TWO LAYERED BALLAST SYSTEM FOR IMPROVED PERFORMANCE OF RAILWAY TRACK

CHAITANYA CALLA

A thesis submitted in partial fulfilment of the University's requirements for the Degree of Doctor of Philosophy

December 2003

Coventry University

Abstract

Considerable evidence suggests that, ballast is the main cause of uniform and non-uniform settlement of ballasted railway track, provided the subgrade is adequately specified. The requirement of a good track is that the sleepers are firmly supported by the ballast bed but over a period of time uneven settlement of the ballast will cause voids to form under the sleepers leading to unacceptable ride quality of track. Voids below sleepers can lead to major track defects and in worst cases can be the cause of vehicle derailment (Ball 2003, Cope and Ellis 2001- p206). Regular maintenance is required to remove voids below sleepers and correct other track geometry faults for smooth, safe and efficient running of the railways.

The fundamental principle of track maintenance is to lift the track wherever it is low and pack ballast firmly under the sleepers (Tazwell 1928, Frazer 1938, Cope and Ellis 2001 - p231). Track maintenance has evolved from manual methods of track maintenance, beater packing and measured shovel packing, of early railways to today's sophisticated mechanised automated systems of maintenance, tamping and stoneblowing, but the basic principles of maintenance still remain the same. Beater packing or tamping works by compressing existing ballast below and around the sleepers into the void below the sleeper while in measured shovel packing and stoneblowing new stones of smaller size are introduced into the void below the sleeper. Ideally ballast below sleepers once compacted by traffic should be left undisturbed, which is the case for measured shovel packing and stoneblowing techniques of maintenance but beater packing and tamping disturbs ballast below the sleepers (Tratman 1909 - p361, Cope and Ellis 2001 – p260). The durability of track geometry of track maintained by the stoneblower is higher, but tamping still remains the preferred option as opposed to stoneblower for track maintenance (Ball 2003). Both stoneblowing and tamping require expensive on-track plant and are expensive to carry out, overall a large percentage of the railway budget is spent on ballast maintenance (Ball 2003).

The proposed two layered ballast system described in this thesis replaces the crib ballast around the sleepers by stones of size smaller than standard railway ballast. The aim is to fill the voids below the sleepers before they become unacceptably large, without use of expensive plant or manual intervention. Model and full scale laboratory tests carried out using the proposed two layered ballast system have demonstrated that with smaller stone as crib ballast (ballast around the sleepers) a void below the sleeper will be filled up to the average particle size of the crib ballast, by smaller crib ballast particles flowing into the void below the sleeper (Claisse et al 2002, Claisse and Calla 2003). The system is self-maintaining and does not require manual intervention or use of mechanical tools or plant once the smaller ballast has been placed in the crib.

ACKNOWLEDGEMENTS

Work on this thesis has been carried out under the guidance of Dr Peter Claisse and late Dr Michael Keedwell. The author wants to express his deep and sincere gratitude to his guides Dr Claisse and Dr Keedwell for giving him the opportunity to work on this project and for their invaluable guidance and deep insight into the subject. The research project has been funded by Balfour Beatty Rail Company and RMC Concrete products and the author would like to thank Tony Darroch of RMC and Charles Penny of Balfour Beatty Rail for their invaluable advice on various practical aspects of this project. The author is grateful to the technicians at the School of Science and the Environment for their support and encouragement throughout the project. The author also wants to thank Austin Reeves and Jim McCartney for their cooperation and support while writing the thesis.

Contents

List of figures

List of tables

Executive Summary of Research

The research involved laboratory, testing at both model scale and full scale on the proposed two-layered ballast system. The different types of tests carried out during the research are shown in the chart on page xxvi. A voided sleeper was simulated in all the tests by lifting the sleeper up between cycles. In type A runs the sleeper was lifted up after each load cycle. In type B runs the sleeper was lifted up after the passage of a 'train' on the track i.e. 10 load cycles. In uplift equal to displacement cycles the sleeper uplift was equal to sleeper displacement into the ballast, i.e. the sleeper was lifted up to the datum zero level set at the start of each test.

A typical track settlement curve after tamping of ballast or on a newly constructed track is shown in figure (i). Track settlement immediately after tamping or in a newly constructed track is very rapid initially but reduces with time as shown in the graph. The laboratory testing for the research was carried out in the region of the track settlement graph (Figure (i)) where the rate of settlement was very low, again as shown in the graph.

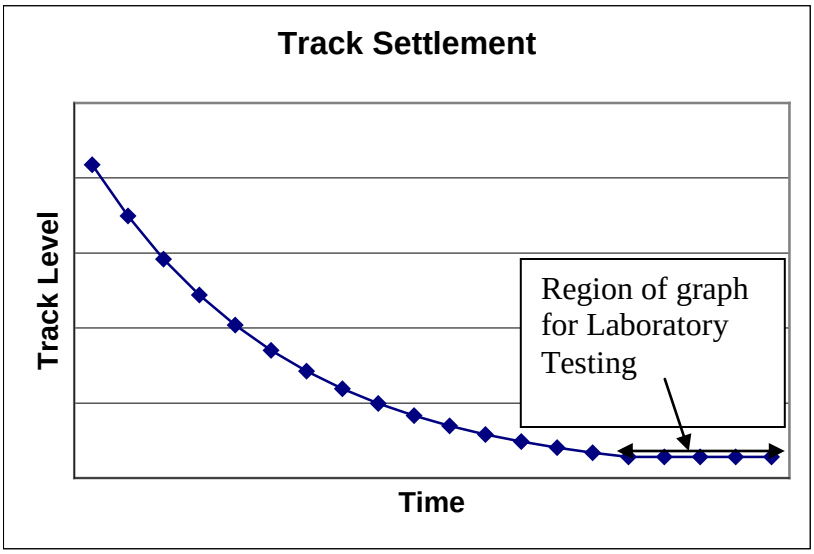

Figure (i) Track Settlement with time.

Test Summary

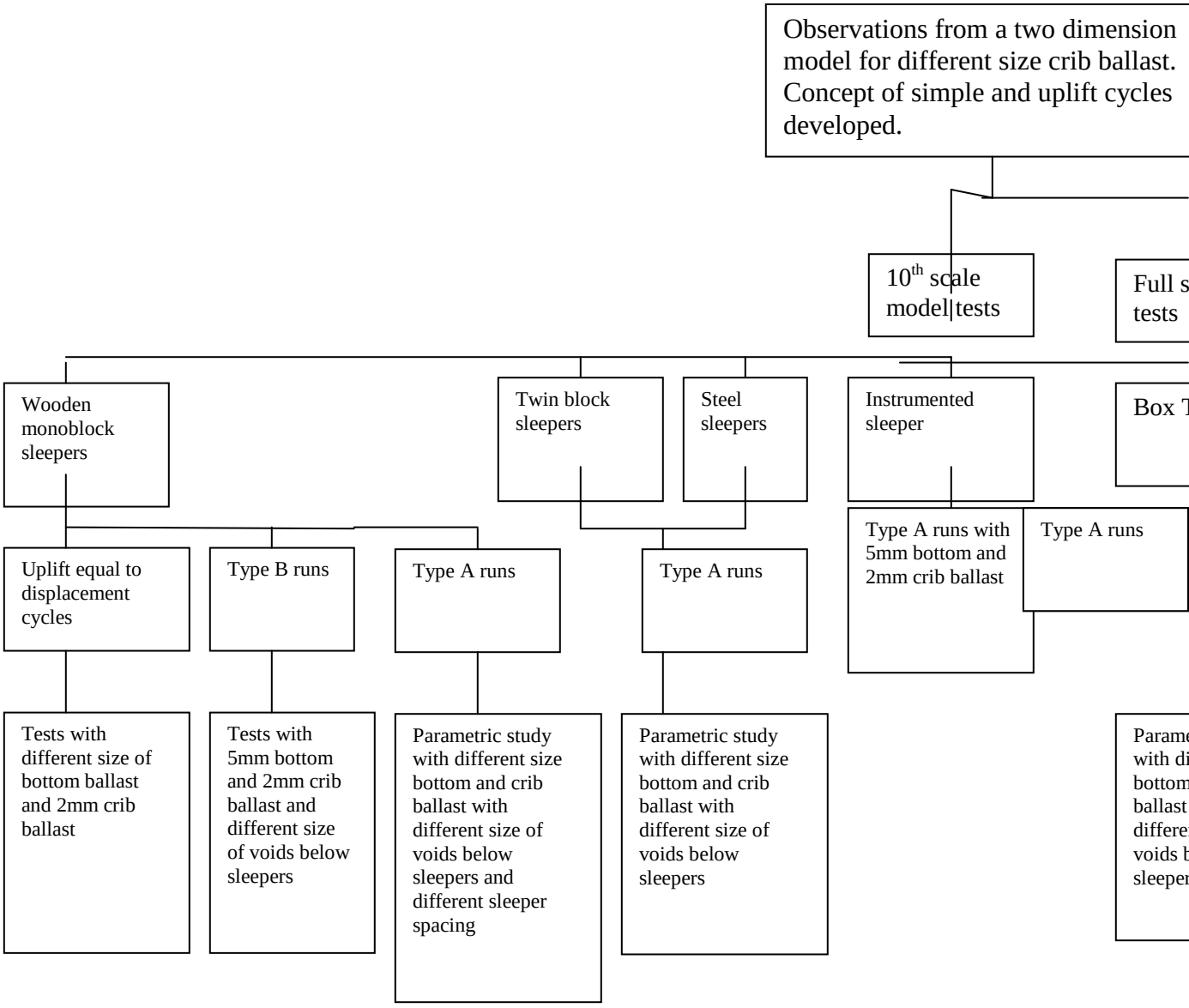

1. Introduction

Ballasted railway track consists of track superstructure of rails and sleepers supported on a layer of granular material (stones) called ballast. Ballast provides a 'firm but elastic' support to the track superstructure and distributes stresses from the sleepers to the subgrade. Ballast also provides for immediate drainage of rainwater from the track but arguably the most important function of ballast is to allow maintenance of track, required to keep the track geometry within certain tolerances for safe and efficient running of trains. Ballast by weight and by volume is the largest component of the track and cost of buying and distributing ballast forms a significant part of the entire Civil Engineering budget of the railways (Cope 1993, p314). In spite of the fact that ballast is the most important component of the permanent way most attention has been focused on the track super structure of rails, fasteners and sleepers, not much consideration has been given to understand the behaviour of ballast in detail (Selig and Waters 1994, p1.1).

Loss of track geometry can be broadly defined as departure beyond a certain tolerance, of the track from its design horizontal and vertical alignment, referred to in the Railway terminology as loss of 'line' and 'level'. Many authors are of the opinion that of all the components of the permanent way ballast is the controlling factor of loss of geometry of track (Shenton 1984, Selig & Waters 1994 – p8.3, Tratman 1909 – p25). Ballast has been identified as the main cause of average and differential settlement of railway track with passage of traffic. Track settlement is also influenced by the inherently variable nature of the formation but if the formation is adequately specified ballast remains the main cause of loss of geometry and subsequent loss in ride quality of the track (Selig and Waters 1994, p8.32). Differential settlement of ballast can cause voids to be formed under the sleepers, which is a major maintenance issue in Railways around the world. Voids below sleepers can lead to major track defects and in worst cases can be the cause of vehicle derailment (Ball 2003, Cope and Ellis 2001 – p206). Continuous inspection of track is required to identify problem areas and carry out maintenance to the track, to correct track geometry problems including voids below the sleepers. Track maintenance has evolved from manual methods of track maintenance like beater packing and measured shovel packing in the

1930’s to today’s sophisticated mechanised automated systems of maintenance like tamping and stoneblowing, these are described in detail in the literature review. Both modern systems of track maintenance viz. tamping and stoneblowing are in principle automation of beater packing and measured shovel packing methods. Thus both tamping and stoneblowing inherit the drawbacks of the manual track maintenance methods.

The proposed two layered ballast system described in this thesis replaces the crib ballast around the sleepers by stones of size smaller than standard railway ballast. The aim is to fill the voids below the sleepers before they become unacceptably large, without use of expensive plant or manual intervention.

1.1 Two layered ballast system

The concept of two layered ballast system was proposed by Dr Michael Keedwell of Coventry University and patented by him (Keedwell 2003). The system consists of replacing 50mm boxing ballast (crib ballast) around the sleepers with stone of smaller size as shown in figure 1.1.

The research reported in this thesis shows that, with smaller size crib ballast when a void is formed under the sleeper larger than a certain size the smaller crib ballast rolls into the void maintaining sleeper vertical alignment. Dr Keedwell likened this idea to the potato masher principle as illustrated in figure 1.2. The potato masher placed in a cylinder filled with sand once lifted, will not be able to move to its original position as the void below will be filled with sand.

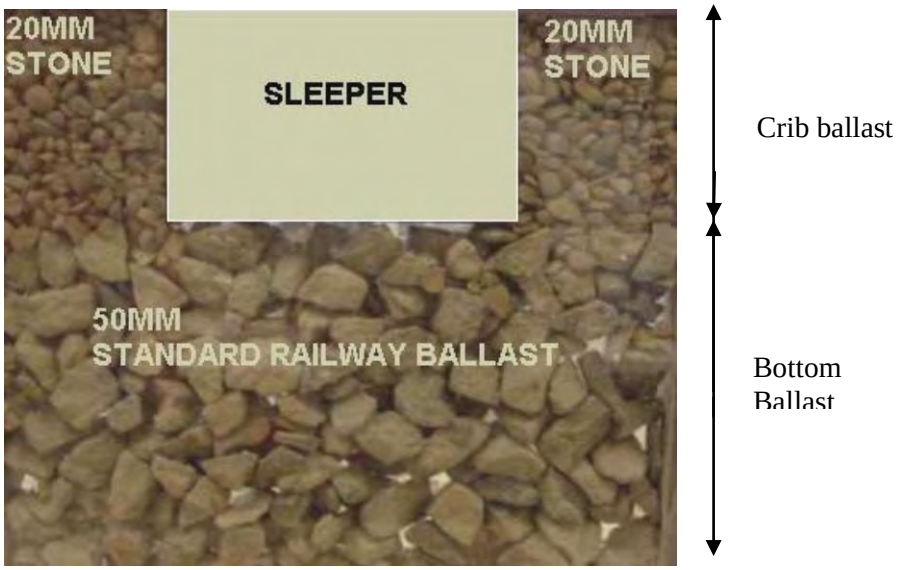

Figure 1.1 Cross-section through proposed two layered ballast system

The system has been patented in the US and Australia (Keedwell 2003). The patent is for a system supporting a rail of a rail track above a substrate. The rail is supported on the upper face of a support (sleeper) with the lower surface facing the substrate, the support is maintained between the lower surface (of the sleeper) and the substrate and the movement of the rail towards the substrate is inhibited. The patented system is designed to deal with the problems of voids below the sleepers and provide a better alternative to the maintenance process of tamping and stoneblowing. The scope of the patent covers continuous support for road or rail vehicles in form of beams or rails placed under the wheels in the direction of travel with cross members (sleepers) resting on a substrate called ballast or road pavement materials placed over ground surface or formation and space between cross members filled with granular material. The spacing and dimensions of the cross members and particle size of the granular material is to be selected such that granular material may flow freely into

any gaps that form between the cross members and ballast or road pavement materials, thus compensating for uneven settlement of ballast or road pavement materials and providing a self – levelling support system

.

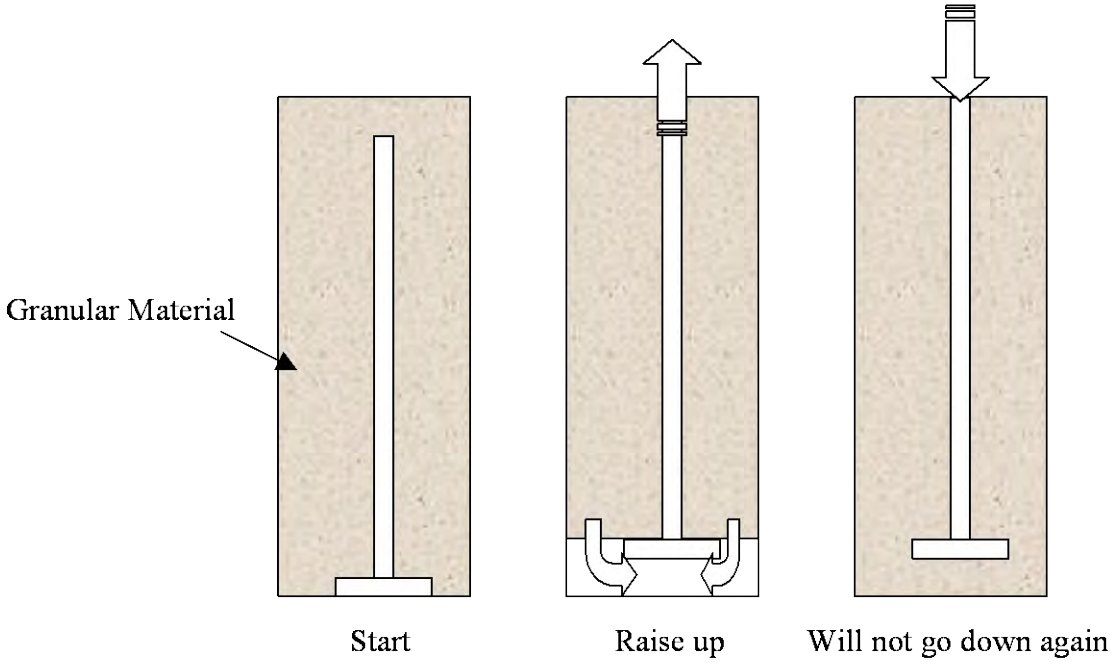

Figure 1.2 The potato masher principle

The research in this thesis looks at practical application of the system to ballasted railway track. A history of development of specifications for the permanent way components and permanent way maintenance methods is given in chapter 2 along with a literature review of research on ballast and railway track maintenance. Virtual instrumentation and measurement methods are described in Chapter 3. The laboratory test set up for model tests and full scale tests is described in Chapter 4. Results from model tests are described in Chapter 5 and results from full scale tests are described in Chapter 6. A discussion on the results of model tests and full scale tests is presented in chapter 7. A description of the preparation for the live track trials is given in Chapter 8. Conclusions of the research are described in chapter 7.

2. Literature review

2.1 Introduction

Railway is considered as one of the fundamental innovations in the development of transportation.

The railway is distinguished from other modes of transport by carriages with smooth metal wheels running on smooth metal rail supported by sleepers resting on a track bed of graded stone known as ballast (more recently the slab track). The great advantage of railway is that the friction or rolling resistance of a smooth metal wheel running along a smooth rail is much lower than that of any type of road vehicle (Rolt 1968, p11). One of the main disadvantages is the regular maintenance required by the ballasted railway track. It is accepted that the cost of maintaining a railway track is several times greater than that of an equivalent length of road lane.

Railways as seen today are not a result of some instantaneous development but is the result of combination of ideas which have been around for a few hundred years. The figure 2.1 below shows a typical modern ballasted track with concrete sleepers laid to a good standard (Cope and Ellis 2001, p – 'inside cover page').The history of development of the railways is described in this chapter with particular emphasis on development of ballast specification and maintenance techniques.

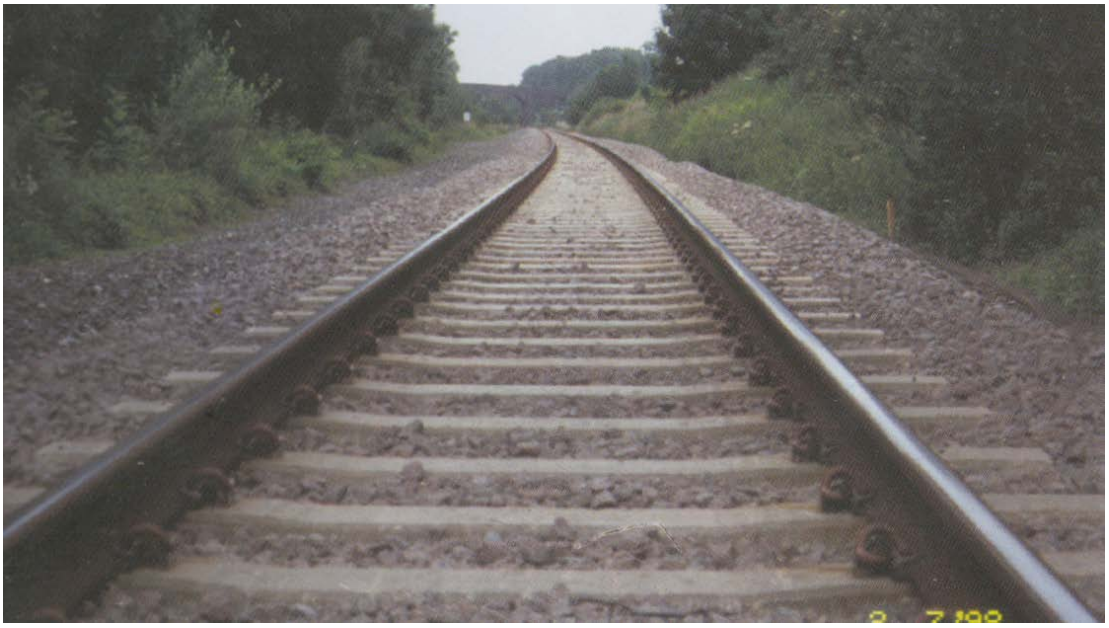

Figure 2.1 Ballasted railway track with concrete sleepers (Cope and Ellis 2001)

2.2 Rails

The rails support and guide the wheels of the vehicle. Their profile has been the object of continuous improvement since the appearance of the railways. Wooden railways were used in the mines from the sixteenth century onwards.

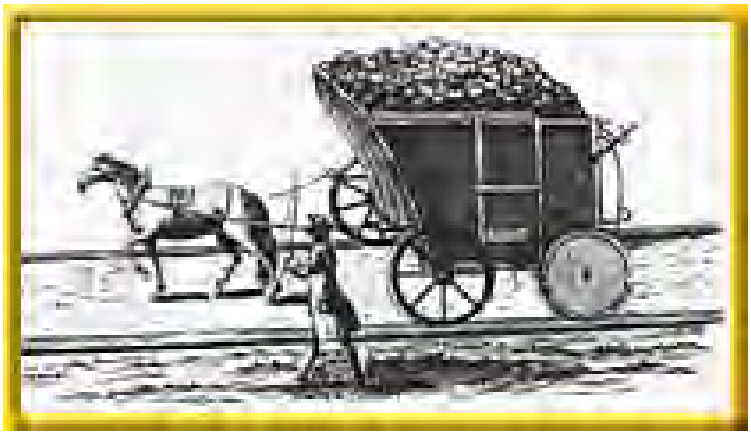

Figure 2.2 An early horse drawn railway on wooden longitudinal sleepers (www.railwaycentre.com 2003)

These wooden wheels were initially provided with a running surface made of wooden blocks, which was subsequently replaced by wrought iron plates in the industrial revolution. This evolved further to cast iron plates and later to edge rails with flanged iron wheels. In 1825, the Stockton and Darlington Railway was constructed adopting track of wrought iron rails resting in cast iron chairs supported on stone blocks set in the ground at three feet (0.9m) intervals. The rails used in the Stockton and Darlington railways were of 'T' section, 4.5m long and weighed approximately 120N per metre. Soon with the development of new technology steel rails substituted the cast iron rails. Until the second world war the bullhead or 'dumbbell' section was standard throughout. The first trials with the flat bottom rails were carried out at Cheddington in 1936 . This rail became the British Standard in February 1949. The flat bottom rail has been redesigned continuously to suit the increasing needs of traffic and high speed trains and recently the British railway has opted for the 60 kg/m section for its railways in place of the existing 56 kg/m section (Hope 2000).

2.3 Sleepers

The sleepers (also known as ties) maintain the line, level and the gauge of the rails and resist action of those forces tending to alter the line and level of the rails. The early makers of the permanent way mistakenly aimed at complete rigidity of the railway track by laying the track on massive stone blocks or stone sleepers. George Stephenson stuck to the system of track on rigid stone blocks for his Liverpool and Manchester railway (See figure 2.3) but it soon became evident to other engineers that laying track on rigid stone blocks led to frequent rail breakage under the heavy locomotives and these stone blocks were soon replaced by timber cross sleepers (Rolt 1968, p14).

Figure 2.3 An artists impression showing the first passenger train ever run. It seems a horse drawn carriage was run alongside to compare the 'horsepower' of six horses to steam power but note the track in the foreground with rails sitting on top of massive stone blocks with no ballast (www.railcentre.co.uk 2003)

The need to find a replacement to wooden sleepers arose at the start of World War -II. Reinforced concrete sleepers were not found satisfactory and steel sleepers were not approved for use in UK because of the cost and fear of corrosion in the variable weather environment. During World War II the first prestressed concrete sleepers were put in the West Coast mainline at Cheddington near Tring on 21st February, 1943 (Taylor 1993). Development of prestressed concrete sleepers took place about the same time as the development of the flat-bottomed rail. Prestressed concrete sleepers have been the Standard for British rail but the use of steel sleepers is slowly gaining acceptance in the UK. The standard prestressed concrete sleepers used in the UK are normally 2515 mm. long by 264 mm. wide. The depth varies from 203mm. at the rail seat to 165mm. at the center (RMC 2000). Alongwith monoblock concrete sleepers twin block sleepers were developed in France (Profillidis 1995, p123), which consisted of two trapezoidal reinforced concrete blocks joined by a connecting bar. Standard concrete monoblock and twin block sleepers are shown in Figure 2.4.

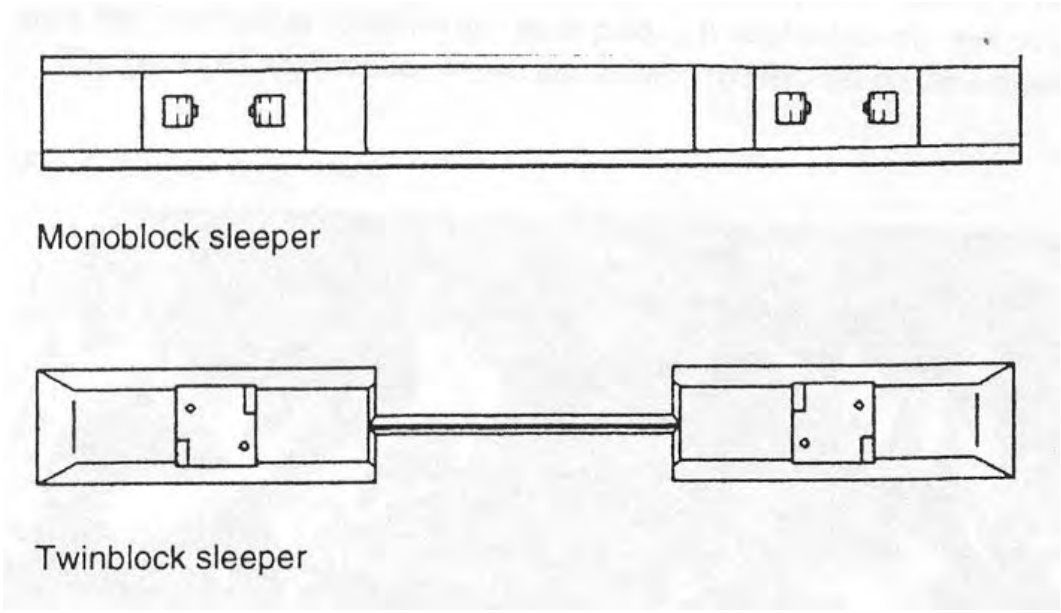

Figure 2.4 Concrete sleepers

Figure 2.5 Track being laid on steel sleepers

Higher stresses are developed in the ballast below a twin block sleeper and thus adequate ballast depth should be provided for optimum performance. In monoblock sleepers the stress distribution is better leading to lower stresses in ballast compared to twin block sleepers but as twin block sleepers are heavier they provide better transverse stability to the track. Due to the flexible tie bar in between the twin block sleeper the track requires extra maintenance to ensure that the blocks do not tilt differentially and the track does not loose gauge.

The use of steel sleepers is being promoted on British rail when relaying sections of track but this is still in its trial period (Hope 2000). Steel sleepers as seen in figure 2.5 have an inverted trough shape with spade ends. Initially when the sleepers are laid on the ballast the sleepers sit on their spade ends but passage of traffic soon forces the spade ends into ballast with the ballast partially filling the inverted trough shape of the sleeper. The remainder of the trough is filled by tamping the ballast. Steel sleepers are being considered for use in tunnels as they can be laid with reduced depth of bottom ballast as compared to wood or concrete. One of the problems with steel sleepers is the reduced lateral resistance to track movement, but better lateral resistance is offered by the spade ended sleepers. Track laid with steel sleepers can be maintained by tamping machines but not by stoneblowing machines, the working of the stoneblowing and tamping machines has been described further.

It is interesting to note that the treated wood sleeper is the material of choice for the majority of track in the U.S. and that 98% of the 14 million sleepers installed in 1988 were of wood (Anon. 1989). Wood is expected to remain the first choice for sleepers in USA in the near future with concrete sleepers coming second (Wanek 2001). Plastic and composite sleepers are being tried in the USA as an environment friendly recyclable alternative to conventional sleepers.

Sleepers are spaced below rails so as to spread the wheel loads over an area of ballast large enough to ensure that neither the ballast nor the sub-grade are overstressed (Cope 1993). Slightly different sleeper spacing is used in different railways around the world but the sleeper spacing varies from 500mm minimum to 700mm maximum. In the U.K. sleeper spacing is in the range of 650mm to 700mm (Profillidis 1995, p128) but recently on the Channel Tunnel Rail Link sleeper spacing of 600mm has been used to reduce stresses on ballast and subgrade. Decreased sleeper spacing results in more uniform track response (Selig and Stewart 1982) but decreased spacing below the existing standards will inhibit maintenance and sleeper spacing above existing standards gives increasingly unfavourable response (Selig and Stewart 1982). Thus current industry standards for sleeper spacing already reflect an optimal design considering costs, maintenance procedures and foundation load distribution (Selig and Stewart 1982)

2.4 Ballast

Ballast forms the largest component of ballasted railway track in terms of cost and volume. It is estimated that British rail will be spending approximately £ 136 million per annum on ballast supply alone by 2005, this does not include the cost of placing the ballast (Ball 2003).

The term ballast as a part of railway track originated on Tyneside in the UK. In the Guinness Railway Book (Marshall 1989), John Marshall has said that ships carrying coal away from Newcastle returned ‘in ballast’ laden with gravel and other materials to maintain stability. This ‘ballast’ was dumped by the quays and was used to provide a solid bed for the tramways, which carried the coal. This association of the word ballast with the tramways was continued and was adopted for the railways.

It has been mentioned that early railway engineers aimed at complete rigidity of track by installing track on massive stone blocks laid on level ground (See figure 2.3). Randell (1913) describes the efforts of early engineers who “sought to form a solid bed, by pounding mother earth with the blocks of stone which were to carry the track”. He also

describes an instance on a railway track between Manchester and Leeds where sleepers were fastened directly to a dressed rock cutting, this track lasted a few weeks. Instead of laying the sleepers directly onto the ground the engineers realised the need for a resilient base to the sleepers, more importantly they realised the need to keep the track top 'level' and thus the need for material below the track, which would allow lifting and packing of the track. In many instances a sprinkling of ballast was considered sufficient bed (Randell 1913). Ballast was viewed as a medium for surfacing the track and Ahlf (1995) describes a rule of thumb in early railways that, 'ballasting and raising of the track should not exceed the amount of lift necessary to restore the surface of the track' (Ahlf 1995). The material had to be a right of balance of rigidity and elasticity to carry the load of railway traffic without causing damage to the track superstructure components and to be able to distribute the loads to the subgrade. The material had to be free draining to prevent waterlogging of the track. Thus a set of conflicting requirements led to the development of a layer of granular material under the sleepers called ballast. To summarise the ballast functions: Ballast provides resiliency to the track and distributes stresses from the sleepers to the subgrade. It provides lateral and longitudinal stability to the track and maintains track gauge. The ballast facilitates maintenance and provides immediate drainage of rainwater from the track. As specified by Cope (1993, p312) the above functions are performed in a manner such that the position of the rail:

1. does not, in the loaded condition change with time;
2. returns to its original position after the passage of each train;
3. moves elastically under vehicle loading within tolerable limits for the mechanical design and use of those vehicles.

To perform the above functions ballast depth, size and shape are specified and the best material suited for ballast is also specified. The practice is generally similar in railways around the world with some local variations(Cope 1993, p313).

2.4.1 Ballast depth

A minimum ballast depth is required for the ballast to perform the above functions. Adequate ballast depth must be specified to prevent sub-grade failure (Selig 1984, Shahu et

al 1999). The underlying principle is to have minimum depth of track bed such that pyramids of support from sleeper to subgrade should touch or overlap (see fig. 2.6) (Cope 1993, p313). This ensures that that the loading on the subgrade is uniform. A minimum depth of ballast is also required to facilitate maintenance operations like tamping.

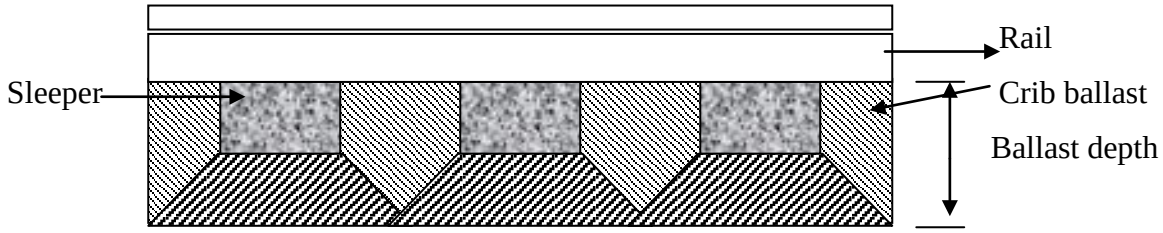

Figure 2.6. Stress distribution from sleeper to subgrade

Various design methods have been in use to design ballast depth, early simplistic methods of design have now been replaced by more rational methods of design, which take into account various factors affecting ballast performance. British railways developed a "threshold stress" design method for the depth of ballast. The design was to limit the stress on subgrade soil to within the 'threshold stress' to prevent subgrade failure by excessive plastic deformation (Heath et al 1972).

Selig has described minimum ballast depths for carrying out different ballast functions as given below in Table 2.1 (Selig 1998).

Function	Ballast depth
To provide resiliency to track on a subgrade less stiff than the ballast	150mm – 300mm
To provide enough ballast for storage of fouling material	300mm – 375mm
To accommodate tamping	Around 225mm
For drainage to keep water surface well below the ties	300mm-375mm

To reduce stress on underlying sub ballast or subgrade	150mm – 450mm

Table 2.1 Proposed ballast depths by Selig and Waters (1994)

Selig concludes that a minimum of 300mm – 450mm ballast is required below the sleepers and this applies to heavily used track. For lightly trafficked track the ballast depths could be reduced but not below 150mm – 300mm. Selig has defined two granular layers under the sleepers one being the ballast just below the sleepers and the other being the sub ballast between the ballast and the subgrade. Li and Selig (1998) have given methods for design of granular layer thickness in railway tracks which include both the sub ballast and the ballast.

Recommended ballast depths on British rail for various track types are given in table 2.2 (Cope 1993).

Line Speed (km/h)	Line Tonnage (tonnes/year)	Ballast Depth (mm.)
177 to 201	7 million upwards Below 7 million	280 230
129 to 169	15 million upwards Below 15 million	280 230
Below 129	All	150

Table 2.2 Ballast depth on British Railways (Cope 1993)

Recently on the West Coast Mainline an increased ballast depth of 300mm has been adopted to account for variable subgrade conditions (Sharp et al 2002).

The stresses in all track components are dependent on elasticity of the ballast. A term, Track Modulus is used to define the elasticity of ballast. The track modulus is a measure of elasticity of ballast and relates pressure imposed on the ballast by the sleeper to the

deflection of the top table of the rail (Cope 1993, p313). Structurally modelling the rail as a beam on an elastic foundation track modulus can be defined as " The uniformly distributed line load required to produce unit deflection of the support" (Cope 1993, p313). An elastic ballast with lower track modulus will deflect more under the load and the bending moment in the rail will be high. To limit deflection of the track it is important that the track modulus is fairly high although a stiffer ballast will transmit vibration into the surrounding ground (Cope 1993, p313).

To provide longitudinal stability to the track ballast is filled in the cribs to the top of the sleepers and to provide lateral stability to the track ballast shoulders are formed on sleeper ends to a typical width of 300 – 600mm depending on the type of track. For track with continuous welded rails track shoulders are heaped 125mm above the sleeper top level to prevent buckling of track. To increase the lateral resistance of track a technique called ballast gluing is used on the British Rail (Railtrack 1996). Approved glue materials are used to bind the stones together at their contact points. To increase lateral stability the gluing is carried out only on shoulder ballast. The depth of gluing is typically 200mm and width is 300mm. Maintenance tamping is permissible after gluing provided gluing has been carried out on shoulder ballast only.

It is interesting to note that as early as 1909, Tratman (1909, p25) recommends minimum depth of ballast below the sleepers as 300mm for track with heavy traffic, with well formed shoulders to provide lateral resistance, similar to current practice. In Britain ballast was laid in two layers with bottom layer of ballast (hardcore ballast) being stones 225mm (9inches) in size and top layer being the standard ballast of granite, flints, gravel or slag (Randell 1913, Hamnett 1956) (See figure 2.7). This practice was discontinued in the 1950's (Hamnett 1956).

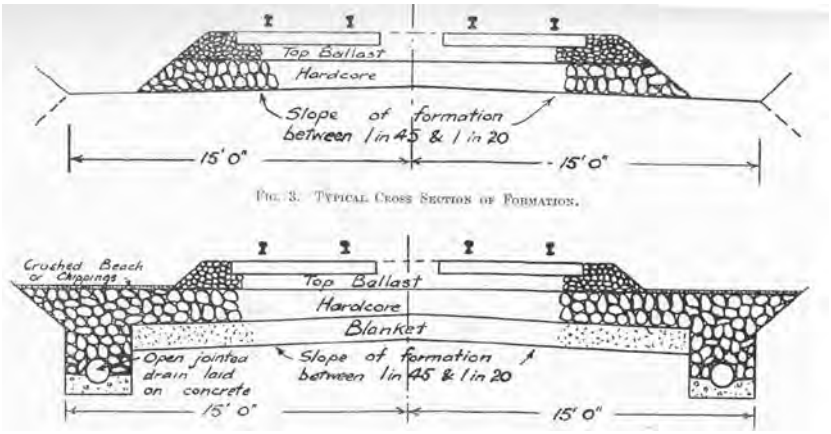

FIG. 3. TYPICAL CROSS SECTION OF FORMATION.

Figure 2.7 Details of ballasted track in UK in the early 1900's with hardcore ballast and top ballast (Hamnett 1956).

2.4.2 Material for ballast

Ballast being the largest component of the permanent way in terms of volume and cost ideally it should be a cheap material capable of being packed (Cope 1993, p314). It is now universally accepted that good quality hard angular stone free from dust and dirt and not prone to cementing action is the best material for ballast. Stone ballast can withstand heavy loads without getting crushed and with a crushed angular rock it is possible to achieve proper frictional interlocking of ballast particles.

Selig (1998) has divided ballast properties into two categories:

a. Individual particles and
b. Assembly of particles.

Individual particle characteristics are
Durability – represents resistance to breakage under mechanical forces.
Shape – is defined by the amount of flat and elongated particles and by angularity.
Surface texture – is the roughness on the surface of ballast particles.

Gradation – is the mean particle size and range of particle sizes.

Selig opines that the normal practice on railways is to put limits on acceptable values of these individual index properties and the problem is that no correlation exists between the ballast index properties and the performance of ballast in the track.

The important properties considering ballast as an assembly of particles are strength, stiffness, resistance to deformation under repeated loading, resistance to flow of water, ease of tamping and voids for storage of fouling materials (Selig 1998). Interestingly these properties change over time as the ballast becomes fouled.

2.4.3 Ballast size

Provided that ballast is good quality durable angular stone, its most important parameter is its size and gradation. Ballast size should be chosen such that it supports the track superstructure, allows for drainage of water, and also lends itself to maintenance for correcting track geometry faults.

The choice for ballast gradation is generally similar in all countries with some local variations but it is interesting to note the difference in the French and the British ballast specifications. Current practice on British rail is to use single size stone with majority of ballast of size 30mm to 50mm. Ballast on French rail is a well graded ballast with stone sizes ranging from 63mm maximum to 15mm minimum with the majority of particles in the size range 20mm to 40mm (Profillidis 1995, p143). French ballast is of a broader gradation with major proportion of the particles being smaller than 40mm (Wood 2002). This is significantly different from what is used on British rail.

Cope (1993, p315) explains the requirement of optimum particle size distribution of ballast as a balance between a very uniform aggregate which will have a higher percentage of voids and larger voids but lower strength and well graded aggregate which will have less voids but higher strength.

Selig concludes that effect of particle size on strength of ballast is unclear (Selig and Waters 1994, p7.26) but tests seems to suggest that strength of ballast is more for a broader gradation than a uniform gradation and some research suggests that broadly graded ballast of smaller size is stronger than uniformly graded ballast of large size, although results are inconclusive. It was observed that ballast compression (cumulative plastic strain) was higher for a uniformly graded ballast as compared to a broadly graded ballast with a smaller mean size. Determining the optimum choice of ballast specification according to Selig is difficult due to the conflicting particle requirements among the various ballast functions. One important observation made by Selig, not mentioned by other authors, is that maintenance by tamping of track is better with a narrow range of particle sizes. Triaxial tests carried out by Indraratna et al (1998) seem to suggest that there is more particle breakage in ballast with a broader gradation which is densely compacted.

2.4.4 Ballast fouling and drainage

The term fouling can be broadly defined as the filling up of the voids in ballast with particles of size smaller than 6mm (Selig and Waters 1994, p8.18). New ballast does not contain more than 2% of the particles smaller than 6mm in size (Selig and Waters 1994 – p8.18). Over a period of time the proportion of smaller particles increases and beyond a certain limit the smaller particles prevent ballast from providing - support to the sleepers, drainage of water from the sleepers and a means of correcting track geometry faults. Such ballast is called spent ballast and has to be replaced.

Main sources of fouling are (Selig and Waters 1994, p8.18):

1. Ballast breakdown due to traffic and tamping
2. Infiltration from ballast surface either airborne or delivered with ballast or dropped from trains i.e. fouling due to external sources
3. Sub grade infiltration and
4. Sleeper wear.

Different railways have different experience with fouling and these have been discussed in detail by Selig et al (Selig and Waters 1994, p8.26). The North American experience

shows that ballast fouling is due to ballast degradation under loads and due to the effect of tamping. 76% of fouling is due to ballast breakage, which could be both from tamping and traffic. The German experience is that majority of ballast fouling is due to external sources of fouling. British Railways have estimated that the maximum contribution to fouling is by the tamping process, this has been discussed in detail in succeeding sections.

Fouling of track, as mentioned earlier, prevents ballast from carrying out its functions but the effect of each fouling material is different (Selig and Waters 1994, p8.31). Selig et al have said that fouling of track by sand and fine gravel size particles increases the shear strength of ballast and increases stability decreasing ballast compression from traffic if coarse ballast particles still form the ballast skeleton. Fouling by sand and gravel also increases frost protection. Track drainage remains adequate until all the voids are filled up although drainage gradually decreases. The problem occurs when fouled track is tamped. This causes segregation of particle sizes and soon all the voids are filled up. On fouled track alignment by tamping is not durable thus frequent tamping is required increasing maintenance costs and further damaging ballast. Still Selig et al are of the opinion that fouling by coarse sand and gravel particles does not increase maintenance costs significantly. They have said that loss of performance of track usually occurs when fouling materials contain silt and clay size particles (fines). Silt and clay size particles combine with the coarser fouling elements to form an abrasive slurry. This will cause problems like sleeper attrition and increased ballast deterioration. There will be severe loss in drainage of track and ponding water will further worsen the problem. Maintenance of such track with tamping is impossible and as ballast is contaminated with clay it cannot be cleaned but has to be totally replaced.

2.5 Ballast and track geometry deterioration

Most authors are of the opinion that of all the components of the permanent way ballast is the controlling factor of loss of geometry of track (Shenton 1984, Selig & Waters 1994 – p 8.32, Tratman 1909 – p25), if the formation is adequately specified. Ballast in a newly laid track or a track just after routine maintenance operations is compacted under traffic and settles. Due to various reasons this settlement is not uniform and thus faults in track

geometry develop, commonly known as twist or cyclic top faults (Cope and Ellis 2001, p45). Track geometry deterioration is also the cause of wet spots on track. These geometric faults have been described in detail in succeeding paragraphs.

Both Selig & Waters (1994, p15.10) and Shenton (1984) have mentioned inherent track quality. It has been observed that track has an inherent shape which it acquires at the time of its original construction. A track constructed with level compacted ballast and straight rails has a good inherent quality. Achieving changes in the inherent track shape is very difficult. A track having good inherent quality has a good ride quality while a track with poor inherent quality requires much maintenance (See figure 2.9). For short distances the rail imprints its shape on the ballast while for longer distances the rail bends to the shape of the ballast bed (See figure 2.8). Thus a track constructed with straight rails and level ballast bed with uniform settlement properties will have low rate of deterioration.

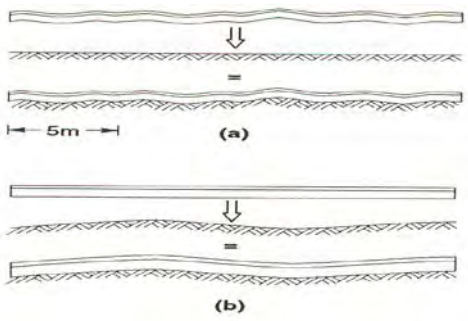

Figure 2.8 Inherent track quality – Influence of rail shape (a) and ballast shape(b) (Selig and Waters 1994)

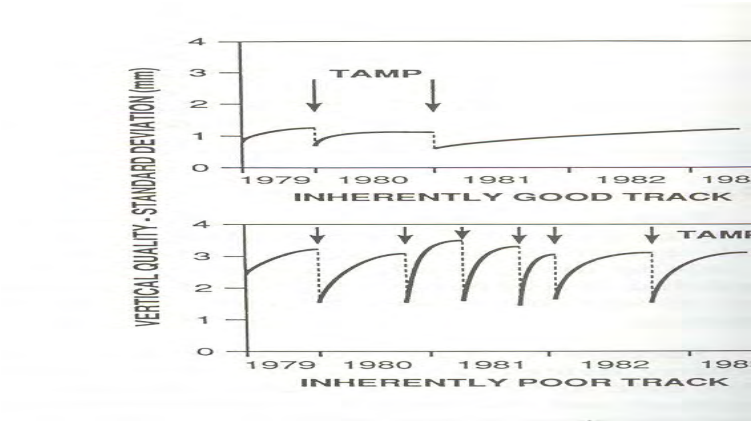

Figure 2.9 Graphs demonstrating frequent maintenance required by inherently poor track (Selig and Waters 1994)

Undulations in the track induce vertical vibrations in passing vehicles and depending on their frequency these vibrations reduce ride quality of track and cause track damage. The minimum geometric quality to which the track has to be maintained is a function of the speed and type of traffic being carried on the track. Tracks carrying high speed or passenger traffic will need to be maintained to a higher geometric quality than will tracks dedicated to low speed and/or freight traffic (Selig & Waters 1994, p15.16). As shown in figure 2.10 maintenance intervention for passenger traffic will be more frequent than for freight traffic. Also shown is the effect of track inherent quality on maintenance cycle of the track.

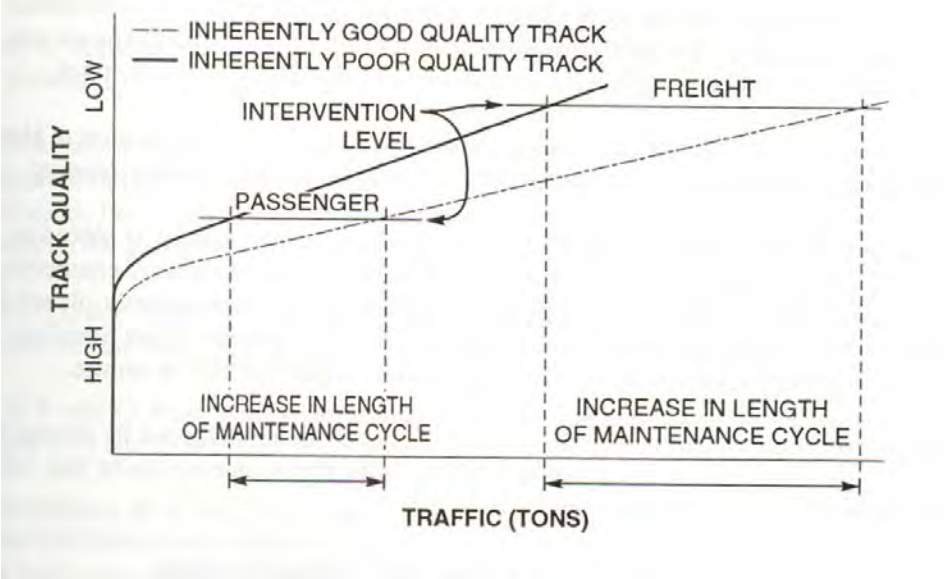

Figure 2.10 Graph showing effect of track quality on maintenance cycle and intervention levels for different traffic (Selig and Waters 1994)

2.5.1 Voids below sleeper

Voids under sleepers are a common occurrence in the railways and are a major cause of track geometry deterioration and ballast degradation. Voids can be detected by watching vertical movement of the sleeper under traffic or by striking the sleeper with a hammer and subsequently measured by installing instruments like void meters on the track (Fig. 2.11). Voided sleepers occur either as single sleepers supported by adjoining sound sleepers or as a group of loose sleepers again supported by adjoining sound sleepers effectively hanging from the rail. A track with a single voided sleeper if not attended to, soon deteriorates to a group of loose sleepers.

Figure 2.11 Showing Pell void meter fixed to bottom flange of the rail (Cope and Ellis 2001)

The author while doing his research was living in Coventry in a house adjacent to the Coventry - Nuneaton line and had to pass a level crossing on his way in to work and back home everyday. Thus whenever the level crossing was closed it presented an opportunity to the author to observe the track when the trains passed. On both the up and down lines the author could observe loose voided sleepers and the movement could be estimated to be around 10-15mm. There already was a speed limit of 35 mph in place on that track and looking along the length of the track one could see that there were dips in the track at several locations very similar to a cyclic top fault described further, a photograph of the track is given in figure2.12.

Figure 2.12a Coventry – Nuneaton railway line as seen from level crossing on Coundon Road in Coventry, close to the author's house. Note the cyclic fault in the track. Speed limit of 35-40 mph is in force on the track as seen in the photograph.

Figure 2.12b Coventry - Nuneaton railway line with cyclic fault.

Similarly on a trip to the Coventry railway station by the author and his supervisor many loose sleepers were observed and on jointed track close to the railway station the sleeper movement was excessive with voids below the sleepers estimated to be more than 15mm. Thus voided sleepers seems to be a common but serious maintenance problem on British Rail network.

Cope and Ellis (2001, p206) has given a detailed description of problems occurring due to voids under the sleepers, which is not discussed in as much detail in any other literature on Railway Track. One of the reasons might be the fact that modern track geometry recording cars measure the loaded profile of the track and thus are not able to differentiate between a track surface irregularity and voids below sleepers as both track defects appear as a similar distortion on the output data of the track geometry recording cars. Cope et al have discussed at length the track defects occurring as a result of voids in ballast below the sleepers. Voids below sleepers lead to development of wet spots, cyclic tops or bad tops and aggravate the effect of twist faults. Voids below sleepers can be easily identified by white powder around the sleepers and rounding of ballast particles in wooden sleepers (See figure 2.13). In concrete sleepers again tell tale signs are white powder around the sleepers and less angular ballast on the upper surfaces (See figure 2.14).

Problems due to voids below sleepers are usually the cause for problems to other track component like loose or missing fittings, missing rail pads, rail weld failure, failure of joints in a jointed track etc. Thus it is important to keep the rail bearing portion of each sleeper well packed and free from voids (Cope and Ellis 2001 – p206, Tazwell 1928, Frazer 1938, Tratman 1909).

Figure 2.13 Voids below wooden sleeper identified by white powder around the sleepers

Figure 2.14 Voids below concrete sleeper again identified by white powder around the sleeper.

2.5.1.1 Wet spots and ballast failure

Cope et al mentions that the most common form of ballast failure is the wet spot or slurry spot, although this perhaps relates to track conditions within the U.K. This occurs where sleepers are poorly packed. When the wheel passes over a loose sleeper it causes the sleeper to impact the ballast damaging the soffit of the sleeper and also causing ballast breakage in that area. The powdered concrete produced due to sleeper damage and particles of stone broken from the ballast, mix with rain water and form a lean mix concrete which in dry weather sets in the form of a trough around the affected sleepers which then helps retain water around the sleepers (Cope and Ellis 2001 – p225, Selig and Waters 1994 – p8.30) (See figures 2.15, 2.16, 2.17, 2.18). The process is self perpetuating if the problem of voids below the sleepers is not corrected and spreads to adjacent sleepers quickly. If only under one rail the slurry spot indicates a twist fault but if under both rails it can lead to development of a cyclic top. It is not possible to correct a track with wet spot by regular maintenance and if in an advanced stage (Figure 2.18) the only solution is track possession and repair or replacement.

Figure 2.15 Wet spot with water ponding in the crib (Ball 2003)

Figure 2.16 An advanced stage of wet with voided sleepers and fouled ballast (Ball 2003)

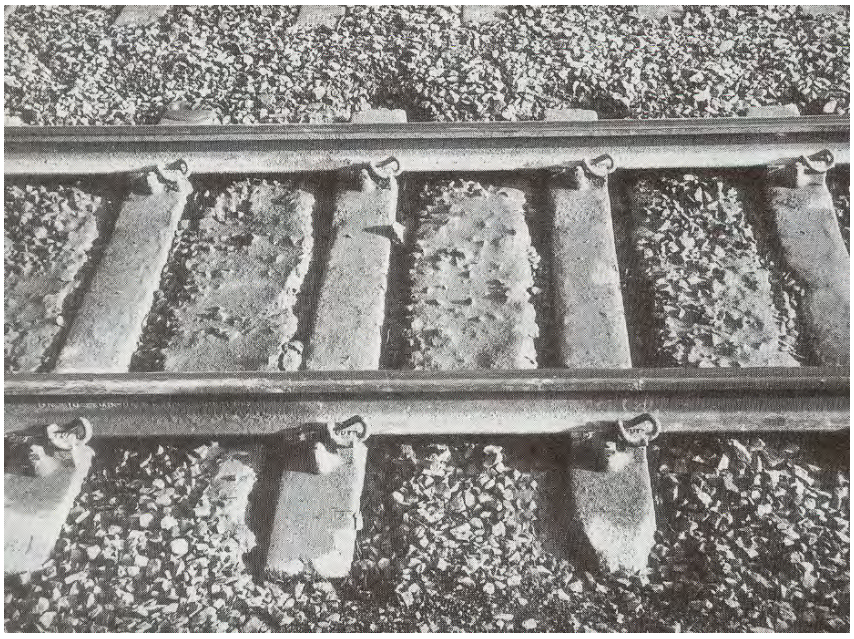

Figure 2.17 Wet spot damage to the sleepers, observe the ballast displaced out of the cribs (Selig and Waters 1994)

Figure 2.18 An advanced stage of wet spot which will require ballast renewal (Cope and Ellis 2001)

Wet spots are one of the major maintenance problems on British Rail. Ball reports that there are 3642 wetbeds in the West Midlands area of the UK over track length of 359 miles (Ball 2003). Ball estimates that there are approximately 173540 wetbeds across the railway network in the U.K. Network Rail has theoretically limited the maximum voiding below sleepers to 7mm but this level of compliance is not possible in all locations and thus a larege proportion of the track remains substandard waiting for renewal (Ball 2003).

2.5.1.2 Twist faults and Cyclic tops

A twist fault is a track condition where there is a difference in cross levels in the track measured on the same sleeper. This is intentional on a curved track to balance the weight of

the train on the curve. On curved track one rail is positioned higher than the other intentionally and this is called cant transition in railway terminology. A cant transition can develop unintentionally in case of badly supported sleepers, this type of fault is called twist fault. Voids below sleepers along with minor faults in track vertical geometry will accelerate the development of twist faults (Cope and Ellis 2001, p45).

A cyclic top is a series of dips and humps at regular intervals on the track (See figure 2.19 and 2.20). Cyclic top causes vehicles to bounce while travelling over the dips and in extreme cases can cause derailment (Cope and Ellis 2001, p48). Voids under the sleepers can be the direct cause for cyclic tops but it is also usual for wet spots to lead to development of cyclic tops thus voids below sleepers indirectly causing cyclic top.

Figure 2.19 Cyclic top in continuous welded track. In extreme cases these dips can cause vehicle derailment (Cope and Ellis 2001)

Figure 2.20 Dipped joints caused by insufficient packing of ballast below joints (Cope and Ellis 2001)

Both the above conditions can be detected by track geometry recording machines and should be treated before they exceed their allowable limits.

2.5.1.3 Track geometry measurement and analysis

To maintain track ride quality within acceptable limits for the passengers and to maintain the permanent way to satisfactory safety standard by cost effective maintenance, track geometry recording is carried out on a regular basis. The data helps set track geometry standards and is a means of scheduling permanent way maintenance. Track quality data can help identify areas requiring urgent attention and thus maximises the use of resources.

Track quality measurement is carried out by track inspection cars and the use of these cars can be traced back to the 1920's in France when the 'hallade' system was used for track recording (Cope 1993, p487). Prior to the 1920's the track quality was assessed by visual inspection of the track and observing voided sleepers moving under the track. Since the 1970's British Rail Research has developed track geometry recording cars with on board computer systems for recording and analysing data, these are known as High Speed Track Recording Cars (HSTRC) (Figure 2.21). These cars are operated over the entire railway network periodically at set intervals to record the condition of track geometry. The output then forms the base for planning and carrying out railway maintenance. It also generates a number of key performance indicators, which allows monitoring of track maintenance being carried out.

Figure 2.21 High speed track recording car capable of recording at speeds of 125miles per hour (Cope and Ellis 2001)

The HSTRC makes use of an inertial system of measurement which makes use of the displacement arising from the inertia of a spring mounted mass in an accelerometer to sense and quantify accelaration. The data can be integrated twice to give a very accurate electrical analogue of the displacement, or movement of the surface to which it is mounted. When

fixed to a railway vehicle this arrangement provides a reference line form which vertical and horizontal track profile measurements can be made. Displacement sensors across the suspension are used for vertical profile measurements while optical sensors are used to measure the horizontal profile (Cope 1993, p488). Additional instrumentation is used to measure cross level, curvature, gradient and corrugation amplitude. The magnitude of track irregularities is obtained in the form of standard deviation of the vertical and horizontal profiles. Standard deviation of track provides a convenient way of quantifying the track geometric quality. Standard deviation is calculated as the square root of the mean of the squares of the individual data samples, each of which represents a departure from an assumed mean whose value is zero. A standard deviation of zero corresponds to a perfect track and maximum reported value of 9.9mm corresponds to an extremely poor quality. A scale of intermediate values is thus available to specify the quality of all classes of line (Cope 1993, p500). Figure 2.22a shows a track with poor geometric quality, standard deviation 6.8mm and 2.22b shows the same track after maintenance, standard deviation 3.1mm.

Figure 2.22a Track with poor geometric quality – Standard deviation 6.8mm

Figure 2.22b Track geometric quality restored by maintenance, standard deviation 3.1mm

2.6 Track Maintenance

The fundamental principle of track maintenance is “To maintain a good ‘top’ on a line it must be lifted wherever it is low and the ballast must be packed firmly under the sleepers at the points where it has been lifted” (Cope and Ellis 2001 – p231, Tazwell 1928, Frazer 1938). This will prevent the development of track geometry faults as discussed above. One of the disadvantages of ballasted railway track is the continuous inspection and maintenance required to keep the track geometry within certain tolerances.

Track maintenance has evolved from the early days of beater packing to modern mechanised maintenance of the present and the requirement of ballast to lend itself easily to maintenance has influenced the development of ballast specifications (Claisse and Calla 2003).

2.6.1 Beater packing

In the earliest days of railways, track was maintained by beater packing (Mc Dougall 1938, Randell 1913, Tratman 1909 - p365). Maintenance involved treating dips in the vertical profile of the track termed as ‘slack’ in the track and voids under the sleepers. A ganger by visual inspection would identify low areas on the track, this being done by looking along the length of the track with eye at rail level. Loose sleepers would be identified by marking sleepers observed moving under the passage of a train or by striking sleepers with a hammer. On each side of the sleeper to be packed ballast would be opened out to the bottom of the sleeper. A beater is a pick-axe with a blunt tee-shaped end for driving the ballast under sleepers. Track would be lifted up by the required amount, estimated by the ganger, using jacks. The ballast under the sleepers would be loosened by the sharp end of the beater and then beaten by the blunt end into the void from both sides of the sleeper. The mechanized version of this technique is tamping. The track top obtained using beater packing was down to the expertise of the ganger and uniformity of track top was not obtained. It is also mentioned in early literature that the pair of workmen carrying out the beater packing should be of about the same strength and activity (Tratman 1909, p365) to achieve uniformity of packing. Another disadvantage was that repeated use of beater packing damaged the sleeper undersides and the ballast making it rounded due to the repeated blows of the beater and old ballast below the sleeper was loosened and weakened

by beater packing. Before the introduction of ordinary shovel packing and subsequently measured shovel packing beater packing was the only means of maintenance.

It is interesting to note that as early as 1909 mechanisation of the beater packing process was introduced. Tratman mentions the trials of the Collet machine in France in which a bar was operated with a reciprocating movement (Tratman 1909, p366). Four of these machines were mounted on a truck or a push car two on each side of the sleeper. Similar Collet machines are mentioned by Mcdougall (1931) although the observation by Mcdougall is that British method of Shovel packing was superior to the tampers used on the continent.

2.6.2 Ordinary and measured shovel packing

Due to the inherent drawbacks of the beater packing method shovel packing was introduced in the U.K in early 1930's (McDougall M 1931). In this method the track was raised and small stone chips 5 to 10mm in size were filled in the void to provide a firm bearing to the sleeper at the required level. Its use was limited to small lifts and again its effectiveness depended on the skill of the ganger in estimating the slack in the track and amount of chips required for each sleeper. This was until 'Measured Shovel Packing' was introduced. Measured Shovel Packing was introduced in France and its use in Great Britain started in 1930's-40's. In this method by simple levelling techniques the amount of 'slack' in the track was determined. A set of three sighting boards was used to identify low spots in the track (Figure 2.23), with two boards being set on high spots on the track and the third board placed in between on a low spot. As shown in figure 2.23 the ganger through the first board would sight the distant board on the high spot and signal his assistant to raise the intermediate board up till it completely covered the distant board. The amount by which the intermediate board was raised was calibrated to give the number of chips required to raise the track to bring it in level with the high spots.

Void meters were used to measure depression of loose sleepers into the track on passage of traffic. Measuring equipment was calibrated to give directly the amount of chippings required under each sleeper, which were then spread evenly 450mm (15 inches) either side of the running edge of the rail to provide a firm bearing (Figure 2.24). The stone chips would consolidate by a small amount under initial traffic and it was general practice to pack the track slightly higher to allow for this consolidation, although Heeler (1979) cautions that this should not leave high spots on the track after packing.

It seems that ordinary shovel packing was introduced first in Britain but the idea of removing the uncertainity of the final outcome of the packing process, which was based entirely on the gangers experience in estimating the amount of lift required by the track, was devised by Monsieur Lemaire in France (Frazer 1938).

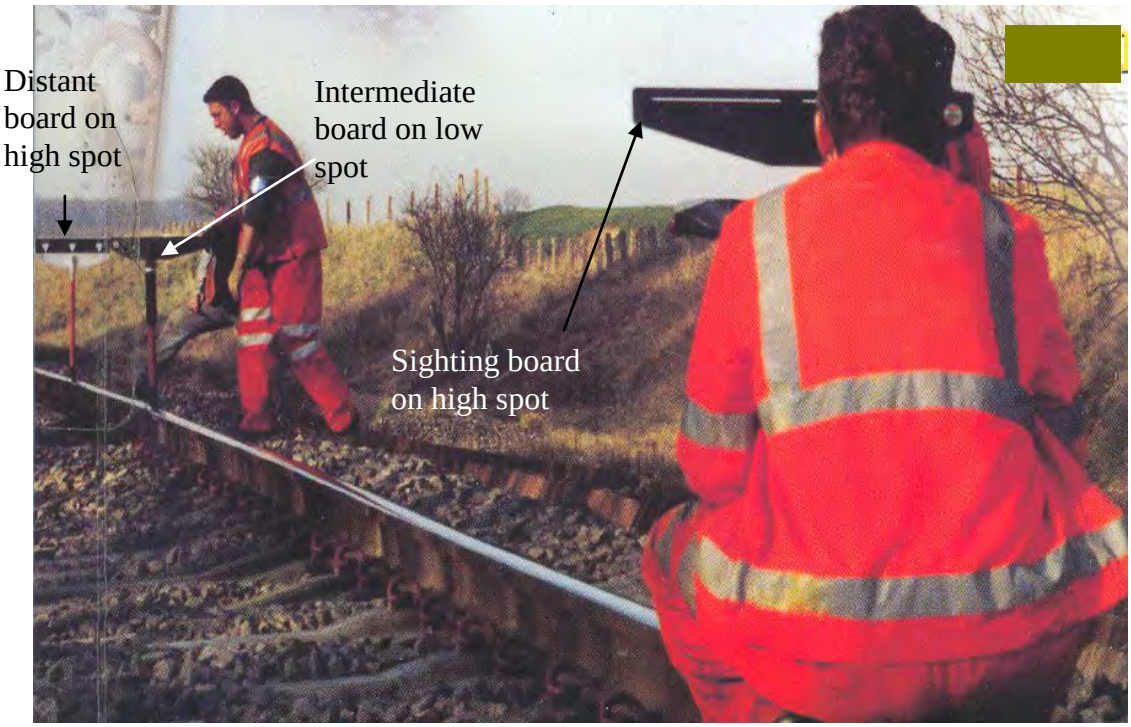

Figure 2.23 Identifying slack in the track using simple levelling techniques of three sighting boards prior to measured shovel packing (Cope and Ellis 2001)

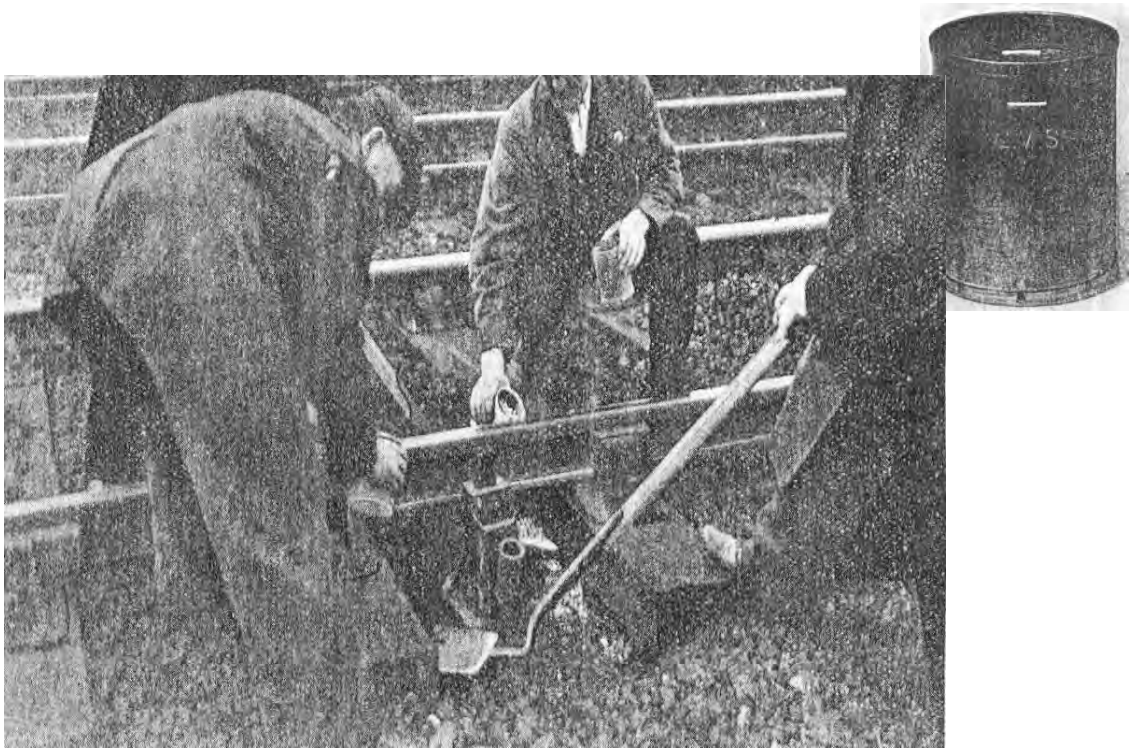

Figure 2.24 Measured shovel packing in progress, note the can used to measure the amount of chips required for packing (Fraser 1938)

The mechanised version of this technique is the hand held stone blowing machine and the pnuematic ballast injection machine. This technique was found to be much superior to beater packing or ‘tamping’ and it superseeded beater packing completely on British rail (Cope 1993, Fraser 1938). Although not without difficulty, the time shovel packing was introduced it was not taken favourably by some engineers in Britain and Tazwell (1928) argues that beater packing is the best way to maintain ballasted track and he was confident that ‘it will not be replaced by an inferior method like shovel packing’. It is interesting to note that Tazwell mentions that shovel packing has evolved from ‘fly packing’ which he says is ‘an old fashioned method, used on old longitudinal timber lines with continuous bearing’. Shovel packing did provide a more durable track top, the frequency of maintenance required was reduced and beater packing was superseded. It has been recorded that track aligned by measured shovel packing stood for six years without requirements of further packing (Coombs 1971). Measured shovel packing was not considered suitable for

lifts higher than 50mm and Hamnett (1943) mentions that track requiring more than 50mm of lift will require further packing in 2-3 months time. Mc Dougal (1931) has noted that there was increased occurrence of broken plates on track since shovel packing was introduced for maintenance, this is due to increased stiffness of the track due to the introduction of smaller stone below the sleepers and due to the fact that the sleeper is better supported when measured shovel packing is used to pack loose sleepers.

Fraser (1938) favouring the measured shovel packing process has made an interesting comment on the term 'resilient track' suggesting that the railway track once consolidated is a rigid mat and the resilience arises from other elements of the track i.e. sleepers, rail and the pad. Also it should be noted that there is a mention of a plant similar to hand held stone blowing machine being used in America in 1909 (Tratman 1909, p365), in which compressed air was used to blow stone chips 18-20mm size into the void below the sleeper, again this was considered a better technique than beater packing and Tratman mentions that this technique will "do away with tamping which necessarily disturbs the old bed of tie to some extent".

2.6.3 Mechanised tamping

Mechanised tamping has evolved from the beater packing into two forms

1. Use of hand held tamping tools.
2. Use of fully mechanised automatic tamping machines.

2.6.3.1 Use of hand held tamping tools

These electrically powered tools like the 'Kango' hammer have taken the place of the manual beater type tool used earlier (Cope 1993, p531). These are used in much the same way as the beater pick with a pair of hammers being used either side of the sleeper to

be packed. The user of the hammer with experience is able to sense when adequate consolidation of the ballast has been achieved. Care has to be taken to prevent excessive crushing of the ballast or damage to the sleeper undersides. The ballast should be free from fine material otherwise the hammers will not be effective in packing as the fine material would flow around the vibrating hammer (Cope and Ellis 2001, p233). This technique although useful for localised maintenance and around switches and crossings is unsuitable for use on wet spots as it could aggravate the problem of wet spots by creating holes in the ballast, allowing water to pond (Cope 1993, p531).

2.6.3.2 Use of fully mechanised automatic tamping machines

The principal maintenance machine in general use from the 1960's to date is the on-track tamping machine and although stoneblowers were introduced in 1997 tamping still remains the mainstay of track maintenance operations in Britain. The objective of tamping is to improve the vertical and horizontal geometry of track with the minimum amount of disturbance and the minimum use of ballast (Cope and Ellis 2001, p255). Tamping is the process of lifting and laterally adjusting track to the desired geometry while rearranging the upper portion of the ballast layer to fill resulting voids under the sleepers (Selig and Waters 1994, p8.1), it is thus a mechanisation of the beater packing process. When the sleepers are lifted, vibrating tamping tines are introduced into the ballast on both sides of the sleeper, the vibration easing the entry of the tamping tines. The vibration frequency is chosen so as to fluidise the ballast, which then is compacted inwards and upwards towards the bottom of the sleeper (See figure 2.25). The modern tamping machines carry out their operations without the machine coming to rest within the cycles and working rates achieved by the modern tamper are more than 1200m per hour (Cope and Ellis 2001, p255). Figure 2.26 and 2.27 shows details of tamping tines.

Due to the vibrating action of the tamping tines the best results for tamping are achieved on a 'good' track, which is not fouled (Selig and Waters 1994). The ballast should be single graded stone for optimum performance of the tamping machine (Selig 1998) and it is difficult to tamp ballast size smaller than 37mm (Wood 2002).

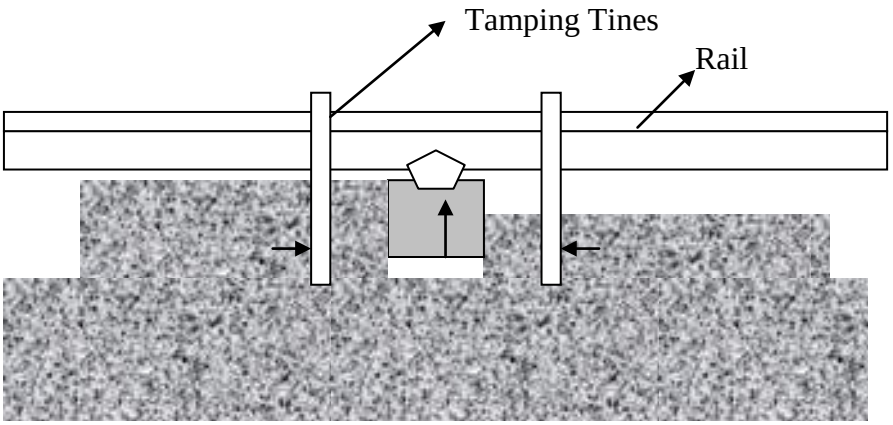

Fig. 2.25 Schematic diagram showing tamping operation

Figure 2.26 A close up view of on track tamping machine showing the tamping tines.

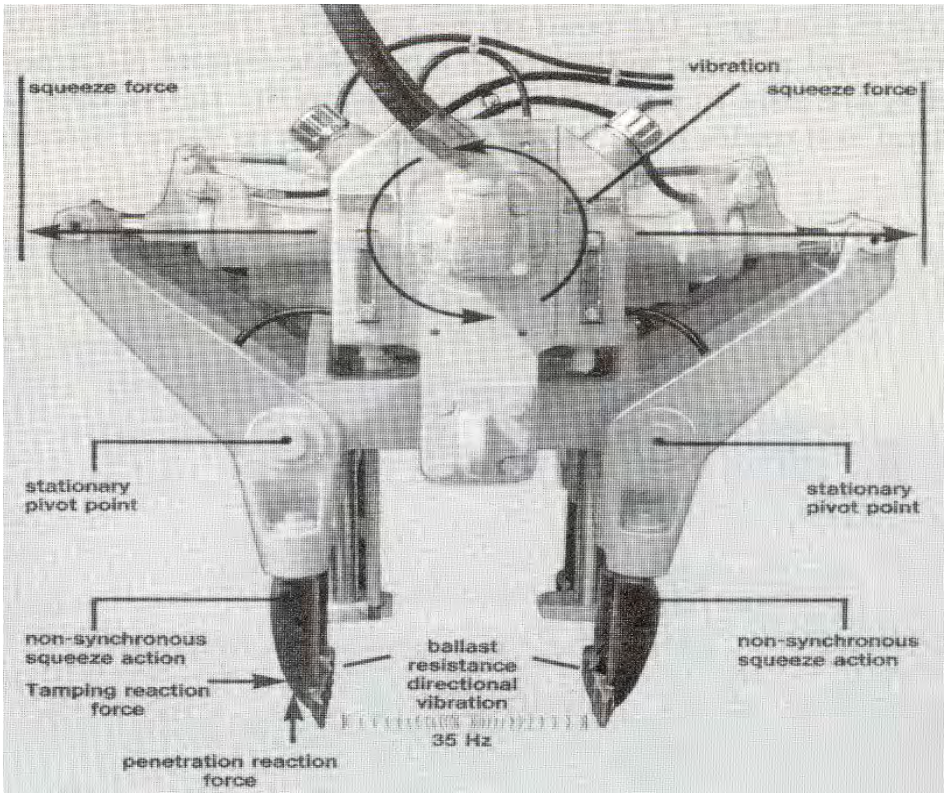

Figure 2.27 Tamping tines attached to a power unit (Selig and Waters 1994)

This is because the vibration frequency and the shape of the tamping tines is designed such that stones smaller than 37mm size cannot be compacted and will flow around the tamping tines (Wood 2002). Graded ballast if vibrated to make it fluid will cause segregation of ballast with the smaller particles moving towards the subgrade.

The tamping process although quick does not produce a durable track geometry. The tampers disturb the compacted ballast beneath the sleepers and vertical track geometry deteriorates rapidly after tamping. The resultant track profile after tamping rapidly assumes its original pretamp condition, a phenomenon known as ballast memory. Also the tamping process damages the ballast and each tamping cycle produces substantial amount of dust, thus repeated tamping of the track hastens track renewal as the track becomes fouled (See Fig. 2.28 and 2.29). Selig and Waters (1994) through laboratory box tests have also demonstrated that locked in horizontal stresses develop in ballast due to long term vertical

loading and these locked in stresses help stabilize the ballast against movement. Tamping disturbs these residual stresses and results in increased settlement.

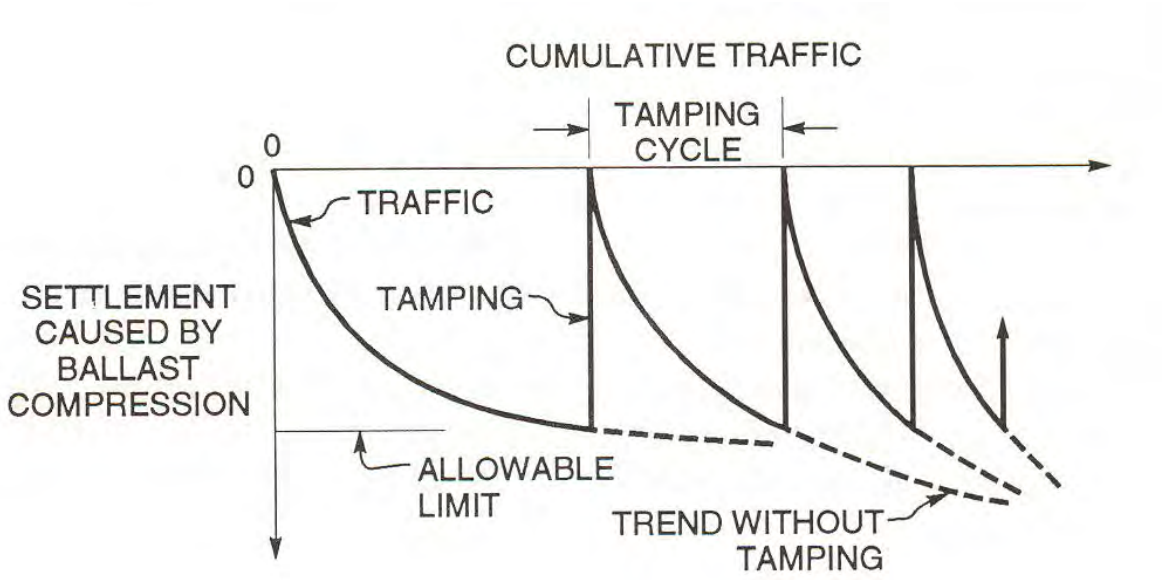

Figure 2.28 Effect of progressive fouling on length of tamping cycle (Selig and Waters 1994)

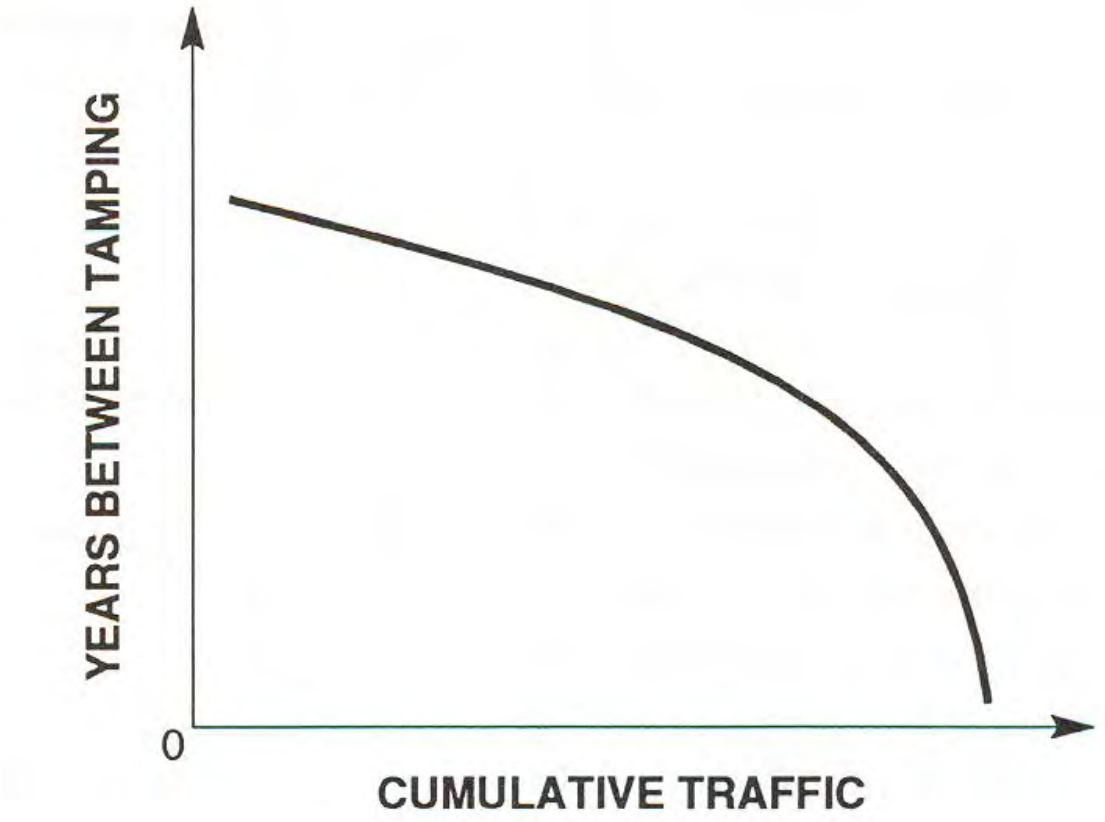

Figure 2.29 Progressive decrease in time between tamping (Selig and Waters 1994)

Selig attributes the lack of durability of track geometry of tamped track to lift/settlement relationship, also known as ballast memory (Selig and Waters 1994, p15.16). For low lifts given by tamping the track reverts back to its original profile repeatedly after each tamping, thus there is not change to the track inherent profile. For lifts greater than 25mm a lasting improvement in the track inherent profile is achieved. An explanation of this phenomenon is given by Selig & Waters (1994, p15.16). It has been observed that for low tamping lifts the ballast below the sleepers is squeezed upwards and dilates into the void between the sleeper and the ballast surface. As the lift is small on contacting the underside of the sleeper further deformation of ballast cannot take place and thus arrangement of ballast particles within the ballast is unchanged. The passage of traffic re-compacts the ballast and the particles adopt their original position with respect to each other and thus the track assumes it original pretamp shape. A solution to this problem as suggested by Selig and Waters is high lift tamping. In high lift tamping the ballast will have

sufficient room for maximum ballast dilation and rearrangement of particles will take place with new particles being absorbed into the skeleton. Re-compaction of this new ballast skeleton by traffic will introduce a new geometry to the track. It is claimed that high lift tamping can produce three times greater track durability compared to when low lifts are given to track although limited head room and shortage of crib ballast may inhibit use of high lift tamping process. Also after high lift tamping ballast consolidation is required before traffic can be run at normal speeds. Mc Michael et al have said that this process is of limited value to British Rail because of limited headroom available on majority of British Railway track (Mc Michael and Strange 1992).

Ball (2003) has analysed the pre-maintenance vertical standard deviation of track (prior to tamping) and post-maintenance vertical standard deviation of track achieved by tamping. According to Ball tamping machines are not able to implement their vertical design effectively. The standard deviation data is supplied to the tamper via its own 'Automatic Track Top Alignment' (ATTA) design system. The tamping machine makes a design run on the section of track to be corrected collecting track geometry data, which is processed by the on-board computer using the ATTA to produce a design alignment. This data then is supplied to the machine for its implementation run and at the end of the implementation run the machine provides data of standard deviation measured after the work. Ball has compared data from 150 tamping shifts and has produced graphs showing design vertical standard deviation values (compiled after the design run) and implemented values (compiled after the implementation run). The graphs are shown in figure 2.30

The graphs show that for vertical standard deviation the tamper is unable to implement its own design profile on the track. For a pre treatment standard deviation of 4mm the design standard deviation designed by the ATTA was 0.9mm but the tamper could implement a standard deviation of 2.6mm. Ball attributes this phenomenon to the fact that tampers disturb the ballast below the sleepers and the ballast tends to sink back to its original position. When the raised track is lowered back onto the ballast bed the self-weight of the track is sufficient to cause the ballast to settle by some amount and thus design lift of the track is never achieved. Due to the size of the ballast (50mm) any small lifts given to

the track are unsuccessful as the ballast structure after tamping is not altered and the large particles settle back to their original position even under small loads.

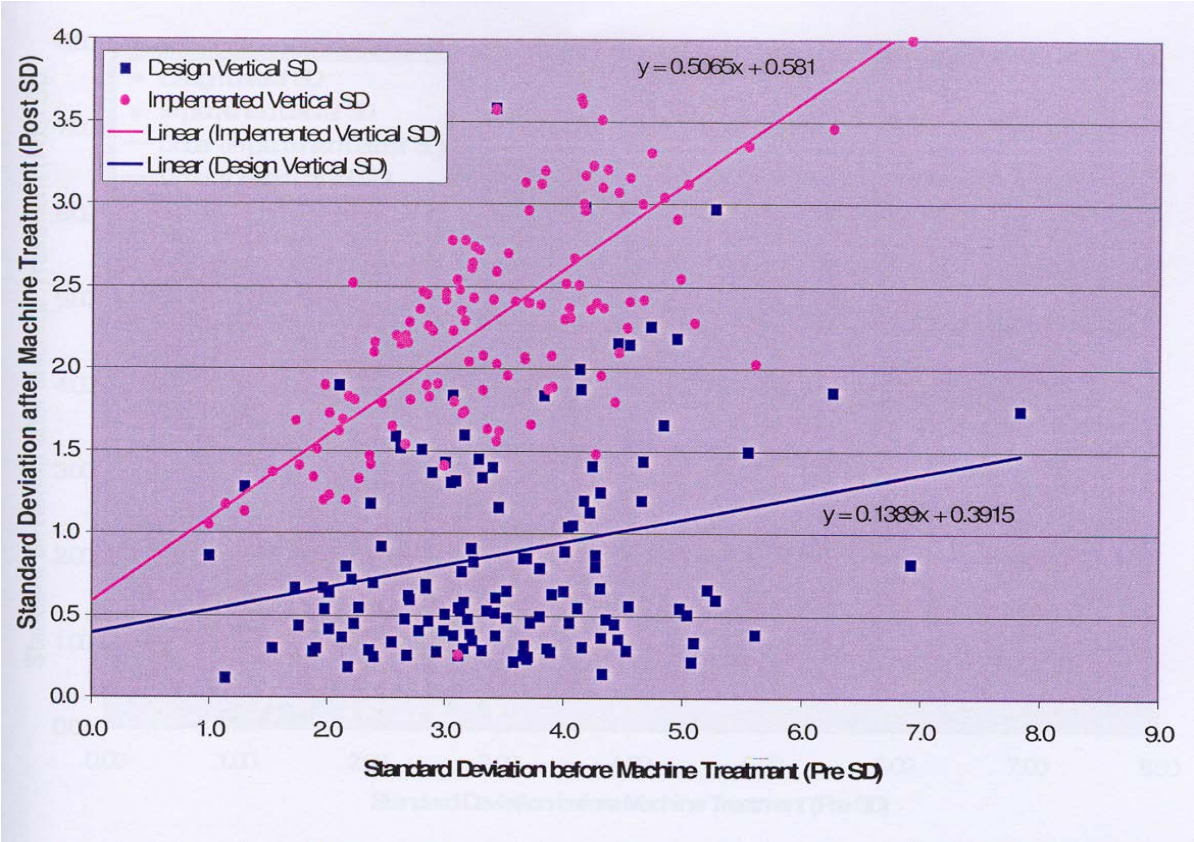

Figure 2.30 Tamper design standard deviation and implemented standard deviation (Ball 2003).

Ball has also compared the standard deviation measured by the ATTA of the tamping machine and the HSTRC. This was done because although the ATTA measures the standard deviation implemented by the tamper in its implementation run this data is not considered definitive and the HSTRC data is used to measure the track geometry, the results of which are used to classify the track in quality bands e.g. good or poor. Ideally the track geometry measurements over a piece of track by the ATTA of the tamper or the HSTRC should be the same if the HSTRC measurements are carried out within a month of the tamping work. Ball has demonstrated that track quality measured for the same piece of

track by the HSTRC is different than that measured by the ATTA of the tamper (See figure 2.31), although the difference measurements by the ATTA are fairly close to that of the HSTRC.

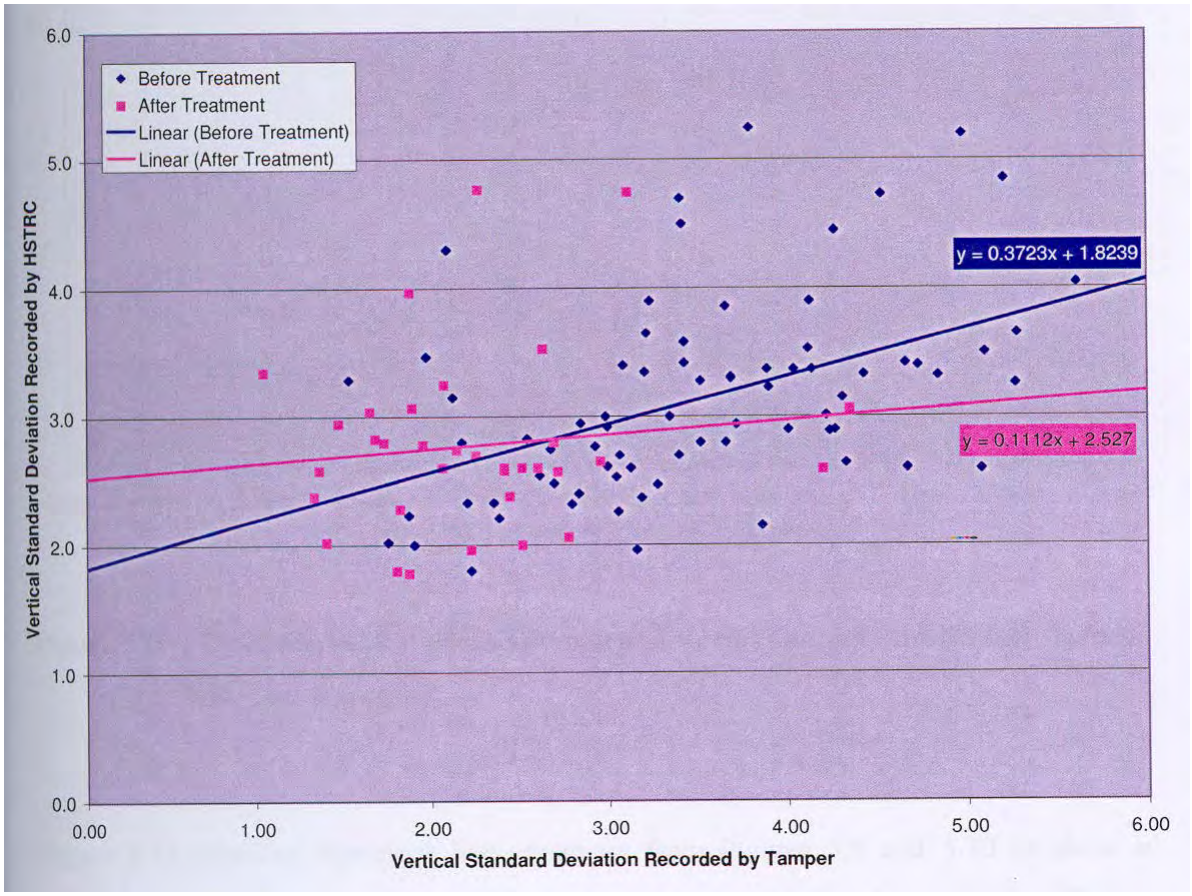

Figure 2.31 Comparision of vertical Standard deviation recorded by the tamper and the HSTRC before and after treatment (Ball 2003).

Ball has also studied track deterioration following tamping by analysing standard deviation data from the HSTRC measured at intervals of 1 month, 3 months, 6months and

12 months after tamping (See figure 2.32). Ball concludes that tamping has little effect on track quality if carried out on track with standard deviation values between 2.2-3mm but below these values the track quality worsens after tamping. Tamping is effective when implemented in track with standard deviation values above 3.0mm.

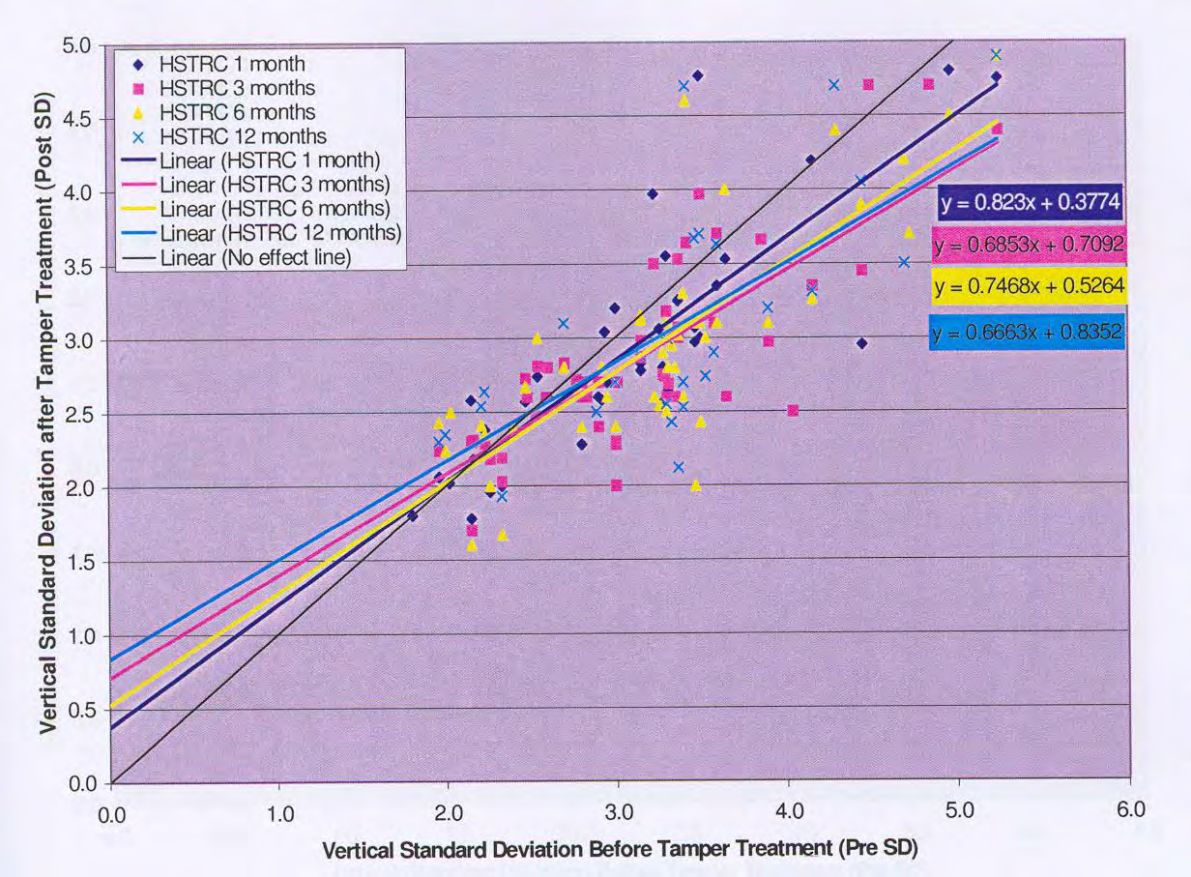

Figure 2.32 Vertical standard deviation recorded by the HSTRC 1, 3, 6, 12 months after tamper treatment of the track (Ball 2003).

Selig and Waters (1994, p8.2) have studied the particle breakage caused by the tamping process by carrying out laboratory tests on a sleeper section in a ballast box. Track tamping was simulated by rearranging particles in the box after 100,000 cycles and running further load cycles on the ballast. This doubled the particle breakage when compared to tests on ballast with no disturbance. It should be noted that breakage from the tamping action itself was not taken into account in this study. The reason as put forward by Selig and Waters is that with particle rearrangement in the ballast new particle contact points are established after tamping and this causes additional breakage under traffic. British Railways have estimated the contribution of each source of ballast fouling to a fully fouled ballast. Fully fouled ballast was defined as when 30% of the total sample by weight consists of particles less than 14mm in size. A representative estimate is shown in table2.3 (Selig and Waters 1994, p8.27).

British Railway Sources of Fouling (Selig and Waters 1994)			
No.	Source	Kg/Sleeper	% of total
1.	Delivered with ballast	29	7
2.	Tamping: 7 insertions during renewals and 1tamp/yr for 15 years at 4 kg/tamp	88	20
3.	Attrition from various causes	90	21
4.	External input - Wagon spillage, airborne dirt etc.	225	52
	Total	432	100

Table 2.3 British Railways sources of fouling (Selig and Waters 1994)

Thus tamping contribution to fouling is comparable to contribution due to attrition caused by traffic loading etc. It has been observed by British Rail that ballast particles remaining after removal of fouled ballast are still sharp and angular after 15 years in service (Selig and Waters 1994, p8.27). Thus wearing of the particles is not the main source of fouling on British Rail. The above table assumes a single tamp per year for maintenance while Ball (2003) in preparing his estimate of contribution of various fouling sources to ballast fouling has assumed two tamping runs per year on the track and his findings are slightly different. These are given in table 2.4 and Figure 2.33.

Source of ballast contamination	Amount of fines generated
Mechanical Maintenance	4kg fines/tamp/sleeper
Wagon Spillage (e.g. near quarrries)	4kg fines/m^2/year
Air borne fines	0.8 kg/m^2/year
Traffic loading	0.2 kg/sleeper/million tons of traffic

Table 2.4 Ballast contamination on British Railways (Ball 2003)

Ball argues that as each ballast bed between sleepers is approximately $1m^2$ and assuming two tamping runs per year the fines generated by tamping are 61% of the total fines generated. A pie chart describes the % contribution of each source. A similar pie chart (Figure 2.34) given by Mc Michael and Strange (1992) gives contribution of fouling due to tamping at 53% thus estimate by Ball and Mc Michael and Strange is fairly similar. The reason these estimates differ from Selig and Waters is because Selig and Waters have made a conservative estimate of a single tamping run per year.

In a study conducted in a track laboratory at British Rail it was observed that 2-4 kg of material less than 14mm in size was generated per tamp for a single sleeper i.e. single insertion of the tamping tie. The ballast degradation was actually much greater as the sizes larger than 14mm were excluded from measurement. In one field investigation carried out by British Rail ballast breakage was measured after 20 consecutive tine insertions with a tamping machine. It was observed that there was 15%-45% reduction in the 38-51mm size particles.

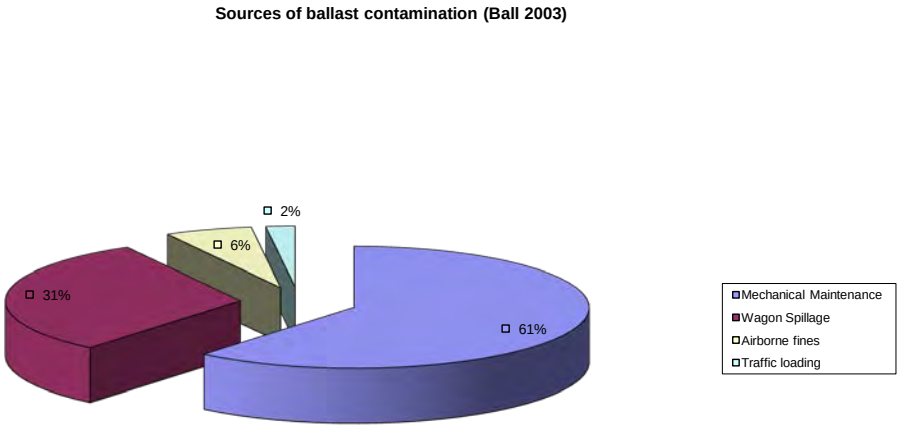

Figure 2.33 Track fouling on British Railways (Ball 2003)

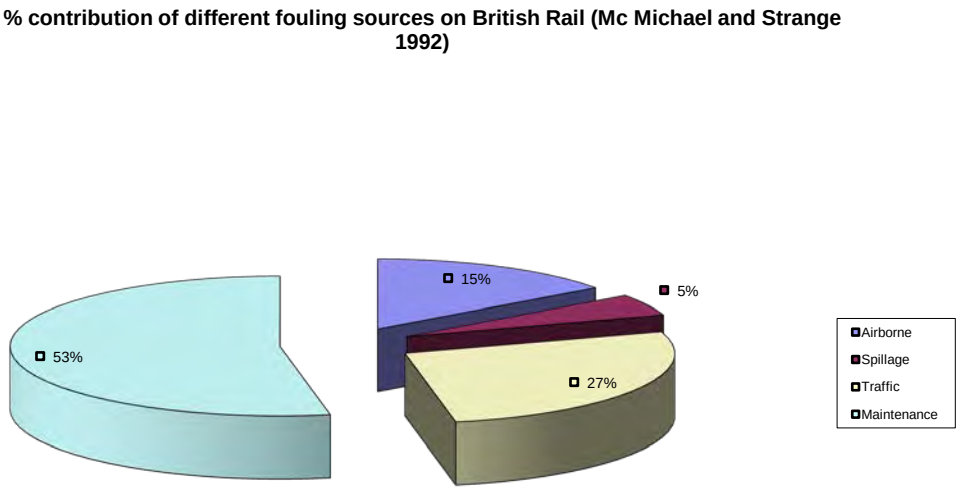

Figure 2.34 Track fouling on British Railways (Mc Michael and Strange 1992)

Thus it should be noted that although tamping is the mechanisation of the beater packing process the drawbacks of beater packing have also been taken on board in tamping. The drawbacks of beater packing were:

1. Ballast breakage due to beater packing.
2. Shortlived track geometry improvement after maintenance.

These are still present with the tamping process, the only improvement above the manual beater packing technique is the uniformity of packing and the speed of operation achieved by mechanisation of the process. Ball (2003) also noted that in the U.K. the situation is made worse by over-tamping to meet productivity targets.

2.6.4 Pnuematic ballast injection machines (Stoneblowers)

Given the inherent shortcomings in the tamping process, pneumatic ballast injection machines (stone blowers) were developed in the U.K. as a mechanisation of the measured shovel packing process. These again can be classified into

2.6.4.1 Hand held stone blowing machines

Hand held stone blowing machines provide a degree of mechanisation of the measured shovel packing process. Figure 2.35 shows a schematic diagram of the working of the pneumatic ballast injection machines. Although the equipment needs to be operated manually there is no need to clear the crib ballast before packing as stones are introduced below the sleepers through tubes inserted adjacent to the sleeper and compressed air is used to blow stone chips in the void below the sleeper. One important difference is the size of stone chips used for the packing process. Measured shovel packing is carried out using stone chips of the size 5-10mm while the hand held stone blowing machines utilise 20mm – 14mm size of stone. Hand held stone blowers are useful to maintain track between operations of the on-track maintenance machines. Figure 2.36 shows the operation of a Hand held stone blowing machine.

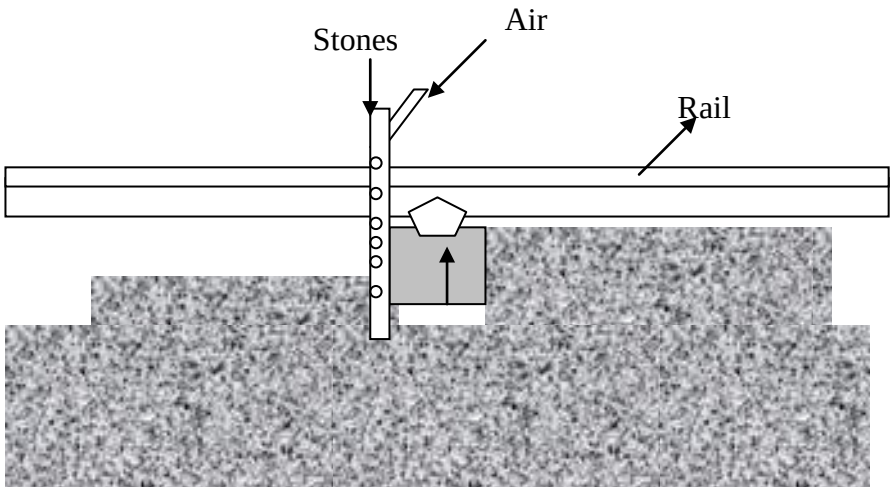

Fig. 2.35 Schematic diagram showing operation of pnuematic ballast injection machines

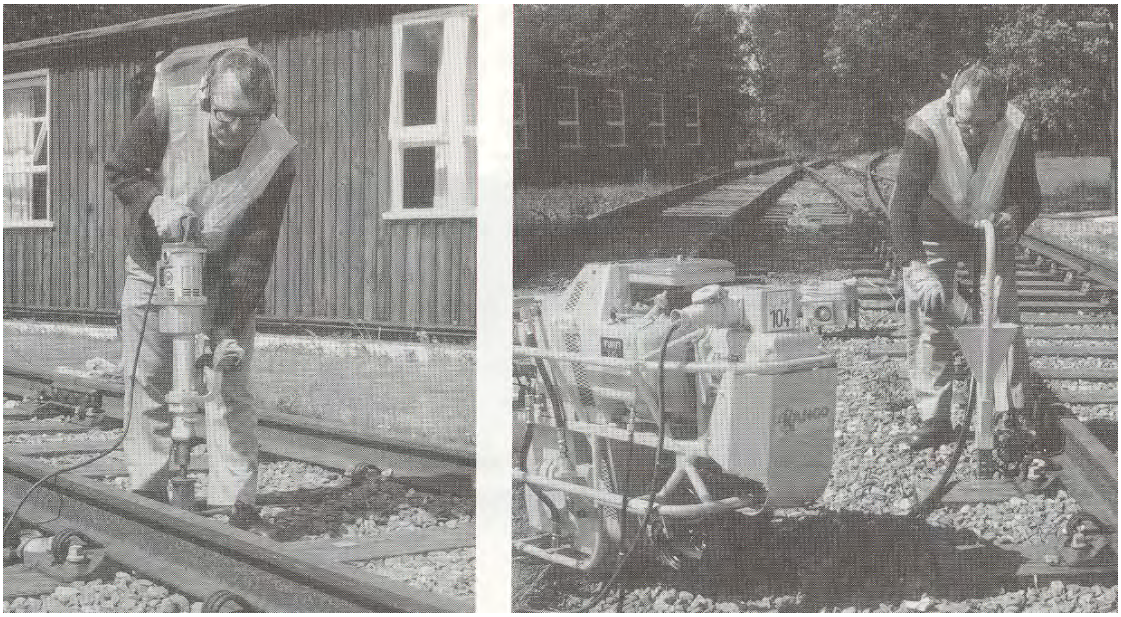

Figure 2.36 Hand held stoneblowing process in operation – In the left the operator is inserting the stoneblowing tubes next to the sleeper and in the right picture stones are being blown under the sleeper (Selig and Waters 1994)

2.6.4.2 Mechanised pneumatic ballast injection machines

Stone blowers are now widely used on British Railway after initial experimental trials were successful in the early 1990's. Figure 2.37 shows a stoneblowing machine and Figure 2.38 shows a closeup photograph of the pipes used to blow stones under the sleepers.

Figure 2.37 Stoneblowing machine


Figure 2.38 Close-up photograph showing the tubes used for blowing stones under the sleepers

Stone blowers use compressed air to blow 20mm stone under the sleeper creating a compact bed under the sleeper. The process takes advantage of the already compacted ballast bed below the sleepers instead of disturbing it as in the tamping process. The durability of the track profile thus achieved is much higher but then the process is not effective on track where the track ballast is new or has been disturbed by the tamping process. Cope (1993, p537) mentions track top durabilities 8 times better than tamping have been recorded with an average figure of 3. Thus fewer stoneblowers are required to maintain a length of track than tampers leading to savings in capital expenditure, machine maintenance, manpower and track possessions. The other advantage is that it is possible to maintain track, which is sub-standard (slurried, wet spots) or even tracks with ash ballast (Cope 1993 - p537, Cope and Ellis 2001 – p260). The stoneblowing stone is placed in position of maximum ballast stress but it has been observed that the stone does not break under traffic (Coenraad 2001). As the stoneblowing stone is of size smaller than the standard ballast more contact points are developed under the sleeper to allow better load distribution, thus ballast breakage is reduced. Coenraad (2001) has noted that contrary to the view that stoneblowing stone impedes track drainage it actually helps improve drainage because it reduces or eliminates the vertical pumping action of the sleeper.

Although all authors are of the opinion that the stone blowing process is advantageous compared to tamping, the process is looked at with some scepticism by railway engineers. One reason is that the track just after stoneblowing looks worse than it was prior to stoneblowing (Ball 2003), which is due to the ‘design overlift’ given to the track during stoneblowing. During the stoneblowing process the track has to be raised to the level required for correcting vertical geometry plus an extra 45mm to enable blowing of stones under the sleepers. This extra 45mm is called the ‘design overlift’ although the term is confusing as it is not the same as high lift tamping. When raising the track the amount of stones blown under the track is calculated based on height gain required for track geometry correction, the stones are not blown in to achieve an extra uplift of 45mm above that required for geometry correction. The extra uplift is to ease the blowing stones under the sleepers. The track after stoneblowing is lowered back onto the new bed of stones blown under the sleepers but the track does not settle through all of its 45mm uplift. It requires

50,000 tonnes of traffic to bring the track down to the design level, designed for correcting the track geometry faults (Cope and Ellis 2001, p261). Thus immediately after stoneblowing the track profile appears sometimes to be worse than what it was before stoneblowing but after the design overlift has been ‘run down’ the track quality usually falls under the satisfactory band and keeps on improving for passage of a further 250,000 tonnes of traffic. Track deteriorates after passage of 300,000 tonnes of traffic after stoneblowing but the rate of deterioration is less compared to that of the tamper.

The stoneblowing machine has its own on board computer system to design the corrected track profile. The stoneblower, like the tamper, carries out a measurement run to gather data for designing the track profile and implements the design in the subsequent run on the track but the design program used in the stoneblower is different from the programs in the ATTA (tampers) and the HSTRC. Ball (2003) has given comparison of vertical track standard deviation measured by the stoneblower and the HSTRC. The results are startling because the existing track pre-maintenance vertical standard deviation measured by the stoneblower is more than that measured by the HSTRC and post maintenance standard deviation for stoneblower is less than that measured by the HSTRC (see figure 2.39). E.g. for a stoneblower measured standard deviation of 3.0mm the HSTRC measured standard deviation pre-treatment is 2.5 mm and post treatment is 4.7mm.

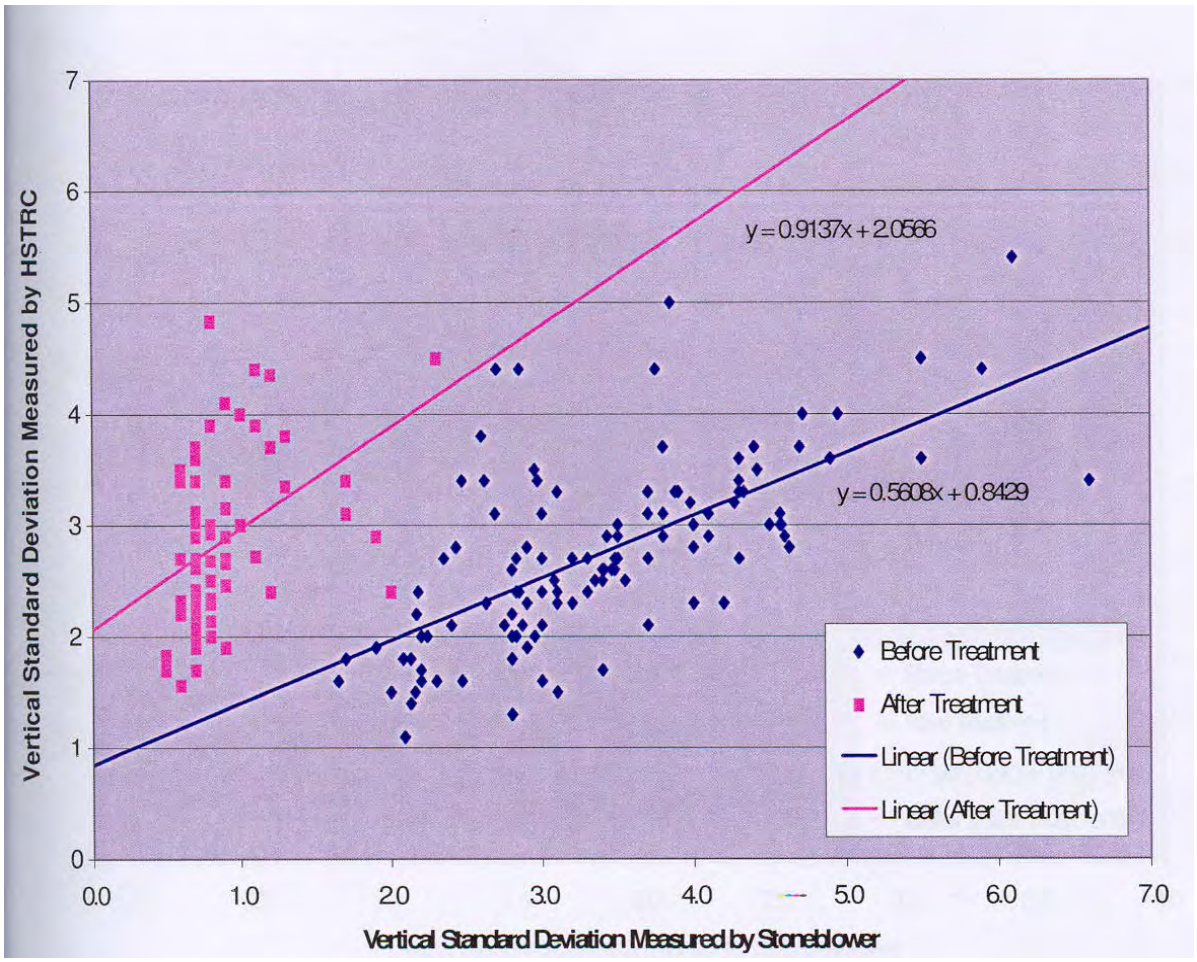

Figure 2.39 Comparison of Standard Deviation data as measured by stoneblower and HSTRC before and after treatment (Ball 2003).

Considering the HSTRC standard deviation values post treatment the track quality instead of improving has become worse. This is explained by the fact that stoneblowing requires 50,000 tonnes of traffic to 'run down' the design overlift and the track geometry appears worse than pre-maintenance immediately after stoneblowing. Ball (2003) has taken HSTRC values 1 month after stoneblowing was carried out on the track. Also the stoneblower does not carry out standard deviation measurements after the design implementation run, thus it assumes that the design has been successfully implemented on the track. While the implemented design is achieved only after the traffic has compacted the design overlift. Ball has also analysed data from HSTRC recordings of a track which

has been stoneblown at the intervals of 1month, 3 months, 6 months and 12 months after stoneblowing (See figure 2.40).

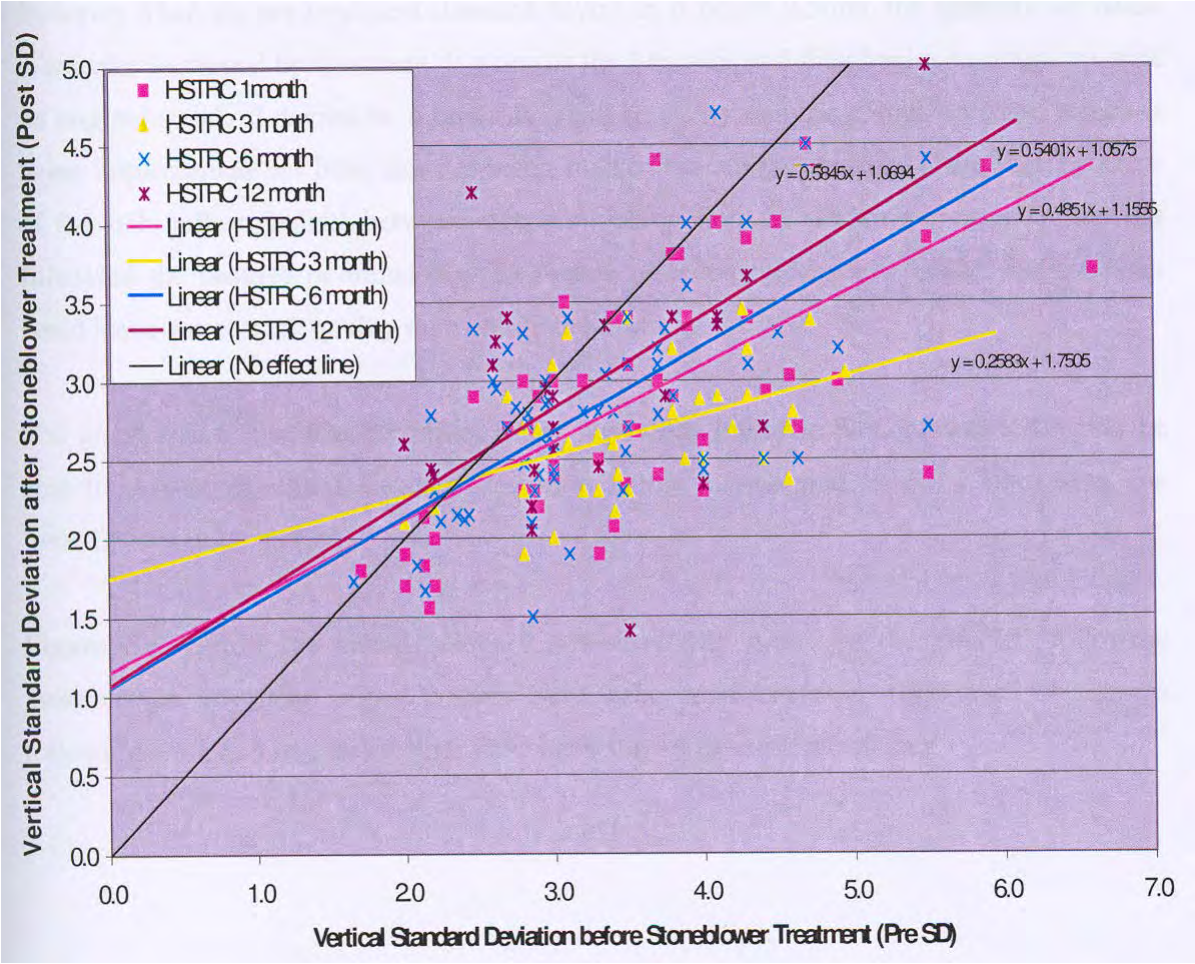

Figure 2.40 Vertical Standard Deviation as recorded by the HSTRC at 1, 3, 6, 12 months after stoneblower treatment.

Ball concludes that for vertical standard deviations above 2.5 mm stoneblowing can achieve improvement in track geometry. For the first 3months the track geometry keeps improving as the design overlift is 'run down'. Then the deterioration begins at six month after stoneblowing but even after a period of 12 months the track vertical standard deviation is better than it was premaintenance. However when the pre treatment vertical standard deviation is below 2.5 mm the track quality worsens after stoneblowing. This implies that stoneblowing should not be implemented on track which is already classified as good track.

Stoneblowing is effectively a mechanisation of the measured shovel packing process but measured shovel packing was carried out using 5-10mm stone chips the stone blower uses 20mm hard angular stone. Private communication with engineers involved in development of the stone blower has revealed that initial trials of the stone blower were carried out using 5-10mm stone chips similar to the measured shovel packing procedure (Strange 2003). It was found that using 5-10 mm chips did give a good packing under sleeper and results similar to measured shovel packing. There were various reasons for abandoning 5-10mm size in favour of larger stone (20mm) but one of the reasons is to allow for tamping of stone blown track if required. As mentioned earlier it is not possible to tamp smaller particles in ballast. Thus it would not have been possible to tamp a piece of track with 5-10mm size stones just under the sleeper, so a compromise solution seems to be the 20mm stone which would allow for tamping of a piece of stone blown track if required (Strange 2003). Although current practice on British Rail is not to tamp a track which has been stoneblown because tamping of track maintained by a stoneblower defeats the purpose of stoneblowing (Cope and Ellis 2001, p260).

Extended trials with the stoneblower on the East Coast Mainline have produced good results and track maintenance costs have been reduced (Anderson et al 2002). There have been two observations on the performance of the stoneblowing process:

- To achieve any significant track quality improvement when using the stoneblower a minimum of 4tonnes/km of stone must be used.
- Excessive lifts when using the stoneblower should be avoided because when the layer thickness of the stones blown below the sleeper is greater than 20mm (size of the stone) the long term settlement of the track may be greater (Anderson and Key 2000). Thus to avoid excessive uplifts stone usage should be restricted to a maximum of 10tonnes/km. Anderson (Anderson et al 2002) has suggested that in such cases maintenance should be carried out by further stoneblowing after the 20mm stone has densified, this is an approach similar to that used by early railway engineers when dealing with high uplifts with measured shovel packing. It is

interesting to note that Anderson has suggested use of either tamping or further stoneblowing in such cases, which he mentions is a matter of debate in the railway industry.

Stoneblower causes less damage to ballast compared to tamping and a comparitive graph of fines created by stoneblower and tamper per 10 maintenance cycles is given below in figure 2.41 (Harsco 1997). Thus stoneblower does give a better track maintenance solution than a tamping machine but its use is not as widespread in the Railway track maintenance regime in the U.K. as one would expect. Tampers still continue to be the mainstay of all maintenance operations in the U.K. with Railtrack prohibiting use of the stoneblower on the East Coast mainline, preferring to use the tampers for track maintenance (Ball 2003). At a few seminars and conferences which the author had the opportunity to attend during the course of his research there was evident 'hostility' in the Railway Engineering fraternity towards the introduction of the stoneblower for track maintenance and the main concern of the engineers was the possibility of reduction in track drainage properties due to stoneblowing. To date none of the literature on track drainage suggests that an increase in smaller size stone particles in the ballast matrix of size 5-20mm will hamper drainage. Instead Selig et al have suggested that even track fouled with sand particles and gravel (<6mm in size) will provide adequate drainage (Selig and Waters 1994). Measured shovel packing in the 70's was carried out using stone ships of size 5-12mm, at a time when maximum train speeds were up to 125 mph and axle loads were comparable to present day axle loads on British Rail. This is not mentioned in any literature as being detrimental to track drainage in any way. Experience with sand ballast suggests that clean sand ballast provides for good track drainage (Tratman 1909, p30). As mentioned earlier more than 50% of the fouling on track on British Railways is on account of tamping and repeated tamping reduces ballast to dust. Thus if tamping was to be replaced by stoneblowing as a maintenance tool track fouling would be dramatically reduced increasing ballast life, potentially saving millions to be spent on track renewals.

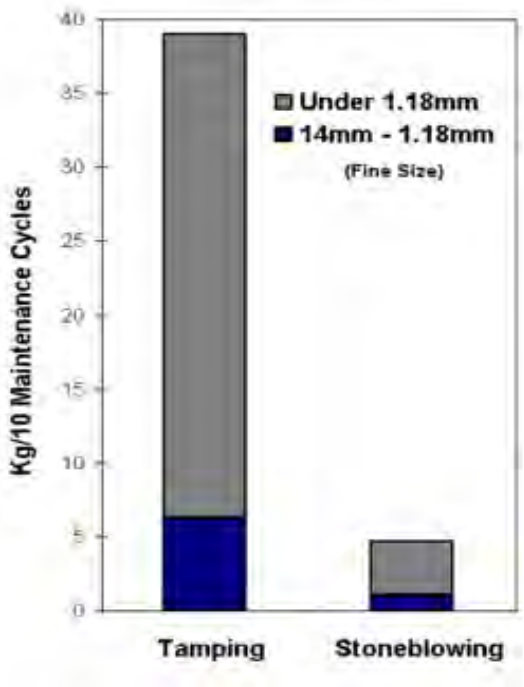

Figure 2.41 Comparision of fouling by tamping and stoneblowing (Harsco track technologies 1997)

2.6.5 Dynamic track stabilizer and crib and shoulder surface compactor:

As discussed earlier tamping disturbs and loosens the ballast below the sleepers and the shoulder and crib ballast. Subsequent traffic would compact the bottom ballast and during this process lateral stability would also be regained but in most cases speed restrictions would have to be imposed and there would be a loss of track geometry (Selig and Waters 1994, p8.2). Dynamic track stabilisers are used to follow the tamping and lining work to consolidate ballast below and around the sleepers (See Figure 2.42). This helps the track to regain its lateral stability (Cope and Ellis 2001, p261).

Figure 2.42 Close-up view of dynamic track stabilizer unit (Cope and Ellis 2001)

Dynamic track stabilizers apply a static vertical load and vibration to the track in horizontal and vertical directions which causes the ballast to fluidise and assume a 'least volume state' (Cope and Ellis 2001, p261). Selig and Waters (1994, p14.16) report that about half the loss in lateral resistance from tamping is regained by the application of the track stabilizer and as per Cope (Cope and Ellis 2001, p261) optimum application of the DTS will cause a track recently lifted, to settle by 50% of the amount of lift applied. Machines can control the amount of settlement given to the track by adjusting the degree of consolidation produced in the ballast (Cope and Ellis 2001, p261). The use of DTS is not recommended in conjunction with the use of the stoneblowers as it could disturb the smaller stone blown in by the stoneblower and cause loss in height achieved by packing (Cope and Ellis 2001, p261).

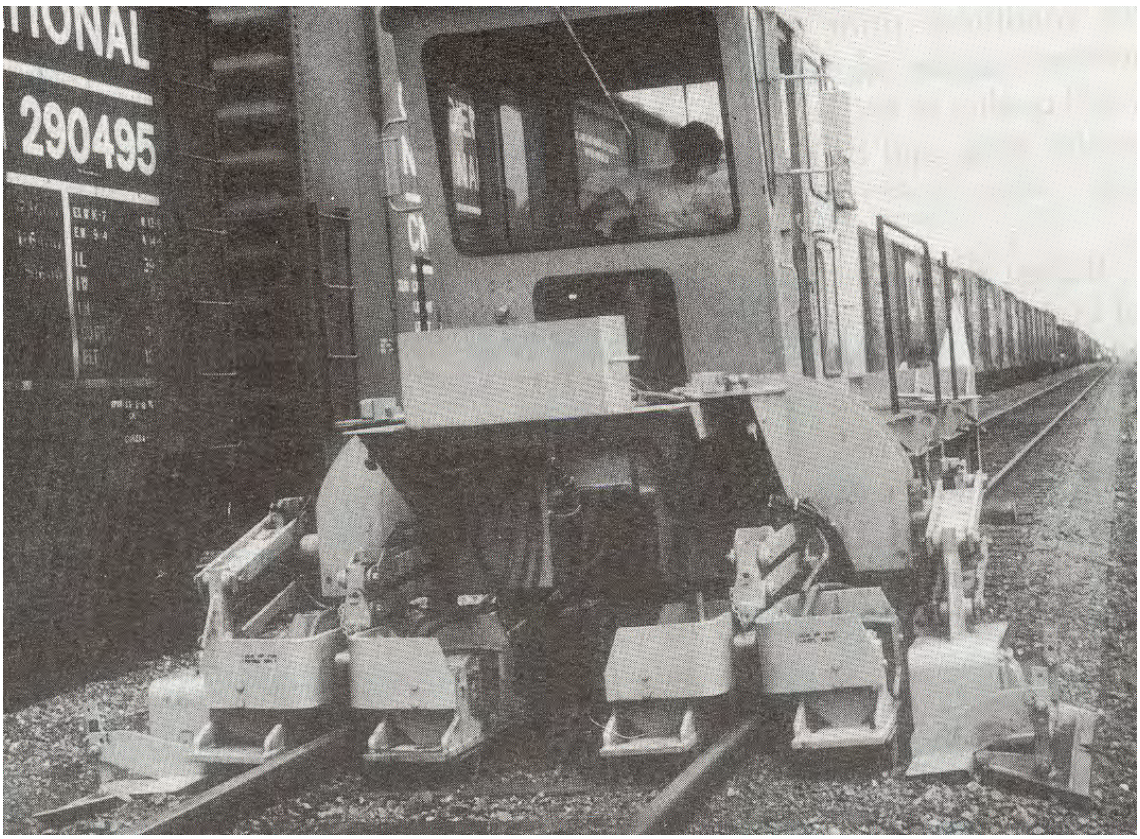

Figure 2.43 Crib and shoulder ballast compactor (Selig and Waters 1994)

Crib and shoulder ballast compacters are used to compact the crib and shoulder ballast by applying a vertical vibratory force to the ballast. The cribs are vibrated in the zone where tamping tines have disturbed the ballast (Selig and Waters 1994, p14.16). Selig reports that a vibration of 2-4 seconds seems to produce optimum performance of the available compacting machines. The compactor helps achieve track lateral resistance subsequent to tamping and retains the tamped geometry for a longer time after tamping as compared to a track not compacted after tamping.

2.7 Ballast specification – a historical perspective and present problems

2.7.1 Ballast Material.

In the early railways easy availability and cost were the two most important factors considered for selection of ballast materials. Any locally available and cheap material was used as ballast. By early 1900's permanent way engineers understood the importance of ballast and its functions with regards to stress distribution to subgrade and drainage. Tratman (1909) has stated that "ballast is a most important item in securing good track, with economy in maintenance and operation." He recommends the use of hard and tough rock for ballast. In literature from the U.K. from early 1900's it is accepted that hard angular stone is the best ballasting material. But various other materials were accepted for use as ballast, the reason could be the great difficulty encountered in trying to transport large quantities of stone to all various locations where track was being constructed. In Britain with no stone quarries in the Southeast it would have been virtually impossible to transport huge amounts of stone from the north without the railway being in existence. Ball (2003) has made an interesting comment that ' track has been for longer on non-stone ballast than on stone ballast' as the first passenger train was run in 1821 and stone ballast was not adopted on all track till the 1930's.

Some ingenuity was used in trying to adapt any locally available material as ballast. Tratman (1909, p30) mentions use of oyster shells as ballast on some lines along the coast in America. Otherwise ashes, sand, slag, broken bricks, clay, etc were used as ballast (Randall 1913, Tratman 1909, p30). Figure 2.44 shows track ballasted with 37.5mm (1.5 inch slag ballast) (Randell 1913). Ashes were considered good material for ballast as they were free draining and provided for good packing under the sleepers although they would disintegrate quickly under heavy loads (Hamnett 1964, p71). Ashes also provided a very silent track (Randall 1913). Even as late as 1922 90% of the mileage of the former North Eastern railway was ballasted with ash (Cope 1993). Ash was accepted as an alternative to stone ballast in "British Railway Track", published by the Permanent Way Institution till the 1971 edition but disappears from the list of acceptable materials for railway ballast in the 1979 edition. The author suggests that the main cause for this may simply have been the end of the supply of ash from steam locomotives, as these were phased out of use. Railway men working with ash used to consider ash as a good material for ballast as it was easy to handle and could be readily packed under the sleeper allowing for fine adjustments to track

vertical alignment (Wood 2002). One problem with ash ballast was that it was chemically harmful to wooden sleepers and track fittings (Randall 1913).

Another material used as ballast worth of note is sand (Tratman 1909 – p30, Arora and Saxena 1988 – p120, Randall 1913). Coarse sand was considered as good ballast for light traffic (Tratman 1909 – p30, Arora and Saxena 1988 – p120). The drawback of sand was that it was washed away by rain or drifted away by the wind. Sand was used on tracks in France and India covered with a layer of broken brick or stone to prevent it from washing or blowing away (Tratman 1909) and is still used on some tracks in India as reported by Arora et al (1988). Another means used in America for preventing sand from blowing was to apply a layer of crude oil on the sand, called as oiling of ballast. One notable advantage of sand ballasted track is that it gives a noiseless track. It has been the experience of the author while travelling on a train in the desert regions of India that sand blows off from the desert and enters the stone ballast in many locations. These tracks give a virtually noiseless ride to the trains. Contrary to what one would expect, Tratman (1909, p30) mentions that track drainage is not a problem with sand if it is clean. The British experience with sand was not successful and Randall (1913) mentions the problems with sand ballast in wet weather with the sand becoming spongy and in dry weather flying in all directions. It was difficult to maintain sand ballasted track as it was very difficult to pack the sand using a beater.

2.7.2 Ballast size

From all literature it is evident that ballast size is the most important quality of ballast influencing its performance under heavy loads and also influencing the way ballasted track can be maintained. Importance of having good quality hard stone with sharp edges as ballast was understood by Permanent Way Engineers by 1900's although specification for the stone was not very clear about size and quality. There is mention of an instance, by F.R. Conder in his book 'The men who built the railways' (1983, first

published in 1868), where specification for ballast stated that no bit of broken stone be used as ballast larger than a man could put in his mouth".

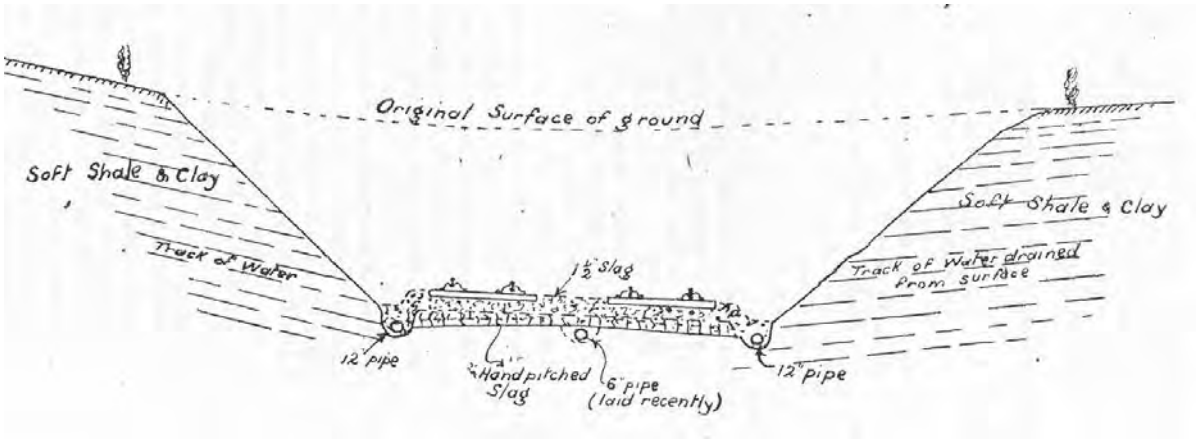

Figure 2.44 Figure showing track ballasted with 37.5mm (1.5 inch) slag ballast (Randell 1913)

A decision regarding the size of ballast was reached based on trial and error with different sizes over the years and it seems that selection was made based on the size, which would allow easy and efficient maintenance of the track. In the days when track was maintained by manual means ballast consisted of smaller stones but with introduction of mechanised on-track tamping machines ballast size has been increased to suit the tamping machines (Wood 2002). The main concern in the days of manual track maintenance was to

achieve fine adjustments to the track vertical alignment, for which ballast consisted of smaller stones (Ahlf 1992). Ballast in the U.S.A. in 1900's used to be smaller stones of size around 20mm and less but this soon was changed to stone size 50mm. Tratman (1909, p26) mentions that stone broken to a ¾ inch (20mm) size is less noisy, wears the ties less, can be tamped more easily and gives a better surface with less labour. Earliest reference, the author could obtain, from the U.K. in 1913 shows a track section ballasted with 37.5mm slag ballast, shown in figure 2.44 (Randall 1913). Another reference from 1928 mentions that 'stone ballast should be of size passing a ring of 50mm (2 inches) diameter however presented' (Tazewell 1928). Tazwell mentions that it was very expensive and difficult to get stone of such specification and he gives an example of a permanent way ballasted with 25mm size slag ballast and also an example of difficulty faced with maintaining a track with ballast larger than 75mm (3 inches). Another factor before railway nationalisation was that different companies used different specifications for the ballast and also different methods for maintenance. It is more likely that with a broad specification of stone passing a 50mm diameter ring with no limit on the minimum size, except 'not to contain small material than is made in the process of crushing (Tazwell 1928)', the ballast used in the early railways was stone of size 10mm to 25mm in size. In the book 'British Railway Track' edition 1943, Hamnett mentions that good qualities of ballast are

a. Good bearing capacity
b. Good drainage capacity
c. High frictional resistance to movement of sleepers
d. Suitability for packing.

It is then mentioned that the first three qualities would be fulfilled by a hard angular material, which will lock together and will not crush into dust. To satisfy the fourth requirement, of packing, the material should pass a 50mm (2inches) mesh sieve. This is the time when beater packing was the preferred means of maintenance for majority of the railway companies in the U.K. with measured shovel packing being used successfully on the LMS railway and was being introduced on other lines. Mechanically operated hand held tamping tools were also widely available during this time. In all subsequent editions until

1979 it is again mentioned that a size of 40-50mm for ballast facilitates packing. It must be noted that no minimum size for the stones has been specified and even in 1979 edition of the book ballast is specified as stone passing 40mm sieve and that a proportion of smaller material is desirable. Thus again it seems likely that ballast consisted of small size stones of average size 20mm to allow for effective maintenance of the track. In the book 'Track laying for underground haulage' published by the British Coal board (1973), ballast for a new track is specified as " the material should pass through 1.5inches (37.5mm) square or 2inches (50mm) round mesh and stand on 3/8 inches (9.5mm) square or ½ (12.5mm) inches round mesh. The coarser material is used for the initial layer of ballast and the finer for the final packing and lifting to grade. The author is of the opinion that the same philosophy was applied when ballasting railway track. Wood (2002) is of the opinion that ballast on British Rail even in the late 60's was of smaller average size with more particles in the range of 15-20mm size, this was before the widespread introduction of the on track tamping machines and when measured shovel packing was still the preferred method of maintaining the track.

Thus it seems that the present ballast specifications were developed between 1980's and 1990's. The requirements of the ballast specifications became more stringent requiring majority of particles in the ballast matrix of a size between 37mm to 50mm. The present ballast specifications have evolved from ballast with a smaller average size i.e. a maximum size of 50mm with a large proportion of particles of size 10-30mm in the 1970's to ballast with larger average size with majority of particles of size between 37-50mm. Wood is of the opinion that the modern ballast size specifications have been developed to allow for better tamping of the track, either manually or by automatic tamping machines (Wood 2002). As described earlier, mechanised tamping machines vibrate the ballast to fluidise it before compacting the ballast in the void below the sleeper. With small size stones the stones would flow around the tamping tines and effective compaction of the ballast will not be achieved. Modern research confirms that to effectively pack ballast by tamping it is required that ballast consists of single size particles (Selig 1998) as tamping of well graded ballast will cause segregation of the ballast with the smaller particles moving down towards the subgrade when vibrated.

It is interesting to compare British Rail specification for ballast in 1988 and Railtrack specification for ballast in 1995 and draft European specification for ballast released in 1997 given in table 2.5.

	% passing sieve		
Size	British Rail specification 1988	Railtrack specification 1995	European specification 1997 for different track categories

80	-	-	100	100	100	100	100
63	-	100	100	97-100	95-100	97-100	95-100
50	97-100	97-100	70-100	70-100	70-100	65-95	55-100
40	-	-	30-65	30-70	25-75	30-60	25-75
37.5	-	65-35	-	-	-	-	-
31.5	-	-	0-25	0-25	0-25	0-25	0-25
28	0-20	0-20	-	-	-	-	-
22.4	-	-	0-3	0-3	0-3	0-3	0-3
14	0-2	0-2	-	-	-	-	-
1.18	0-0.8	0-0.8	-	-	-	-	-

Table 2.5 Development of British Rail ballast specification

As seen in the table 2.5 in 1988 ballast is a broad collection of particles ranging from size 28mm to 50mm with up to 20% of the particles of size between 14 and 28mm. In the 1995 specification majority of the ballast is stone of size 40mm and 37.5mm with a small percentage of stones between size 14mm and 28mm (up to 20%). In the draft European specification particles of size 63mm have also been introduced into the ballast and the minimum size possible is between 32mm and 22mm. The major proportion of ballast is of size 40mm.

2.8 Railway Track loads

The forces acting on the railway track structure can be classified broadly into the following (Selig and Waters 1994, p2.10):

1. Vertical Forces
2. Lateral Forces
3. Longitudinal Forces

1. Vertical forces

Vertical forces act perpendicular to the plane of the rail and the actual direction depends on the track level and grade (Selig and Waters 1994, p2.10). For all practical purposes the railway track structure is idealised as rails supported by a continuous elastic foundation. It is assumed that as the sleeper spacing is very small they form a continuous foundation for the rail, which acts as an infinite beam. Thus bending moment, shear force

and deflection of rail can be worked out based on the above hypothesis. It is found that the bending moment, shear force and deflection peak under the wheel but reverse at a distance from the wheel (Cope 1993). This phenomenon is called the 'precession wave effect', which causes the sleepers in front of and behind the wheels to lift up out of the ballast. With the advancing wheel the lifted sleeper is forced down creating a pumping action which causes wear of the track components (Selig and Waters 1994, p2.11)

The vertical wheel load consists of a static load which is total vehicle weight divided by the number of wheels and a dynamic load due to track geometry faults and wheel impact forces due to wheel flats, rail corrugations etc (Selig and Waters 1994, p2.11). The standard wheel load on British Railways including dynamic components is 100kN. For a firm track bed about 42% of the wheel load is transmitted to the sleeper directly below the wheel and 26% is taken by the adjacent sleepers, termed as the rail seat reaction (Cope 1993, p247). For soft track bed the rail seat reaction for the sleeper directly under the wheel reduces to 25% of the wheel load. It is obvious that reducing sleeper spacing will reduce rail seat reaction and increasing sleeper spacing will increase rail seat reaction.

2. Lateral forces

Lateral forces act perpendicular to the direction of traffic. Principal sources are the lateral wheel force which is due to lateral friction force between wheel and rail and force of wheel flange pushing against the rail. The above may be as a result of track geometry irregularities causing the vehicles to sway or due to weaving motion of vehicles at high speeds. Another source is the track buckling in the lateral direction caused by increase in rail temperature (Selig and Waters 1994, p2.14).

3. Longitudinal forces

These are applied in direction parallel to the rails and can be caused due to braking or accelerating of the train and thermal expansion and contraction of the rail (Selig and Waters 1994, p2.14).

2.9 Ballast settlement equations

Ballast immediately after tamping or ballast in a newly laid track settles rapidly initially and then rate of settlement decreases with increasing traffic on the track. Ballast is the cause for average and differential settlement of the track between surfacing operations (Selig and Waters 1994, p8.32). This being short - term settlement, subgrade contribution to the settlement is negligible. Subgrade being compacted by traffic for decades settles at a very slow rate compared to the ballast. Even if subgrade settlements are large the faults are removed by adding extra ballast in the surfacing operations. Thus with time the ballast depth is increased leading to a reduced rate of subgrade settlement eventually.

Selig and Waters (1994, p6.1) have given the cause of ballast settlement as particle rearrangement in the ballast to a denser state and particle breakage with smaller particles filling the voids in the larger particles. This leads to differential settlement of ballast and hence loss of track geometry. Fouling of track can cause both increase and decrease settlement depending on the fouling material but the worst effect of fouling on track settlement is observed when fouled track is tamped. Vibration of the tamper causes the fines to settle downwards leaving top ballast loosely packed than what it was before tamping. Any subsequent traffic causes such track to settle rapidly.

Various equations have been developed in different railways around the world to explain the phenomenon of track settlement with time, but these are basically empirical in nature (Dahlberg 2001). With load settlement behaviour of railway track being a complex problem with too many variables any theoretical solution to the problem would be impractical (Anderson and Key 2000). Dahlberg has carried out a critical review of available track deformation models and says that track settlement is generally considered to

be a function of the number of loading cycles and magnitude of loading and that there is no correlation of settlement to the properties of ballast and subgrade (Dahlberg 2001). A few settlement models are being described below:

1. Sato's model for track settlement

Sato's (Dahlberg 2001)model for track settlement is given as

$$Y = \gamma (1-e^{-ax}) + \beta x \qquad (2.1)$$

Where x is the loading on the track. The first part of the expression $\gamma (1-e^{-ax})$, is for initial settlement of the track. γ represents the rapid settlement which occurs just after tamping and 'a' controls how quickly this settlement is achieved. The second part βx, represents long term settlement of the track. The value of constant β is chosen such that it does not have any significant effect until the initial settlement is achieved.

The above equation does not distinguish between the effect of a lighter axle and a heavier axle. Similar settlement would occur in the formation for a load of 10tonnes to a load of 20 tonnes (Dahlberg 2001) which is not supported by the research carried out in Britain which concludes that axle load is one of the most important factors influencing the settlement (Shenton 1984, Selig and Waters 1994 – p8.45, Dahlberg 2001).

2. Shenton's model for track settlement

Often track settlement is considered proportional to the logarithm of number of axles passing the track but Shenton (1984) has given a relationship

$$S = k_1 N^{0.2} + k_2 N \qquad (2.2)$$

S is the total settlement of the track after N cycles.

k_1 and k_2 are track constants

$k_1 N^{0.2}$ represents initial rapid settlement for up to 1 million load cycles and k_2 N is a small factor representing settlement due to subsequent traffic. After further investigation on the factors affecting settlement and laboratory tests Shenton (1984) has given a general equation for track settlement

$$S = K_s \, Ae/20 \, ((0.69 + 0.028L) \, N^{0.2} + (2.7 \times 10^{-6} N)) \qquad (2.3)$$

Ae is the equivalent axle load
N is the total number of axles
L the lift given by the tamping machine
Ks is a factor which is a function of sleeper type and size, ballast type and type of subgrade. For a typical British Railway track Ks = 1.1

The equivalent axle load is an attempt to take into account the effect of mixed axle loads on a typical track. The lift given by a tamping machine is found to be one of the most important factors influencing subsequent sleeper settlement after tamping. The other factors taken into account by the above equation are sleeper type and spacing and ballast type.

3. Settlement model of Selig and Alva Hurtado

Assuming that the ballast deformation starts from an uncompressed state Selig and Alva Hurtado proposed the following simple model for ballast deformation (Dahlberg 2001):

$$\varepsilon = \varepsilon_1 [\, 1 + C \log (N)] \qquad (2.4)$$

ε is the total permanent strain.
ε_1 is the permanent strain after first cycle
C is a material constant with typical values of 0.2 – 0.4.
N is the number of cycles

Dahlberg has compared Selig's model with Sato's model and he cautions that for a large number of loading cycles the two models could give different results. However Selig and Waters have demonstrated that the relationship given in (2.4) underestimates the cumulative ballast compression as the number of cycles increases (Selig and Waters 1994, p8.33). Thus there is a danger of overestimating the duration of the tamping cycle by underpredicting the rate of track settlement. Based on laboratory box tests, Selig and Waters (1994, p8.36) have proposed the following power relationship for settlement of ballast,

$$S_N = S_1 N^b \qquad (2.5)$$

Where S_N is the settlement after N load cycles

S_1 is the settlement from the first load cycle

b is an exponent

N is the number of cycles

The above settlement equation can be expressed in terms of strain by dividing both sides of the equation by the appropriate layer thickness (Selig and Waters 1994, p8.34). Based on observations at a newly constructed test track (Selig & Waters 1994, p8.36) the settlement equation was expressed in terms of strain (Selig and Waters 1994, p8.36) as given below

$$\varepsilon_N = \varepsilon_1 N^b \qquad (2.6)$$

Where ε_N is the strain after N load cycles

ε_1 is the strain from the first load cycle

b is an exponent

N is the number of cycles

Thus ballast strain can be defined as ballast layer compression divided by the layer thickness. The above equation represents strain in the top ballast (305mm thick directly below the sleeper). Similar power equations have been proposed for the settlement of sub-

ballast and subgrade and the total settlement is the sum of each of these three components of settlement. Although the test track was newly constructed and the subgrade and sub-ballast had not been compacted under previous traffic ballast contributed to more than half of the total settlement. The ballast contribution to total settlement was expected to increase with the subgrade and sub-ballast gradually being compacted by traffic and remaining relatively undisturbed by maintenance operations (Selig and Waters 1994, p6.1).

Some effort has been made by Dahlberg (2001) to present a computer based finite element model to predict track settlement. It is an attempt to relate track settlement to properties of the ballast and subgrade. The model consists of rail, rigid sleepers, non-linear ballast springs (stiffnesses), and ballast damping. Settlement occurs when stresses exceed the yield limit of the ballast and settlement can be accumulated and it is possible to model sleepers hanging from the rail.

2.10 Model and full scale testing of ballast.

To understand ballast behaviour under cyclic vertical loading model tests and full scale tests are carried out on the ballast. Track conditions are simulated in the laboratory and measurements of various parameters taken under control conditions. The most important parameter studied by both model scale and full scale tests to date is the track vertical settlement under simulated track loads. The test set up is fairly similar for most of the tests in references cited in this thesis so only typical examples are described here.

2.10.1 Box test by Selig and Waters (1994, p6.3)

A steel box of 610mm by 305 mm and depth 480mm was used with a standard width sleeper segment of 300mm length, shown in figure 2.45.

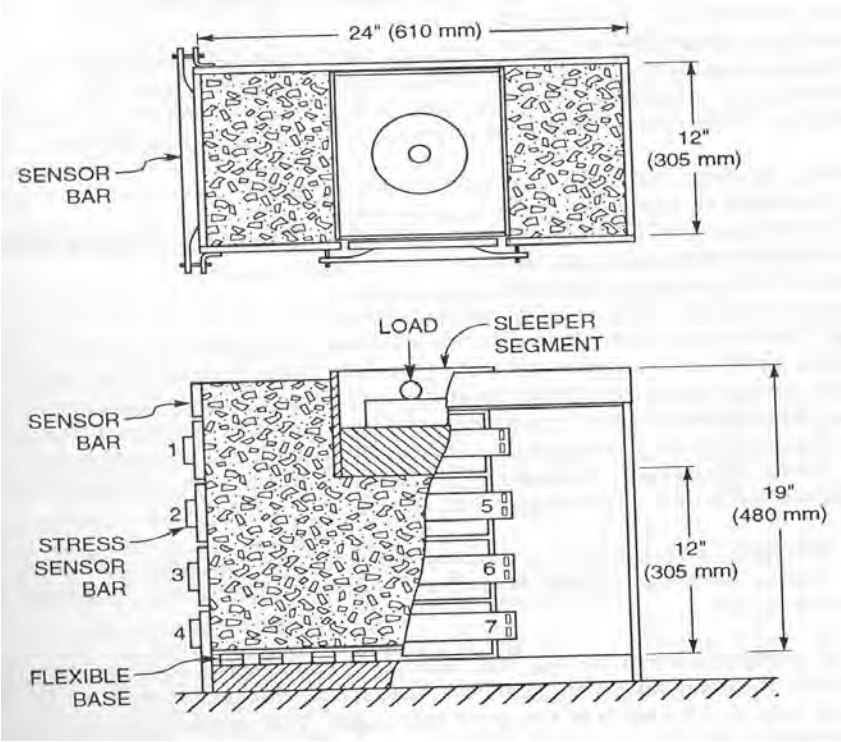

Figure 2.45 Box test arrangement by Selig and Waters 1994

The sleeper segment could be wood or concrete. The box side and end panels were instrumented to read lateral ballast pressure. The bottom of the box was elastic to simulate subgrade elasticity. The thickness of bottom ballast layer provided was 300mm. The sleeper segment was placed on the bottom ballast and crib ballast was filled around the sleeper. The box was then placed in a load frame and loaded by a cyclic vertical load using a servo hydraulic testing machine. Only vertical loading was simulated in the box tests. The following measurements could be made

1. Sleeper settlement
2. Ballast breakage
3. Ballast abrasion
4. Ballast density
5. Change in stiffness
6. Horizontal residual stresses in ballast.

In one of the tests, ballast directly below the sleepers was dyed so than ballast particle breakage and degradation could be studied. The amount of load applied to the sleeper segment simulated the actual ballast pressure in field conditions under axle loading. The sleeper loading in the tests simulated an axle load of 390 kN. The number of cycles could be directly related to the traffic in millions of gross tons. The advantage with the box test was that the ballast could be loosened and rearranged at any time between the test to simulate the process of tamping or stoneblowing of a track.

In one box test a voided sleeper was simulated and ballast breakage and fouling below a voided sleeper was studied. Springs were attached to the sleeper segment to create a gap of approximately 4mm when the sleeper was standing unloaded. The sleeper was pressed down on the ballast when loaded and thus voided sleeper lift up and impact under traffic loading could be simulated in the laboratory. Track settlement and fouling were measured for the voided sleeper test and compared with test results for sleeper without any voids. It was observed that there was increased settlement for sleeper with void compared to sleeper without a void. Fouling was more for a sleeper with void as compared to a sleeper with no voids. Selig and Waters (1994, p8.43) are of the opinion that increasing settlement under a voided sleeper in the test means increasing differential settlement in live track. This would cause an increase in dynamic loads and the settlement under a voided sleeper in live track would be even more than that observed in the box test.

2.10.2 Box tests by Anderson and Key (2000)

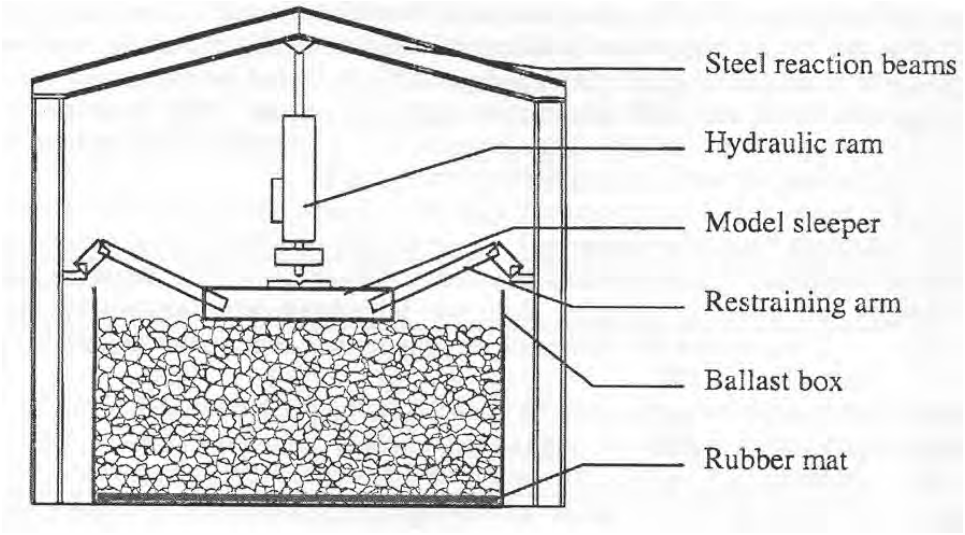

Figure 2.46 Box test set-up by Anderson and Key (2000)

Box tests have also been carried out by Anderson and Key investigating the performance of stoneblown track. A steel plate box 1000mm by 800mm by 600mm deep was used (schematic diagram shown in figure 2.40). A rubber mat with elastic modulus of 5000 kpa was placed at the bottom of the box to stimulate subgrade elasticity. A model sleeper 600mm by 100mm by 100mm was used in the test. 50mm standard railway ballast was used for bottom ballast and smaller stones were placed directly below the sleeper to simulate the effect of stoneblowing. Testing was restricted to vertical loading only. The sleeper was loaded via a hydraulic ram which was fed via a high capacity pump and was computer controlled through a servo-hydraulic valve. A sine wave loading unloading cycle

was used for the tests. The load was cycled between 2.1kN to 18.2kN and the sleeper stresses on the ballast were 35-303 kPa.

Important observations made from the test were:

1. Even slight disturbances to compacted ballast below a sleeper resulted in a change in the load distribution through the ballast bed but for little disturbance the long term deformation was not significantly affected. Thus large disturbances (i.e. tamping) could cause changes to long term deformation characteristics of the ballast.
2. Addition of small size stone below the sleeper reduced settlement but if the layer thickness of small stones added below the sleeper was more than the size of the small stone increased settlement could occur if the sleeper was not restrained by ballast shoulders.
3. After placing the smaller stone layer in the first few loading cycles there was a constant settlement of approximately 2.5mm in all tests.
4. The stone size of 20mm used for stoneblowing is the optimum stone size.

2.10.3 Model test by Ishikawa and Sekine (2002)

Another model test is the moving wheel load test conducted by Ishikawa and Sekine in Japan. In this test the model track is a one fifth scale model of a full scale track in Japan (Figure 2.47).

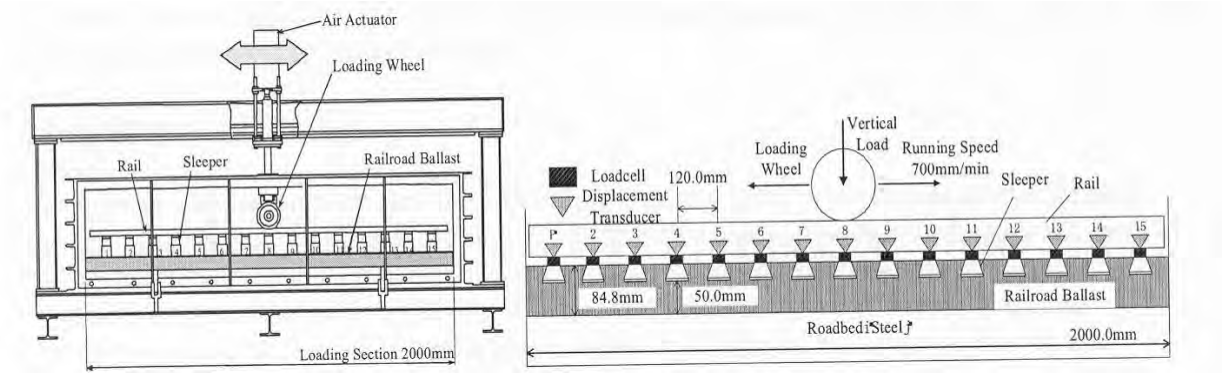

Figure 2.47 Moving wheel load model test set up – Ishikawa and Sekine (2002)

Track components were two steel rails, sleepers made of aluminium and ballast made of crushed stone with a steel subgrade. The important difference from conventional fixed plate cyclic loading tests was that loading was performed through a loading wheel travelling along the rails at a constant speed of 700mm/min. making 100 round trips between both ends of the rail cyclically as actual train loading.

Comparisions were made with a fixed place cyclic load test this time carried out on a one fifth scale model single aluminium sleeper on a steel subgrade and stone ballast with the load directly applied to the sleeper. It was observed that for both moving wheel load test and fixed place cyclic load test ballast deformation and settlement were greater for poorly graded ballast. It was also observed that track settlement was greater for the moving load test as compared to the cyclic fixed place load test.

2.11 Alternatives to conventional ballasted track

From the time of Brunel's broad gauge track with continuously supported sleepers, alternatives to the transverse sleepered ballasted track are continuously being developed. The principal aim is to reduce the maintenance required compared to ballasted track.

Slab track has been developed as an alternative to ballasted track and is widely used in tunnels. In the slab track the rails are supported by a continuous foundation as opposed to discrete support by sleepers in the conventional ballasted track. On slab track the change in track profile is very small and thus the slab track is superior to the ballasted track in this regard. The slab track contributes to a small cross-section of a tunnel and thus it is

economical in tunnels (Watanabe et al 1984, Eisenmann 1995, Profillidis 1995, p35). Maintenance cost of the slab track is almost non existent but initial construction cost in the UK is 30% more than that of a ballasted track and this extra investment could be recovered a savings in maintenance in 5-7 years (Profillidis 1995, p131). Watanabe et al submit that the saving effect of the slab track depends on the usage of the track. For low traffic volumes the track deterioration will be lower and less serious and thus maintenance cost for ballasted track will be low thus a slab track would not be justified in such a situation. According to Watanabe et al slab track should be adopted in tunnels or on elevated structures and ballasted track should be used on ordinary sections (Watanabe et al 1984). Profillidis (1995, p131) has mentioned that although slab track system is virtually maintenance free no correction to track geometry can be applied in case of the slab track loosing its alignment or line due to a poor subgrade. Thus the slab track system cannot be used on poor subgrades. Eisenmann has described different types of innovative track systems being used in Germany for the development of high speed lines and his view is that use of slab track should be considered for new tracks where trains are to be worked at 200 Km/h at a high frequency of operations (Eisenmann 1999). Constructing a slab track on existing ballasted track would require long periods of track possession and disruption to traffic and such operations are difficult to carry out in a country like the UK, which has a fully developed and functional railway with ballasted track on all its main lines.

Cope and Ellis (2001, p289), although agreeing that slab track requires less maintenance, cautions that it is not maintenance free. He has cited that slab track like ballasted track requires routine inspections to check on the fittings, the rail pad and the insulators. A description of the construction process of the British Paved Concrete Track (PACT) is given by Cope and Ellis (2001, p290). The PACT is a continuously reinforced concrete pavement and it has no expansion gaps or construction joints throughout its length (See figure 2.48).

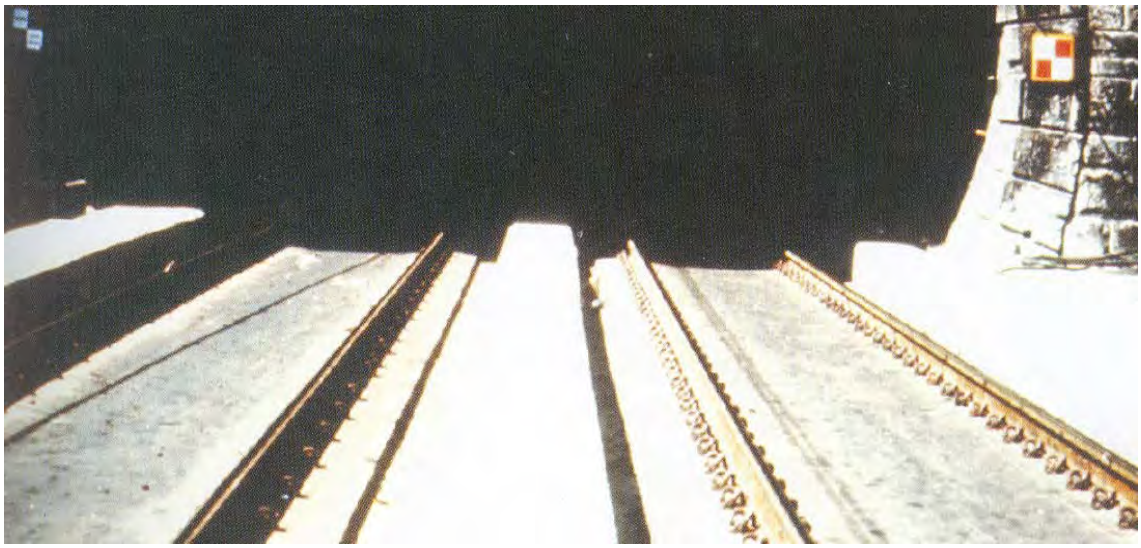

Figure 2.48 PACT track (Cope and Ellis 2001)

Thus fine transverse cracks develop in the concrete which if held tight by the reinforcing steel pose no problems but any vertical movement of the track can cause these cracks to deteriorate allowing seepage of water to the reinforcement. Remedial action in such a situation requires specialised techniques and is expensive. Another problem related to construction of any form of slab track, according to Cope and Ellis (2001), is the transition area where the slab track changes to conventional ballasted form of construction. At this point there is a sudden change in track stiffness and this area of the track requires extra maintenance. Special transition arrangements have to be made in the form of reinforced concrete longitudinal sleeper (ladder units) resting on ballast or by providing a buried concrete slab with a tapering ballast cross-section longitudinally with lower ballast depth at the slab track end and full ballast depth at the ballasted track end, this being done over a length of 4-9m with the track supported by closely spaced sleepers.

Another form of slab track used in the U.K. is conventional concrete sleepers encased in poured concrete and laid on a reinforced concrete slab (Figure 2.49) (Cope and Ellis 2001, p290).

Figure 2.49 Concrete sleepers embedded in concrete base slab (Cope and Ellis 2001)

These sleepers have a tendency to debond from the surrounding concrete and thus during routine track maintenance is important to look for any movement of these sleepers. If detected early the sleeper movement can be repaired in-situ by resin injection, any delay in detection will cause deterioration of the track requiring the sleepers to be broken out and cast in again. A similar arrangement is achieved using the ladder track (figure 2.50) with continuous longitudinal beams connected transversely by precast concrete units with all stirrup reinforcement linked to the surrounding infill concrete (Cope and Ellis 2001, p290). These are used on straight track only or as mentioned earlier in transition zones from slab track to ballasted track.

Figure 2.50 Ladder track used in the U.K.

A different form of ladder track has been experimented in Japan. Ladder track is a modern development of the Brunel system of continuously supported rails on a ballast bed (See figure2.51). Experiments carried out in Japan were on precast concrete longitudinal beams held to the desired gauge by embedded steel pipes. These provide continuous support to the rails and act with the rails as composite rails (Wakui et al 2002). The aim is to reduce the ground pressure on the subgrade and also to reduce sleeper settlement into ballast, thus reducing the requirement of maintenance of the track. It is possible to develop on track tamping machines to maintain the ladder track system.

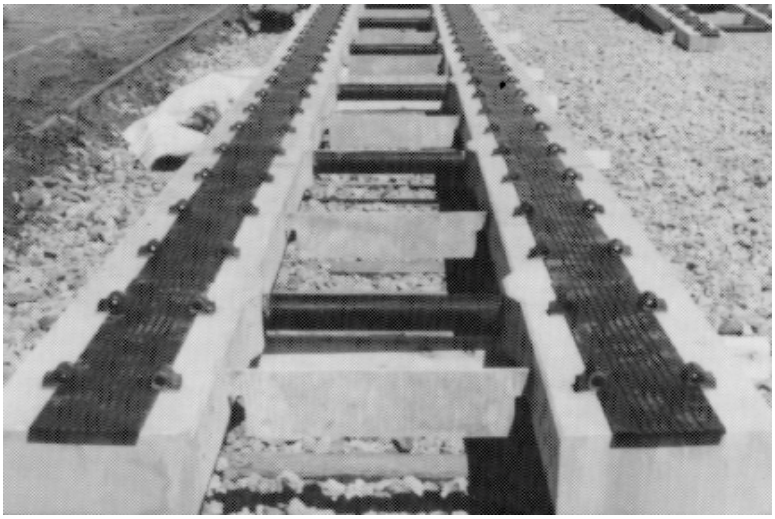

Figure 2.51 Ladder track – Experimental trials have been run on this system of ladder track (Wakui et al 2002)

Lechner et al (2002)have described German experiences with slab track spanning over 30 years. Lechner et al mentions that replacing ballast by a stiff concrete requires provision of additional elastic elements in the track, which are usually provided under the rail in form of elastic pads. Also slab track does not lend itself to maintenance the same way as ballasted track if any irregularities in track geometry are to appear. This must be compensated by suitable track design and strict quality control for slab track construction. On a piece of slab track installed in 1972 Lechner et al report that no rehabilitation or maintenance work was required other than grinding of rails. This track is similar to the British embedded sleeper system. Experimental studies are also being carried out on slab track systems with sleepers resting on an asphalt base instead of reinforced concrete slab and also on precast prefabricated concrete slab systems (Lechner et al 2002).

3. Measurement and virtual instrumentation

3.1 Introduction

In this chapter the computer methods, which were developed for the laboratory testing are reviewed.

Virtual instrumentation is a combination of computer based hardware and software to create user defined instrumentation solutions (National Instruments Corporation 2000)

A virtual instrumentation system generally consists of

1. A data acquisition instrument (transducer)
2. A data acquisition device (board) e.g. Das 16 board used for this project
3. A driver software for the data acquisition board e.g. Instacal Universal library for DAS 16 board
4. Application software e.g. Labview used for this project

The fundamental task of all measurement systems is the measurement and/or generation of real world physical signals (National Instruments Corporation 2000). Acquisition is the means by which physical signals, such as voltage, current, pressure, displacement etc are converted into digital formats and brought into the computer. A data acquisition instrument (transducer) acquires raw data, which is converted to an electrical signal. The data acquisition (DAQ) device converts the electrical signal into digital information, which is fed into the computer. The driver software enables the data acquisition board to communicate with the computer. The application software e.g. Labview acquires the raw data from the data acquisition board, analyses the data and presents the results. It also controls the Data acquisition system telling it when to acquire data and which channels to acquire data from and can be used to control operation of machines through the data acquisition system.

3.2 Data acquisition instruments

Data acquisition instruments (transducers) are used to convert physical signals into electrical signals, which can be read by a DAQ device and converted into an digital signal to be input into a computer. Thus a displacement transducer will convert information of displacement into an electrical signal. Similar instruments are available to measure physical quantities like strain, pressure etc.

Data acquisition devices are usually classified into two categories: general purpose DAQ devices and special purpose instruments. General purpose DAQ devices typically connect directly to the computers internal bus through a plug - in slot. The general purpose DAQ devices convert the incoming signal into a digital signal that is sent to the computer. The DAQ device does not compute the final measurement, this is done by the software inside the computer e.g. Labview. Thus the advantage to the user is that the same device can be used for a wide range of measurement applications but the downside is that the user needs to create programs for each different measurement application. Special purpose instruments carry out the same function as DAQ devices but the software required to produce the final measurement is built in into the device and cannot be modified. The DAS 16 board used in this project is a general purpose plug in DAQ board. The maximum analog input range of the board is +/- 10 volts and the digital input range of the board is 0-5 volts (Computer boards inc. 1994).

3.3 DAQ drivers or driver softwares

DAQ drivers or driver softwares enable the DAQ board to communicate with the application software (e.g. Labview) in the computer and vice versa. Instrument drivers are a key factor in test development. An instrument driver is a collection of functions that implement the commands necessary to perform the instrument's operations (National Instruments Corporation 2000). The instrument drivers save time for the user as the user does not have to write programs for each function of the instrument driver. Application software such as Labview controls the data acquisition process and communicates with data

acquisition instruments (transducers) through the instrument drivers. For example Labview can send command to the drivers to acquire a load cell reading via a certain input channel and also to increase load on the load cell via a certain output channel.

The instrument driver for the DAS 16 DAQ board is the instacal software with a Computer Boards Universal Library which the users can utilise to write their own programs for data acquisition and control (Computer boards inc. 1994). The library contains all high level functions for all the common operations for the DAS 16 board. For example to read a single analog reading the function available is ‘Ain’. This function takes a single reading from an analog input channel. Thus a set of different functions of the type above are available to the application software (e.g. Labview) to enable it to control input output operations through the DAS 16 board.

Given in figure 3.1 is an example of a simple program in Labview to read analog signals using a DAQ board. The program for reading analog signals is available to Labview as a function ‘AI one pt’ through the Universal library of the instrument driver, which allows the user to specify the board to use and the channel number to which the transducer is connected. The incoming data, which is in the form of an analog electrical signal is converted to a digital signal by the DAQ board. The data then can be displayed in Labview on a Waveform chart as shown in figure 3.1. The display in the example shown will display raw data straight from the DAQ board but using Labview it is possible to calibrate the data and display the final measurements.

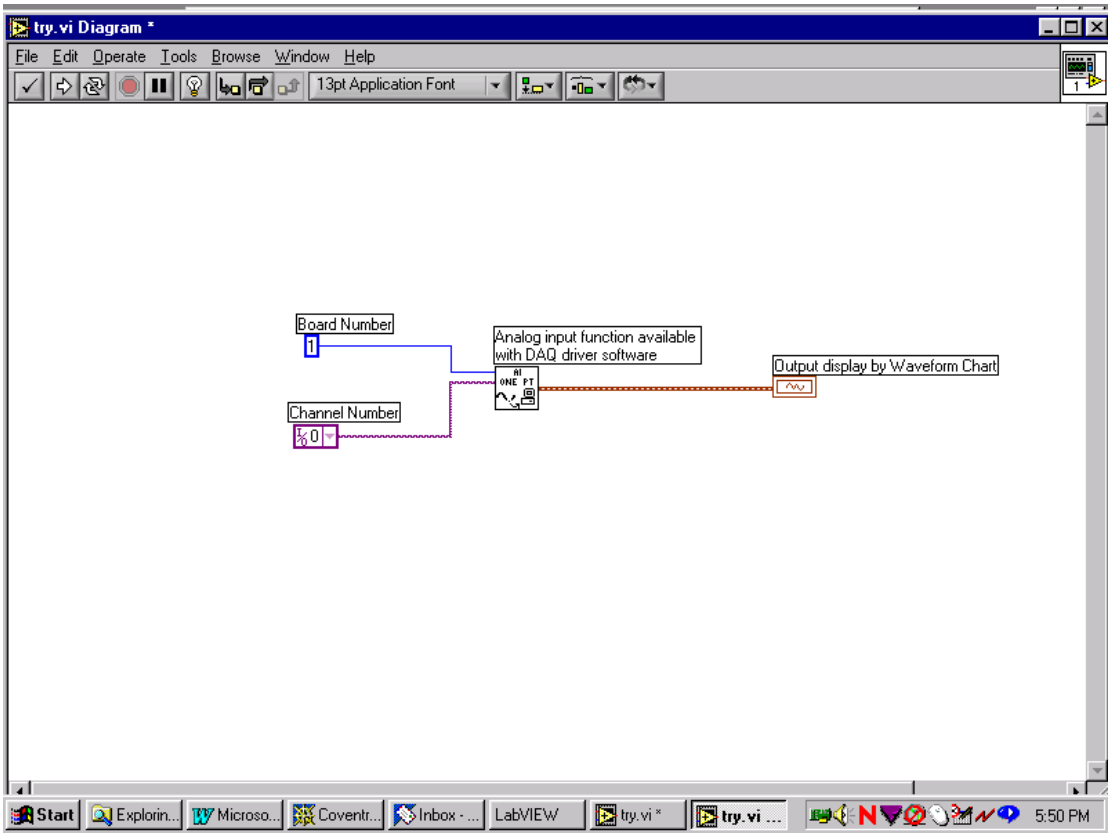

Figure 3.1 A simple program for reading analog signals using DAQ board

3.4 Application software (Labview)

As mentioned earlier, Labview is an application software which can acquire raw data from the DAQ boards and analyse and present it and it can also control the data acquisition process by specifying when to acquire data and which channel to acquire it from. Using the output channels in tandem with the input channels on the DAQ board Labview can also be used to control machine functions thus allowing full computer control over any testing facility. Labview is a graphical programming language that uses icons instead of lines of text to create applications. In contrast to text-based programming languages, where instructions determine program execution, Labview uses dataflow programming, where flow of data determines execution (National Instruments Inc. 2000). Labview programs are called virtual instruments or VI's because their 'appearance and operation imitate physical instruments' (National Instruments Inc. 2000). As defined in the Labview user manual every VI has the following three components:

1. Front panel – Works as the user interface
2. Block diagram – Contains the graphical source code that runs the VI
3. Icon and Connector pane – Identifies the VI so that you can use the VI in another VI. A VI in another VI is called a sub VI similar to a subroutine in a text based programming language.

3.4.1 Front Panel and Block Diagram

The user interface in Labview is known as the front panel or the control panel. The front panel is built using controls and indicators available in the front panels functions pallete shown in figure 3.2. Controls simulate input devices and supply data to the block diagram of the VI and indicators simulate output devices and display data the block diagram acquires or generates. Controls are knobs, push buttons, dials etc. and indicators are graphs, LED's and other displays. Examples of a few controls and indicators in the front panel and their corresponding graphical representations in the block diagram are shown in fig. 3.2 and 3.3.

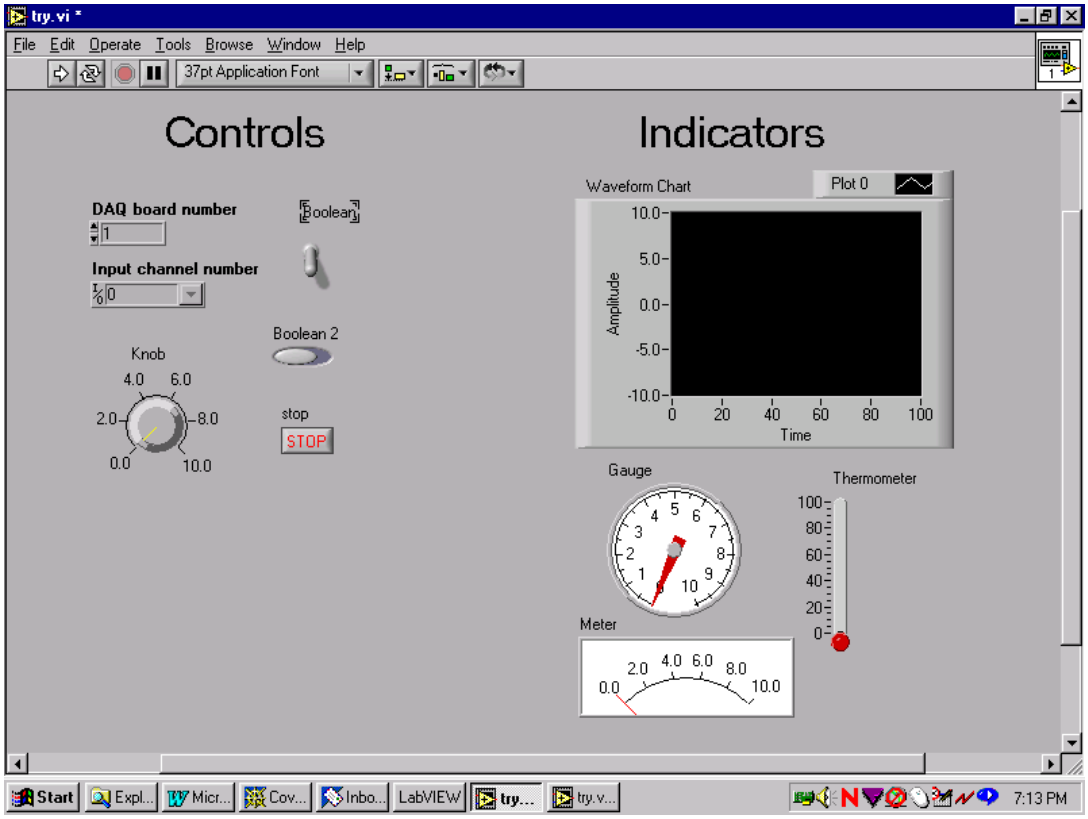

Figure 3.2 Controls and Indicators on Labview Control (Front) panel.

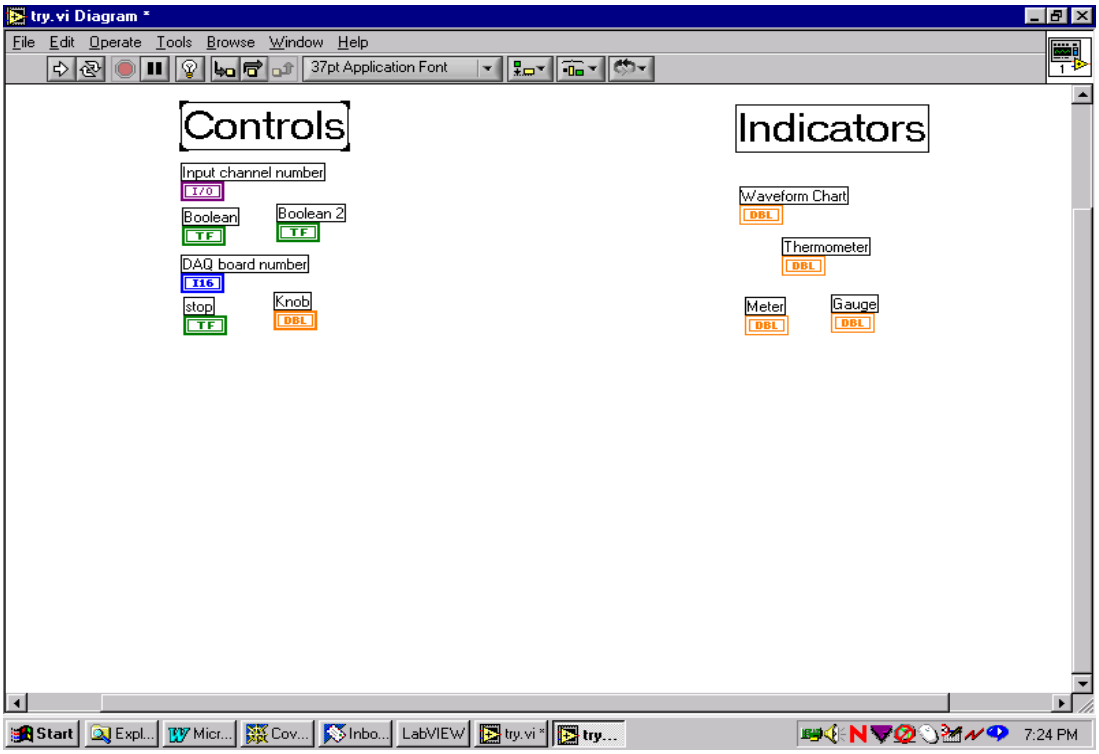

Figure 3.3 Controls and indicators of figure 3.2 as they appear on Labview Block Diagram.

The source code for the program is written in the block diagram using graphical representations of functions in the control panel and also the functions from the Universal library of the DAQ board, available through the functions pallete in the block diagram as shown in figure.

Graphical representations of the front panel objects, known as terminals, appear in the block diagram as shown in figure 3.3. The terminals represent the data type of the control or indicator. For example a True/False terminal represents a Boolean control or indicator.

A simple example of addition and subtraction of two data values using a Labview program is shown in figure 3.4. When the VI is run, data enters the block diagram through the terminals A and B in the front panel. The data then enters add and subtract functions, known as nodes, before flowing to the indicator terminals, which display the result on the front panel. The addition and subtraction functions are known as nodes and they have inputs and /or outputs and perform operations when a VI runs. They are analogous to

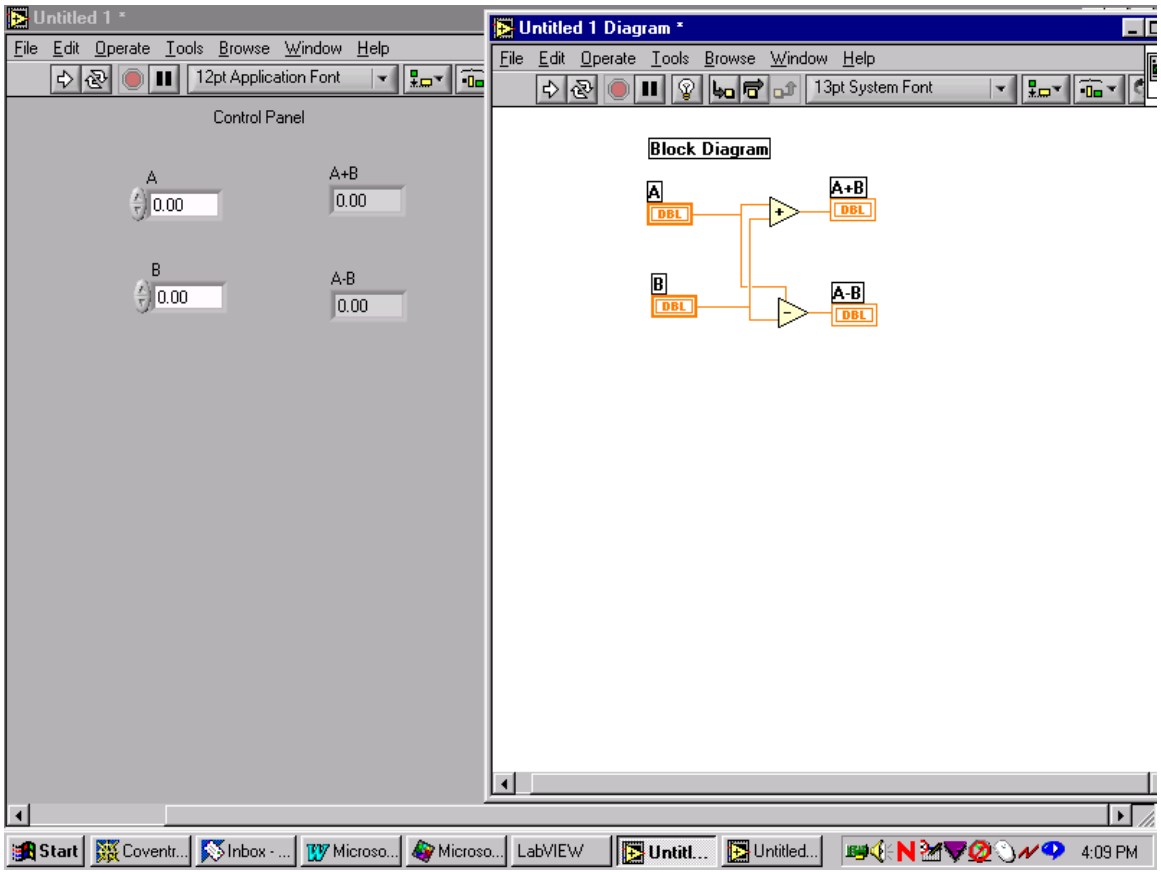

Figure 3.4 Control Panel and block diagram showing an example of addition and subtraction in Labview.

statements, operators, functions and subroutines in text-based programming languages and are available through the functions palette of the block diagram.

The transfer of data among block diagrams is through wires. In figure 3.4 wires connect the control terminals to the nodes and the nodes to the indicator terminals. Each wire would have a single data source but can be connected to many VI's and functions that read data. Wires are different colours, styles and thickness depending on their data type. A broken wire appears as a dashed black line and occurs when there is some error in the program.

Labview graphically represents the loop and case statements of text based programming languages using 'structures'. Structures can be used while writing the source code in the block diagram to execute code conditionally or in a specific order.

A VI can be represented by its icon and the connector pane to be used as a sub VI. As mentioned earlier a sub VI is similar to a subroutine in text based programming languages.

3.4.2 Functions

Functions are the essential operating elements of programming in Labview. Functions are available in the block diagram but do not appear in the front panel. A few functions are being described below:

1. Numeric functions – These are used to create and perform arithmetic, trigonometric, logarithmic and complex mathematical operations on numbers and to convert numbers from one data type to another (National instruments inc. 2000).
2. Boolean functions – These perform logical operations on single Boolean values or arrays of Boolean values such as change in true and false value and vice versa, determine which Boolean value to return if you receied two or more Boolean values, convert Boolean value to number etc.
3. Array functions – are used to create and manipulate arrays. E.g. extract individual data elements from an array, add or subtract data to an array, rearrange arrays etc.
4. Comparison functions – are used to compare Boolean numbers, strings, numeric values etc.
5. Time and dialog functions – are used to control the speed of operation of the program or an activity and to register data with a time reference.
6. File input output functions – used to open and close files and to read from and write to files. These facilitate creating directories and files to the path specified.
7. Loop and case structures – Structures in Labview are available in the block diagram through the functions palette and represent loop and case statements of the text based programming languages. Structures are like nodes and have terminals to connect them to other nodes. Once the data is received the function is executed automatically and the output is supplied through output wires to other nodes or to indicators on the front panel. An example of a few structures is shown in figure3.5

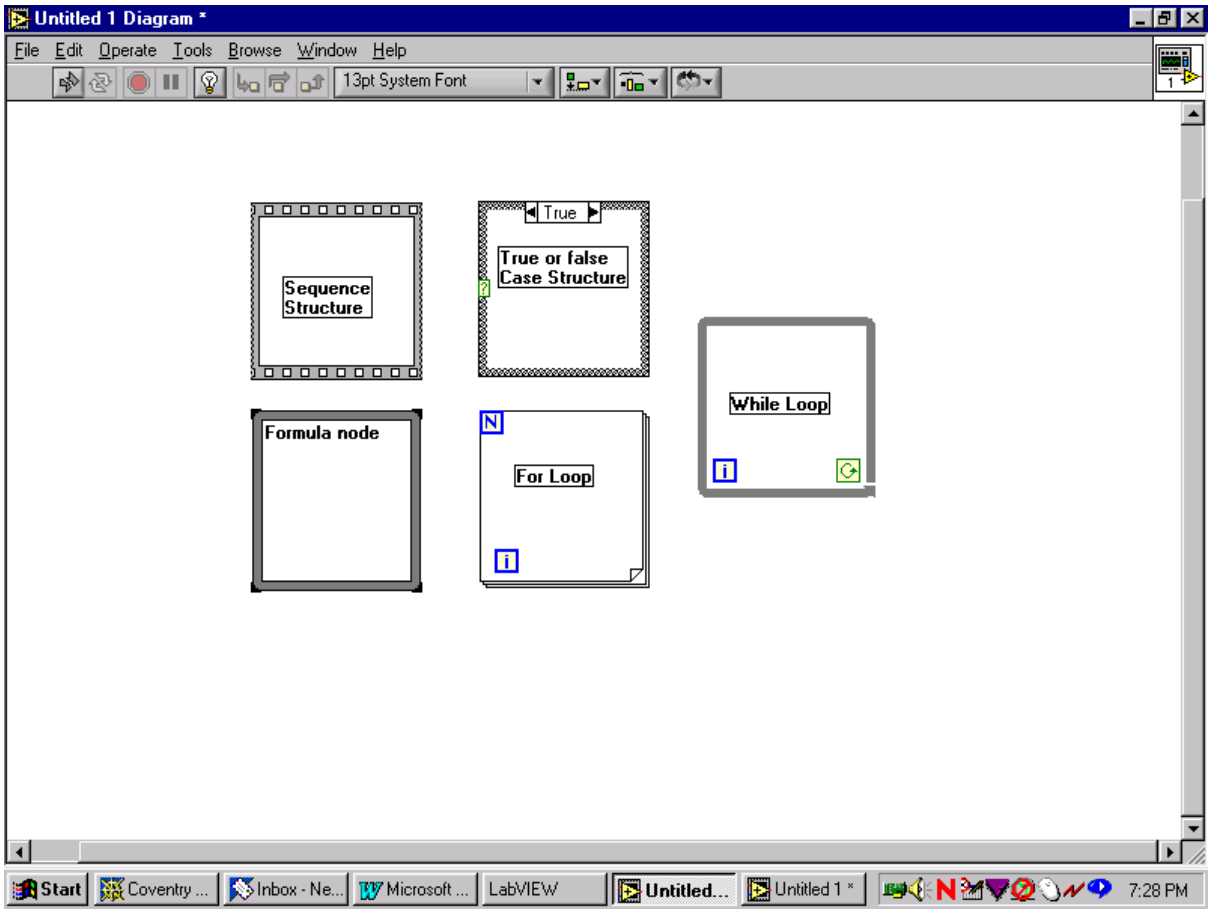

Figure 3.5 Examples of Structures in Labview.

Each structure appears on the block diagram in form of a box with a distinct resizable border. The program to be executed by the structure is enclosed within the box of the structure and is called a subdiagram. The data is fed into and out of the structure through nodes called tunnels. The following structures are available through the functions palette on the block diagram:

1. For loop – The For loop is used to control repetitive operations. It executes a subdiagram for the number of times specified. For loop example is shown in figure 3.6.

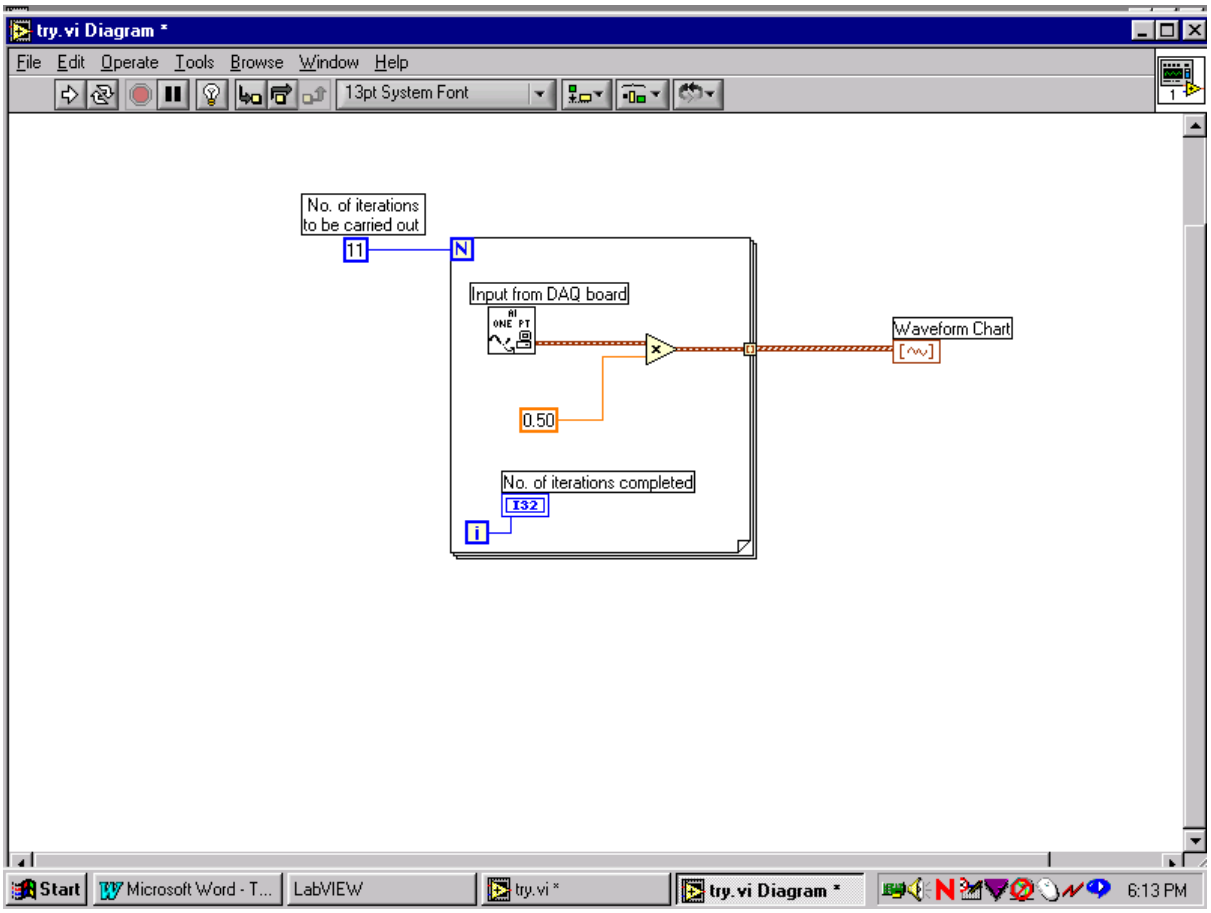

Figure 3.6 For loop example

In the figure above the For loop is represented as the square box, N is the count terminal and it specifies the number of times the For loop needs to be iterated. i is the iteration terminal and gives the number of iterations completed at any time while loop is being executed. The subdiagram is enclosed within the For loop boundary and it is programmed to read the DAQ board for an analog input, the value of which will be multiplied by a constant and the final value will be displayed on the graph in the control panel. As the iteration count is set at eleven the For loop will carry out the above subdiagram eleven times and the output data will be displayed in the graph. The iteration terminal has been wired to a digital indicator which will display the number of iterations carried out while the program execution is in progress.

2. While loop – This is similar to a Do loop of a text based programming language. It carries out conditional execution of the subdiagram. An example of the while loop is shown in figure 3.7.

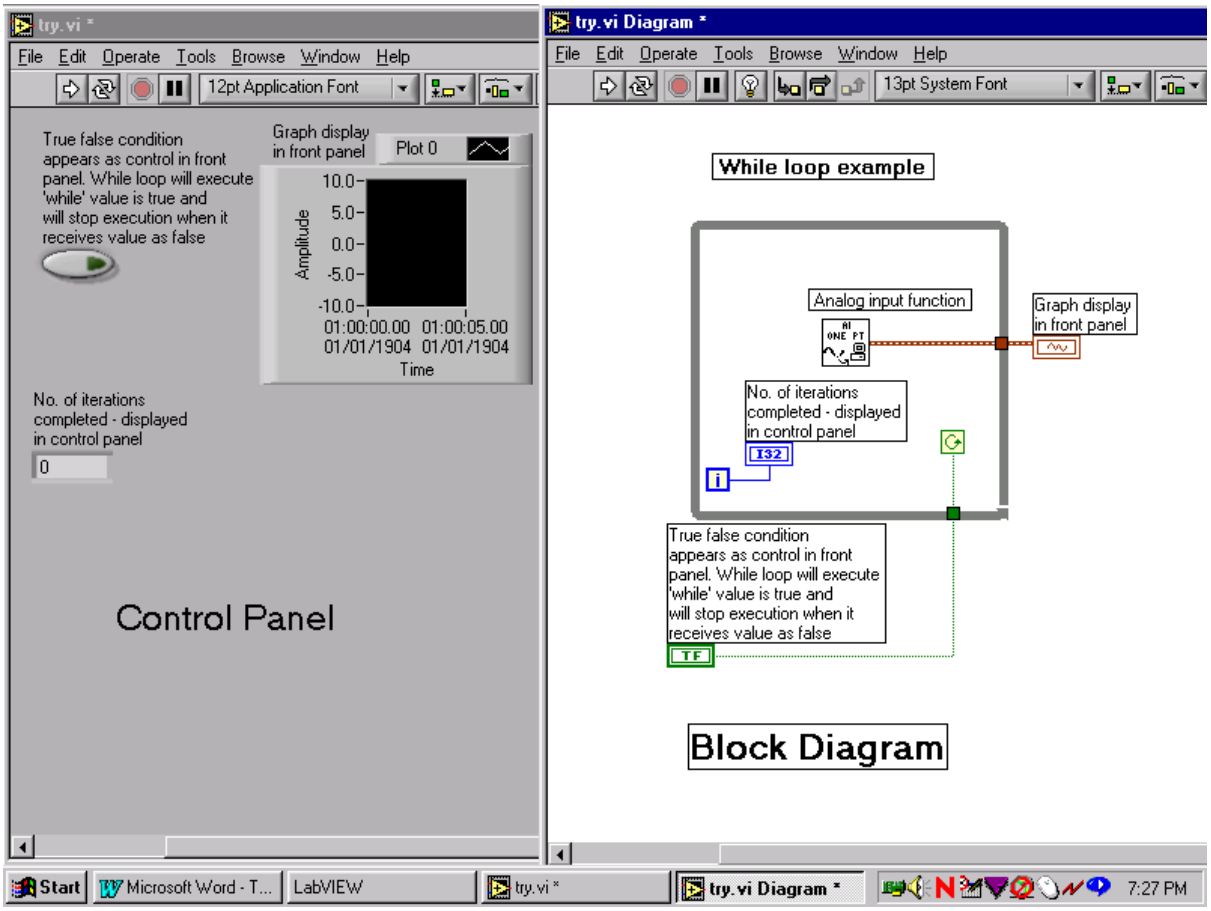

Figure 3.7 While Loop example

While loop is represented by a box with bold grey border. The subdiagram is enclosed within the while loop. The while Loop executes the subdiagram until the conditional terminal, which is an input terminal represented by a circular green arrow, receives a specific boolean value. In the figure the conditional terminal has been wired to a boolean control visible in the control panel as a control button. The default condition of the conditional terminal is to 'continue if true' and the loop will continue executing until the user presses the control button in the control panel and passes a false value to the conditional terminal, on which the execution will stop. The iteration terminal is similar to the iteration terminal of the For Loop and gives the number of iterations carried out. Thus

in the example of While Loop in the figure the subdiagram will receive input from the DAQ board analog channel until the user presses the control button on the control panel.

3. Case structure – Executes subdiagram based on the input value passed to the structure. An example showing use of case structure is shown in figure 3.8

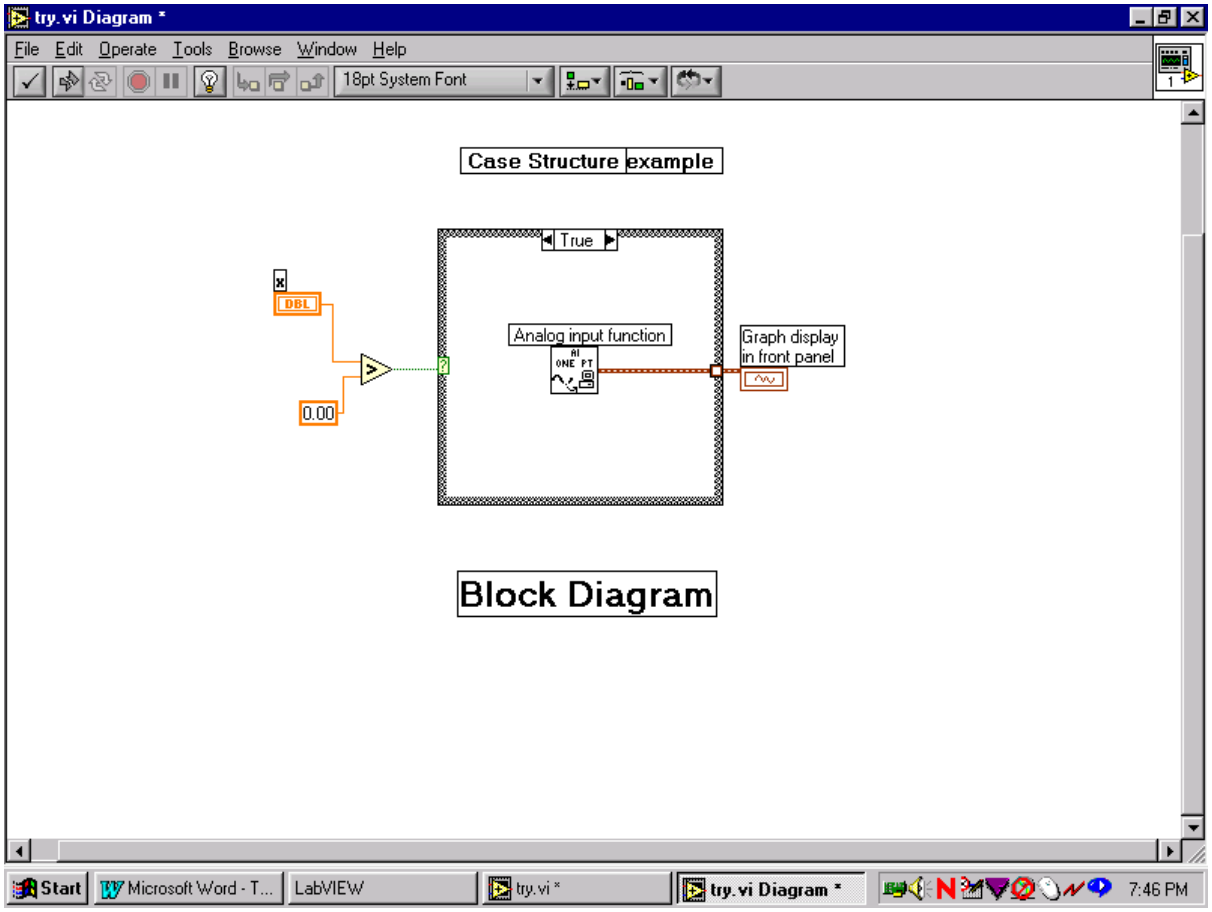

Figure 3.8 Case Structure example

In the above diagram the Case Structure is represented by a box with a hatched border. A Case Structure has two or more subdiagrams each with a case selector identifier at the top, which in the figure is shown as 'True'. Only one subdiagram is executed at a time based on the input value received by the case structure. The input value is wired to the selector terminal which appears as a green '?' on the side of the case structure as shown in the figure 3.8. For example in figure 3.8 the case structure has a subdiagram which will read an analog input signal from the DAQ board and display it in the graph on the front panel. The execution will depend on the condition that a value 'x' input by the user from

the control panel is greater than zero. If the value is greater than zero the control passes to the case structure 'True' subdiagram (shown in the figure above) and the program will be executed with the final measurement being displayed in the graph on the control panel. If the value input by the user is less than zero the control will pass onto the Case Structure 'False' subdiagram and the program will not be executed.

4. Sequence structure – Executes subdiagrams in sequential order can have infinite number of subdiagrams. An example of the sequence structure is shown in figure 3.9

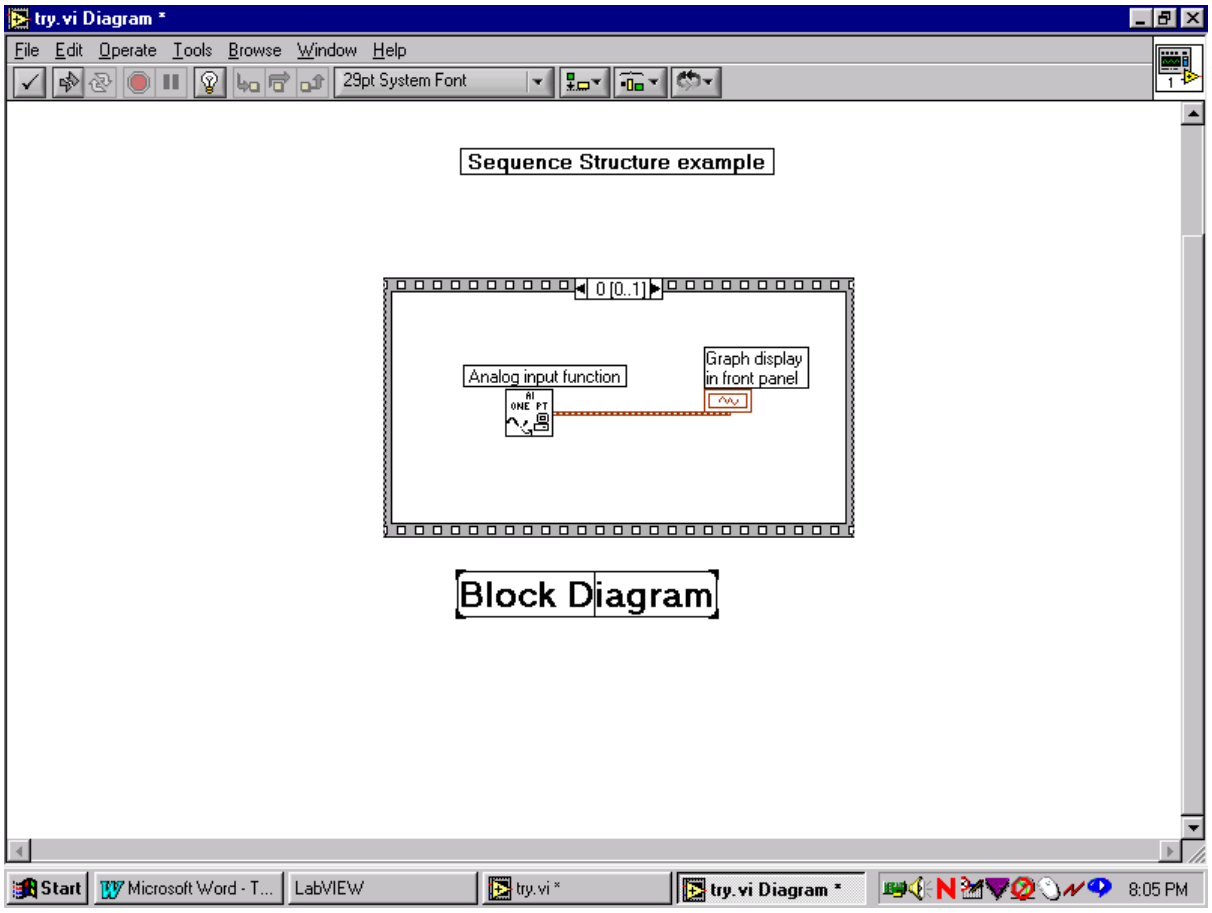

Figure 3.9 Sequence structure

A sequence structure executes frame 0, 1, 2, 3……until the last frame executes. The sequence structure does not complete execution or return any data until the last frame executes.

5. Formula node – used for performing mathematical operations on numeric input. The formula node allows the user to develop mathematical equations in a mathematical environment and the equations are integrated into an application (National Instruments Inc. 2000). An example of a formula node is shown in figure 3.10.

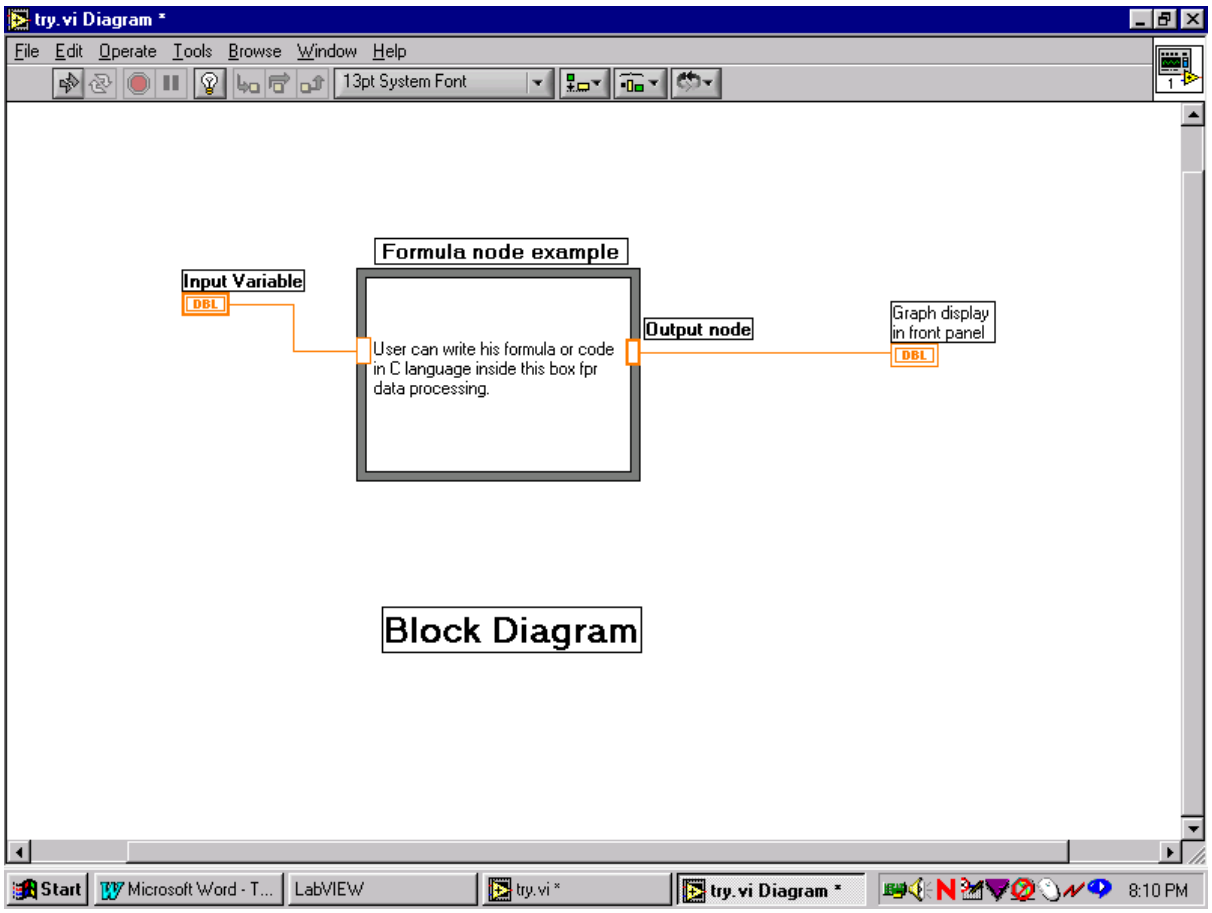

Figure 3.10 Formula node example

The formula node has an input terminal and an output terminal as shown in the above figure as orange boxes on the border of the formula node. The users can write formulae or their own code for data processing inside the box. In the above example shown in the figure the input data will be processed and output data displayed on a graph in the Control Panel.

4. Laboratory test set up

4.1 Introduction

The philosophy of all testing (model scale and full scale) on the two layered ballast system was to investigate the various parameters affecting the two layered ballast system and to be able to specify these parameters to keep voids below sleepers within tolerances specified on the railways. Initial tests were carried out on model scale and the results of the model tests were validated by carrying out full scale tests in the laboratory.

Figure 4.1 Two dimensional representation of track ballast and sleepers

As a general principle, it was decided to try and simulate a voided sleeper in all the tests. Voided sleepers occur on railway track as a single sleeper or a group of sleepers, which move vertically under the traffic loading. A voided sleeper or a group of voided sleepers are supported by adjoining sound sleepers sitting on ballast. Thus when loaded by traffic the voided sleepers move downwards to the bottom of the void but move up again to their position of 'rest' when the load is removed, effectively hanging from the rail supported by adjoining sound sleepers.

A two dimensional crosssection of ballast was created between two glass plates as shown in figure 4.1 to help develop the testing methodology. The above set up, in the initial stages of the project, helped visualise the working of the system. 50mm standard railway ballast was placed to a standard depth in the box and a sleeper cross-section was placed on top of the ballast. Thus 50mm stones formed the bottom ballast. Smaller stone was filled around the sleeper. This position of the sleeper represented a voided sleeper in live track under maximum load at the bottom of the void. The sleeper was then lifted up by a specified amount (say 25mm). This movement represented a loose sleeper on track, supported by adjacent sleepers, moving upwards once the axle has passed above it. When the sleeper was lifted up the small ballast was observed moving into the void below the sleeper and the sleeper section could not be pressed down to its original level. It was also observed that if a series of vertical movements were given to the sleeper the crib ballast gradually moved in to fill the void. Thus, simulation of a loose sleeper, as described above, by lifting the sleeper up after each load cycle formed the basic principle of all subsequent tests on the two layered ballast system.

4.2 Simple and Uplift cycles

A typical test 'run' both for model and full scale tests consisted of 'simple' and 'uplift' cycles, these have been described schematically in Figure 4.2. Bottom ballast was placed first and levelled out. The sleeper(s) were placed on the bottom ballast with a minimum seating load, which represented the self weight of the track assembly. The level

of the sleepers at this minimum load was set as zero, which became the datum for the test. Smaller crib ballast was filled in the crib around the sleeper and the test was started. In the simple cycles the load on the sleepers was cycled from the minimum seating load to a maximum, simulating passage of traffic on a perfect track without voids. The uplift cycles were used to simulate formation of voids below the sleepers. In the uplift cycles the sleepers were lifted up by a specified amount (void size) after each load cycle. This simulated a group of loose sleepers in a track which are effectively 'hanging' from the rail. Different combination of simple and uplift cycles were run in the tests to simulate live track loading on the model sleepers. These have been described in detail in succeeding sections.

The maximum displacement of the sleeper(s) in the ballast, relative to the set datum level, was measured for each simple and uplift load cycle at the maximum load. The displacement data from simple and uplift cycles has been presented in the form of graphs of maximum sleeper displacement for each load cycle. A typical graph for a type A run (described later) has been shown in figure 4.3. The first 20 readings of sleeper displacement are for the 'simple' cycles and the subsequent 20 readings of sleeper displacement are for the 'uplift' cycles. It is clear from the graph that in the uplift cycles the void below the sleeper is slowly reducing as the crib ballast flows into the void and sleeper rises up in level. In the simple cycles the sleeper has moved down by 0.5mm compressing the bottom ballast. In this way simple cycles simulated a sleeper on sound track without any voids below the sleeper and the uplift cycles simulated a poor track with void below the sleeper.

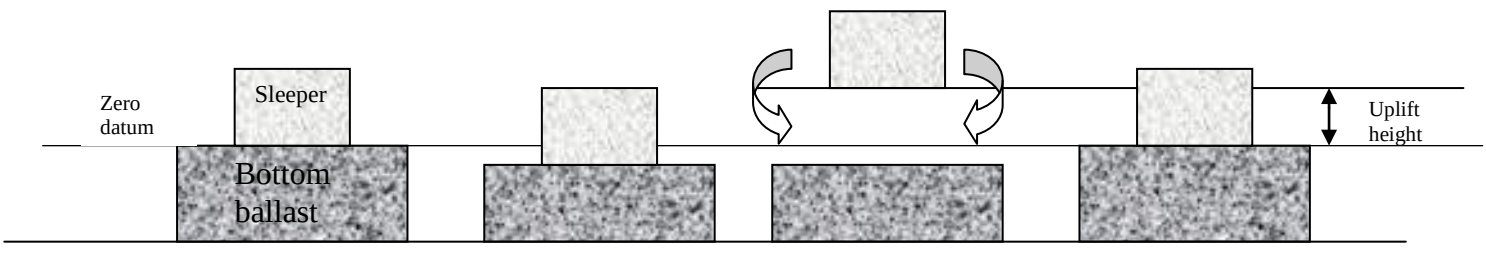

Sleeper on ballast with minimum seating load. Zero datum	Simple cycles: Load cycled from seating load to maximum. Sleeper at maximum load causing ballast	Uplift cycle: Load zero - Sleeper lifted up by specified amount from zero datum level. Crib	Uplift cycle: Sleeper load maximum. Movement of crib ballast has filled the void below the

Figure 4.2 Schematic diagram showing ‘simple’ and ‘uplift’ cycles

Figure 4.3 A typical result from a test run with 20 ‘simple cycles’ and 20 uplift cycles. The crib ballast was stone of smaller size.

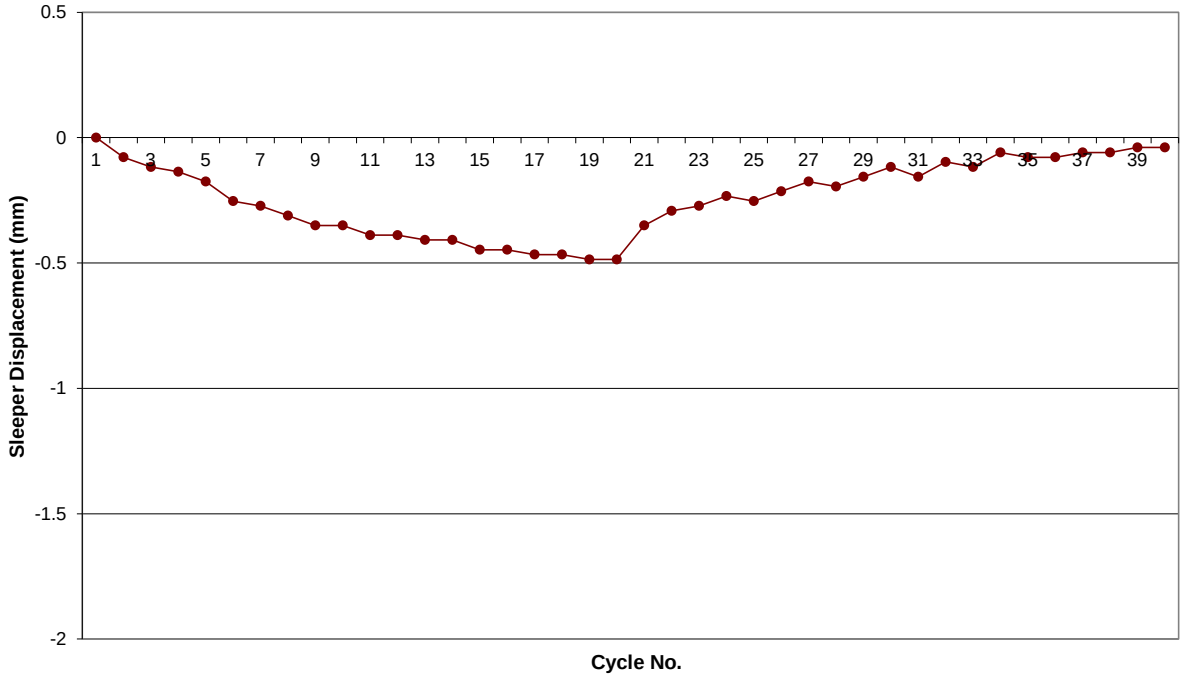

4.3 Model test set up

Model tests were carried out at tenth scale on model sleepers and ballast. The model tests comprised the first stage of testing on the two layered ballast system. The first aim was to establish if the two layered ballast system would perform as proposed by Dr Keedwell i.e. if standard railway ballast in the crib around a loose (voided) sleeper was replaced by smaller stone will the void below the sleeper be filled up by the smaller stones as the sleeper moved vertically under cyclic load and if the system did work as proposed then what factors would affect the working of the system and to what extent will the void below the sleeper be filled up.

Model tests were carried out on both wooden and steel sleepers and an instrumented sleeper, instrumented with strain gauges. These are described in detail in this section.

4.3.1 Model test components

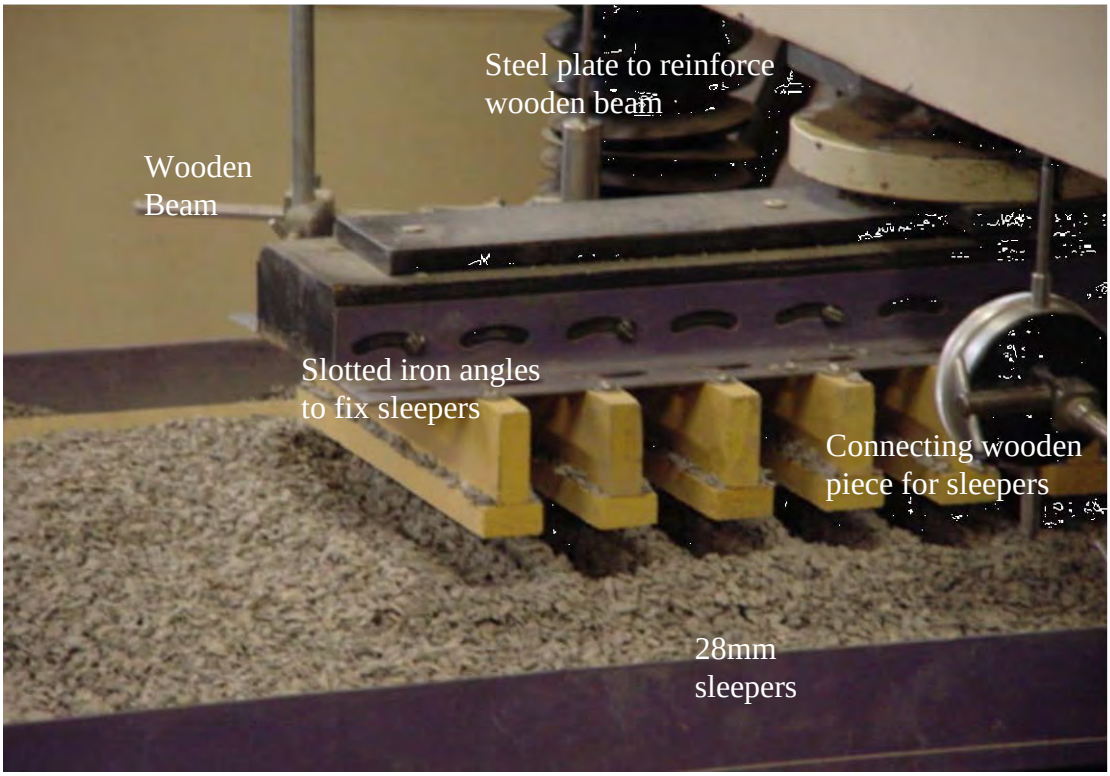

Figure 4.4a Monoblock

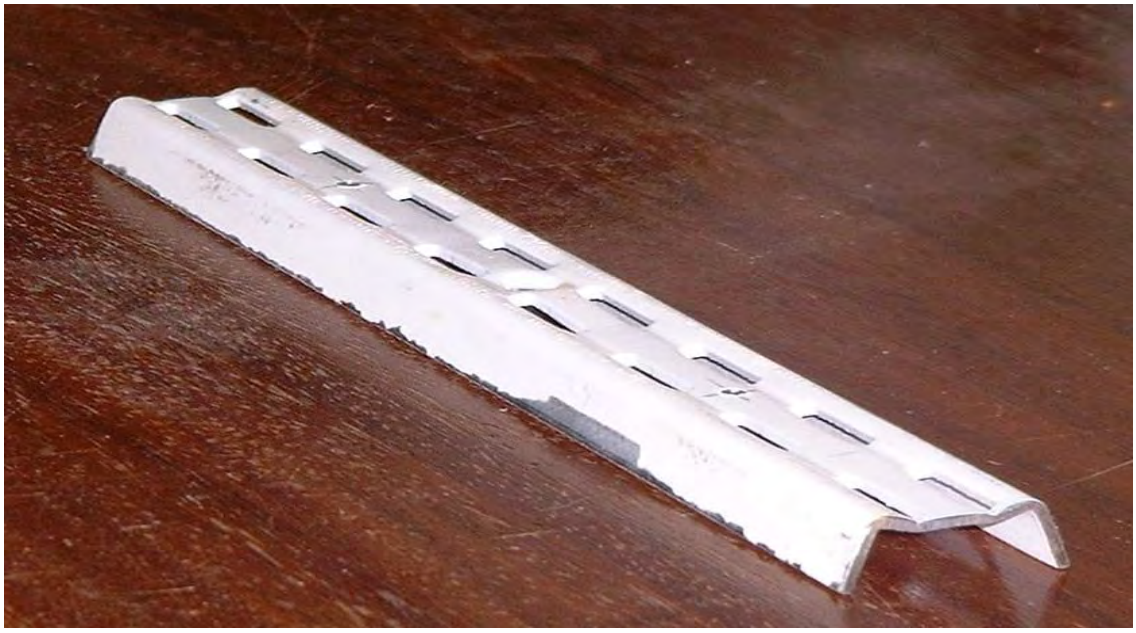

Figure 4.4b Steel sleeper used for the model test

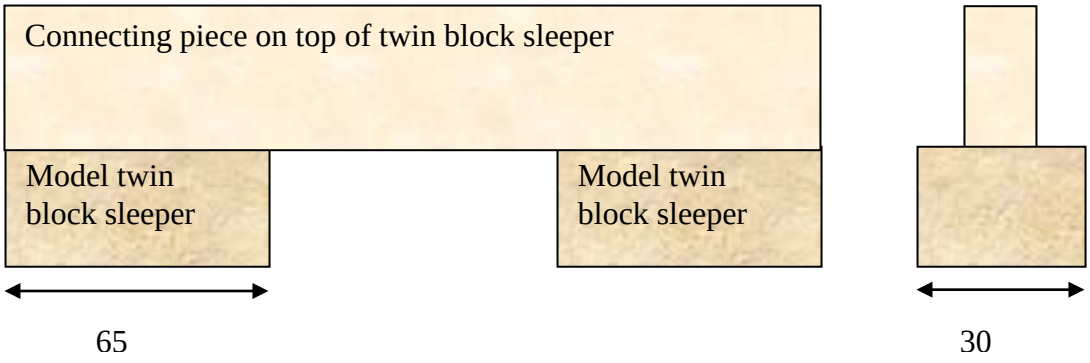

Figure 4.4c Twin block sleepers

Figure 4.4 Model sleepers

4.3.1.1 Sleepers

Wooden sleepers were used to model at tenth scale monoblock and twin block sleepers used on British Rail. Monoblock sleepers modelled in wood with two different width were used, 28mm (10^{th} scale of standard British Rail sleeper width of 280mm) and 15mm (as an alternative to the standard sleeper in the initial tests). The length of the sleeper was 245mm (10^{th} scale of 2450mm, length of standard British Rail sleeper). The twin block sleepers modelled the concrete twin block sleepers used on the Channel Tunnel Rail Link but were made of wood. The twin block sleepers were 30mm wide and 65mm long each and were connected at the top by a wooden connecting piece which simulated the connecting steel angle between two concrete blocks of a twin block sleeper.

10^{th} scale steel sleepers were fabricated in the shape of inverted troughs. The sleepers are shown in figure 4.4. Steel sleepers were manufactured by bending slotted steel flats to simulate the inverted trough shape of the steel sleepers used in British rail.

The sleepers were fixed to a wooden beam, which was bolted onto the beam of the loading machine. Small steel angles were fixed to the side of the wooden beam as shown in figure 4.4a and the sleepers were screwed on to the steel angle. This arrangement allowed

sleeper spacing to be adjusted easily and sleeper types could be changed without much difficulty, between tests. To increase the stiffness of the wooden beam a steel plate was attached to the wooden beam along its length. The metal plate allowed the assembly to be bolted to the loading beam of the compression machine (See figure 4.5b). For the loading range of the model test the beam was assumed as being infinitely rigid which implies that infinite rigidity of the rails was assumed.

4.3.1.2 Ballast and subgrade

As discussed earlier the standard railway ballast on British rail consists of stones of size ranging from 50mm to 28mm thus the standard ballast for model tests at tenth scale was ballast of size ranging from 5.0mm to 2.8mm. The grading of standard railway ballast and model railway ballast is given in table 4.1. Various sizes of small stones were used as crib ballast in the model tests carried out on the system but major part of the testing was carried out using crib ballast modelling the stoneblowing stone used on the stoneblowers. Stoneblowing stone was modelled as 2.0mm stone, tenth scale of 20mm. The grading of stoneblowing stone used for the tests is given in table4.1.

Table 4.1 Grading of full scale and model scale railway ballast

Sieve size (mm.) Full Scale	Standard railway ballast % Passing	Stoneblowing stone % Passing	Equivalent sieve size (mm.) Model scale	Model size railway ballast % Passing	Model size Stoneblowing stone % Passing
50	100	100	5	100	100
37.5	30	100	3.75	30	100
28	0	100	2.8	0	100
20		100	2		100
14		17	1.4		25
1.0		0	1.2		0

To produce the required grading of model 5mm railway ballast, ballast sizes retained on 3.75mm and 2.8mm sieves were mixed in proportion 70:30 by weight. The ballast used in the initial testing was sieved from 5-10 mm aggregate piles in the laboratory, the aggregate for this initial trial was black in colour. The stoneblowing stone (model scale) was sieved from the laboratory sand pile. To simplify sieving of stoneblowing stone it was sieved on 2mm sieve and all particles retained on 1.2mm sieve were used for the test. A detailed sieve analysis of random samples of the crib ballast was then carried out to check the percentage of particles larger than 1.4mm. The percentage of particles larger than 1.4mm in the model scale stoneblowing stone was 70-75% which is the percentage of stones size larger than 14mm stone in the full scale stoneblowing stone(see table 4.1). Thus the stoneblowing stone at model scale was a true representation of full scale stoneblowing stone. It should be noted that in full scale the stoneblowing stone consists of particles passing 14mm sieve and retained on 1.0mm sieve but for model scale the size of 1.0mm was not used as stone size of 1mm would qualify as dust.

The 5mm-2mm mix ballast after each test was separated into 5.0mm ballast and 2mm ballast by sieving on a 2mm sieve and reused. After a few tests it was observed that the 5.0mm black ballast was breaking up into smaller fragments. When at the end of the test the two ballast sizes were separated on a 2mm sieve as described above it was observed that the 2mm ballast sieved originally from sand was contaminated by fragments of the black 5mm ballast smaller than 2mm in size. The black particles in the sand ballast, by visual inspection were confirmed to be flaky shaped and thus could potentially affect the working of the two layered ballast system. It was clear that the stones from the aggregate pile used in the tests were not able to sustain repeated cyclic loading simulating railway axle load at model scale. To prevent the contamination of the crib ballast by fragments of larger bottom ballast it was decided to procure the model size ballast from a granite quarry which supplies ballast and stone blowing stone to the railways. The quarry was located in Coalville in Leicester. Stones from the 5mm residue and the 2mm fines waste pile in the quarry were

procured and were sieved in the lab to the required grading. After running a few tests with the new ballast it was observed that there was no contamination of the smaller crib ballast and ballast breakage was considerably reduced.

The ballast for the tests was placed on a steel plate base 5mm thick, which represented the subgrade. The steel plate was placed on the steel loading platform of the loading machine. Thus the subgrade was effectively assumed as being rigid. As the steel surface provided a very smooth base for the ballast sand paper was fixed to the steel surface to simulate subgrade roughness.

4.3.1.3 Loading machine

The loading machine used for the model tests was an Avery Denison (hydraulic) compression loading machine shown in Figure 4.5a. The complete test set up is shown in figure 4.5b.

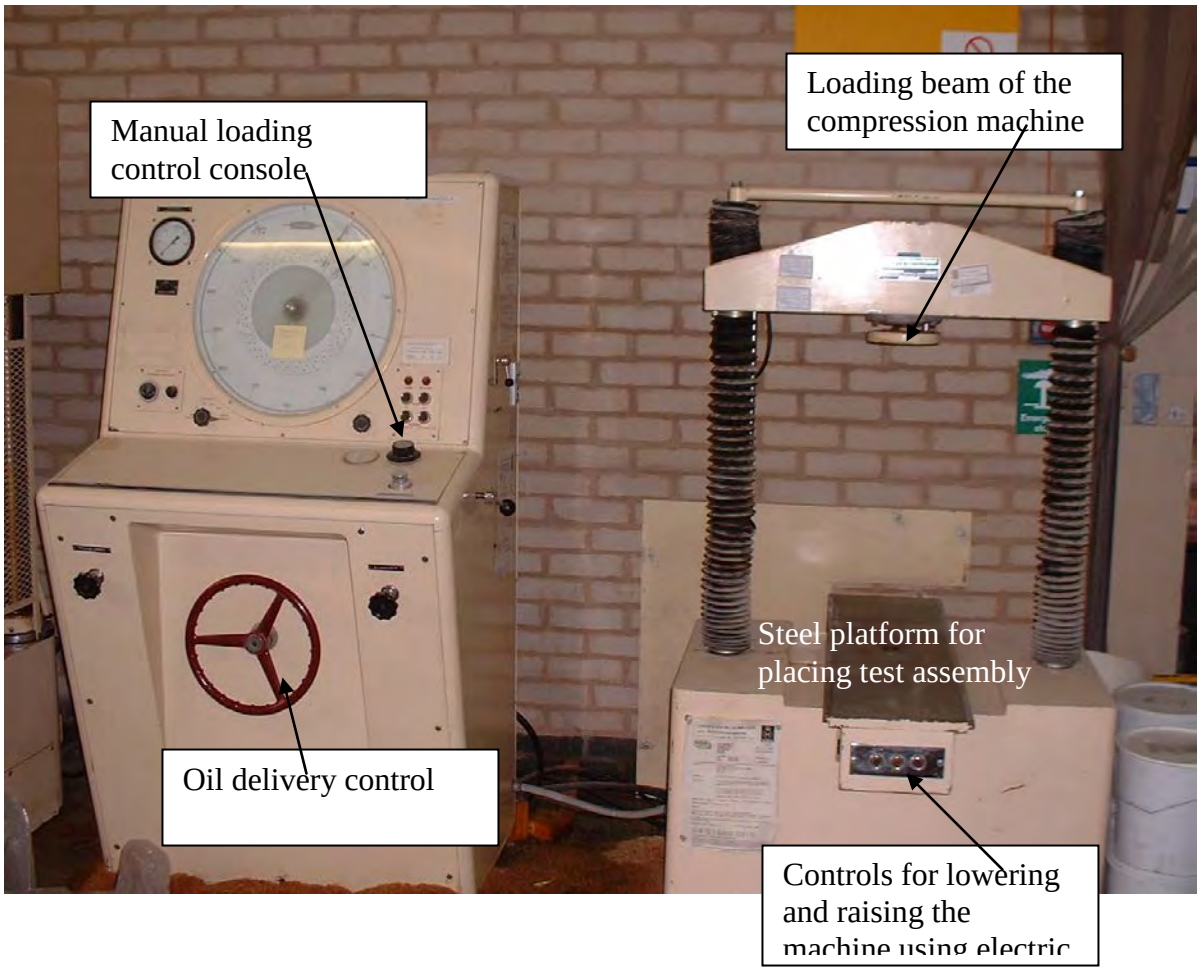

Figure 4.5a Avery Denison loading machine used for testing.

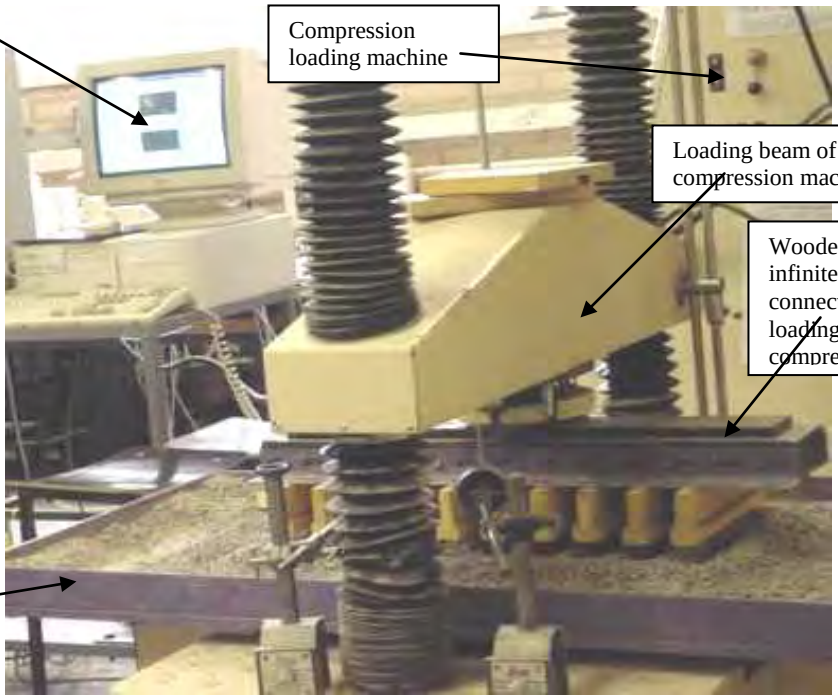
Computer controlling the test
Compression loading machine
Loading beam of compression machine
Wooden beam of infinite stiffness connected to the loading beam of compression machine
Rigid steel plate base

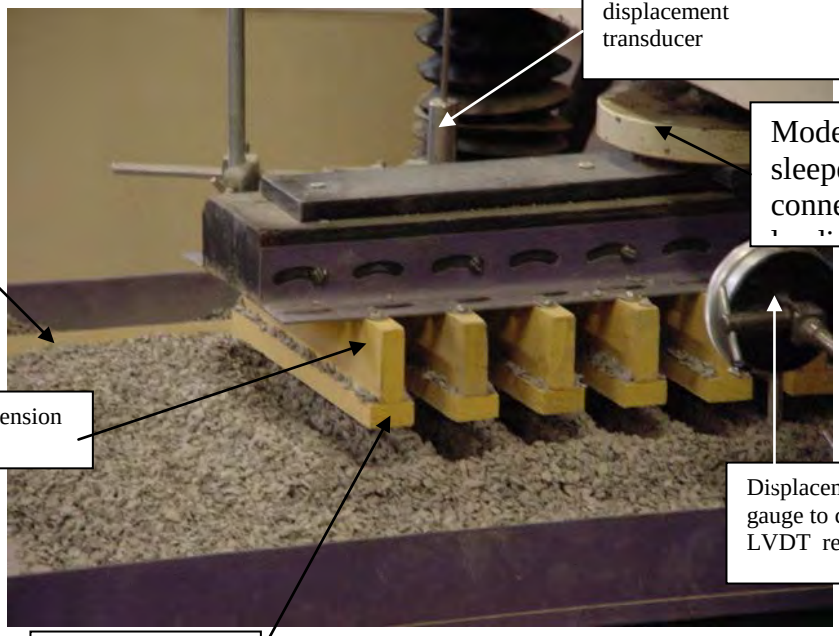
Linear variable displacement transducer
Model sleepers connected to
Sand paper fixed on top of steel base below ballast
Wooden extension pieces
Displacement dial gauge to check on LVDT readings
Wooden sleepers

Figure 4.5b Photographs of the model test set-up

The loading machine was a general purpose compression machine which was used for a variety of tests in the laboratory including concrete beam tests. The loading beam of the machine prior to loading could be positioned as required in the vertical plane by moving it with the help of an electric motor. The load was applied, by hydraulic oil delivery, between the loading beam and the steel base of the machine as shown in figure 4.5a. For simple testing like beam tests etc. the machine could be handled manually via the Loading console as shown in the figure 4.5a. Also the machine could be controlled electronically via a solenoid valve. The solenoid valve worked on a "dump" circuit and it was closed for loading. As part of this project software was written in Labview (National Instruments Inc. 2000) to enable the loading machine to be connected to, and run by a computer. Complex load cycles programmed on the computer could then be run on the machine.

For testing on the two layered ballast system the sleeper assembly was fixed to the loading beam of the compression machine. A steel plate was fixed on to the wooden beam and the assembly was bolted on to the loading beam via the steel plate. As described earlier a steel tray was used as a base to represent the subgrade. The ballast and the model assembly were placed on the steel tray for testing. The arrangement is shown in figure 4.5b. First ballast was placed on the steel tray and levelled. A piece of plywood was placed on the ballast and a few load cycles were run to properly level the ballast and consolidate it to some extent. The sleeper assembly was lowered into a position 25-50mm clear of the top of the bottom ballast, using the electric motor in the compression machine. No load could be applied using the electric motor as it was used only for positioning the loading beam at the start of the test. When the test was started the sleepers were lowered onto the ballast by hydraulic pressure and loaded to a minimum seating load as described earlier, the seating load represented the self weight of the sleeper assembly. Once crib ballast was filled in loading cycles could be run. In the 'uplift' cycles to lift the sleepers up the load was reduced to zero, the solenoid valve would 'dump' the oil delivery and the sleepers would start lifting up to their original level of 25-50 mm above the ballast, as before the start of the test. This upward movement of the sleepers was monitored using a linear variable

displacement transducer (LVDT) and at the required 'uplift' the sleepers were loaded again. This formed the mechanism of the 'uplift' cycles. For the 'simple' cycles the sleeper would be loaded with a cyclic load.

The load was cycled between 1kN and 8kN (Fig. 4.6, 4.7, 4.8). As 40% of the axle load is transferred to the sleeper through the rail (Cope 1993 – p247, Profillidis 1995 – p81), the maximum load represents 40% of a 200kN axle load (per sleeper) transmitted to the sleepers with an area effect of 1/100. The beam to which the sleepers were connected was assumed to be infinitely rigid thus the load was transferred equally to all sleepers. Thus each sleeper was loaded to a maximum load of 0.8kN. The ballast pressure under the full length of the sleeper at maximum load for different types of model sleepers is given in table 4.2 The ballast pressures achieved in the tests are comparable to those generally encountered in live railway (Anderson and Key 2000). As the load to be applied at tenth scale was very small compared to the capacity of the Denison machine it was operated at low oil delivery, which allowed the better control over the machine for small loads.

Table 4.2 Ballast pressures for model tests

Sleeper type	Ballast pressure, N/mm^2
Monoblock sleeper width, 28mm	0.11
Monoblock sleeper width, 15mm	0.21
Twin block sleeper width 30mm	0.20

4.3.1.4 Types of runs

Three types of tests were carried out on the model sleepers named as type A runs, uplift equal to displacement runs and type B runs. These tests were carried out with different combination of 'simple' and 'uplift' load cycles to try and simulate the effect of live traffic in the model tests.

1. Type A runs

These runs consisted of 20 simple loading cycles followed by uplift loading cycles. A typical loading graph with three simple load cycles and uplift load cycle for type A runs is shown in figure 4.6.

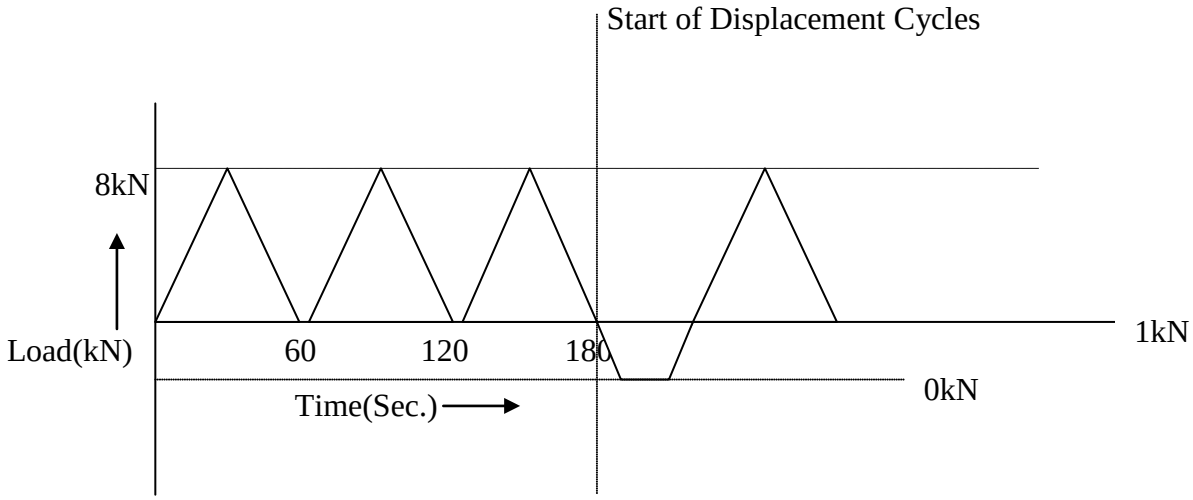

Figure 4.6 Typical model test load cycles, three simple load cycle followed by one uplift cycle

As discussed earlier the first twenty simple load cycles simulated a track without voided sleepers while the uplift load cycles simulated a track with voided sleepers. It was assumed that a voided sleeper would be pushed down onto the top of the ballast under axle load of vehicles but on passage of the axle would rise up to its original level supported by adjoining sound sleepers. Thus in the uplift cycles the sleepers were lifted up after each load cycle. A typical test would consist of 20 ‘simple’ cycles without uplift followed by uplift cycles and the uplift cycles would be continued until there was no further correction in sleeper height. Sleeper displacement at maximum load was measured for each load cycle.

2. Uplift equal to displacement runs

As described earlier the basic principle of all testing on two layered ballast system was to simulate a loose sleeper (s) in the track. In type A runs after running 20 simple load cycles, which simulate a properly packed sleeper in the track , in the uplift cycles the sleeper was lifted up between load cycles to simulate a voided sleeper in the track. The aim was to understand how a void of a certain size below the sleeper would be filled up with crib ballast of a given size.

In the type A runs after 20 load cycles a large void dramatically appears below the sleeper, an occurrence, which is very rare in live railway track. The development of a voided sleeper(s) in the railways is a slow process occurring due to various reasons over a long time period. The uplift equal to displacement cycles, were run to simulate the gradual development of void below a sleeper.

It was observed from the results of type A runs, that under cyclic loading (in simple cycles) the ballast undergoes plastic compression (non-recoverable) with each cycle, although the compression in each cycle is very small. Thus in the uplift equal to displacement cycles, after each load cycle the sleepers were brought back to their datum zero level. As the sleeper sunk into the ballast for each load cycle it was brought back up to the original zero datum level which was set up at the start of the test. This simulated the slow formation of void below the sleeper. After a single simple load cycle, uplift cycles were run with uplift height equal to displacement of the sleeper in the previous cycle. Sleeper displacement was measured at maximum load for each load cycle. A typical loading graph for these runs is given in figure 4.7.

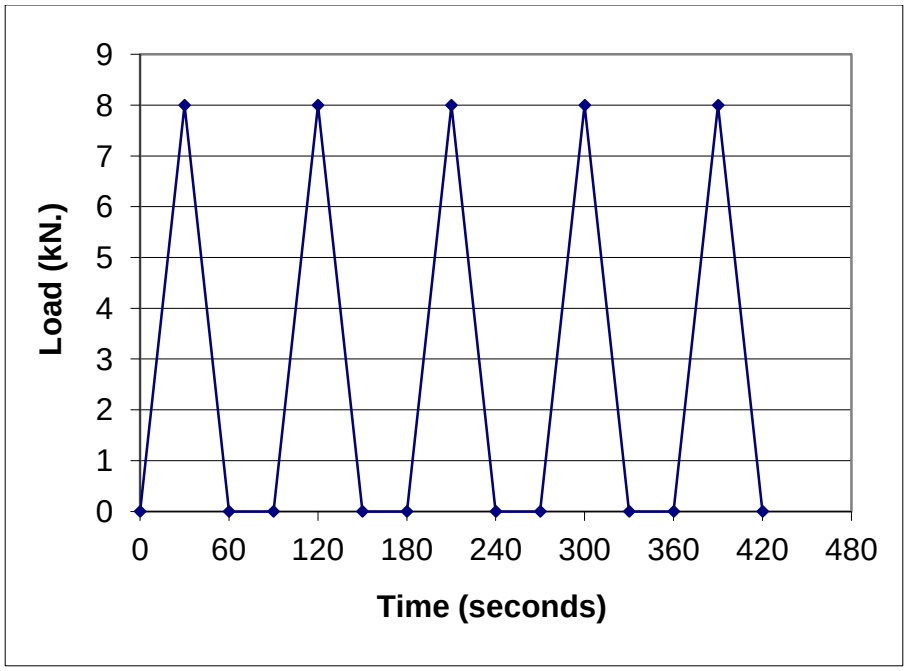

Figure4.7 Typical loading graph for uplift equal to displacement run, one simple load cycle followed by uplift cycles with uplift height equal to displacement.

3. Type B runs

For these tests the configuration of the simple and uplift cycles for the tests was changed. These tests were carried out with the initial model tests to try and finalise how detailed testing on the two layered ballast system would be carried out. For type B runs a loose sleeper was simulated by continuously loading it for 10 simple load cycles (simulating 10 axles on live track) without uplift and then lifting the sleeper up once by a specified amount before again loading it for 10 simple load cycles. This process was repeated for a few times in a test. In the type B runs it was assumed that while a train (railway traffic) was passing on top of a loose sleeper it would not lift up to its original level until all the axles had passed. Thus the sleeper was lifted up between 'trains', each train assumed to have 10 axles. Sleeper displacement was measured at maximum load for

each load cycle. It soon became apparent that this was not a correct simulation of live track conditions and after a few runs these tests were abandoned but some interesting observations were made from the results of these tests so these have been described in brief in Chapter 5.

A typical loading graph for type B runs is shown in figure 4.8. The load was cycled between 1kN and 8kN, same as for the type A runs.

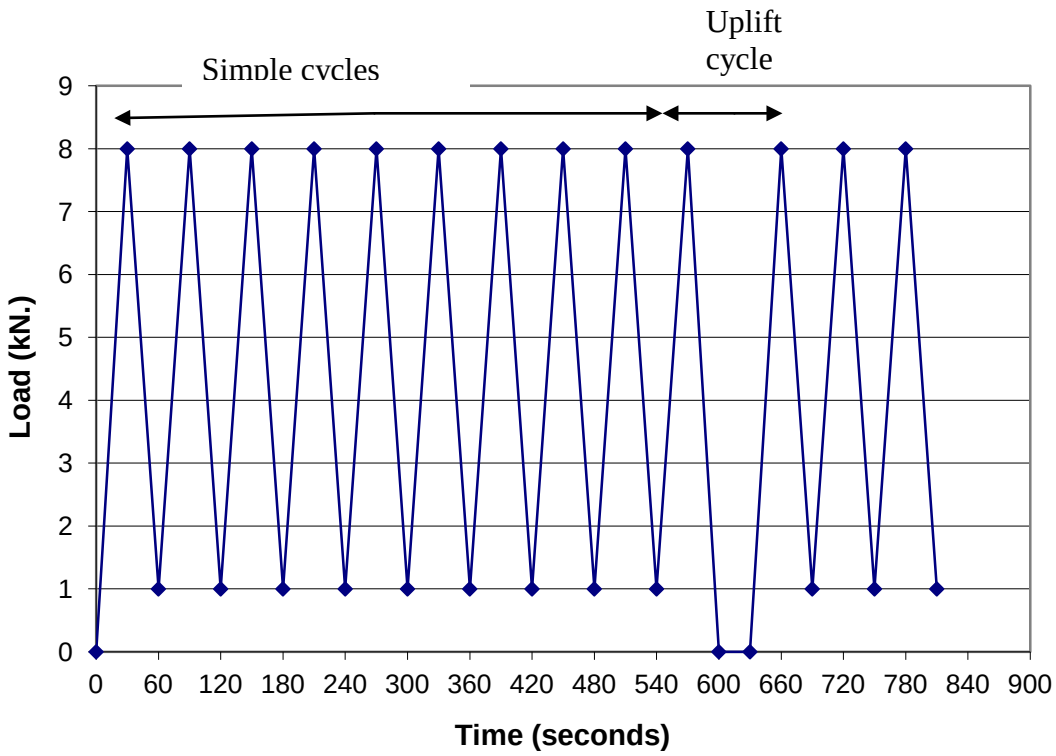

Figure 4.8 A typical loading graph for type B runs.

For all model tests, although the maximum load represents 10^{th} scale of standard railway axle loading, including dynamic loads, transmitted to the sleeper, the rate of loading in the tests did not simulate live track loading.

4.3.1.5 Problems with oil delivery

As mentioned earlier, the initial tests were run under a very low oil delivery in the Denison compression machine. Thus very good control over the loading machine was possible with the load gradually being increased to maximum for each loading cycle and the same maximum load was applied for each loading cycle. The elastic compression for the model assembly was the same for all load cycles and thus the graph lines are smooth with no spikes in the graph. This was possible only when running short tests with a small number of loading cycles.

It has been explained in the model test set up that a LVDT was used to measure the uplift displacement in each uplift cycle. The load would be reduced to zero and the sleeper assembly would rise up slowly to its position of rest. This movement of the sleepers was continuously monitored by the LVDT. When the sleeper level was 2.5mm above the datum zero level the computer would instruct the machine to apply the load again i.e. a voltage input would be given by the computer to apply the load. The LVDT would stop reading the displacement and the control would pass to the computer. The computer would assume that the correct uplift has been achieved as the load was applied as soon as the uplift was 2.5mmon the LVDT and the uplift achieved would be displayed in the indicator on the front panel. To cross check on this dial gauges were fitted to the loading beam of the compression machine in a manner similar to the LVDT. The dial gauge readings for the uplift revealed that in some uplift cycles the uplift was more than that specified for the test. The error was within 0.5mm of the actual uplift and occurred for a few cycles. This was happening because of very slow rate of loading at low oil delivery. As mentioned above the computer on receiving data from the LVDT of the uplift being achieved would apply the load and it would assume that the correct uplift has been achieved. In reality what happened was that although the computer would instruct the machine to apply the load, at very low oil delivery the machine took sometime to start applying the load. Although this time lag was of perhaps a few seconds the sleeper assembly for this time span would still be slowly moving upwards until load was applied. Thus it was clear that better control over the coordination of the machine and the LVDT was required. In the short term this was resolved by suddenly giving a very high voltage input from the computer to the machine to

apply the load, when the correct uplift was achieved and checked by the LVDT. This resulted in the load being applied almost instantly to the sleeper assembly and thus the extra uplift as before did not occur. These changes were made in the computer program in Labview. Also the calibration equation for the LVDT was also refined and made more accurate. After carrying out these changes the uplift was again checked by the dial gauges and was found to be within 0.1mm of the specified uplift height. When carrying out detailed testing, described further, the problem was resolved as the tests were run on a higher oil delivery in the Denison machine, this has been discussed in section 4.3.3.

4.3.2 Virtual Instrumentation of model test set up

The model tests were run under full computer control and once all the parameters had been input at the start of the test the test continued to the end without any further intervention from the user. A Das 16 data logging board (Computer Boards inc. 1994) coupled with Labview software (National Instruments inc. 2000) was used to enable the computer to communicate with the various equipment used in the test (See Fig. 4.9). Two analogue input and one analogue output channel of the Das 16 board were used.

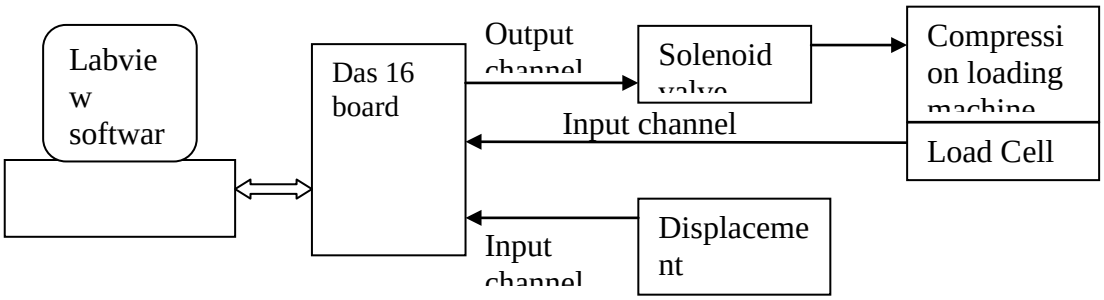

Figure 4.9 Hardware and software set up for test control.

The output channel of the DAS 16 board was connected to the solenoid valve to control increase and decrease of oil delivery on the compression machine. An in-built oil pressure transducer in the compression machine was connected to the input channel on the DAS 16 board, which read the load on the machine. One input channel on the board was dedicated to reading the Linear Variable Displacement Transducer (LVDT), connected to the beam of the compression loading machine as shown in Figure 4.9, to read the displacement of the sleeper assembly and also to check on the uplift height of the sleepers in the uplift cycle. A computer program was written in Labview to run the tests on the model. The computer program is given in appendix A.

4.3.2.1 Calibration of compression machine and displacement transducer

As described earlier, in virtual instrumentation, computer software like Labview (National Instruments inc. 2000) communicates with various machines through the output and input channels on a data acquisition board like DAS 16 (Computer boards inc. 1994). The data acquisition board acquires data from data acquisition instruments like displacement transducers and load cells and passes them on to the computer software for processing. The data communication between the above components of virtual instrumentation is in the form of a low voltage signal within the range of –10v to +10v.

Labview software has inbuilt functions like ‘Aout’ and ‘Ain’ which respectively give a voltage output to the output channel of the DAS 16 board and read a voltage input from the input channel of the DAS 16 board. Again all data is supplied to Labview in the form of a low voltage signal which is uncalibrated. Uncalibrated voltage reading in Labview appears as a data value on the Front Panel. For known voltage input and small increments in the voltage input the input voltage can be calibrated to read a real time voltage in Labview. To carry out the above operation a voltage source was connected to Labview via the DAS 16 board. The ‘Ain’ function in Labview was used to read the input voltage from the voltage source. The uncalibrated voltage appeared as a data value on the screen. Small load increments within the voltage range of +-10 v were input into Labview and corresponding data values read on the screen for each voltage increment. Thus Labview was calibrated very accurately to read realtime voltage from any voltage source (Figure 4.10).

This formed the basis of calibration of all data acquisition instruments in Labview. All voltage inputs from a data acquisition instrument were calibrated to read the real time voltage in Labview and for known increments in the said data value (voltage) the data calibrated in Labview.

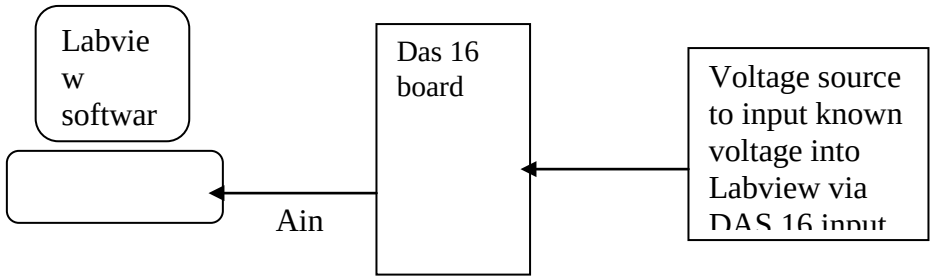

Figure 4.10 Calibration of voltage in Labview.

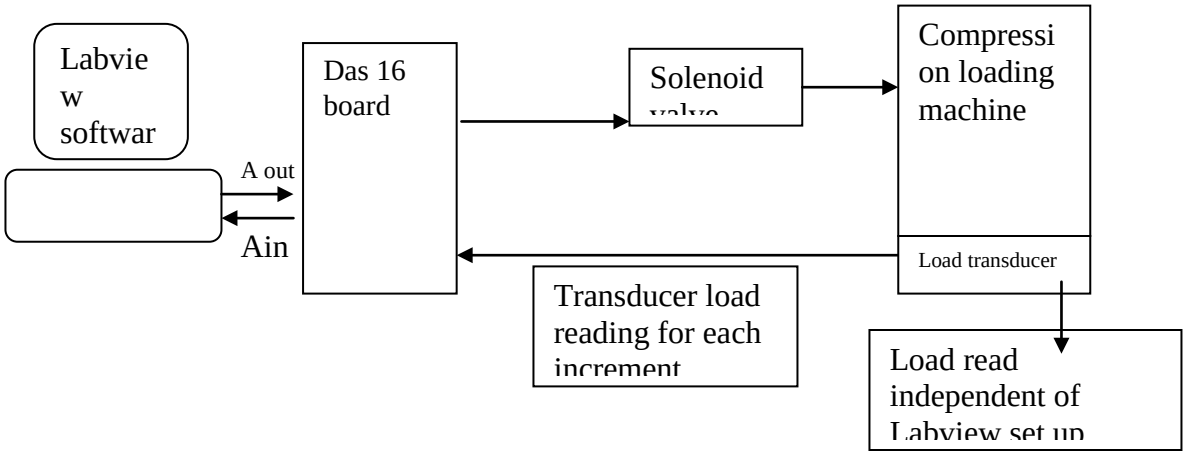

Figure 4.11a Calibration of compression machine

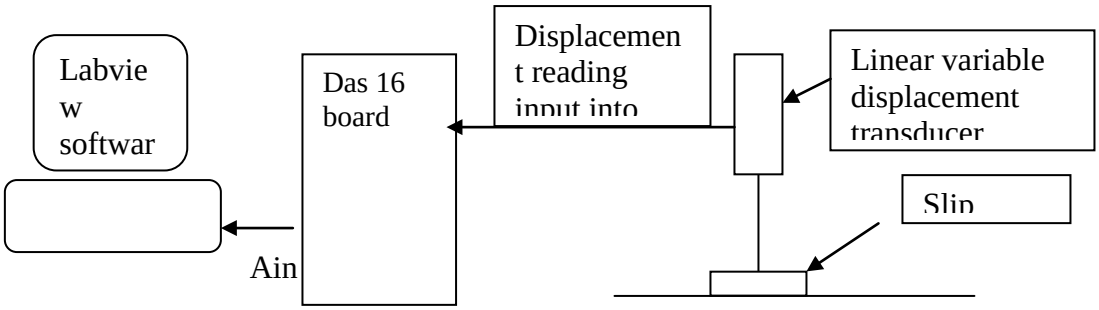

Figure 4.11b Calibration of displacement transducer

Figure 4.11 Calibration of LVDT and compression machine.

bading machine and the linear voltage displacement transducer via the DAS 16 board. An output channel on the DAS 16 board was used to control the increase or decrease in load on the compression machine. Using the 'Aout' function in Labview, small increments in voltage were given to the solenoid valve via the output channel to load the compression machine in small increments. The 'Aout' function as described earlier is available in labview, which allows the computer to give voltage increments or decrements via the output channels of the DAS 16 board. An inbuilt oil pressure transducer in the compression machine was

connected to the input channel on the DAS 16 board. The Labview function Ain was used to read transducer data. The data acquired from the load cell was calibrated in Labview as real time voltage. After each increment the load cell reading of the compression machine was read in Labview in form of real time voltage. The load cell was also connected to a display unit independent of the Labview set up from where load readings could be taken. Thus both the load and the voltage signal generated by the load in Labview were known. In this way using known loads the compression machine could be calibrated in Labview. The calibration equation could be created in Labview program using its mathematical functions and saved as a subroutine (subVI) in the program. The subVI is shown in appendix.

Similarly the linear variable displacement transducer readings were input into Labview via an input channel on the DAS 16 board and read by the function Ain in Labview. These readings were calibrated in Labview to give real time voltage. The displacement transducer was given known displacements using slip gauges and the voltage signal for each displacement value was read in Labview. Thus using known displacements the displacement transducer was calibrated in Labview.

4.3.2.2 Labview Control Panel

Parameters required to control the test were input through the Labview interactive screen known as the Control Panel. Data output, which was the sleeper position at maximum load for each cycle, was stored in a floppy disc and also plotted on screen as a graph of maximum sleeper displacement for each load cycle. As shown in figure 3.6 the following parameters could be set up in the control panel

1. Number of simple cycles
2. Number of uplift cycles
3. Uplift height for each uplift cycle
4. ‘Main cycles’ for different combination of simple and uplift cycles

The simple and uplift cycles were run under a main loop shown in figure 4.12 as control named ‘Main cycles’. The Main cycles control was used to specify the number of times any combination of simple and uplift cycles would be run. For type A runs the Main cycles parameter was 1, so the test would run once for the specified number of simple and uplift cycles and stop. While for the type B runs the Main cycles parameter was specified greater than 1, the number of simple cycles specified as 10 and the number of uplift cycles specified as 1. If the value of Main cycles for type B runs was specified as 3, the test would run for 10 simple cycles followed by a single uplift cycle and this loading pattern would be repeated three times.

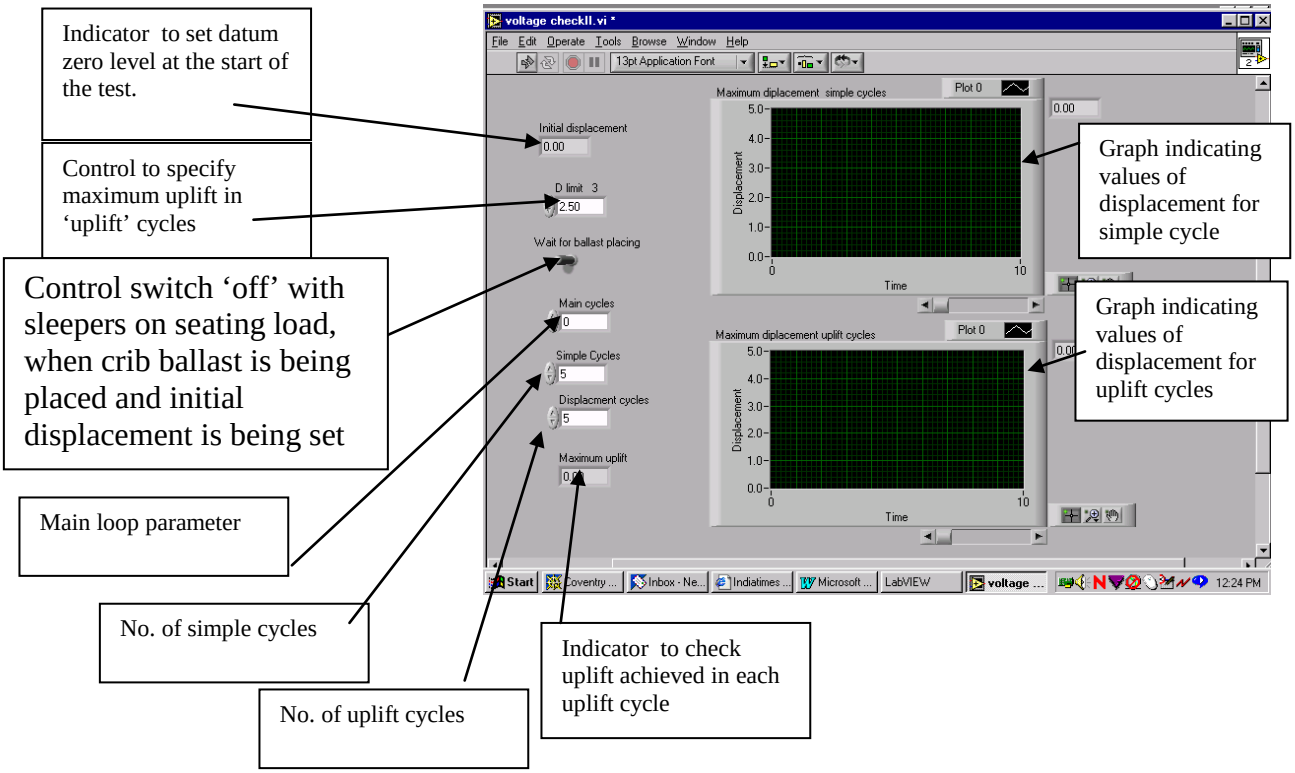

Figure 4.12 Control panel

With the value of main loop as 1 and simple cycles specified as 20 and uplift cycles specified as 20 the test would run once for 20 simple cycles and 20 uplift cycles. If the main loop value in the Labview front panel was specified as 2 then the test would be run for

20 simple cycles followed by 20 uplift cycles and then repeated a second time for 20 simple and 20 uplift cycles. In this way if required different combinations of simple and uplift cycles could be run although for most of the model tests the main cycles control was specified as 1.

The sleepers were lowered on top of the bottom ballast with a minimum seating load of 1kN. The control switch named ‘wait for ballast placing’ was on the ‘off’ position and the load was maintained at the seating load while the control switch was in the ‘off’ position i.e. load cycles were not started until the switch was toggled to its ‘on’ position. This allowed the user to place the crib ballast around the sleepers. The LVDT reading for the sleeper displacement was displayed in the indicator ‘initial displacement’ as shown in figure 4.12. The LVDT was manipulated manually to read zero displacement and this position of the sleepers formed the datum level for the test. The maximum uplift to be achieved in the uplift cycles (the void size) was specified and the number of simple cycles and uplift cycles to be run were also specified. Smaller crib ballast was filled around the sleepers and the control switch was toggled to its ‘on’ position and the loading cycles were started. The loading sequence was simple cycles followed by uplift cycles. The maximum sleeper displacement for each load cycle was measured. The data was written to the floppy drive and also plotted as a graph of maximum sleeper displacement for each load cycle on the Labview Front panel as shown in figure 4.12. Thus the results could be observed while the test was in progress. The data file in the floppy drive was accessed through MS – excel and the data could be processed in form of charts.

While the test was in progress, in the uplift cycles the maximum uplift achieved by the sleeper was displayed in the indicator ‘maximum uplift’ as shown in figure 4.12. This allowed a check on the uplift achieved in each cycle. The displacement readings taken by the LVDT were cross-checked by installing dial gauges to read the displacement of the loading beam to which the sleepers were fixed.

The load cell readings of the compression machine and the calibrated load readings of Labview were cross checked by reading load using a different load cell independent of the

test set-up. The load cell was placed in the compression machine and the reading from the load cell was compared with the load reading from the digital readout of the compression machine, both were same. This was done in addition to the regular calibration of all the equipment in the laboratory.

4.3.3 Data processing

Data from a test was obtained as a data file in the floppy disc. This data file could be accessed through MS – excel program and the data could be processed. It was expected that there would be some elastic compression of the model assembly under load. To check this the sleeper assembly was placed directly on the sandpaper with a minimum seating load, datum level was set to zero at this load. Load cycles were run without any ballast. Displacement of
the sleeper assembly, relative to datum zero level, under maximum load (8kN.) for each cycle was recorded.

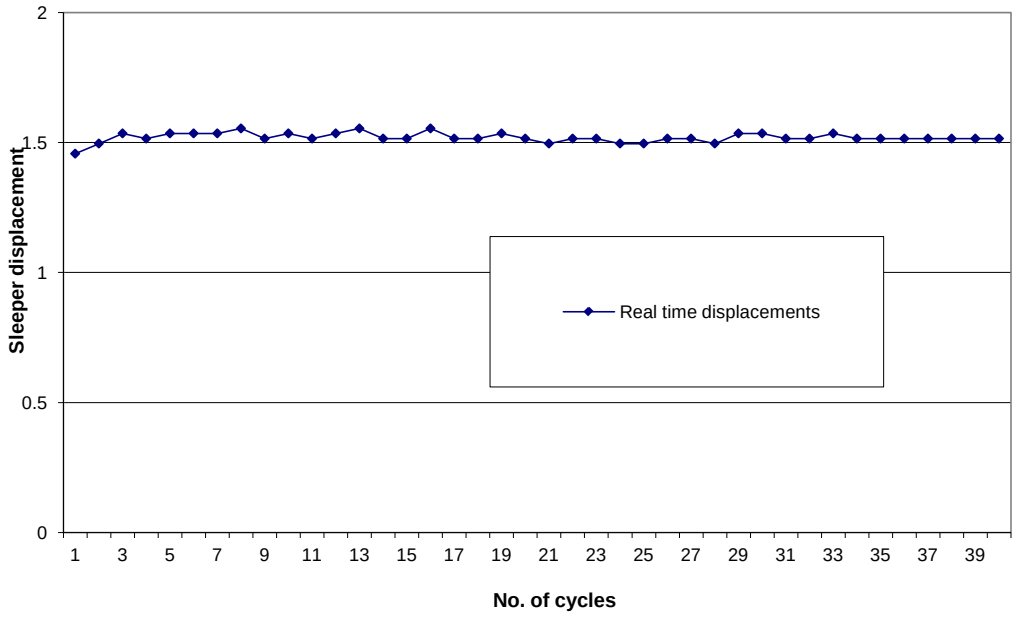

Figure 4.13 Test run without ballast - Elastic compression of model assembly at maximum load

A graph of sleeper displacement against cycle number is shown in figure 4.13. It can be seen that the maximum elastic compression of the model assembly under the applied load is 1.5mm and it is constant for the given loading. The same data was then plotted against the number of cycles by subtracting the first displacement reading from the rest of the data. The results are shown in figure 4.13.

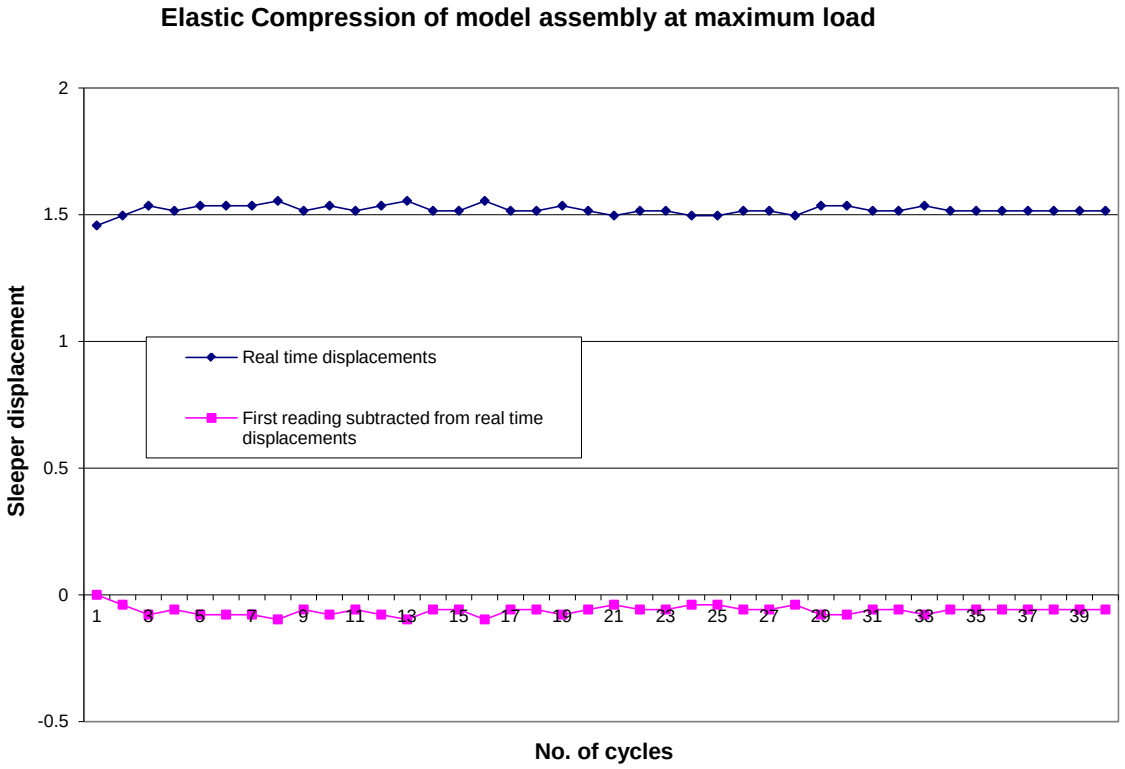

Figure 4.14 Test run without ballast.

With the first reading subtracted from the data the elastic compression of the model assembly is zero. With load cycles run with the sleeper assembly placed on bottom ballast the sleeper displacement readings will also measure the elastic compression of the assembly for each load cycle. To eliminate the elastic compression of the model assembly from the data for each model test the first displacement reading was subtracted from the data. An

example is shown in figure 4.15, where the test was run with smaller crib ballast for 20 simple and 20 uplift cycles. The data was processed to subtract the first displacement reading from all data. The results are shown in the figure 4.15.

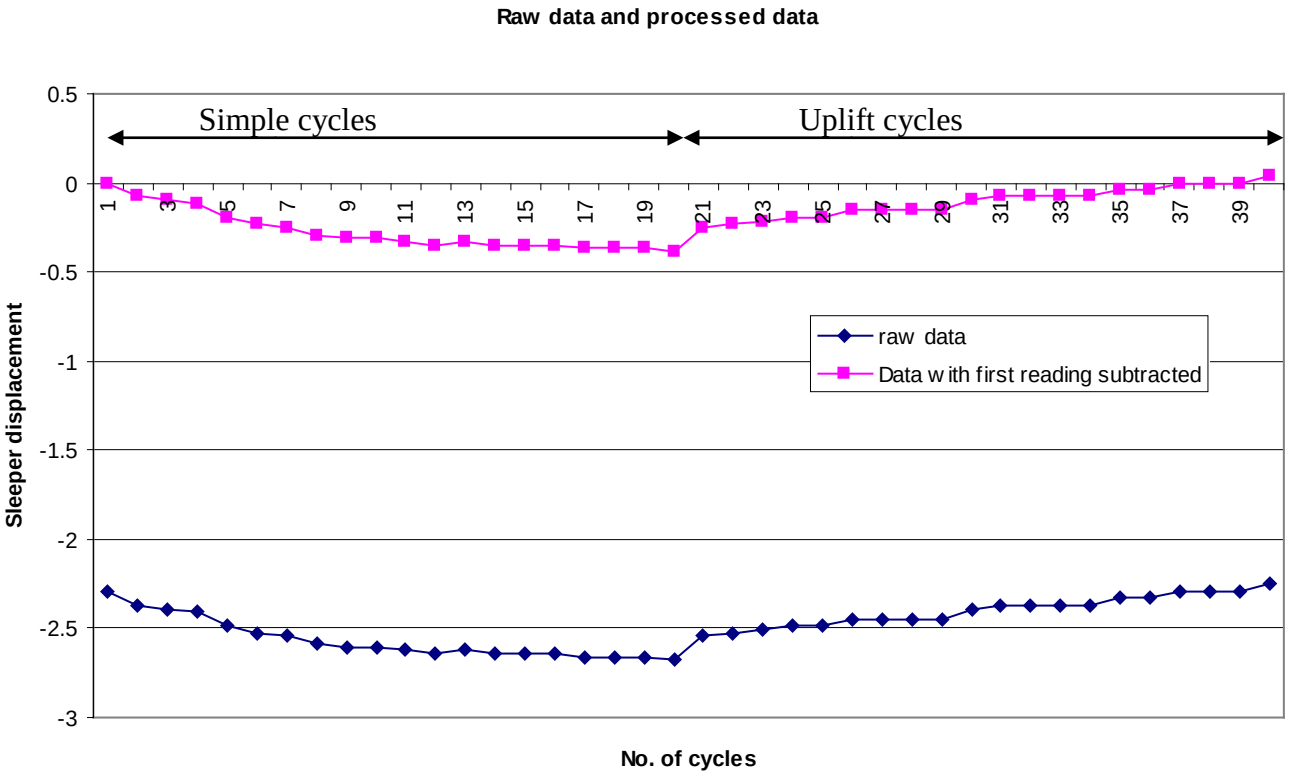

Figure 4.15 Comparison of raw data and processed data from a model test.

Thus it is clear from figure 4.15 that by subtracting the first displacement reading into the ballast the elasticity of the model assembly has been removed from the measurements.

This approach has been consistently followed in all testing, both model and full scale. The first displacement reading is subtracted from all subsequent displacement readings to eliminate the elastic compression of the system from the data.

While running the sleeper assembly directly on sandpaper to measure the elastic compression of the test assembly it was also noted that the elastic compression measured was sensitive to very slight changes in the maximum load. For a very small change in the maximum load the elastic compression would also change. E.g. If the elastic compression of the assembly for a load of 8kN was 1.5mm for a load of 7.8 kN would be 1.3mm and for a load of 8.4kN would be 1.6mm. Considering the small displacement being measured it was thus important to achieve the same maximum load for each cycle. In the initial tests this was achieved by running the Denison machine at very low oil deliverys and the set up worked properly as very short tests with small number of load cycles were run. When it was required to run a large number of cycles in subsequent tests it was observed that after running a few cycles the Denison machine could not run further cycles as it could not run for longer periods on very low oil deliverys. Thus the oil delivery on the machine had to be increased slightly to facilitate running the tests for a longer duration. It was observed that for higher oil delivery it was virtually impossible to maintain exactly the same maximum load for each cycle. The load would be within a certain range either side of the specified maximum load. As mentioned earlier the load on the machine was increased by giving a low voltage signal to the solenoid valve through Labview. It was observed that for higher oil deliverys the relation between the voltage increase and the load was not linear. When at zero load a large voltage input from the computer was required to load the sleeper assembly but as the load increased the same amount of voltage increase would push the load past the maximum load. Thus to achieve better control over the machine and the maximum load achieved, the input voltage increments as the load increased were made smaller. Even after making these changes in the Labview program given the limitation of the equipment it was not possible to achieve the same maximum load for each load cycle. Thus the maximum specified load was 8kN but the maximum load achieved would be within the range of 7.8kN to 8.4kN. Thus elastic compression under maximum load would vary between ± 0.3 mm approximately. This resulted in spiky graphs when running long tests with large number of load cycles, although it did not alter the final results as the trend of the graph was still the same. The lines were not smooth but it was observed that the error in the displacement measurement was similar both sides of an average reading as seen in the

graphs and for large number of cycles the trends in the graphs are similar. Thus in case of model tests the graphs were represented as moving average of the data as shown in figure 4.9, for a typical model test data.

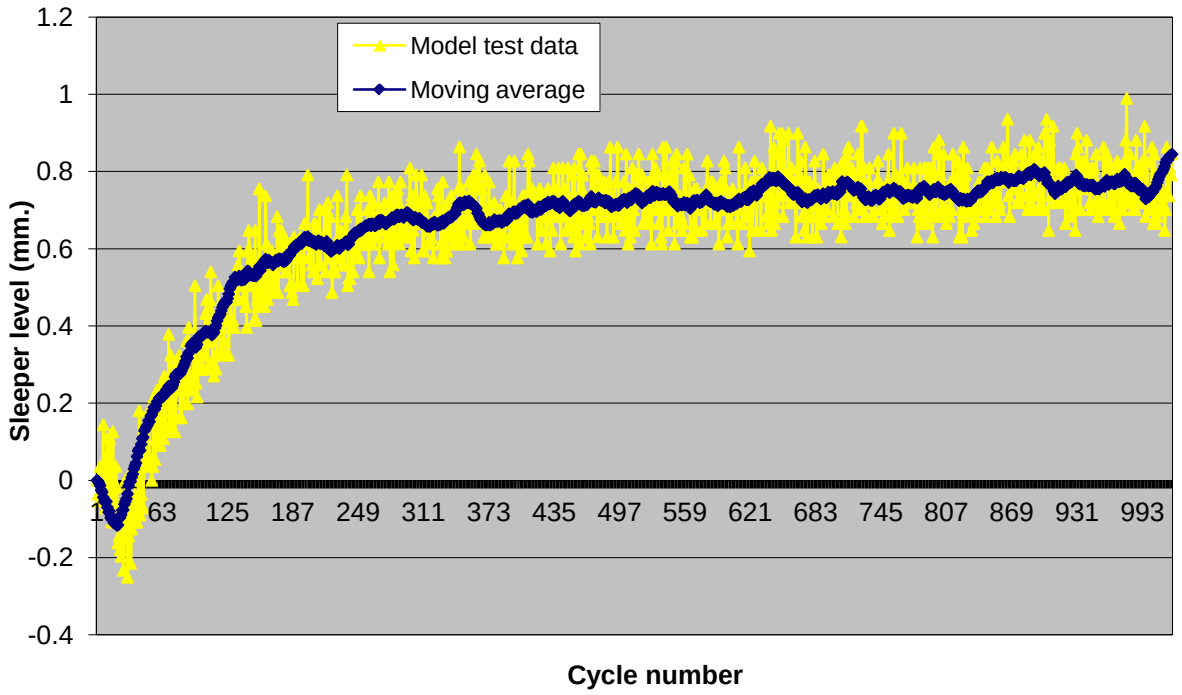

Figure 4.15a Model test data fitted with a moving average curve.

4.3.4 Instrumented sleeper

The instrumented sleeper was a monoblock sleeper instrumented with strain gauges. This sleeper was used to study the movement of ballast under the sleeper in uplift cycles and the change in stress state along the width of the sleeper in the uplift cycles, as the crib ballast migrated towards the centre of the sleeper cross-section. It was assumed that the crib ballast would move gradually from the edge of the sleeper to the centre of the sleeper during the uplift cycles in the course of the test and the aim of the instrumented sleeper was to observe the change in state of stress below the sleeper as the ballast moves towards the

sleeper centre. A diagram of the sleeper is shown in figure 4.16. The strain gauge sleeper was of the same size as the wooden sleepers with five metal bars 10mm square fixed to the bottom of the wooden sleeper. The thickness of the wooden sleeper was reduced to allow fixing of the metal bars such that the final thickness of the straingauge sleeper was the same as that of the wooden sleeper. The metal bars were screwed on to the wooden sleeper (See figure 4.16). As shown in figure 4.16 the central portion of the metal bars was suspended free of the wooden sleepers by a few mm. The remaining length of the metal bars was supported continuously on the wooden sleeper. The screws used to fix the steel bars to the beam were fixed as shown in figure 4.16 to isolate the central portion of the metal bars which was not supported by the wooden beams from the continuously supported part of the metal bars. It was expected that when loaded the central portion of the metal bars would act like a simply supported beam. Strain gauges were fixed to four metal bars at midspan. The strain gauges were fixed to steel bars numbered 1, 3, 4 and 5 as shown in figure 4.16. The strain in the strain gauges under load could be measured and calibrated to give the state of stress under the sleeper. The strain gauge sleeper through its wooden top piece could be connected to the loading beam similar to the wooden sleepers. It was used at the centre of the sleeper assembly directly under the loading beam of the compression machine.

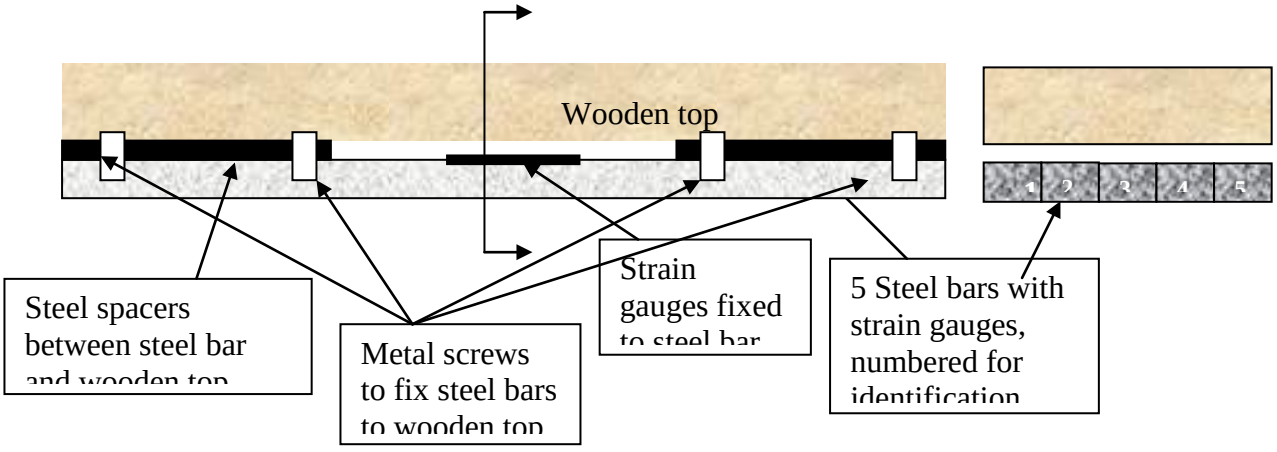

Elevation Section

Figure 4.16 Details of strain gauge sleeper.

4.3.4.1 Computer set up for the instrumented sleeper.

The strain gauges were connected to Labview through the input channels on the DAS 16 board. The same Labview program used for running tests on other model sleepers was used to run test on the instrumented sleeper. Changes were made to the Labview program for running model tests, to read the strain in the sleeper at maximum load for each cycle starting from the ‘simple’ cycles. Thus both the displacement of the sleeper and strain in the sleeper were read at maximum load. The hardware arrangement is shown in the schematic diagram in figure 4.17

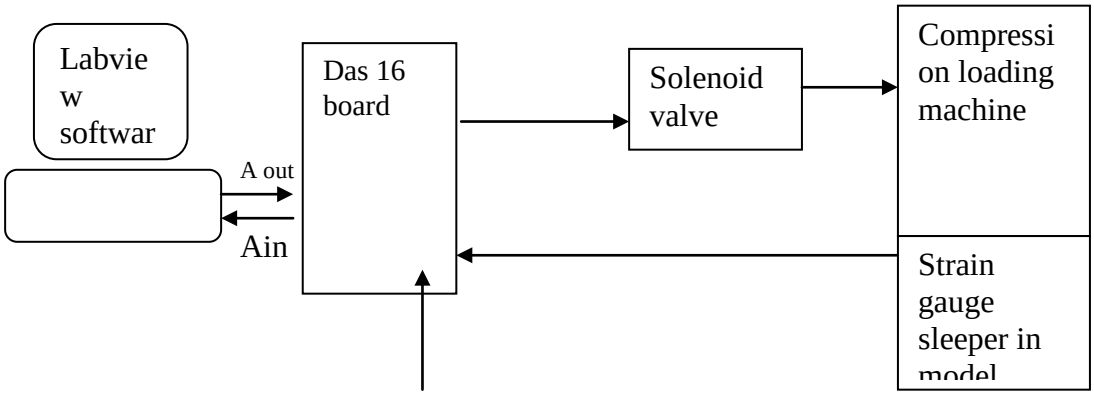

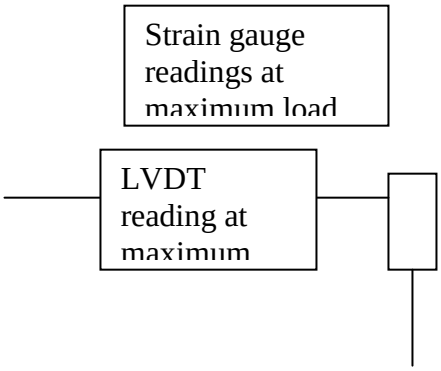

Figure 4.17 Hardware set up for instrumented sleeper

The data again was stored as a data file on a floppy disc and was also plotted on the Labview front panel in form of graph of strain readings against number of cycles, as the test progressed. Raw strain gauge data was collected from a test and calibrated later. The labview Control panel for the straingauge program is shown in figure 4.18 The four lines in the graphs of straingauge readings is the data value from the four strain gauges. As seen in the figure strain gauge readings were also displayed in digital indicators for the simple and uplift cycles

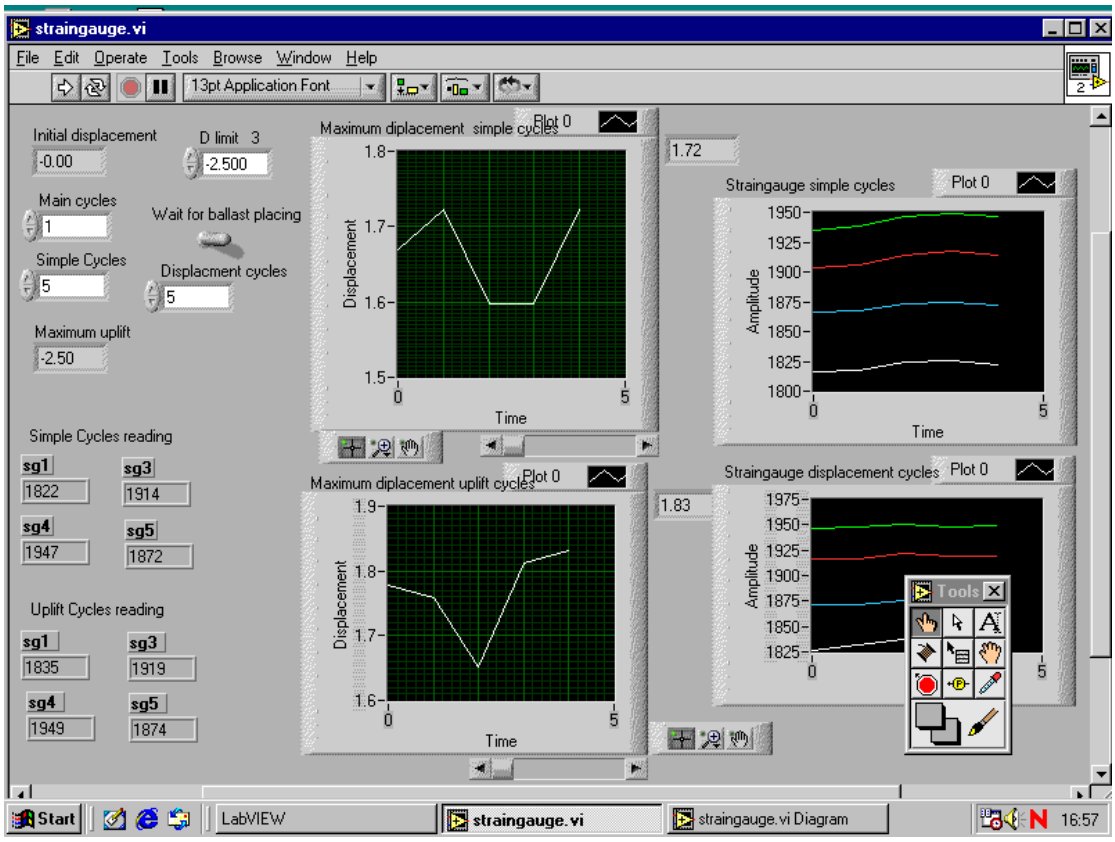

Figure 4.18 Labview Control panel for strain gauge program

4.3.4.2 Calibration of strain gauges.

Raw data from the strain gauge was acquired in Labview to be calibrated later. The object of interest here was not the level of strain in the sleeper but the presence or lack of it. The strain gauges were placed across the width of the sleeper. It was expected that with the first few uplift cycles the edge gauges would be stressed more than the centre gauges as the crib ballast moved into the void below the sleeper but progressively the stress would level out to the same level in all the strain gauges as the ballast would travel to the centre of the sleeper cross section.

The strain gauges installed in the instrumented sleeper were capable of reading compression as well as tension loads. While designing the strain gauge sleeper it was

assumed that the metal bars to which the strain gauges were fixed would behave like a simply supported beam. The sleepers were to be placed on a ballast bed and for the simple cycles it was easily evident that all the metal bars would bend in hogging and thus the strain gauges would be in tension (See figure 4.19). It was expected that with the start of the uplift load cycles as the crib ballast migrated to the sleeper bottom the crib ballast initially would be supporting the edges of the sleeper . Thus the edge bars would be supported along their length by the crib ballast and the edge strain gauges 1 and 5 would be in tension . The ends of all metal bars would be supported on the smaller crib ballast as well because the ballast would migrate to under the sleeper from all sides (shown in figure 4.19). Thus the central portion of the central metal bars with strain gauge number 3 and 4 would be free, off the ballast top and would bend in sagging under the load and the strain gauges would be in compression. It was expected that with gradual movement of the crib ballast towards the centre of the sleeper cross-section the stress in strain gauges 3 and 4 would change from compression to tension.

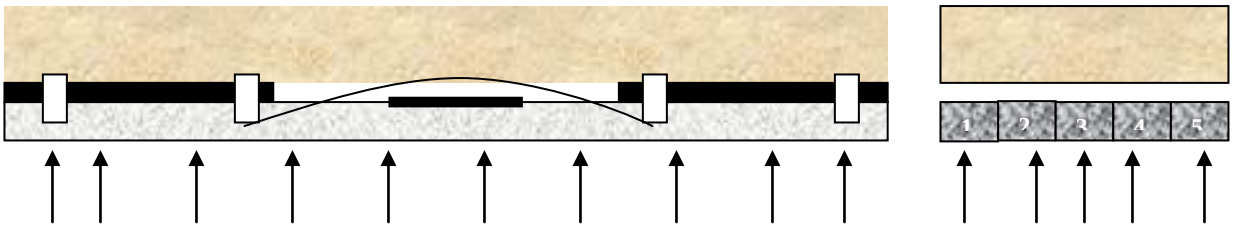

Strain gauge sleeper on bottom ballast in simple loading cycles, all strain gauges are in tension

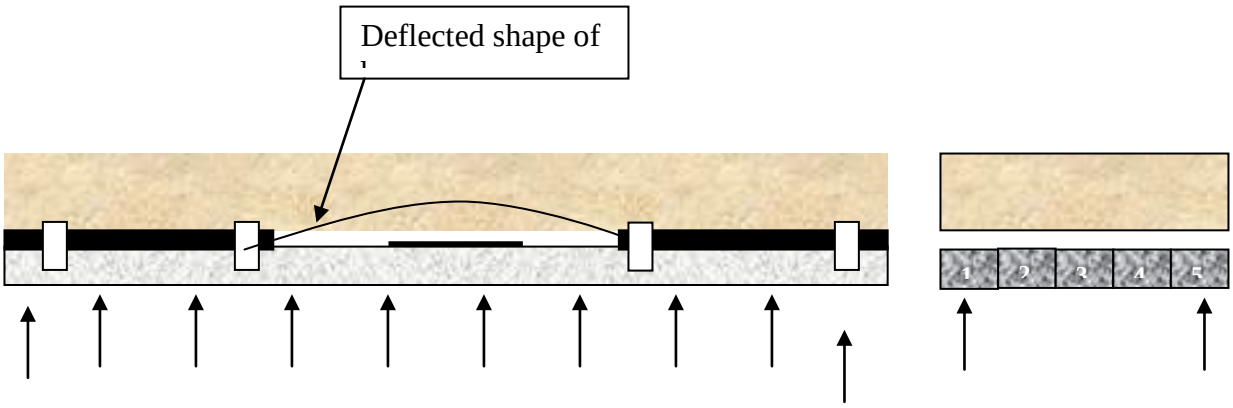

Strain gauge sleeper on migrating crib ballast in uplift load cycles, long section through bar with strain gauge 1, strain gauge in tension

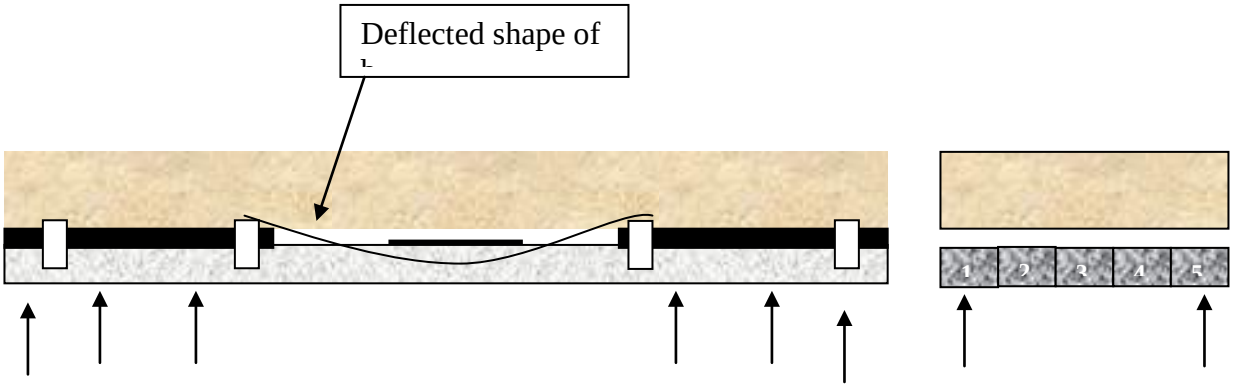

Strain gauge sleeper on migrating crib ballast in uplift load cycles, long section through bar with strain gauge 3, strain gauge in compression.

Figure 4.19 Change in stress under the strain gauge sleeper in simple and uplift load cycles.

It was decided to calibrate and present results for strain gauge readings of strain gauge no. 1 and no. 3 as the aim was to observe the time taken by the crib ballast to reach the centre of the sleeper cross-section. Based on description of stress change under sleeper as discussed in the preceding paragraphs and as described in figure 4.19 the strain gauge sleeper was calibrated as follows:

1. Load at the centre of the sleeper

This is shown in figure 4.20. The sleeper was placed on top of two metal bars as shown in figure 4.20 and load was applied in small increments from 0kN to 5kN. This represented sleeper on ballast in simple loading cycles with the strain gauges measuring tension in the bars. The total load was assumed to be equally distributed to five metal bars.

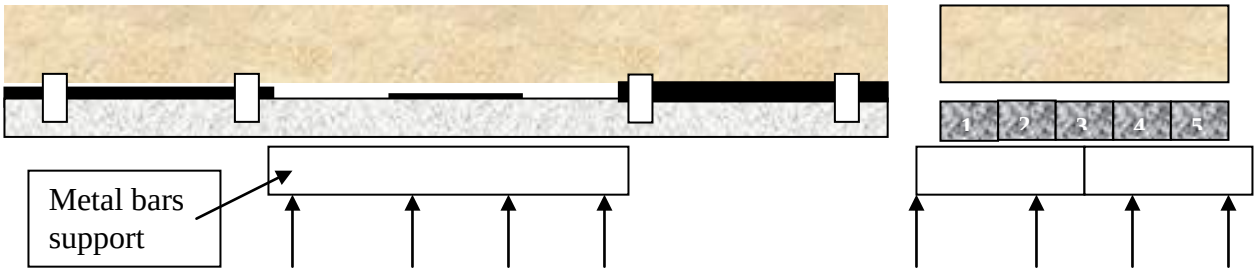

Figure 4.20 Strain gauge sleeper calibrated for tension in metal bars.

In all the model tests the maximum load applied on the 10 sleeper assembly was 8kN. It has been discussed earlier that the load was distributed equally to all ten sleepers as the sleepers were connected to a wooden beam of infinite stiffness. Thus the load on one

sleeper would be 0.8kN. Further distributing the load equally between five metal bars with strain gauges the maximum load on one bar should be 0.16kN. So the strain gauges were calibrated in tension in the range from 0kN to 0.4kN. The calibration of strain gauges 1 and 3 is shown in figure 4.21

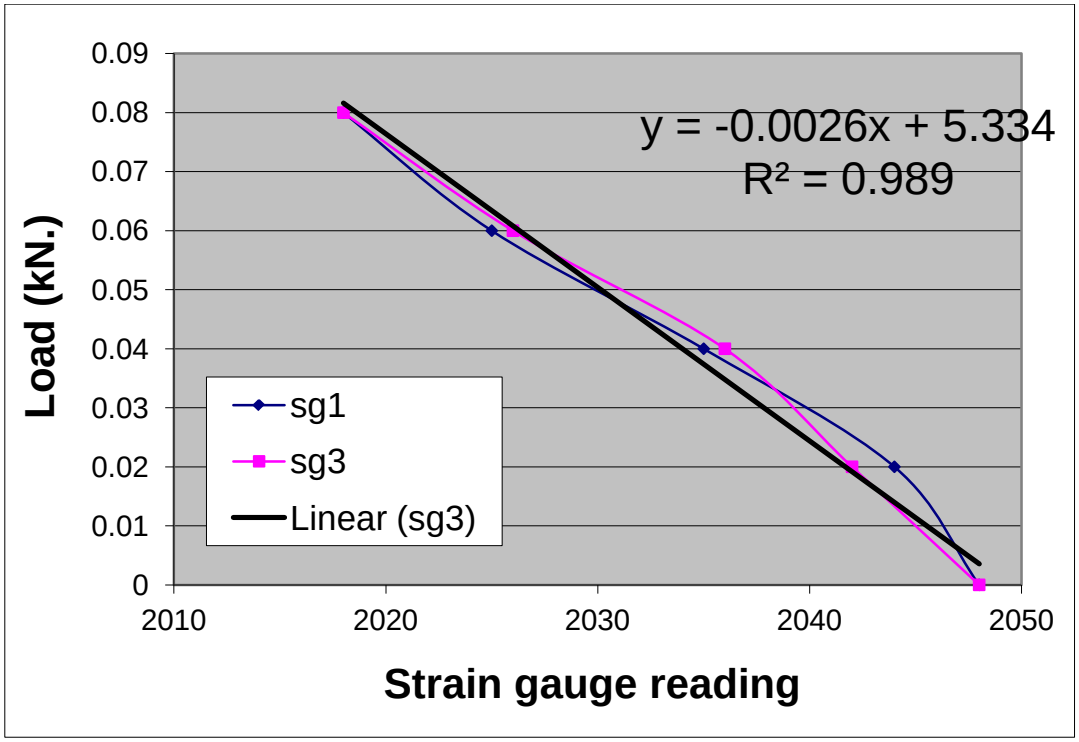

Figure 4.21 Calibration of strain gauge 1 and 3 for tension in metal bar.

It can be seen from figure 4.21 that the response of both the strain gauges in tension is similar.

2. Load at sleeper ends

This method was used to calibrate the strain gauges to read compression in the metal bars. To create compression in the metal bars the sleeper was supported on both

ends (as shown in figure 4.22) again using metal strips and load was applied in small increments to a maximum of 2.5kN although again for calibration loads upto 0.4kN were used.

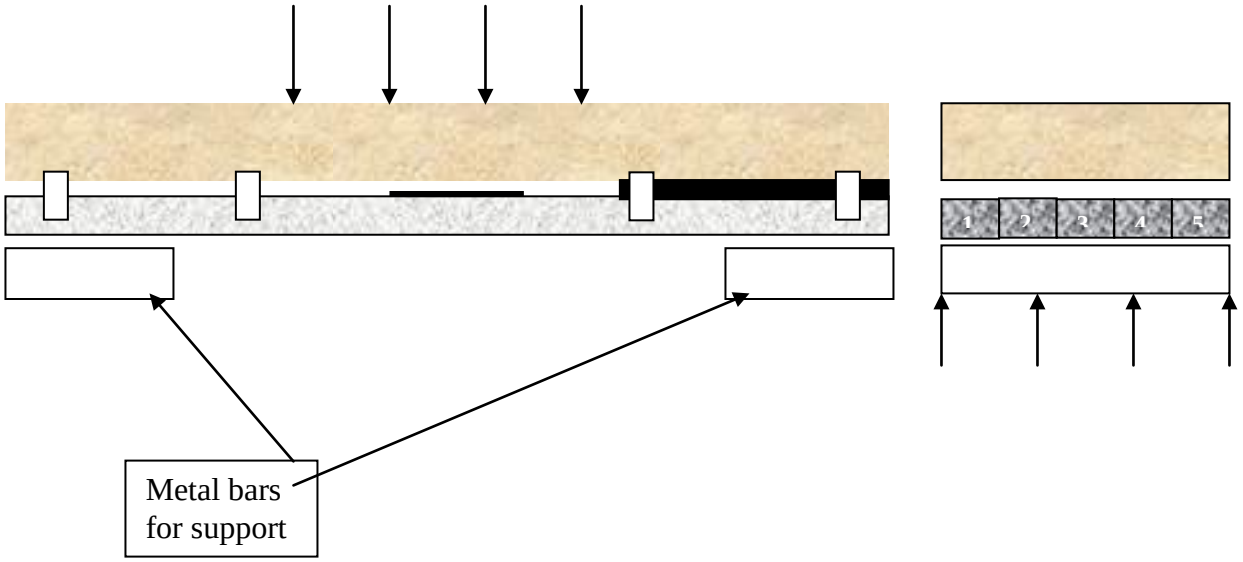

Figure 4.22 Strain gauges calibrated for compression in the metal bars.

The graph showing the calibration is given in figure 4.23. A combined graph showing calibration for both compression and tension in the strain gauges is shown in figure 4.24.

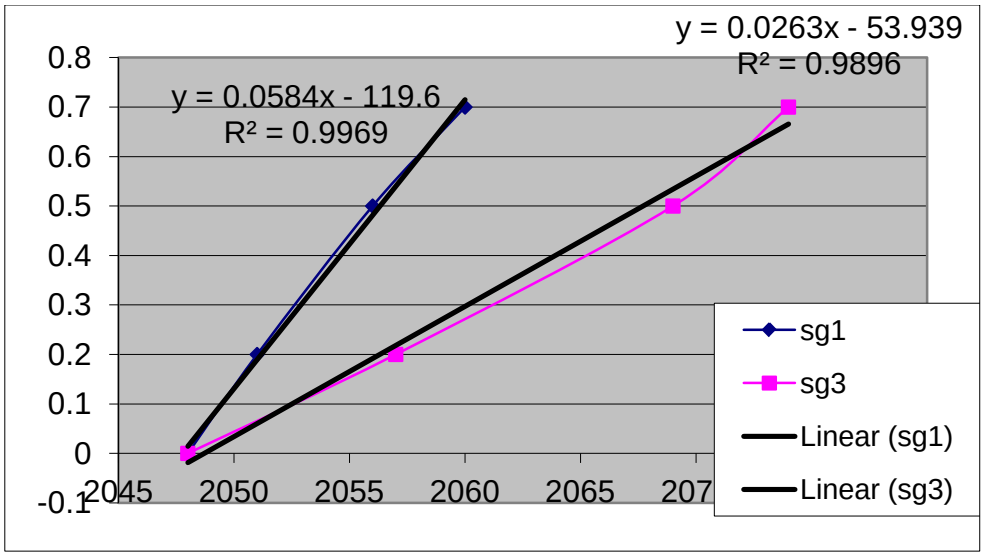

Figure 4.23 Calibration of compression load on instrumented sleeper.

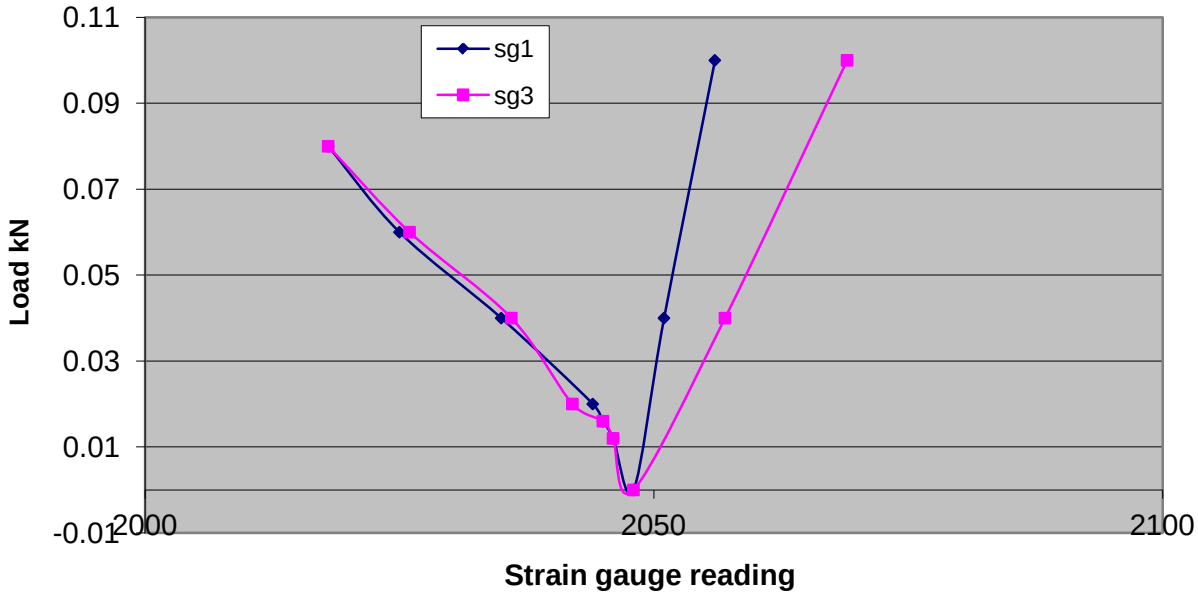

Figure 4.24 Combined graph for calibration in compression and tension

From figure 4.23 and 4.24 it can be seen that the response of strain gauge 1 and 3 is different in compression while it is the same when the strain gauges are in tension. Thus the same calibration equation was used for calibrating both strain gauges in tension (as shown in figure 4.21) and two different calibration equation in compression were used for the strain gauges as shown in figure 4.23. For strain gauge readings relating to compression load data the load value was taken as negative and for tension load data the load value was taken as positive.

Two initial runs with 'simple' load cycles was carried out by placing the sleepers directly on the sandpaper for one test and on 5mm bottom ballast in the other with the strain gauge sleeper in the centre of the model assembly as shown in figure 4.26. Strain readings were noted for maximum load in each loading cycle. Using the calibration equation discussed in the preceding article the load in the strain gauges was calculated, the strain gauges were in tension. The results are shown in figure 4.25 in form of a graph of maximum load against cycle number for strain gauge 1, fixed on the edge of the sleeper.

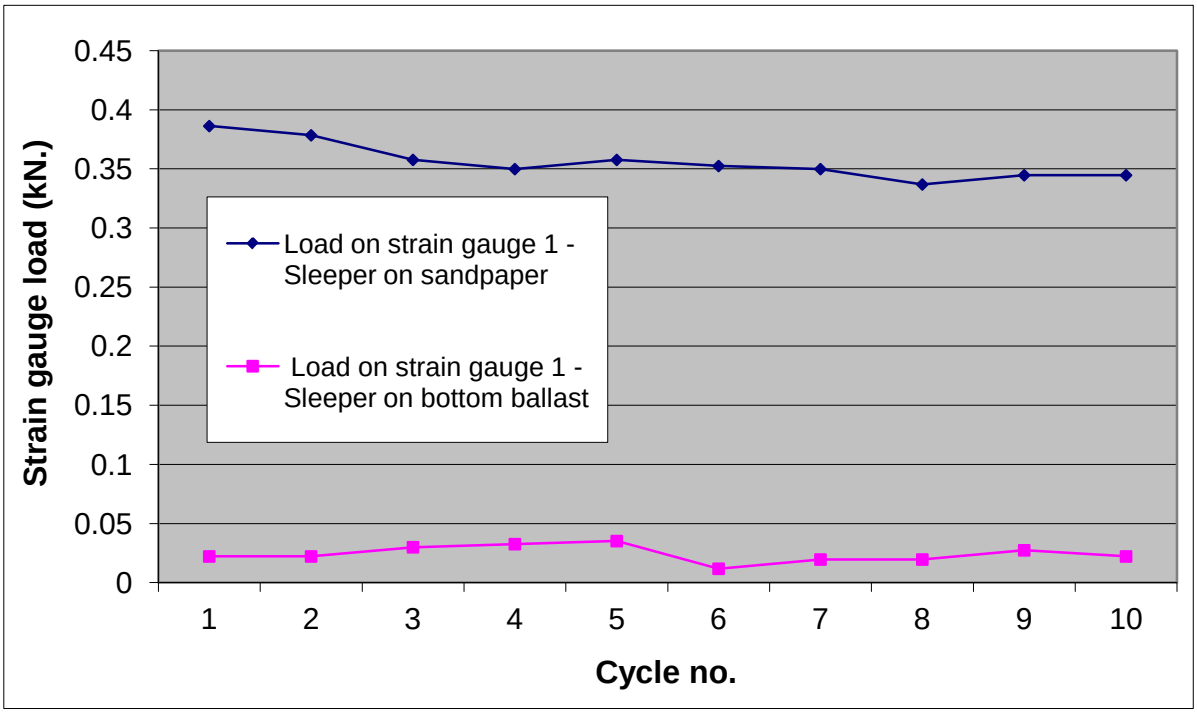

Figure 4.25 Strain gauge readings for test with no ballast.

Figure 4.26 Strain gauge sleeper in model assembly

It can be seen from figure 4.25 that the load on the strain gauge sleeper when placed on a rigid surface is higher than the assumed maximum load for each strain gauge of 0.16kN but when placed on ballast the load on the sleeper is drastically reduced. This directly relates to the fact that a resilient layer is required below the sleepers to keep the stress in the sleeper and track components to a minimum. The efforts in the early railways to create a rigid track below the rails as described in the literature review led to rail breakage and wear and tear of track components. On a rigid surface the load on the sleeper is approximately 10 times the load as compared to, when the sleeper is placed on 5mm bottom ballast.

4.4 Box test set up

4.4.1 The ballast box

In the box test boundary conditions of a section of track were created inside a box made of wood reinforced by a steel frame. The box is shown in the photograph in figure 4.27 and 4.28.

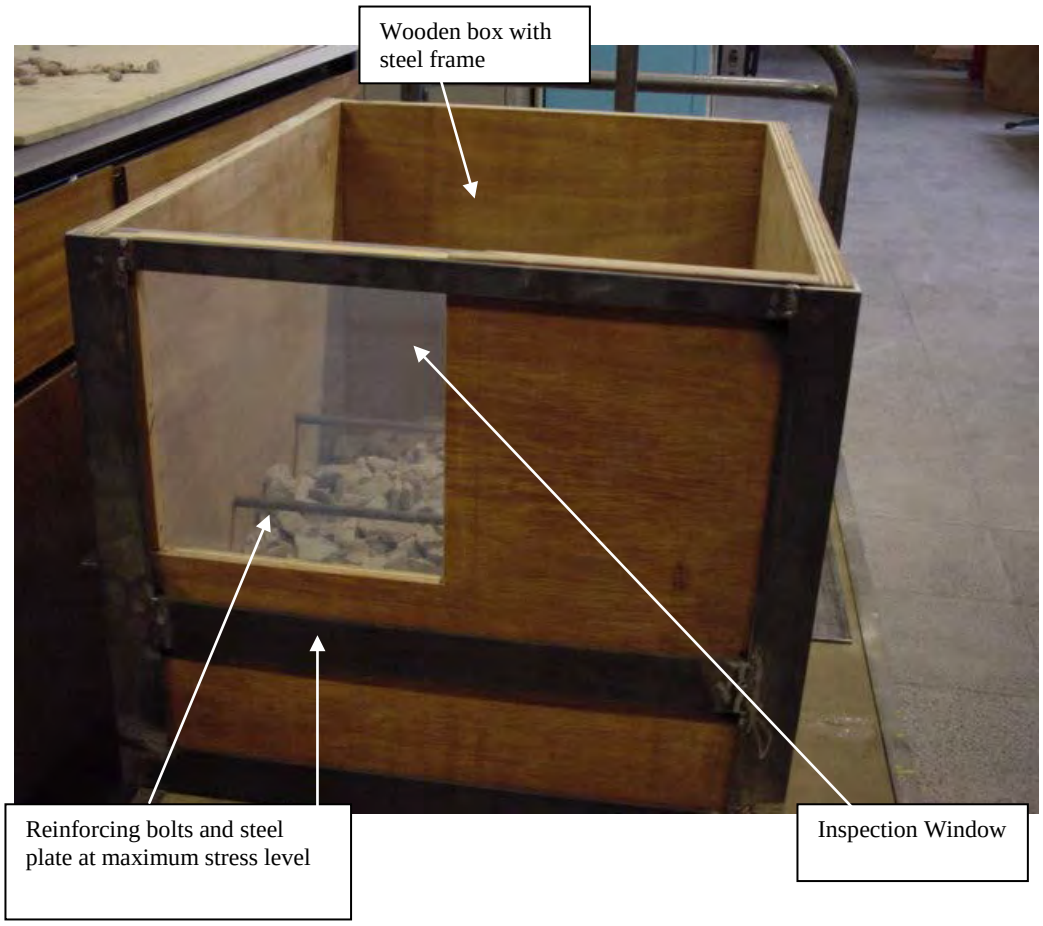

Figure 4.27 Wooden box reinforced with steel frame for full scale laboratory testing

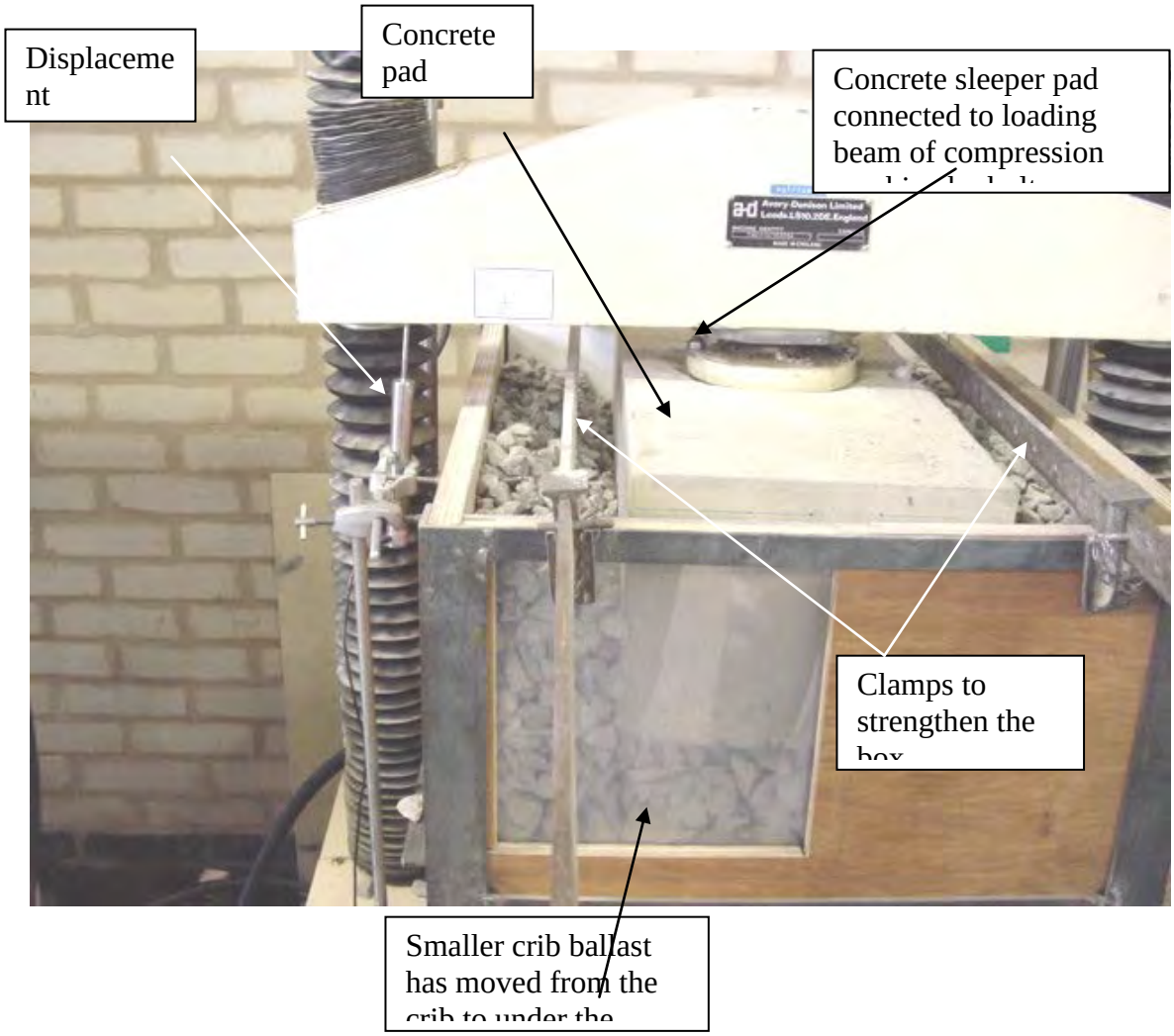

Figure 4.28 Ballast box

The length of the box was kept at 460mm to accommodate a concrete sleeper pad 450mm long. The width of the box was kept at 550mm, which is the minimum recommended centre to centre distance between two sleepers on British Rail. The effect of loading in the transverse direction (along sleeper length) was considered negligible and thus eliminated from the test set-up. A rigid boundary was assumed at the centre of distance between two sleepers thus it was assumed that load applied on one sleeper will not effect ballast beyond the centre of distance between two sleepers. The wooden sides of the box were reinforced with steel members as seen in figure 4.27 and 4.28. Considering load dispersal from the sleeper bottom at 45 degrees a steel flat was welded to the frame at the

depth where the sleeper loading pyramid would intersect the side of the box. At the level where the load pyramid would intersect the box sides, extra bolts were inserted, which are visible in the photograph, to reinforce the box and prevent it from flexing.

The depth of ballast below the sleeper was 280mm which is the standard depth of ballast on British Rail. The bottom of the box was a wooden board on which ballast was placed, but with the box being placed on top of the solid steel platform of the loading machine the subgrade could be assumed as being effectively rigid, similar to model tests.

An inspection window was detailed on one side of the ballast box as shown in figure4.27. The inspection window was dimensioned such that half the sleeper cross-section was visible through the window. The inspection window was positioned to allow for observing the ballast cross-section just below the sleeper and the crib ballast. Thus any movement of ballast from the crib to below the sleeper, during the uplift cycles could be observed through this window. On initially test running the set-up in the box it was observed in the first run that the box' frame was distressed in the location where the inspection window had been installed. The stress of the load was causing the plywood and steel frame to bend in that location. As large number of cycles were to be run on the set-up, to prevent any flexing of the frame and the box in the longitudinal direction clamps were fixed (as seen in photograph) along the longitudinal direction on the top of the box.

4.4.2 Hardware set up for the test

The same hardware set up as used for the model tests was used for the full-scale box test. The Denison compression loading machine used for the model test was again used for the box test to run cyclic loading. The oil delivery in the machine was increased to allow for higher loading required for the box tests, a railway track wheel load at full scale was simulated in the box tests. Better control could be exercised on the machine because it was running on higher oil delivery as compared to the model tests. Similar to the model test assembly the sleeper pad was connected to the loading beam of the compression machine. It was observed that there was some elastic compression at the sleeper connection with the

loading beam of the compression machine. This was removed from the readings by taking the first displacement reading to be zero and subtracting the first displacement reading from all subsequent displacement measurements.

A concrete sleeper pad was used in the test with dimensions of 450mm long by 280mm wide by 230mm deep. A steel plate was cast in to the concrete pad in the centre, with bolts welded onto the steel plate. These bolts were then used to connect the sleeper pad to the loading beam of the Denison loading machine (See figure 4.28).

As with model tests the box tests were run under full computer control with the same set up of Labview program with the DAS 16 board. The labview program was modified to increase the loading to full scale loading for the box test and the program had to be modified to allow for uplift of 25mm (full scale) in the uplift cycles, other functions of the program remained the same.

The load was applied directly to the sleeper. As 40% of the wheel load is transferred to the sleeper through the rail (Cope 1993 – p247, Profillids 1995 – p81) the maximum load applied to the sleeper was 40 kN (40% of standard wheel load of 100kN on British Rail). Thus a maximum ballast pressure of 0.317N/mm2 was achieved at the sleeper bottom, which is the ballast pressure experienced on live track. ‘Simple’ and ‘Uplift’ cycles similar to model test were run on the system. The rate of loading was the same as for model tests. First twenty load cycles were run without uplift and then subsequent cycles with an uplift of 25mm, to simulate a void of 25mm under the sleeper. Displacement was measured at maximum load for each cycle. Data was written to a data file on the floppy disc and also plotted in a chart of sleeper displacement against number of cycles on the screen. To remove the elasticity of the sleeper assembly from the load readings the first reading was subtracted from all readings. This data was then presented as graphs in MS - Excel.

A linear variable displacement transducer (LVDT) was used to measure the sleeper displacement and also the sleeper uplift in uplift cycles. As with model tests the LVDT was fixed to the loading beam of the compression machine. The linear voltage displacement

transducer was calibrated using slip gauges to read displacements of 12.5mm both sides of the zero reading.

Dial gauges were set up on the outside of the box to observe flex in the box with each load cycle. The maximum flex in the transverse direction was 1.5mm for each load cycle, which was consistent throughout the test. The maximum flex in the longitudinal direction was 0.5mm again constant throughout the test. A way of checking sleeper height correction achieved in the uplift cycles and also the uplift height was to mark the level of the top of the box on the side of the sleeper with a pen. As the sleeper would lift up in the uplift cycles when the load was reduced to zero the uplift height could be checked by holding a measure tape on the top of the box and reading the height by which the pen mark on the sleeper travelled. As the sleeper moved up in the uplift cycles with the void being filled by crib ballast the pen mark on the sleeper which was level with the top of the ballast box at the start of the test moved up relative to the top of the box. The total height gain could be checked at the end of the test by measuring the distance from the top of the box to the pen mark on the sleeper.

Thus the box test provided a means to run a full scale test which was ‘portable’ or manageable in size. As small quantities of ballast were required to run the test and the test was run under full computer control it was easy to set – up a test and run test with different configurations of top and bottom ballast.

4.4.3 Ballast for box test

Standard 50mm railway ballast was used for the box test. 20mm stone blowing stone and stones smaller than 20mm were used as crib ballast. The concern was that under heavy full scale loads any stones other than proper railway ballast would be easily crushed. To prevent this the 20mm stoneblowing stone and the 50mm railway ballast were procured from a quarry in Coalville, which supplies ballast and stoneblowing stone to the railways. Smaller stones used as crib ballast were taken from the aggregate piles in the laboratory.

4.5 Test set-up for full scale laboratory test

These tests were carried out on a full scale monoblock concrete sleeper and rail assembly in the laboratory. The aim of the full scale tests was to validate the results from the model tests and box tests.

4.5.1 Sleeper, rail and ballast

The sleeper used for the test was a standard monoblock concrete sleeper. The sleeper was 2400 mm long, 280mm wide and 230mm deep. The sleeper was supplied by RMC concrete products complete with pandrol fastclip fittings and insulating rubber pad below the rail seat. A 4m length of used rail weighing 56kg/m was supplied by Balfour Beatty Rail for the test. This was cut into 2m sections and fixed to the sleeper using the pandrol fastenings. Standard railway ballast of 50mm size and stoneblowing stone of 20mm size same as used for the box test were used for the full scale test. The depth of ballast below the sleeper was 230mm., which is the standard depth of ballast on lightly trafficked lines in the U.K. A few tests were also carried out by using stones smaller than 20mm size in the crib. These included tests with 10mm and 5mm stones and sand as crib ballast. These were taken from the aggregate stores in the laboratory.

4.5.2 Boundary conditions

A small section of track around the concrete sleeper was created in the laboratory as shown in figure 4.29.

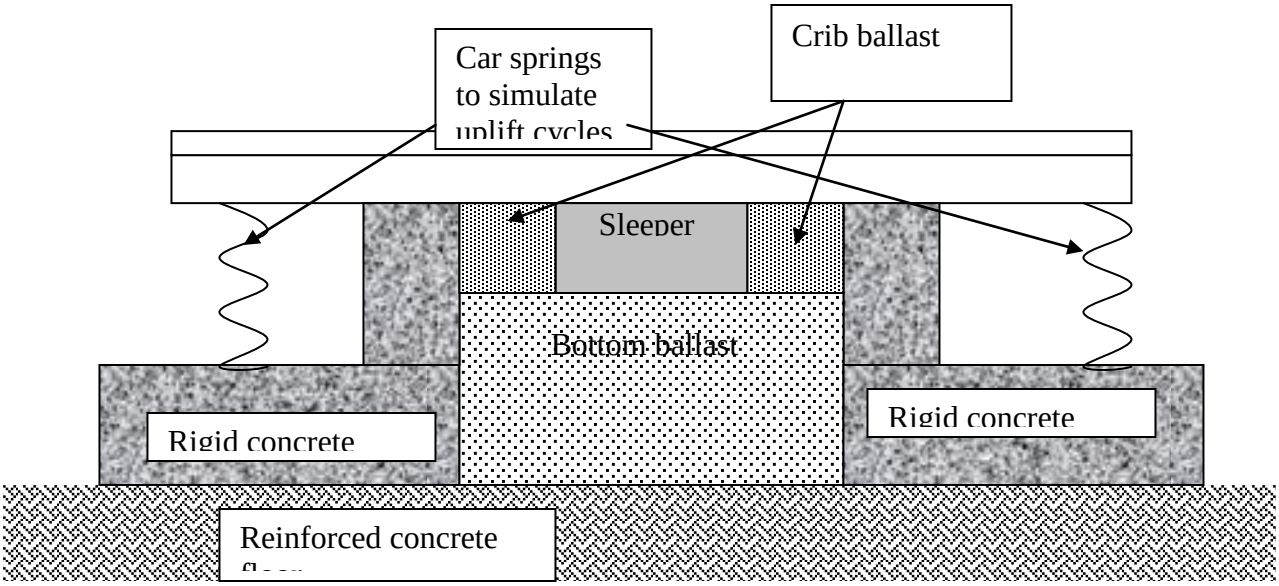

Figure 4.29 Cross-section through full scale test set up

The tests were carried out by placing the ballast on a reinforced concrete strong floor in the laboratory. To be consistent with the model and the box tests the subgrade was assumed to be infinitely rigid. Two reinforced concrete panels were placed, one on each side of the sleeper 600mm apart as shown in figure 4.29. The sleeper was placed in the centre. The concrete panels were assumed to provide a rigid boundary at the centre of the distance between two sleepers thus it was assumed that load distribution from a sleeper does not affect ballast beyond the centre of distance between two sleepers. A few tests were carried out with the concrete panels 550mm apart and 800mm apart, thus simulating different sleeper spacing. In the initial test runs the concrete panels moved apart by 20-25mm on application of about a 100 load cycles as the test progressed. Thus these panels were supported from one end by packing up against a steel column and the other end against the wall, using wooden blocks. This prevented any movement of the concrete panels and thus a rigid boundary was provided to the ballast. To record that no movement occurred in the concrete panels the distance between the panels was measured at the start of the test and then monitored while the test was running and then recorded again at the end of the test.

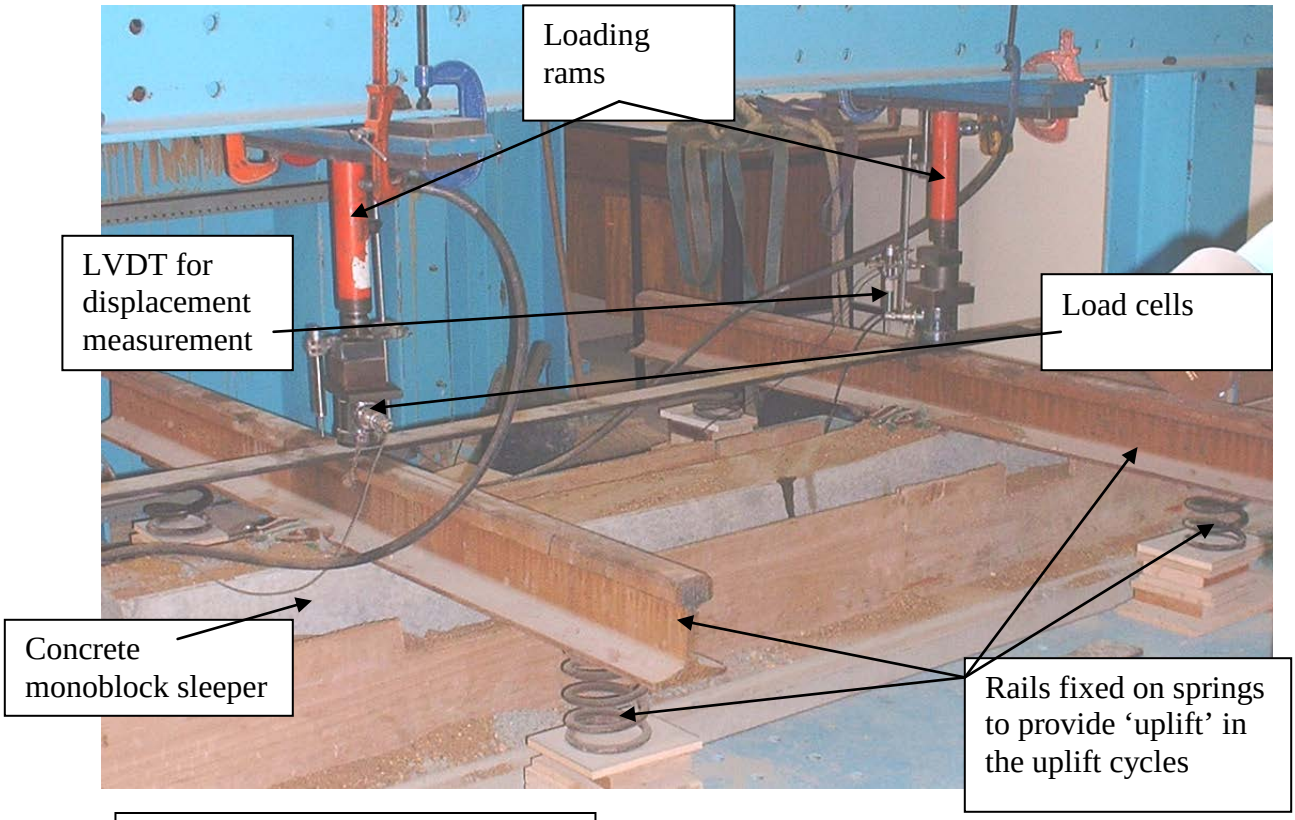

Figure 4.30 Full scale test set up

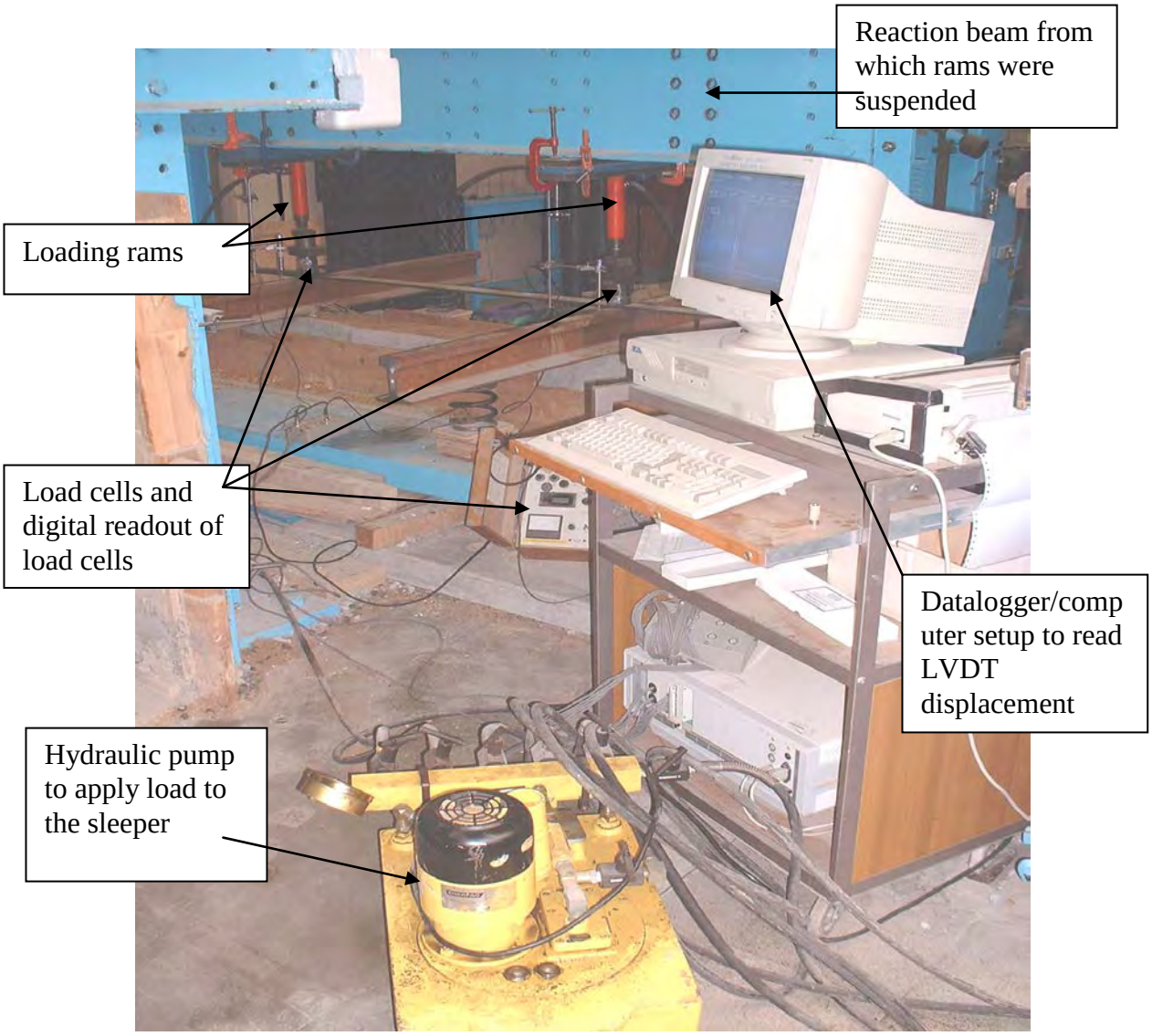

Figure 4.31 Full scale test set - up

Load was applied directly to the rails by two hydraulic loading rams as shown in figure 4.30. A steel beam was positioned on top of the sleeper and the rams were fixed to the beam. The rams were loaded by using an electrical hydraulic pump. The sleepers were loaded by manually operating a valve on the pump to increase or decrease the load. Two load cells, one below each ram were positioned on top of the rail and the load to the rail was applied through the load cells. The load cells were connected to a digital readout, thus

the load on the rails could be monitored by reading the two load cells. The rate of loading for both the rams was consistent and thus by constantly monitoring the digital readout from the load cells the same maximum load for each loading ram for each cycle could be achieved by manually handling the hydraulic pump. As mentioned above the load was applied directly to the rails and the maximum load applied was 60kN per ram (120 kN per axle) which is the axle loading on lightly trafficked lines in the U.K. (Cope 1993).

4.5.3 Displacement measurement

Sleeper displacement and uplift was measured using Linear variable displacement transducers (LVDT). An LVDT was fixed to each rail to measure track displacement under maximum load. The LVDT were suspended from the reaction beam independent of the test assembly. The LVDT were connected to two input channels of a computer based data logger. Each reading of the LVDT was taken by operating the return key on the computer keyboard. Thus during the test the valve on the hydraulic pump was operated manually to increase the load to maximum and keeping the load at maximum the return key on the computer was operated to log the LVDT readings. The data was logged in the computer and could be retrieved as an MS - Excel file.

The LVDT were calibrated using the datalogging program in the computer by giving known displacements to the LVDT by using slip gauges. The LVDT were calibrated for displacements of 25 mm either side of the zero reading.

4.5.4 Simple and uplift cycles

Simple and uplift cycles similar to the model tests were carried out. Two lengths of rail fixed to the sleeper were supported at the ends by springs to keep the sleeper clear of the ballast top by 25mm(or more) when unloaded and in a position of rest before the start of a test. The springs were cut from standard car coil springs. Considering average weight of a car at 1000kgs. each spring was capable of supporting a load of 250 kg without showing any appreciable deflection. The total self weight of the rail sleeper assembly was

approximately 700 kg and thus the springs could support the selfweight of the sleeper assembly when unloaded (at rest) without any appreciable deflection. The sleepers were loaded with the loading rams to a minimum seating load of 10kN which represented the self weight of the sleeper rail assembly. When the load was released the sleeper assembly supported by the springs moved back to the position of rest. This formed the mechanism of the uplift cycles.

Before starting a test the computer data logger was used to scan the LVDT reading for the sleeper assembly at rest supported by the springs, as zero. The loading rams were used to press the sleeper down onto the bottom ballast to a minimum seating load of 10kN. At this position again the LVDT reading was logged, this gave the distance the sleeper would move when the load was released. This became the uplift height of the sleeper for the uplift cycles. It was observed that the ballast in the first few load cycles would compress by a large amount as the ballast was not compacted or levelled correctly after placing in the box. Thus before the start of each test a few load cycles were run on the ballast till it stablised after which the uplift height was measured as described above and the test was started.

For starting a test the sleeper was lowered on the bottom ballast with a minimum seating load of 10kN. The LVDT reading at this position of the rail assembly was scanned as a zero reading. This formed a datum for the subsequent load cycles of the test. Keeping the load at a minimum seating load the crib ballast was filled in around the sleeper and the test was started. Twenty simple load cycles were run with the load cycled between 10kN and 60kN care being taken to ensure that the sleeper did not lift up off the ballast during the simple cycles. Load was applied by manually operating the control valve on the hydraulic pump. Load readings from the two load cells were observed. At each maximum load the return key on the computer was operated to log in the LVDT displacement readings. After the first twenty simple load cycles the load was released to zero causing the sleeper to move to its position of rest supported on the springs, this formed the mechanism of the uplift cycles. In this way a loose sleeper in the track was simulated in the uplift cycles. This also ensured that the same uplift height was achieved in each cycle.

During the uplift cycles when the load was released after reaching maximum the sleeper would move quite quickly to its position of rest supported by the springs. One concern was that the sleeper due to the elastic reaction of the spring when the load was suddenly released would move up beyond its original position of rest before coming back to its position of rest. Although this seemed highly unlikely as the stiffness of the springs was sufficient to support the self weight of the sleeper assembly. A dial gauge was used to measure the sleeper uplift. At initial position of rest of the sleeper the dial gauge was adjusted to read zero. During the uplift cycle when the load was released the dial gauge was monitored to see if the sleeper moved higher than its original position of rest. It was observed that the sleeper did not move up from its original position by more than 0.2mm which can be considered as negligible.

5. Model test results

In this chapter laboratory test results have been described for different tests carried out on both model and full scale test set-up. The results have been described as follows:

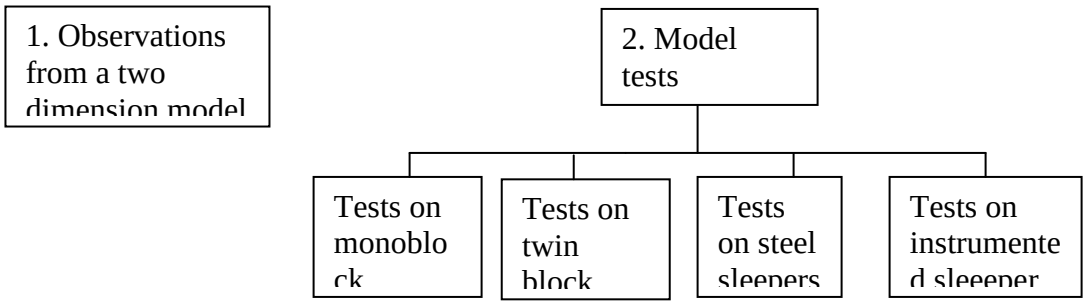

Figure 5.1 Two dimensional glass model

5.1 Observations from two dimensional glass model

As mentioned in chapter 4 a full scale two dimension model was used in the initial stages of research to help visualise how the two layered ballast system would work with a voided sleeper and also to help formulate a methodology for both model and full scale testing on the system.

The crosssection of ballast enclosed within two glass surfaces is shown in figure 5.1. The sleeper crosssection was placed on 50mm standard railway ballast and smaller crib ballast was filled around the sleeper. The sleeper bottom was marked on the glass surface with the help of a felt tipped pen. A level 25mm above the sleeper bottom level was marked as the uplift to be given to the sleeper. Smaller stones were filled around the sleeper representing the crib ballast. The different sizes of smaller stones used were 20mm stoneblowing stone, 10mm aggregate, 5mm aggregate and sand. The sleeper was lifted up manually by 25mm and the smaller crib ballast could be observed moving to the sleeper bottom. The common observation for all small size crib ballast was that once the sleeper was lifted up it was not possible to push the sleeper back to its original position and the other observation was that repeated movement of the sleeper was required for the crib ballast to move to the sleeper bottom and fill the void below the sleeper completely.

For 20mm stoneblowing stone in the crib when the sleeper was lifted up by 25mm some stones from the crib migrated to the sleeper bottom most of them lost in the voids in the 50mm ballast and a few stones were wedged in between the sleeper edge and the crib ballast. The sleeper was pushed down with lot of difficulty but could not be pushed down to its original level. When the sleeper was lifted again to 25mm level it could not be pushed down at all by hand as the few particles below the block did not allow the sleeper to be pushed down. A few jerky motions given to the sleeper displaced and rearranged the ballast after which it was possible to press the sleeper down by a small amount but once it was lifted two or three times it was virtually impossible to push it down by hand. While

carrying out this exercise it was observed that even lifting the sleeper up the first time by 25mm was difficult due to the high friction between the angular 20mm stone and the sides of the sleeper. When the sleeper was lifted up it was observed that the 20mm stone filled up the voids in the 50mm bottom ballast but it remained in the top 50mm layer of bottom ballast (approximately) and did not migrate further down for the compressive force applied by hand.

For 5-10mm crib ballast when the sleeper was lifted up by 25mm the number of stones migrating to the sleeper bottom were more than that for 20mm crib ballast and stones moved further under the sleeper, towards the centre of the sleeper cross-section. It was possible to push the sleeper by a very small amount a few times and when the sleeper was lifted to the 25mm level more ballast from the crib migrated to the bottom of the sleeper and soon it was not possible to press the sleeper down by even a small amount. It was observed that the friction between the aggregate in the crib and the sleeper sides was less than that for the 20mm stone but this was perhaps because the 5-10mm aggregate was not as angular shaped as the 20mm stoneblowing stone. The 5-10mm stones filled all the voids in the top layer of the 50mm bottom ballast and quite a few stones migrated further down in the 50mm ballast even without any load to compress them.

When sand was filled in the crib around the sleeper section a large amount of sand percolated immediately to the bottom of the ballast layer and thus it took some time to fill the cribs with sand. When the sleeper was lifted up by 25mm the sand immediately flowed to the sleeper bottom and travelled further across the width of the sleeper. It was possible to push the sleeper down a few times but very quickly the void below the sleeper got filled with sand and it was not possible to push the sleeper down by hand. The friction between the sleeper wall and the sand in the crib was observed to be less than that for stone ballast used earlier. It was also observed that even for very small lifts sand particles from the crib migrated to the bottom of the sleeper. This implies that the smaller the size of crib ballast the more effective it will be in filling the void below the sleeper.

5.2 Model tests

As described in the previous chapter these were carried out on wooden monoblock sleepers, wooden twin block sleepers, steel sleepers and an instrumented sleeper. The simple observations from the two dimension full scale model demonstrated that if a small size stone is filled in the crib around the sleeper any void below the sleeper will be filled up by the crib ballast migrating into the void. It was easy to identify that the void would be filled up with the crib ballast depending on the size of the void and the size of the crib ballast but an important factor missing from the observations was that the load applied to the sleeper was by hand and thus was very small. Thus the aim of the model tests was firstly to establish that the two layered ballast system would work under full railway axle loads albeit at model scale, and also to investigate in detail the various parameters affecting the two layered ballast system. The test set up has been described in detail in chapter 4 so this chapter will concentrate only on presenting the results.

5.2.1 Tests on monoblock sleepers

Major proportion of the model tests was carried out on wooden monoblock sleepers with type A runs (described in Chapter 4). Initial tests were run to confirm the working of the two layered ballast system as observed in the glass model and to identify various parameters affecting the working of the system. Once the parameters were identified detailed testing on the system for each parameter was carried out. These have been described in detail in this section.

5.2.1.1 Initial tests on the two layered ballast system – Type A runs

Initial tests on the system were carried out to confirm that the observation made in the glass model that a void below the sleeper would be filled up by smaller crib ballast. Initial tests were carried out with 5mm bottom ballast and both 5mm and 2mm stones as crib ballast simulating standard railway ballast and stoneblowing stone. This was done to allow comparison between the present system of 5mm bottom and top ballast and the two layered ballast system with smaller ballast in the crib. Two sleeper widths of 28mm and 15mm were used. 28mm sleeper width is 10^{th} scale of standard railway sleeper width on British Rail while the 15 mm sleeper width was chosen as an alternative to the standard

sleeper width. Two sleeper spacing were used at 55mm and 70mm which is tenth scale of 550mm and 700mm sleeper spacing. As mentioned in the literature review in Chapter 2 the sleeper spacing of 550mm is the minimum recommended sleeper spacing on British Rail and 700mm is slightly higher than the standard sleeper spacing on British Rail of 600-650mm.

The uplift height in uplift cycles was maintained as 2.5mm (10^{th} scale of 25mm). Twenty simple cycles followed by twenty uplift cycles were run in the tests. The various parameters are listed in table 5.1.

Table 5.1 Initial model test parameters

Sleeper size (mm.)	Sleeper spacing (mm.)	Bottom ballast	Crib ballast	Void below sleeper (uplift height in uplift cycles) (mm.)
28	55	5	2	2.5
28	70	5	2	2.5
28	55	5	5	2.5
28	70	5	5	2.5
15	55	5	2	2.5
15	70	5	2	2.5
15	55	5	5	2.5
15	70	5	5	2.5

Thus a total of eight tests were carried out. Data was plotted as maximum sleeper displacement for each load cycle as shown in figure 5.2

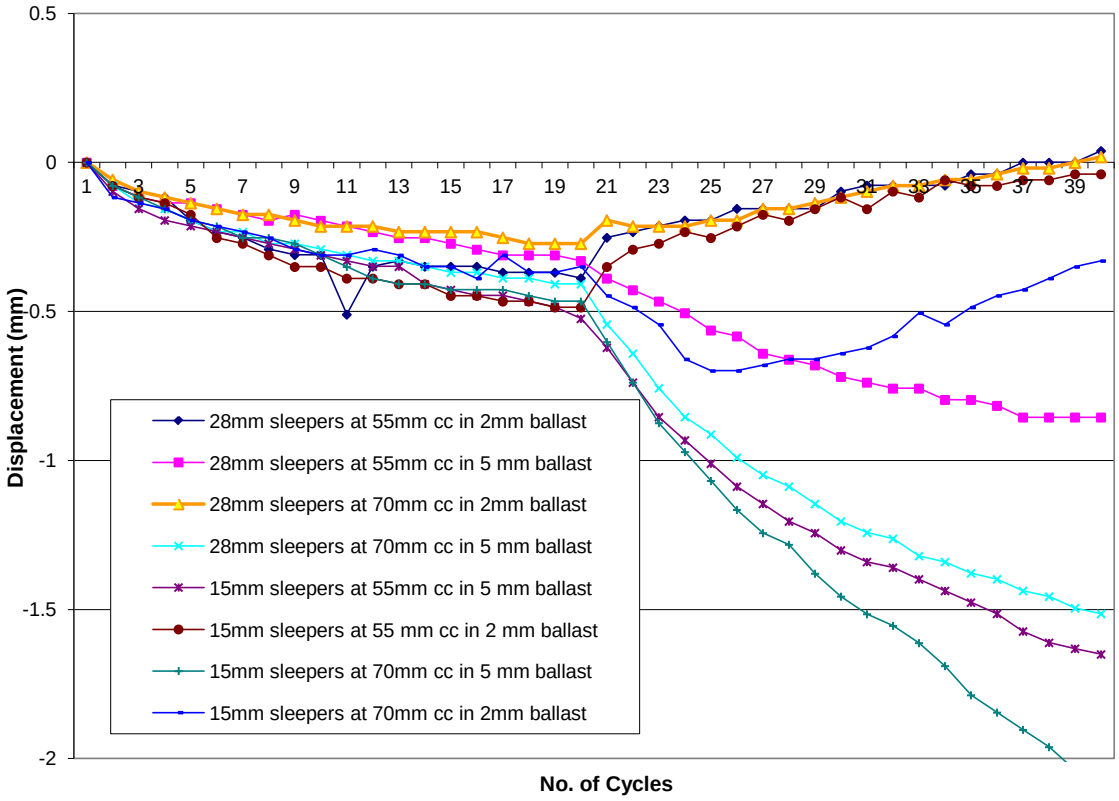

Fig. 5.2 Results from initial tests on two layered ballast system

5.2.1.1.1 Observations on the initial tests

a. Tests with 5mm crib ballast

For both sleeper size and spacing the void below the sleeper of 2.5mm was not filled up in the uplift cycles. The crib ballast particle of 5mm size did not migrate into the void below the sleepers in the uplift cycles. This suggests that a void size of 25mm full scale will not be filled up if the crib ballast is of size 50mm (current system of ballasting the railways).

For the first twenty simple cycles the ballast is being progressively compacted and compressed below the sleeper with each load cycle as the sleeper sinks into the ballast. Ballast compression is maximum in the first few load cycles after which it is more gradual and by the end of twenty simple cycles the line is progressively levelling out. This is consistent with observations from other model and full scale tests studying ballast degradation (Dahlberg 2001) where ballast compression below the sleeper is maximum for the first few load cycles and then is gradually compacted under continuous cyclic loading. After the start of the uplift cycles the ballast compression is suddenly accelerated. The sleeper displacement into ballast in the twenty uplift cycles is almost twice the displacement in the first twenty simple cycles. This demonstrates that with a loose sleeper in the track track geometry deterioration is accelerated.

For smaller sleeper spacing of 55mm the ballast compression is less as the sleeper displacement for sleeper at 55mm spacing is less than the sleeper displacement for sleeper at 70mm spacing. E.g. for 28mm sleeper at 55mm spacing the final displacement into ballast is 0.8mm at the end of 40 cycles while for the same sleeper at 70mm spacing the final displacement into ballast is 1.5mm. This is explained by the fact that with closely spaced sleepers the load distribution into the ballast is better resulting in lower stress in ballast thus ballast compression is less.

For smaller sleeper size of 15mm the sleeper displacement into ballast is more than that for sleeper size of 28mm e.g. the final displacement into ballast for 28mm sleeper at 55mm spacing is 0.8mm while for 15mm sleeper at 55mm spacing is 1.7mm at the end of 40 load cycles. The sleeper displacement for 15mm sleeper at 55mm spacing is even more than that of 28mm sleeper at 70mm spacing as seen figure 5.2. This is due to higher ballast

pressures under sleeper with smaller width. The load distribution under a wider sleeper is better than a sleeper with small width. The ballast pressure under a 15mm sleeper is almost twice that under a 28mm sleeper as shown in table 4.2 in chapter 4.

b. Tests with 2mm crib ballast

The first important observation is that for tests with 2mm crib ballast, after the first twenty simple cycles when the uplift cycles were started i.e. the sleeper was lifted up after each load cycle by 2.5mm the sleeper starts rising in the ballast. Thus the smaller crib ballast is migrating from the crib into the void below the sleeper gradually filling the void. Thus the two layered ballast system is capable of working under effect of heavy axle loading of the railways, as demonstrated by the model test results.

With the sleeper in the glass model, described earlier, once it was lifted up it was not possible to push it down to its original level by hand and after lifting the sleeper up a few times it was not possible to push it even by a small amount by hand. While as seen in the test results (figure 5.2) the sleeper height correction in the model tests is very gradual and even after 20 uplift cycles the sleeper has reached only to its original zero datum level set up before the start of the test. Thus with heavier loads in the uplift cycles as the crib ballast migrates into the void below the sleeper it is compressed into the bottom ballast. With each uplift cycle as new particles from the crib flow into the void they are compacted by the sleeper and thus sleeper height gain is gradual. The friction force between the crib ballast particles and the sleeper face is also negligible when compared with the axle load.

The sleeper height gain after the first uplift cycle is maximum after which the height gain is more gradual. Thus as the void size below the sleeper reduces the migration of the crib ballast particles into the void is reduced.

Except for 15mm sleeper at 70mm spacing the sleeper height gain in the uplift cycles is similar for all sleeper size and spacing. For 15mm sleeper at 70mm spacing the sleeper

sinks a bit more into the bottom ballast before gaining in height and the final sleeper level is lower than for the other tests.

The above tests were carried out on ballast sieved from the aggregates in the laboratory. It was mentioned in Chapter 4 about the ballast being contaminated by smaller flaky particles created due to particle breakage of bottom ballast under cyclic load. As the ballast was recycled after each test the flaky particles remained within the ballast matrix. When the last few tests were being run it was observed that the crib ballast was particularly contaminated by these flaky particles. Thus new ballast was procured from a granite quarry supplying ballast to the railways. The ballast was in the form of small size fractions which were a by - product of the rock being crushed for railway ballast. These were used for all further testing and it was observed that the ballast fouling in subsequent tests was negligible.

5.2.1.1.2 Discussion

These initial tests demonstrated that with smaller particle size of crib ballast the void below the sleeper would gradually be filled up by the crib ballast migrating into the void with the passage of traffic and the vertical pumping movement of voided sleeper in the ballast. From the observations made above from the initial tests and also from the two dimensional model following parameters were identified which would affect the working of the two layered ballast system:

1. Sleeper spacing
2. Particle size of crib ballast
3. Uplift height for uplift cycles
4. Size of bottom ballast

At this stage of the project it was decided to rule out sleeper size as a parameter and thus all further testing was carried out using standard sleepers of 28mm width (280mm full scale). In a progress meeting with the project sponsors to discuss the initial model test

results, sponsors RMC concrete products advised that it would not be practical to look at different sleeper sizes because of the cost involved in adapting existing sleeper manufacturing systems to produce different sleeper sizes. The model tests had demonstrated that the 28mm wide standard sleeper gave better results as compared to the 15mm wide non-standard sleeper, so it was decided to carry out all further testing using 28mm standard width sleeper.

It was decided to run tests with more uplift cycles to get the final height correction for the sleepers and also observe how the above parameters affected the final height gain of the sleeper for a large number of uplift cycles. As explained in the literature review the sleeper tends to lift up by 1-2mm in front of the wheel load in live railway track thus a concern was that if a large number of uplift cycles were run the sleeper would eventually climb out of the ballast as the smaller crib ballast would migrate to below the sleeper as the sleeper lifted up in front of each wheel and lift the sleeper out of the ballast. Thus further tests were carried out with small uplift heights to simulate the above condition and with smaller crib ballast.

5.2.1.2 Effect of sleeper spacing – Type A runs

These tests were carried out to understand the effect of sleeper spacing on the working of the two layered ballast system. Thus all other parameters mentioned earlier were kept constant for the tests while the sleeper spacing was changed for each test. Tests were run for different sleeper spacing and consisted of 20 simple cycles and a large number of uplift cycles. Uplift cycles were run until there was no further height gain for the sleepers. As for the initial tests 5mm stones were used as bottom ballast while both 5mm and 2mm stones were used as crib ballast. The uplift height for all tests was maintained constant at 2.5mm.The results are presented as a graph of sleeper displacement for each cycle. The different sleeper spacing used and other parameters for the test are described in table 5.2

Table 5.2 Tests with different sleeper spacing (Holbourn 2003)

Sleeper spacing (mm.)		Bottom ballast size (mm.)	Crib ballast size (mm.)	Uplift height in uplift cycles (mm.)
Model scale	Full scale			
45	450	5	5	2.5
45	450	5	2	2.5
60	600	5	5	2.5
60	600	5	2	2.5
70	700	5	5	2.5
70	700	5	2	2.5
80	800	5	5	2.5
80	800	5	2	2.5

45mm (450mm full scale) is less than the minimum possible sleeper spacing recommended on British Rail while 600mm is the standard sleeper spacing on British Rail. The maximum sleeper spacing allowed on British rail is 700mm. Thus the sleeper spacing selected covered the full range of sleeper spacing possible on live track in the U.K. The results are shown in two graphs below in figure 5.3. The first graph is for tests run with 5mm crib ballast and the second graph is for tests run with 2mm crib ballast. In the graphs maximum sleeper displacement for each load cycle has been plotted against cycle number.

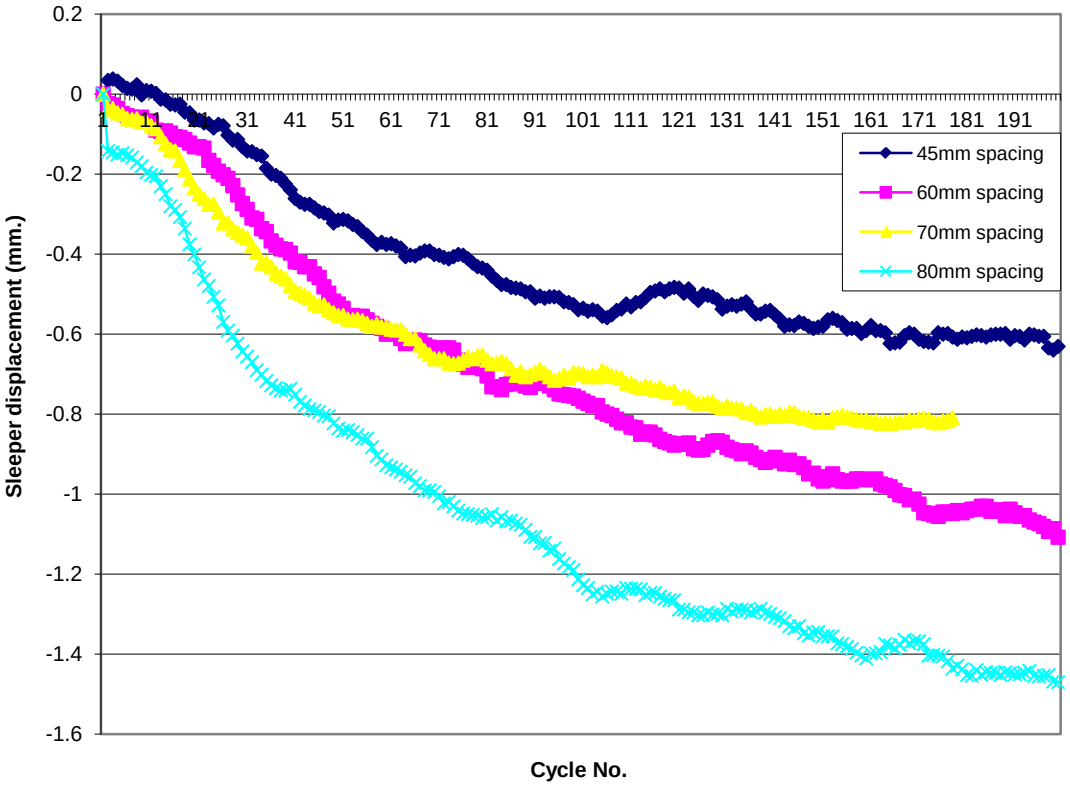

Figure 5.3 a Test with sleepers in 5mm crib ballast and different spacing

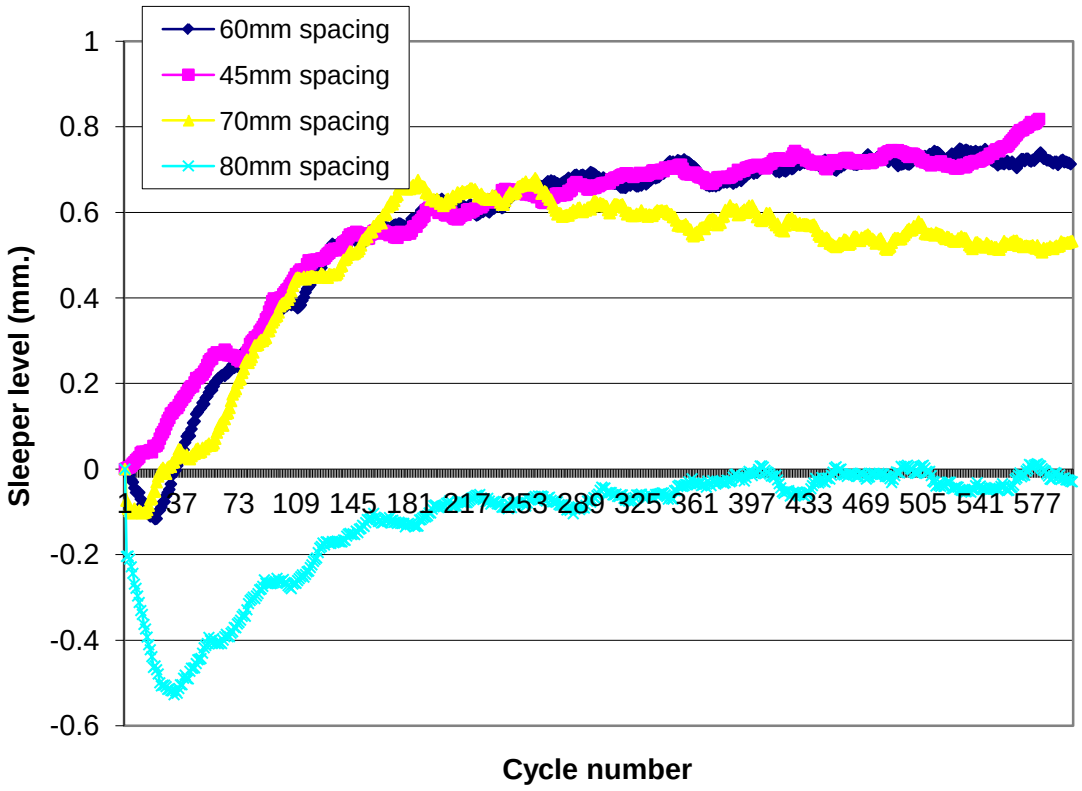

Figure 5.3 b Tests with sleepers in 2mm crib ballast and different spacing.

5.2.1.2.1 Observations:

a. 5mm crib ballast

The test results confirm observations made in the initial tests that better load distribution is achieved by closely spaced sleepers. Ballast permanent deformation is minimum for sleepers spaced at 45mm and maximum for sleepers spaced at 80mm. In the uplift cycles for an uplift of 2.5mm there is no sleeper height gain. For sleeper spacing of 80mm the final sleeper displacement at the end of the test is 1.5mm measured from the datum zero level set before the test. Thus the total void below the sleeper has increased from 2.5mm to 5mm as the void is not filled up by crib ballast.

b. 2mm crib ballast

These tests again confirm that with smaller crib ballast of size 2mm a void of 2.5mm below the sleeper would be filled up by the crib ballast. In the initial tests for 40 uplift cycles the void below the sleeper was filled up to the datum zero level of the test thus the sleeper was still moving 2.5mm in the void at the end of the uplift cycles. A large number of uplift cycles were run for these tests until there was no more height gain for the sleepers. Thus the final height correction in the sleepers could be measured. It can be seen in the graph that final sleeper height achieved is different for different sleeper spacing but the form of the graph is similar for all sleeper spacing. Maximum sleeper height correction is achieved for 60mm sleeper spacing while the minimum height correction is for sleeper spacing 80mm. Sleeper height correction at 100, 200, 300, and 400 cycles is given in table 5.3

Table 5.3 Sleeper height correction

Sleeper spacing (mm.)	Cycle number				
	100	200	300	400	Final height correction
	Sleeper level with respect to datum zero level (mm.)				
45	0.018	0.324	0.467	0.48	0.5
60	0.22	0.63	0.66	0.66	0.8
70	0.32	0.63	0.719	0.63	0.5
80	-0.19	-0.072	-0.054	-0.01	0

For sleeper spacing 45mm and 70mm the final sleeper height correction is 0.5mm while sleeper height correction for 60mm spacing is 0.6mm. For 80mm sleeper spacing the height correction is minimum and the sleeper level is 0mm at the end of the test. This seems to suggest that a sleeper spacing less than 45mm (450mm full scale) and larger than 70mm (700mm full scale) is detrimental to the working of the two layered ballast system. A general conclusion would be that the current industry standards on sleeper spacing seem to be optimum for the performance of the two layered ballast system.

Considering system performance as optimum for sleeper spacing of 60mm the maximum correction in sleeper height is 0.7mm. For the above test the parameter varied was the sleeper spacing while the other two parameters of uplift height and crib ballast particle size were kept constant at 2.5mm and 2mm respectively. A sleeper height correction of 0.7mm means that at the end of the test the void below the sleeper was 2.5mm (initial void size) minus 0.7mm (sleeper height gain) equal to 1.7mm. Thus at the end of the test the sleeper was moving vertically by 1.7mm in the uplift cycles.

It is easy to visualise that a void below the sleeper will never be filled up by a particle larger than the void size i.e. a particle in the crib larger than the void size below the sleeper will not automatically flow into the void under the effect of gravity. From this simple rule it can be predicted that with a 2mm particle size of crib ballast any void below the sleeper would be filled up to size equal to 2mm after which the flow of crib ballast into the void would cease. Thus for the above test with void size 2.5mm and crib ballast size of 2mm the final void size at the end of the test could be predicted to be 2mm but the final void size is 1.7mm. An explanation of this anomaly requires a study of the grading of the crib ballast. The crib ballast grading was adopted from the grading of the stoneblowing stone used on the railways. The grading of both model scale and full scale ballast is given in Chapter 4. The crib ballast largest particle size is 2mm and that size is used to designate the ballast as 2mm ballast similar to the designation of stoneblowing stone as 20mm stone. The model scale stoneblowing stone is a mix of particles ranging from size 2.0mm to 1.4mm with a very small proportion of particles of size less than 1.4mm. 70% of the crib ballast particles are of size between 1.4mm and 2.0mm. Ignoring the particle size smaller

than 1.2mm the average size of crib ballast is 1.7mm, which is the residual void size below the sleeper at the end of the test. This explains why the final sleeper void size at the end of the test at the end of the test is 1.7mm as against 2mm. Thus a simple relation between crib ballast particle size and void size below the sleeper can be derived as

Final void size below the sleeper = Void size – average particle size of crib ballast

The final void size in the above test has been achieved in approximately 600 cycles and the rate of height correction would be affected by sleeper spacing.

The above relationship implies that there would always be a residual void below the sleeper and the void below the sleeper will not be completely filled up. The final void size below the sleeper would depend on the average particle size of the crib ballast if the sleeper spacing is optimum. Thus the earlier concern about the sleeper lifting out of the ballast by passage of trains (lifting in front of the wheel) is not applicable to crib ballast sizes of 2mm i.e. 20mm at full scale. The uplift of the wheel in front of the wheel on live railway track is 1-2mm thus for the crib ballast to flow into void 2mm size, the size of the crib ballast should be less than 2mm.

One observation was made in the initial trial runs for large number of uplift cycles (more than 500) At the end of the test it was observed that the crib ballast of 2mm size had mixed with the bottom ballast of 5mm size and a few particles of the bottom ballast were visible in the top layer of the crib ballast. Also at the end of the test when the sleeper set up was raised from the top of the 5mm ballast it was observed that the 2mm ballast had not reached to the centre of the sleeper. The ballast was neatly packed on top of the crib ballast along the edge of the sleeper. It was then realised that the crib ballast was not filled up to the right depth before starting the test. Thus all further testing was done with the crib ballast filled in to the correct depth. It was then observed that with proper depth of crib ballast the mixing of crib and bottom ballast did not occur and at the end of the test when the sleepers were lifted off the bottom ballast the crib ballast had migrated to the centre of the sleeper and was neatly packed as a layer of smaller stone on top of the bottom ballast.

5.2.1.2.2 Discussion

Observations from the above test validated the results of the initial tests and conclusively demonstrated that a void below the sleeper will be filled up by the crib ballast depending on the average size of particle in the crib ballast. It also demonstrated that the current industry standard spacing was optimum for the performance of the two layered ballast system. The process of filling the void would be done in approximately 600 load cycles which is equivalent to the passage of a few trains in live railway track.

5.2.1.3 Effect of crib ballast particle size and uplift height in uplift cycles

These tests were run to investigate the effect of the crib ballast particle size and void size below the sleeper on the working of the two layered ballast system and to validate the relationship between the final void size below the sleeper and particles size of crib ballast developed based on the results of the preceding tests.

These tests were carried out using 28mm sleepers at 55mm spacing. 55mm sleeper spacing (550mm full scale) is the minimum allowable sleeper spacing on British Rail. It has been observed from the earlier tests that current industry standards for sleeper spacing are optimum for the performance of the two layered ballast system so the minimum allowable spacing on British Rail of 55mm was used for these tests.

The tests were carried out without any bottom ballast to eliminate the effect of bottom ballast as a variable in the test. Earlier observations have shown that in the uplift cycle when the crib ballast flows into the void below the sleeper, in the first few cycles some crib ballast is lost in the voids of the bottom ballast. A percentage of the height gain achieved by the crib ballast filling the void is lost due to compression of the bottom ballast and due to the crib ballast filling the voids in the bottom ballast. For these tests the sleeper assembly was placed directly on the rigid floor without any bottom ballast thus the effect of bottom ballast on sleeper displacement was eliminated. The sandpaper now represented the

surface roughness of the bottom ballast (Fig. 5.4). At the start of the test the sleeper assembly was placed directly on the sandpaper base with a minimum seating load, crib ballast was filled around the sleepers and the test was started. No simple cycles were run as there was no bottom ballast used. Uplift cycles were continued until there was no further height gain for the sleeper assembly in the uplift cycles. Thus for these tests, any height gain in the sleeper could now directly be related to the two parameters viz. void size below the sleeper and crib ballast particle size. The aim was to carryout a parametric study and develop parametric graphs relating maximum height gain of sleeper to void size (uplift height in uplift cycles) below the sleeper and maximum height gain of sleeper to particle size of crib ballast.

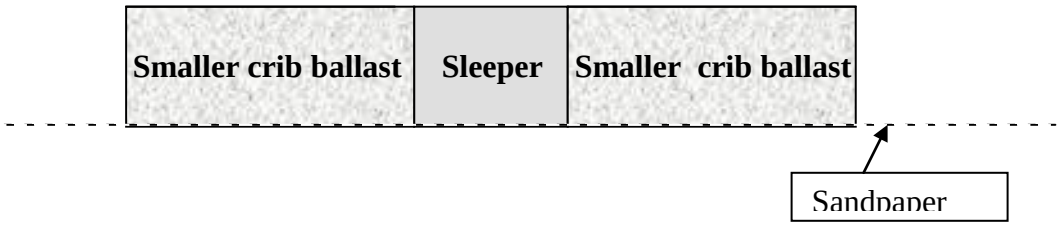

Fig. 5.4 Test set up without 5mm bottom ballast

5.2.1.3.1 Uplift height

In these tests the uplift height of the sleeper assembly in the uplift cycles was varied and the size of crib ballast was kept constant. 2mm stone was used as crib ballast which again was 10^{th} scale of the stoneblowing stone specification. Thus the average particle size

of the crib ballast was 1.7mm as described earlier. Four test runs were carried out with uplift height for each run as 1.5mm, 2.5mm, 3.5mm and 4.5 mm in the uplift cycles to simulate formation of different void sizes under the sleeper, and study the effect of void size on the sleeper height gain. The tests were continued until there was no further height gain for the sleepers. Results are presented as a graph of maximum sleeper displacement (level) against the number of cycles, for different uplift heights, in figure 5.5a. A graph of maximum sleeper height gain against sleeper uplift height is shown in figure 5.5b.

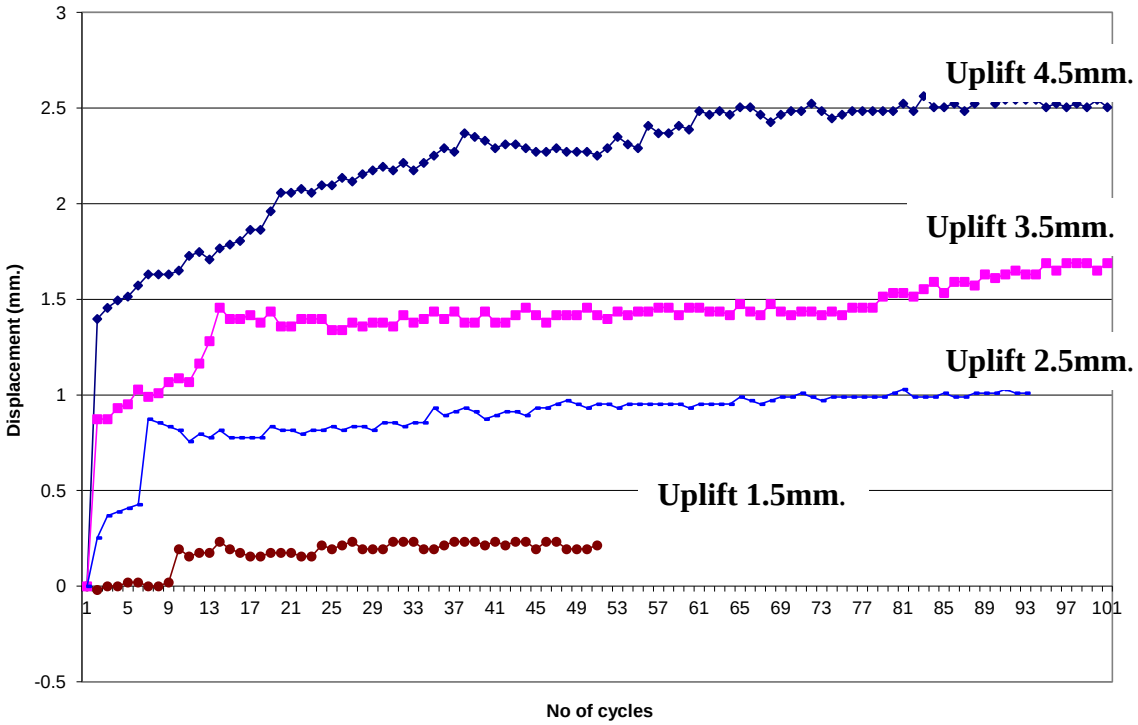

Fig5.5a Effect of uplift height on sleeper height gain

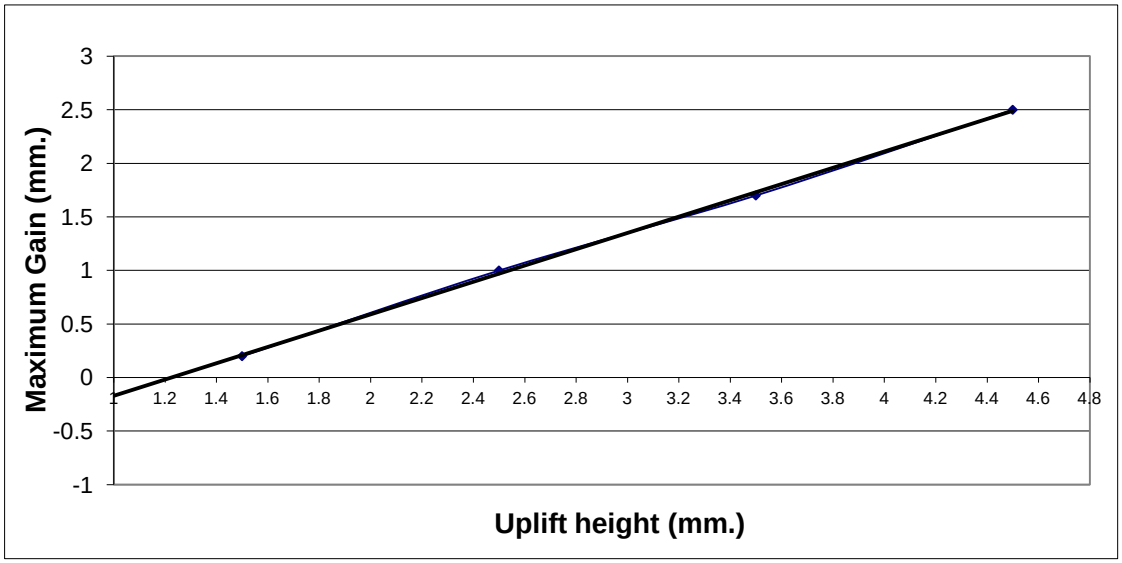

Figure 5.5b Uplift height against maximum height gain.

5.2.1.3.1.1 Observations

The crib ballast migrates into the void below the sleeper in the uplift cycles, as with the start of the uplift cycles the void size below the sleeper reduces. Maximum height gain can be observed in the first uplift cycle after which the height gain is gradual for the remaining cycles. The height gain in the sleeper at intervals of 25 cycles is shown in table 5.4

Table 5.4 Sleeper uplift height gain

Sleeper uplift (mm.)	Cycle number				
	1	25	50	75	Final sleeper height gain (mm.)
Height gain (mm.)					
1.5	0	0.19	0.19	-	0.21
2.5	0.25	0.83	0.95	0.99	1.01
3.5	0.87	1.34	1.45	1.41	1.69
4.5	1.39	2.09	2.27	2.46	2.5

It can be seen that for a void size of 2.5mm 25% of the total height gain occurs in the first uplift cycle while for a void size of 4.5mm more than 50% of the total height gain occurs with the first uplift cycle. The initial height gain in the first uplift cycle for tests run earlier with 5mm bottom ballast and 2mm crib ballast is not as large as for these tests. First few uplift cycles for a test run with bottom ballast and test run without bottom ballast is shown in figure 5.6. The results shown are for an uplift of 2.5mm for 28mm sleepers at 55mm spacing.

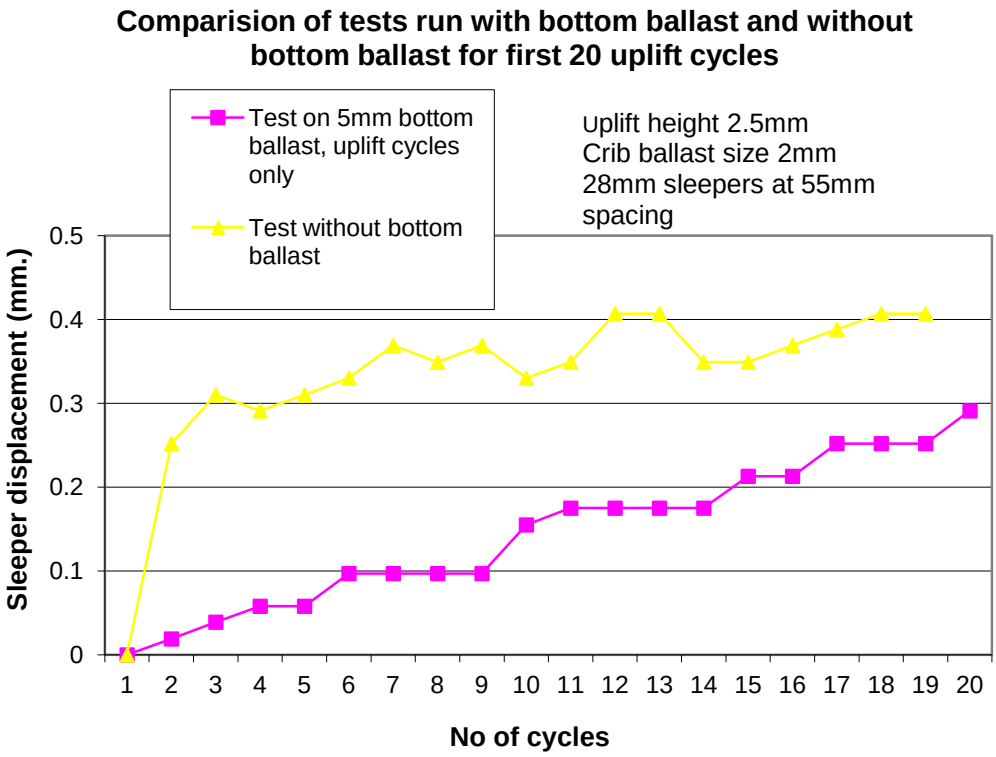

Figure 5.6 Comparision of 20 uplift cycles for test with 5mm bottom ballast and test without bottom ballast.

It can be seen from the graph that the sleeper height gain in the first cycle for tests run with 5mm bottom ballast below the sleepers is very small compared to that of the tests run with sleepers on sandpaper without bottom ballast.

Comparing figure 5.5a and figure 5.3b the final height gain for the sleepers is achieved in 100 cycles for sleepers on sandpaper (without bottom ballast) while for the tests run with 5mm bottom ballast the final height gain is achieved in over 500 cycles.

It is observed in figure 5.3a that maximum height gain of sleepers is at least the uplift height minus the maximum particle size of the crib ballast. The final sleeper height gain for different uplift heights achieved in the tests and the predicted height gain is shown in table 5.5. The predicted height gain was calculated based on the relationship of

final sleeper height gain = uplift height – average particle size of the crib ballast

developed earlier.

The average particle size of crib ballast is 1.7mm for the tests.

Table 5.5 Predicted and measured maximum height gain.

Uplift height (mm.) **A**	Average particle size of crib ballast (mm.) **P**	Predicted maximum height gain (mm.) **Ap= A - P**	Measured height gain (mm.) from test data **Am**
1.5	1.7	0	0.2
2.5	1.7	0.8	1
3.5	1.7	1.8	1.7
4.5	1.7	2.8	2.5

From the table it can be seen that the relationship developed between maximum height gain of sleepers and average particle size of the crib ballast can be used to predict the final void size below the sleepers for a given particle size of the crib ballast. The difference

between predicted and measured maximum height gain is negligible. The equation would apply to standard British Rail sleepers at standard spacing.

The equation used to predict maximum sleeper height gain in table 5.5 implies that any void size larger than 1.7mm it will be reduced to 1.7mm i.e. for a void size of 3.5mm and crib ballast particle size of 1.7mm the maximum sleeper height gain would be 1.8mm thus the residual void size would be 1.7mm. Thus any void below the sleeper larger than the average particle size of crib ballast will be reduced to the average particle size of the crib ballast.

The graph of uplift height gain has been plotted against the maximum height gain in figure 5.5b. A trendline is drawn to forecast the uplift height for which there will be no sleeper height gain for a given crib ballast average particle size of 1.7mm. From figure 5.5b for an uplift height of 1.2mm the trendline's Y intercept is zero. This implies that any void below the sleeper larger than 1.2mm will be reduced to 1.2mm size, and not 1.7mm, after which there will be no sleeper height correction. This is an interesting result as it relates the maximum height gain of the sleeper to the minimum particle size of the crib ballast as compared to the average particle size of the crib ballast. Looking again at the stoneblower stone specification the minimum particle size is 1.2mm, thus the trendline in the graph in figure 5.5b has related the residual void size below the sleeper at the end of the uplift cycles to the smallest particle size of the crib ballast as against the average particle size of the crib ballast

5.2.1.3.2 Particle analysis

These tests were run to determine the effect of particle size of crib ballast on the system. All previous tests have been carried out using stones of size 2mm simulating stoneblowing stone at tenth scale. The 2mm ballast grading is given in chapter 4. The 2mm ballast consists of particles between 2mm and 1.4mm and a small fraction of particles from 1.4mm to 1.2mm. For the particle analysis tests single size fractions of the stones between size 2mm and 1.2mm were used, these are given in table 5.6.

Table 5.6 Single size stone fractions used for particle analysis tests.

Test No.	Passing sieve size (mm)	Retained on sieve size (mm)	Particle size designation (mm.)
1	2.38	2.0	2.4
2	2.0	1.7	2.0
3	1.7	1.4	1.7
4	1.4	1.2	1.4

As the particles have been sieved to a very narrow range of particle sizes they have been designated as single size particles as shown in table 5.6 i.e. the particle size passing 2mm sieve retained on 1.7mm sieve has been designated as a particle of size 2.0mm.

The uplift height was maintained constant at 2.5mm for all the tests while particle size was varied for each test. 28mm sleepers at 55mm spacing were used and the sleepers were placed directly on the sandpaper eliminating the bottom ballast. Only lift cycles needed to be run as the test was run without bottom ballast.

Results were plotted as sleeper maximum displacement for each cycle. The graph of maximum sleeper displacement against number of cycles, for different particle sizes is shown in Fig. 5.7a. The graph of maximum height gain of sleepers against particle size is shown in Fig. 5.7b.

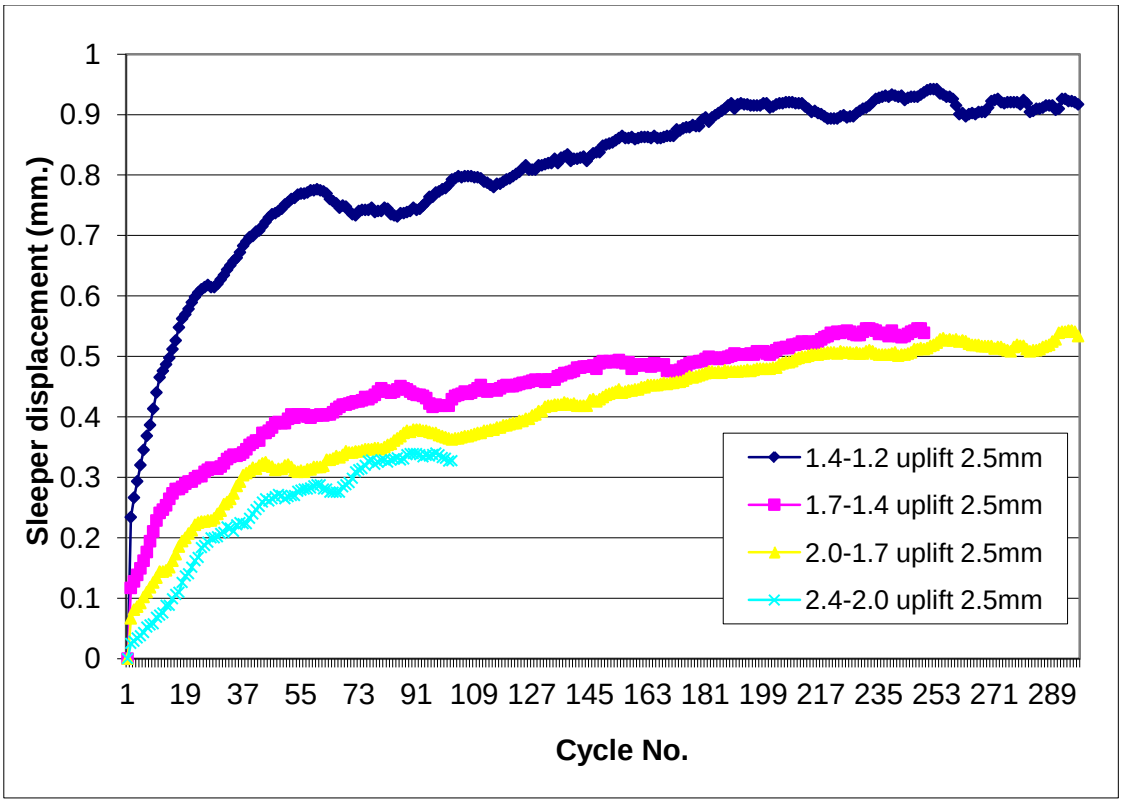

Fig 5.7a Effect of particle size on sleeper height gain

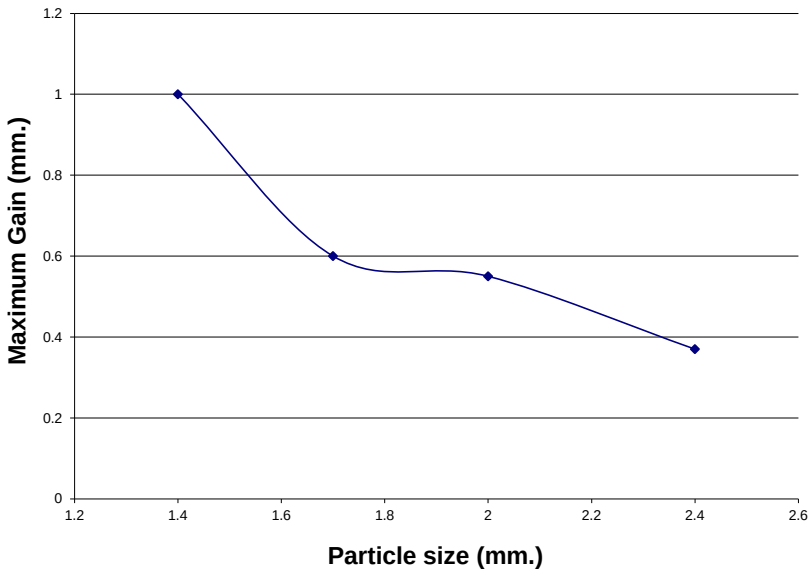

Figure 5.7b Particle size Vs Maximum gain

5.2.1.3.2.1 Observations

The tests have taken more than twice as many load cycles as compared to the uplift height test to achieve maximum sleeper height correction. The uplift height tests were run for approximately 100 cycles while as seen in figure 5.7 the tests have been run for approximately 300 load cycles.

The uplift height achieved at intervals of 50 cycles and the maximum height gain for the sleeper at the end of the test are given in table 5.7.

Table 5.7 Sleeper height gain

Particle fraction (mm.)	Cycle number						
	1	50	100	150	200	250	Maximum height gain
	Sleeper uplift height (mm.)						
2.38 - 2	0	0.3	0.37	-	-	-	0.37
2 - 1.7	0.03	0.32	0.37	0.41	0.48	0.52	0.55
1.7 - 1.4	0.09	0.39	0.43	0.48	0.5	0.5	0.6
1.4 - 1.2	0.1	0.7	0.77	0.84	0.91	0.91	1

It is seen from data in table 5.7 and figure 5.7a that height gain for the sleepers in the uplift cycles is quicker for smaller crib ballast particle size.

The predicted maximum height gain from equation developed earlier and the measured maximum height gain in the test is compared in table 5.8.

Table 5.8 Predicted and measured height gain

Uplift height (mm.) **A**	Particle size (mm.) **P**	Predicted maximum height gain of sleepers (mm.) **Ap = A – B**	Measured maximum height gain of sleepers from test (mm.) **Am**
2.5	2.4	0.1	0.37
2.5	2.0	0.5	0.55
2.5	1.7	0.8	0.6
2.5	1.4	1.1	1

From data in table 5.8 it can be seen that the measured maximum gain in the tests and the predicted height gain are similar. For particle size 2.4mm the maximum gain is more than the predicted gain and for particle size 1.7mm the predicted gain is less than that measured at the end of the test but the difference is not substantial.

5.2.1.3.3 Discussion

The above parametric study for crib ballast particle size and uplift height in the uplift cycles has validated the equation developed to predict the final sleeper height gain. This equation would be valid for optimum sleeper spacing for optimum performance of the two layered ballast system which as demonstrated by model tests is the standard sleeper spacing on British Rail.

The measured maximum sleeper height gain in some instances is less than the predicted height gain and in some instances is more than the predicted height gain although

the difference is not substantial. When the measured height gain is less than the predicted height gain it is because the test has not been run for sufficient number of load cycles and thus the end point for the graph has not been reached. When the measured height gain is more than the predicted height gain it is because of the particles in the crib ballast matrix smaller than the average particle size of the crib ballast. If the void below the sleeper is filled up by the smaller particles in the crib ballast the maximum height gain would be more. This would depend on the percentage of smaller particles in the crib ballast and crib ballast grading. Thus there is some effect of the smaller particles in the crib ballast matrix on the final sleeper height gain in the uplift cycles.

5.2.1.4 Effect of bottom ballast size and grading on the two layered ballast system

These tests were carried out to investigate the effect of size and grading of bottom ballast on the two layered ballast system

It has been observed from the two dimensional glass model and also from results of model tests that when the smaller crib ballast from the crib migrates into the void below the sleeper for the first few uplift cycles some crib ballast is lost in the voids in the bottom ballast. The amount of crib ballast lost in the voids of the bottom ballast depends on the crib ballast particle size. Thus these tests were designed to investigate the effect of changing the grading of the bottom ballast on the performance of the two layered ballast system.

Another concern was that with a voided sleeper in track and smaller crib ballast the crib ballast will migrate to the underside of the sleeper forming a layer of smaller stone on top of the bottom ballast. For example if 20mm stone was to be used as crib ballast with 50mm stone as bottom ballast with time the 50mm stone would be covered by a layer of 20mm stone. These tests were also to investigate the effect of having smaller ballast below a voided sleeper on the performance of the two layered ballast system.

5.2.1.4.1 Effect of bottom ballast grading

The standard railway ballast is essentially a mix of stone sizes ranging from 28mm to 50mm with large proportion of stones of size 40mm. In these tests changes were made to the grading of ballast within the sizes 50mm and 28mm i.e. two different ballast specifications were used (Railtrack specification and 1988 British Rail specification) with different proportions of stone sizes as shown in table 5.9. Tests were run with 2mm stone as crib ballast uplift height in uplift cycles was maintained at 2.5mm. Similar results were achieved for both ballast types. This implies that small changes to ballast grading within the size range 50mm to 28mm does not affect the performance of the two layered ballast system.

Table 5.9 Bottom ballast grading

Grading I (Railtrack specification)		Grading II (Cope 1993)	
Sieve	% passing	Sieve	% passing
5.0mm	100	5.0mm	100
3.75mm	40		
2.8	0	2.8mm	0

5.2.1.4.2 Effect of bottom ballast size.

For this test the 2mm stone (10^{th} scale of stoneblowing stone) was used as bottom and crib ballast. Thus both bottom and crib ballast were of smaller size compared to standard railway ballast. Uplift height in the uplift cycles was 2.5mm and 20 simple cycles were run followed by uplift cycles. 28mm sleepers at 55mm spacing were used. The results are shown in figure 5.8 in form of graph of sleeper displacment against the cycle number. A comparision has been made with similar test run earlier with 5mm stone (10^{th} scale of standard railway ballast) as bottom ballast and 2mm stone as crib ballast.

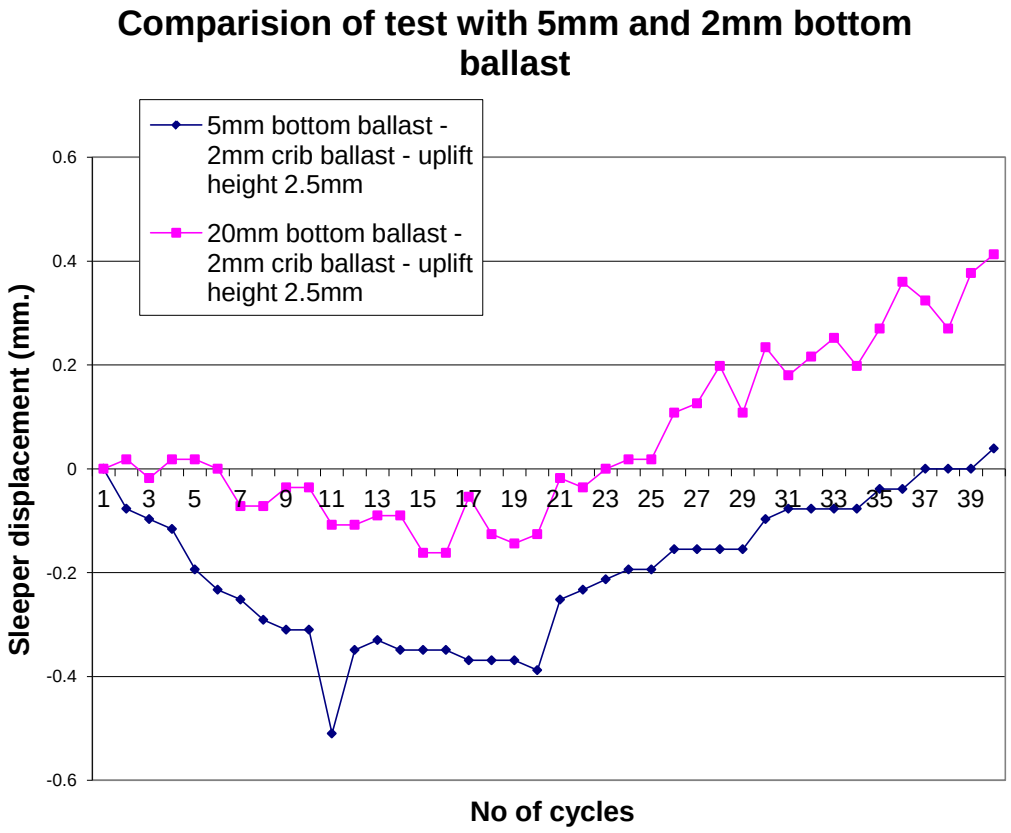

Figure 5.8 Comparision of test runs with 5mm and 2mm bottom ballast

5.2.1.4.2.1 Observation

Ballast compression for the first twenty simple cycles is less for 2mm ballast. At the end of 20 simple cycles ballast compression in 2mm ballast is approximately 0.1mm while in 5mm ballast is approximately 0.4mm. This is because of better stress distribution in smaller ballast. As discussed earlier in the literature review smaller ballast particle size gives better load distribution below the sleeper. This is due to larger number of contact

points below the sleeper for smaller ballast leading to better stress distribution. The plastic compression of ballast is reduced due to better stress distribution in the ballast.

The rate of height correction in the uplift cycles for the test with 2mm bottom ballast is faster as compared to test with 5mm bottom ballast. At the end of 20 uplift cycles the sleeper height correction for 2mm bottom ballast is 0.4mm while for 5mm bottom ballast is 0mm. Thus sleeper height correction is four times more in smaller ballast. An explanation for this phenomenon would be that the 5mm ballast has larger proportion and size of voids and thus any initial migration of crib ballast to under the sleeper would largely be compacted by the sleeper into the voids of the bottom ballast. Also as the ballast compression for 5mm ballast is more some proportion of the height gained by migration of the crib ballast would be lost in the permanent compression of the bottom ballast.

5.2.1.5 Uplift equal to displacement cycles

As described earlier the basic principle of all testing on two layered ballast system was to simulate a loose sleeper (s) in the track. In all the previous tests after running 20 simple load cycles, which simulate a properly packed sleeper in the track , in the uplift cycles the sleeper was lifted up between load cycles to simulate a voided sleeper in the track. The aim was to understand how a void of a certain size would be filled up with crib ballast of a given size.

In the above tests after 20 load cycles a large void dramatically appears below the sleeper, an occurrence, which is very rare in live railway track. The development of a voided sleeper(s) in the railways is a slow process occurring due to various reasons over a long time period. The uplift equal to displacement cycles, were run to simulate the gradual development of void below a sleeper.

It was observed from the earlier tests, that under cyclic loading (in simple cycles) the ballast undergoes plastic compression with each cycle, although the compression in each cycle is very small. Thus in the uplift equal to displacement cycles, after each load cycle the sleepers were brought back to their datum zero level. This meant that the uplift in each

cycle was equal to the displacement of the sleeper in the ballast. As the sleeper sunk into the ballast for each load cycle it was brought back up to the original zero datum level which was set up at the start of the test. This simulated the slow formation of void below the sleeper. The tests were run with both 5mm and 2mm stones as crib and bottom ballast. The test parameters are described in table 5.8.

Table 5.10 Different crib and bottom ballast configuration for uplift equal to displacement cycles

Test number	Sleeper size (mm.)	Sleeper spacing (mm.)	Size of bottom ballast (mm.)	Size of crib ballast (mm.)
1	28	55	5	5
2	28	55	5	2
3	28	55	2	2

After a single simple load cycle, uplift equal to displacement cycles were run. The results are shown in figure 5.9 in form of graphs of maximum sleeper displacement in each cycle. In figure 5.9 a. the results shown are for tests run on 5mm bottom ballast. A comparison has been made between results for test number 1 and 2 from table 5.10 in figure 5.9a. In figure 5.9b a comparison has been done for test carried out on 2mm bottom ballast and 5mm bottom ballast i.e. test number 2 and 3 of table 5.8.

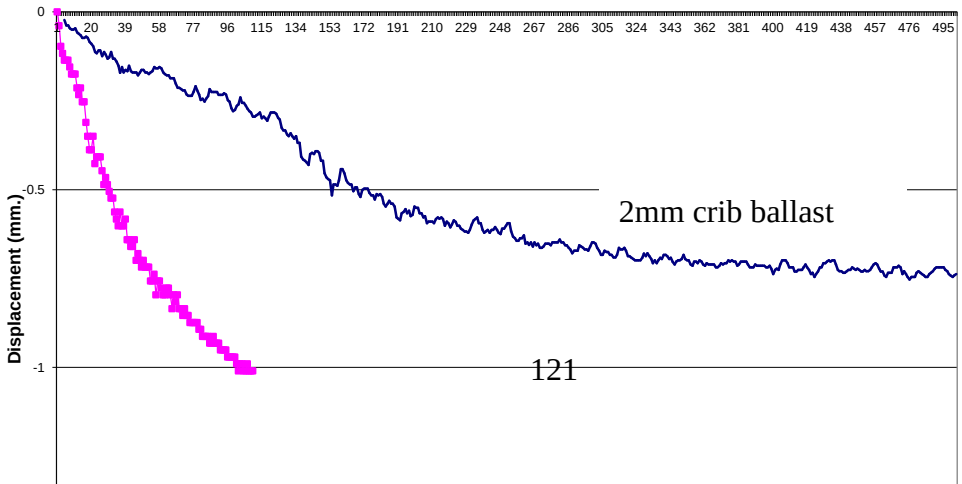

2mm

5mm crib ballast

Fig 5.9a Lift height equal to settlement test for 5mm bottom ballast

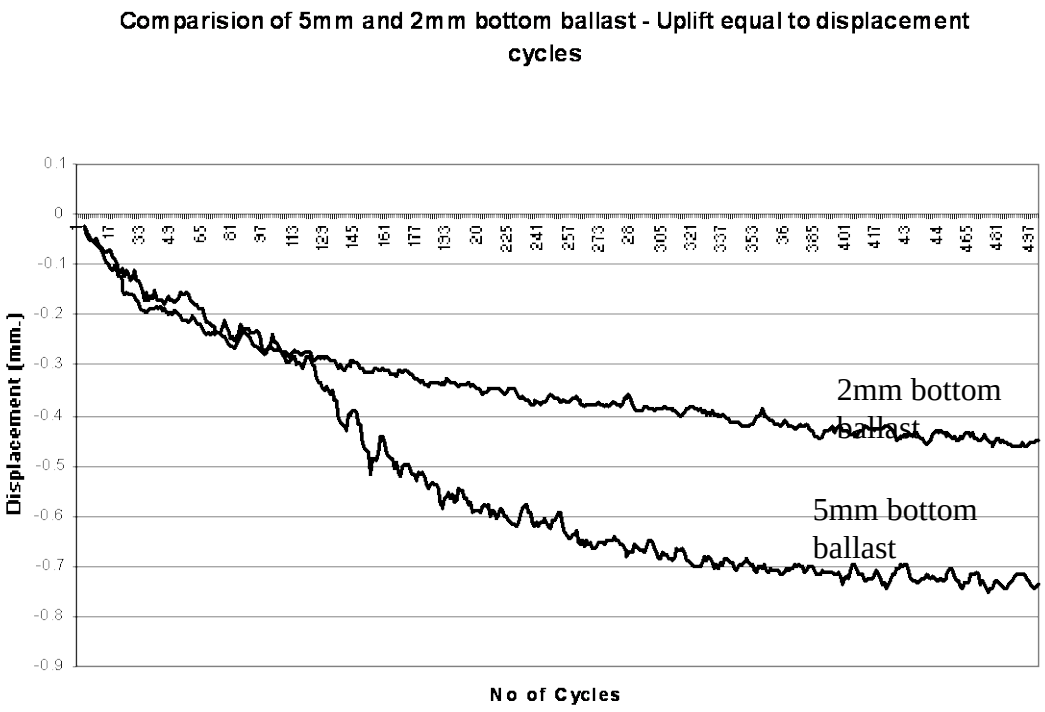

Figure 5.9b Comparison of tests run on 5mm and 2mm bottom ballast.

5.2.1.5.1 Observations

a. Tests run with 5mm bottom ballast

From figure 5.9a it can be seen that with 2mm crib ballast the sleeper displacement into ballast is gradual and the sleeper displacement is arrested at 0.7mm (7mm full scale) in approximately 300 load cycles. While for 5mm crib ballast the sleeper displacement into ballast in approximately 100 load cycles is twice that for the test with 2mm crib ballast.

At the end of approximately 300 uplift equal to displacement cycles there is no further displacement of the sleeper below the ballast for test with 2mm ballast in the crib. Thus the sleeper void has increased from zero to 0.7mm (7mm full scale) but has not increased any further. This implies that for a new track built with the two layered ballast system the track would not deteriorate beyond a certain tolerance based on the size of the crib ballast.

b. Tests run with 2mm bottom ballast

For tests run with 2mm bottom and crib ballast the ballast compression under cyclic loading is less for 2mm bottom ballast. At the end of approximately 300 load cycles the ballast compression is 0.5mm as compared to 0.7mm with 5mm crib ballast. This again reinforces the fact that for smaller bottom ballast, ballast compression is less as compared to larger bottom ballast.

5.2.1.6 Tests with different configuration of simple and uplift cycles – Type B runs.

For these tests the configuration of the simple and uplift cycles for the tests was changed. These tests were carried out with the initial model tests to try and finalise how detailed testing on the two layered ballast system would be carried out. All the previous test described earlier are based on simulating a loose sleeper in the track by lifting it up between load cycles. This simulates a loose sleeper pushed down onto the ballast by the wheel load but rising back to its original level supported by adjoining sleepers once the wheel has passed. This method is a good representation of a loose sleeper in live railway track. For type B runs a loose sleeper was simulated by continuously loading it for 10 simple load cycles (simulating 10 axles on live track) without uplift and then lifting the sleeper up once by a specified amount before again loading it for 10 simple load cycles. This process was

repeated for a few times in a test. In the type B runs it was assumed that while a train (railway traffic) was passing on top of a loose sleeper it would not lift up to its original level until all the axles had passed. Thus the sleeper was lifted up between 'trains', each train assumed to have 10 axles. It soon became apparent that this was not a correct simulation of live track conditions and after a few runs these tests were abandoned but some interesting observations were made from the results of these tests so these are described here.

The procedure for setting up the test was similar to earlier tests. Sleepers were lowered onto 5mm bottom ballast with a minimum seating load and the sleeper datum level was set to zero after which 2mm crib ballast was filled in around the sleepers. The uplift height was specified for the test and test was started. For the simple cycle the load was cycled from the minimum seating load to maximum load of 8kN as before. For the uplift cycle the load was released to zero allowing the sleepers to lift up. Results are presented in form of graphs of maximum sleeper displacement against cycle number in figure 5.10 A few selected results have been shown in the graphs.

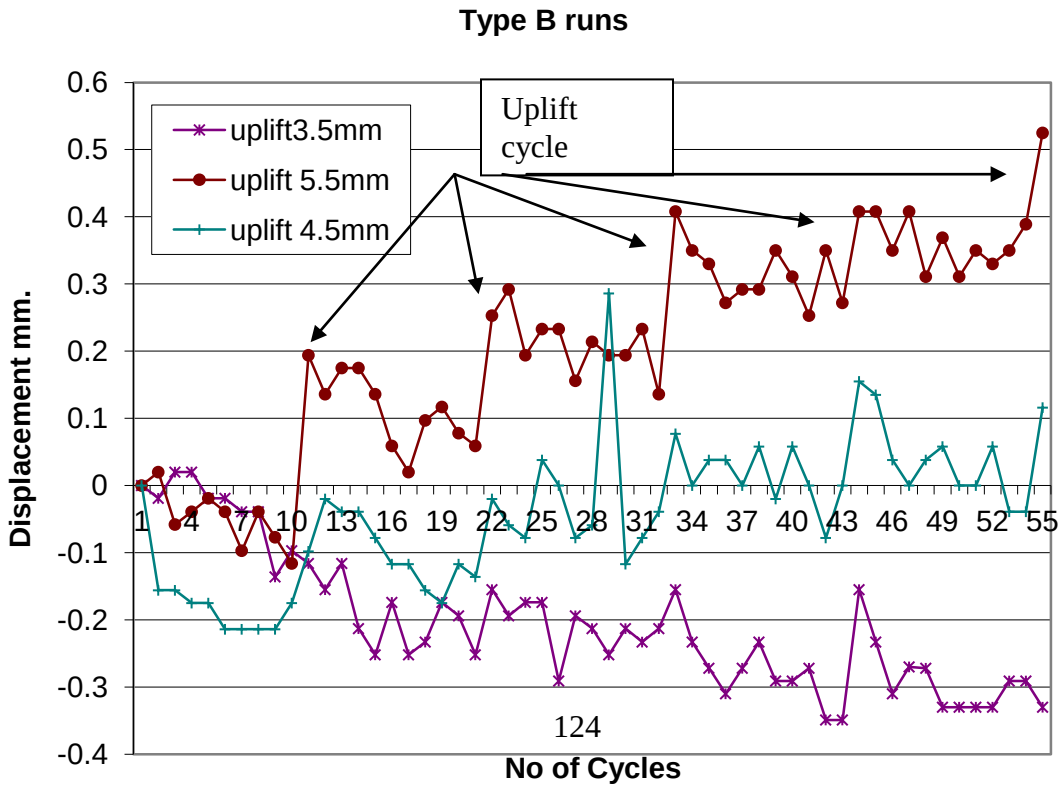

Figure 5.10 Type B

runs with different uplift heights

Results for three tests are shown in the graph for sleeper uplift of 3.5, 4.5 and 5.5mm in the uplift cycle. One uplift cycle was run after 10 simple cycles and the process was repeated for a total of three cycles.

Observations

The graph lines are not smooth and there are a lot of spikes and dips in the graphs although the overall trend can be identified for each graph. One reason for this is that the loading machine was being run on a high oil pressure and the other reason is that due to high uplift heights of 3.5-5.5 mm in the uplift cycles the crib ballast migrated easily into the void below the sleeper and after each uplift cycle the as the new ballast below the sleeper was being compressed the sleeper level kept changing with each loading cycle causing spikes and dips in the graph.

It is possible to identify the load cycles from the uplift cycles. It can be seen that for all graphs for the 10 simple load cycles the ballast undergoes some compression. When the sleeper is lifted up in the eleventh cycle and loaded again to maximum load the sleeper level is raised as the crib ballast moves into the void below the sleeper. Depending on the amount of uplift given in the one uplift cycle the sleeper height gain is lost again in the next set of ten simple load cycles.

For an uplift of 3.5mm in the lift cycle the sleeper height gain is lost as ballast is compressed more than the height gained in the uplift cycle.

For 5.5mm uplift the sleeper gains considerably in height as the amount of crib ballast flowing into the void is more. This height gain is not lost in the subsequent simple cycles causing the sleeper to slowly rise out of the ballast.

For 4.5mm uplift the sleeper height gain in the one uplift cycle balances the ballast compression due to the 10 simple cycles of loading. Thus the graph is close to zero level.

Although the tests are not exhaustive some simple conclusions can be drawn. It has been mentioned earlier that due to various reasons the ballast below the sleepers settles differentially causing the track to loose its vertical alignment. To maintain a proper track 'top' the track needs to be lifted and the ballast packed under the sleepers either by tamping or by stoneblowing. The above graphs can be used to develop a potential tool for track maintenance with the two layered ballast system. The graphs seem to suggest that on a good track with smaller crib ballast if after a few loading cycles the sleepers are lifted up the loss of sleeper vertical alignment due to ballast compression under traffic could be recovered keeping the track in proper vertical alignment. The amount by which the track needs to be lifted could be worked out and would depend on the size of crib ballast and the amount the track deteriorates periodically.

The property of the crib ballast to move into the void below sleepers depending on the size of the void would also affect the working of the stoneblower and tampers. As discussed earlier to maintain a good 'top' on a track the low spots on the track need to be lifted up and the void below the sleeper packed with ballast. This is the basic principle of operation of the tamper and the stoneblower. The tamping machine raises the track and compresses the ballast into the void below the sleeper while the stoneblower fills the void by injecting new stones of smaller size. To get better results tampers resort to high lift tamping lifting the track up by 40-50mm and packing the ballast into this void. The stoneblowers have to raise the track by an amount equal to the void size and an extra 45mm to ease the process of injecting stones into the void. Thus the maintenance operation of raising the track is similar to type B runs where the track has been raised by 3-5mm(30-50mm full scale) after a few simple loading cycles. From type B runs and also from results of earlier tests it is evident that even raising the track once by as much as 3 – 5mm (30-50mm full scale) a large amount of stone will migrate from the crib into the void below the sleeper causing the sleeper level to rise. This gain in height by the sleeper would not be

accounted for in the design for the track 'top' prepared by the on board computers on the tampers and stoneblowers thus there is a risk of track levels being over corrected as demonstrated by the study by Ball (2003). With the tampers vibrating and compacting the ballast after raising the track the problem would not be severe. For the stoneblower it could lead to unexpected, poor post maintenance track quality as the stoneblower does not disturb the ballast and after the stoneblowing process the sleeper is lowered back onto the ballast, again this corroborates research by Ball (2003) on stoneblower performance.

5.2.1.7 Tests on twin block sleepers

Tests on twin block sleepers were a repeat of the type A runs carried out on monoblock sleepers with different sleeper spacing. The different configurations of sleeper spacing and crib ballast particle size used are described in table5.11. The size of bottom ballast was 5 mm. (50mm full scale). The method of setting up the test was the same as that for model test on wooden monoblock sleepers. The results are shown as graphs of sleeper displacement against cycle number for each test in figure 5.11.

Table 5.11 Sleeper spacing and crib ballast combination for tests on twin block sleepers (Holbourn P. 2003).

Sleeper spacing (mm.)		Bottom ballast size (mm.)	Crib ballast size (mm.)	Uplift height in uplift cycles (mm.)
Model scale	Full scale			
45	450	5	5	2.5
45	450	5	2	2.5
60	600	5	2	2.5
70	700	5	2	2.5

80	800	5	5	2.5
80	800	5	2	2.5

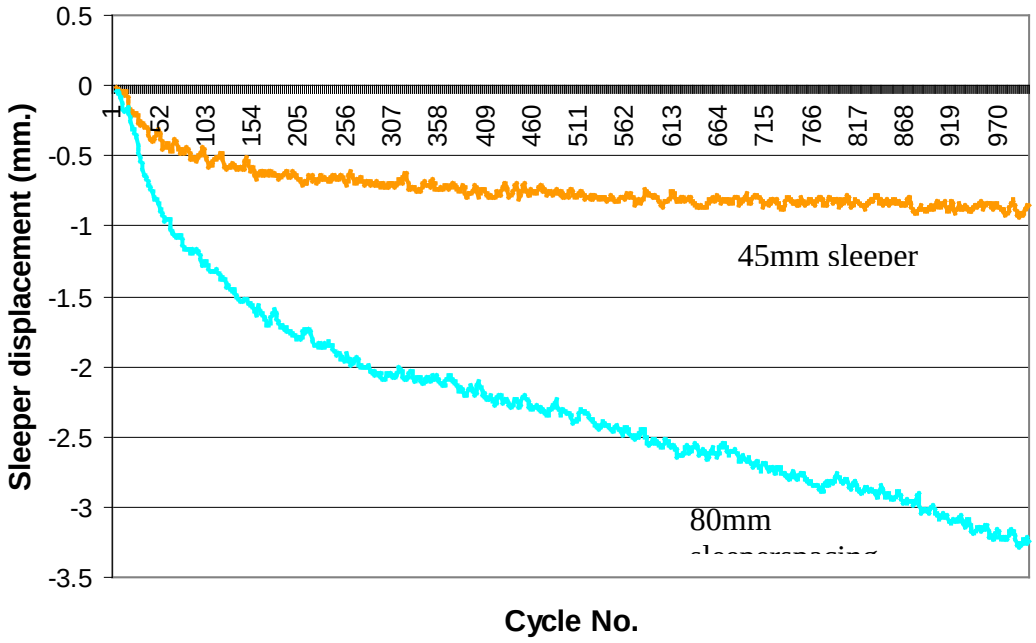

Figure 5.11a Tests on twin block sleepers – Type A runs with 5mm bottom and crib ballast.

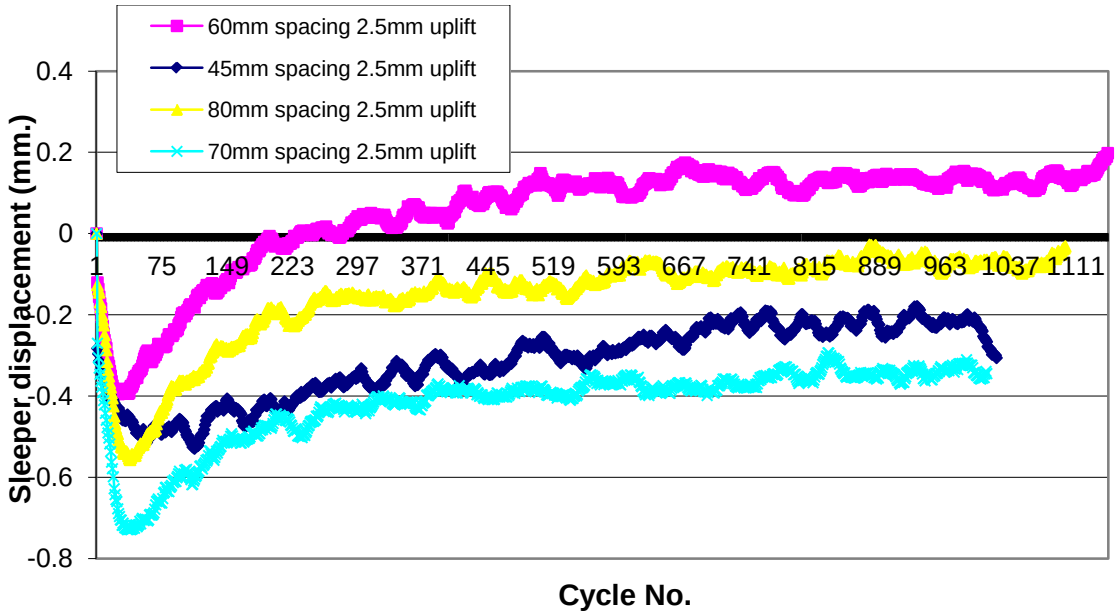

Figure 5.11b Tests on twin block sleepers - Type A runs in 2mm crib ballast

Observations

a. 5mm crib ballast

These tests were run for two sleeper spacing of 45mm (450mm full scale) and 80mm (800mm full scale). Twenty simple cycles followed by uplift cycles with 2.5mm uplift were run. The results for twin block sleepers in 5mm crib ballast are similar to those of monoblock sleepers with 5mm crib ballast. There is no sleeper height gain in the uplift cycles and the sleeper continues to sink into the bottom ballast in the uplift cycles. The total sleeper displacement in the bottom ballast for sleepers with 45mm spacing is approximately 1mm while for sleepers at 80mm spacing the sleeper displacement is 3mm, thus again for increased sleeper spacing the ballast compression below the sleepers is more. Comparing with similar tests on monoblock sleepers (Figure 5.3a) it can be seen that for monoblock sleepers at 45mm spacing the sleeper displacement into bottom ballast at the end of 1000

cycles is 0.6mm while for twin block sleepers at 45mm spacing the total displacement is 1mm at the end of 1000 load cycles. Similarly for tests with sleepers at 80mm spacing the sleeper displacement into ballast for monoblock sleepers is 1.5mm while for twin block sleepers is 3mm.

b. 2mm crib ballast

The two layered ballast system works better with monoblock sleepers as compared to twin block sleepers. From Figure 5.11b it can be seen that the void below the sleeper with 2mm crib ballast for all sleeper spacing has not filled up to the total void size minus the average particle size of crib ballast (i.e. upto 0.8mm). The optimum sleeper spacing for performance of two layered ballast system is 60mm (600 mm full scale) which is the same as observed from tests on monoblock sleepers, although the total sleeper height gain for twin block sleepers is less.

5.2.3 Tests on steel sleepers

Tests on the two layered ballast system were carried out using model steel sleepers fabricated from slotted iron angles and bent to the shape of an inverted trough. The aim was to study if the system worked on track with steel sleepers.

The same set up as for the wooden sleepers was used to carry out the test. Steel sleepers were fixed to the loading beam at a spacing of 55mm centres. As the test set up has been described in detail in chapter 4 only results will be discussed here.

For the first test the sleepers were lowered on to the bottom ballast in a similar manner as the wooden sleepers with a minimum seating load, the crib ballast was filled around the

sleepers and the test was carried out with 20 simple cycles and uplift cycles. Uplift height in uplift cycles was 2.5mm. Tests were carried out on 5mm bottom ballast with both 5mm and 2mm stones used as crib ballast. Results are shown as graph of sleeper displacement of each load cycle.

5.2.3.1 Initial testing

The first test was carried out with 5mm bottom and 2mm crib ballast. The sleeper was lowered onto the crib ballast with a minimum seating load and after filling in the crib ballast the test was started. The results are shown in figure5.12.

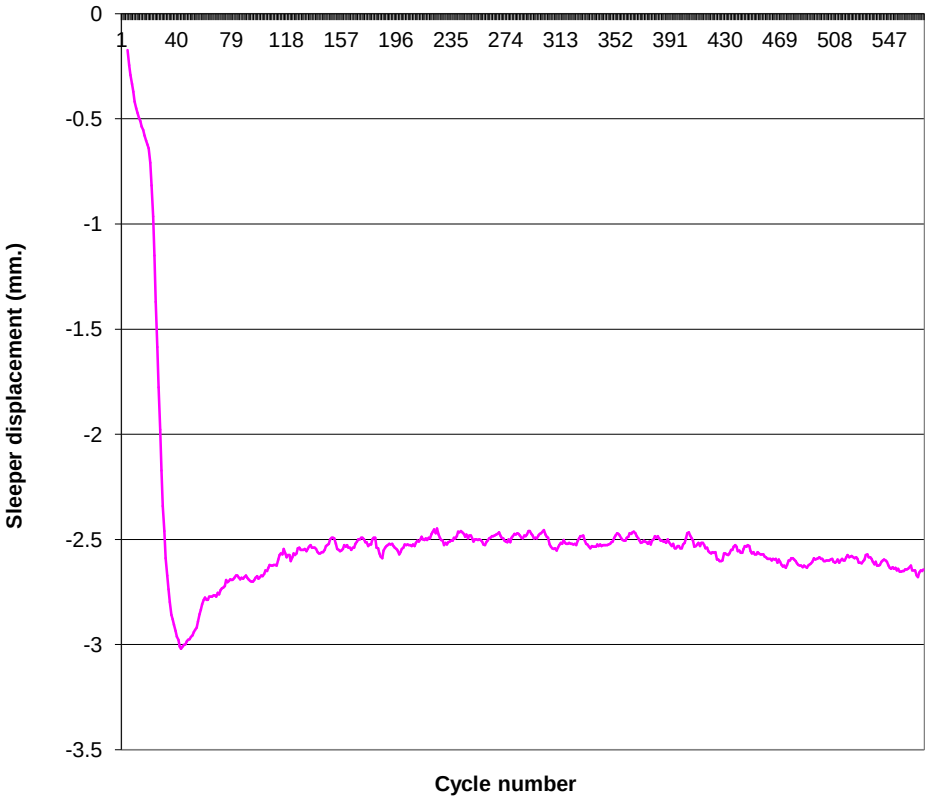

Figure 5.12 Steel sleeper placed on ballast with no initial displacement – Type A run – 2mm crib ballast – uplift height 2.5mm

Observations

The sleeper displacement into the ballast is quite rapid till the displacement is 3mm in approximately 43 cycles i.e. 20 simple cycles and 23 uplift cycles. Subsequently there is a slight correction in sleeper height of approximately 0.5mm as the sleeper rises to 2.5mm from 3mm.

The rapid sleeper displacement into the ballast is because of the sleeper being pushed into the bottom ballast until the inverted trough shape of the sleeper was completely

filled with ballast. Steel sleepers when laid in live track are placed on the ballast and tamped to push the bottom ballast into the void in the trough shape of the sleeper, this being done before the track is opened to traffic. In the test above the steel sleepers were placed on the bottom ballast but the test was started without ensuring the void in the sleeper trough was filled with ballast. Thus the sleeper displaced rapidly into the ballast for 3mm until the void below the sleeper was filled up completely.

5.2.3.2 Comparision of results for 5mm and 2mm crib ballast

For all subsequent tests using the steel sleepers, before starting the test the sleepers were compressed into the 5mm bottom ballast until the inverted trough shape of the sleepers was filled up with ballast. This is similar to the procedure of installing steel sleepers on the railway. The sleepers were pushed into the ballast and by visual inspection it could be verified that the sleeper underside was full of ballast. The sleepers were than maintained in this position with a minimum seating load. The datum zero level for the test was set and the crib ballast filled around the sleepers before starting the test. Tests were run with both 5mm stones and 2mm stones as crib ballast with 20 simple cycles followed by uplift cycles, results are shown in figure 5.13 as graph of sleeper displacement for each cycle.

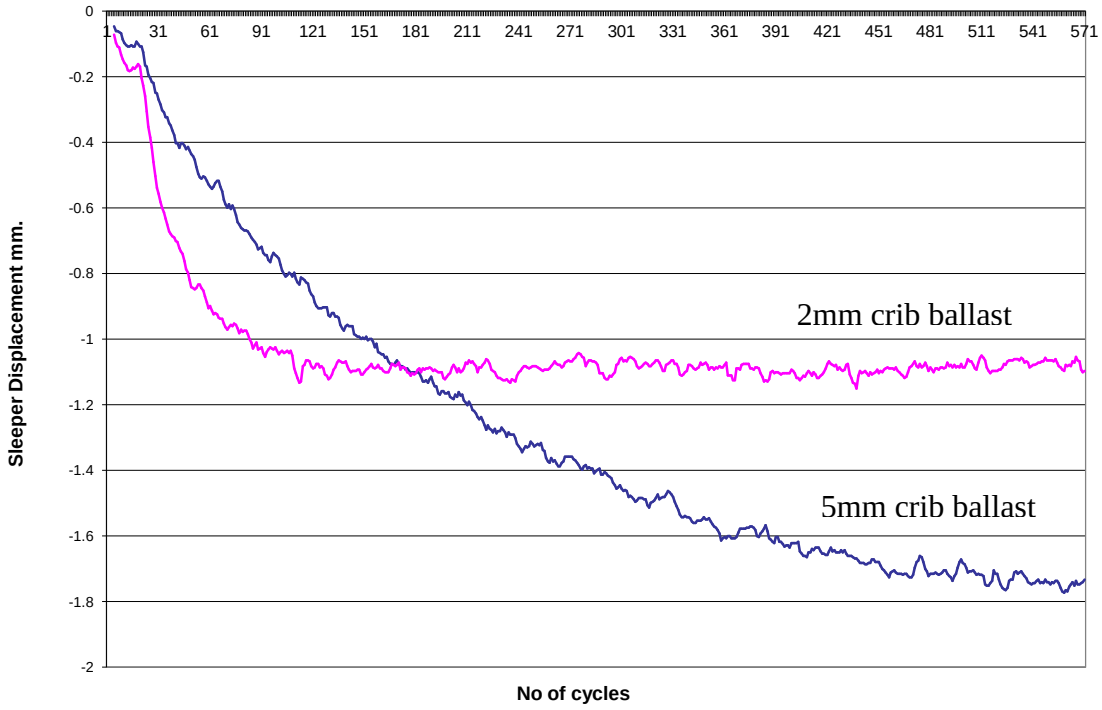

Figure 5.13 Tests on steel sleepers – Type A runs – uplift height 2.5mm.

Observations

For sleepers with 5mm crib ballast the final sleeper displacement is 1.8mm against the 1.2mm for sleepers with 2mm crib ballast. There is no correction in sleeper height for the uplift cycles for both 5mm and 2mm ballast in the crib but the sleeper displacement with 2mm crib ballast is more than for 5mm crib ballast.

The reason why there is no sleeper height gain in the uplift cycles even with 2mm crib ballast is the inverted trough shape of the steel sleeper. The inverted trough shape for the steel sleeper once filled with ballast will not allow new material to move in to the underside of the sleeper for the uplift cycles. Thus the proposed system of filling voids under the sleepers will not work with steel sleepers.

5.2.4 Tests on instrumented sleeper

The model tests above demonstrated that with smaller crib ballast any void below the sleeper would be filled up to the void size minus the average particle size of the crib ballast. One concern while observing these tests was to determine the extent of flow of the crib ballast below the sleeper. It was important to know when the crib ballast was migrating into the void below the sleeper, whether it was able to reach the centre of the sleeper cross-section or was it just supporting the sleeper on its edges causing high stress in the corners of the sleeper bottom. Visually, at the end of the test when the sleeper was raised up after running over a thousand cycles it was possible to see that the crib ballast had reached the centre of the sleeper and was neatly packed inside the voids of the 5mm ballast. To study the movement of crib ballast into the void below the sleeper, tests were carried out on the instrumented sleeper.

The calibration and hardware and software set up of the strain gauge sleeper has been described in detail in chapter 4. Test on the instrumented sleeper was similar to other type A runs on monoblock sleepers. The instrumented sleeper was placed in the centre of the sleeper assembly by replacing one monoblock sleeper. The sleeper assembly was lowered on to the 5mm bottom ballast and then crib ballast was filled around the sleepers before the test was started. The crib ballast was 2mm stoneblowing stone (model size) and uplift height in the uplift cycles was 2.5mm. As with type A runs twenty simple load cycles followed by uplift cycles were run. Strain gauge readings were recorded for maximum load. Based on the calibration carried out in Chapter 4, load on the strain gauges 1 and 3 was calculated and plotted as a graph of Load Vs cycle number as shown in figures 5.14 and 5.15. Strain gauge 1 was the strain gauge on the edge of the sleeper and strain gauge 3 was the strain gauge in centre of the sleeper cross-section. In figure 5.14 the graph has been plotted for the first twenty simple cycles and eighty uplift cycles while the graph in figure 5.15 has been plotted for all load cycles.

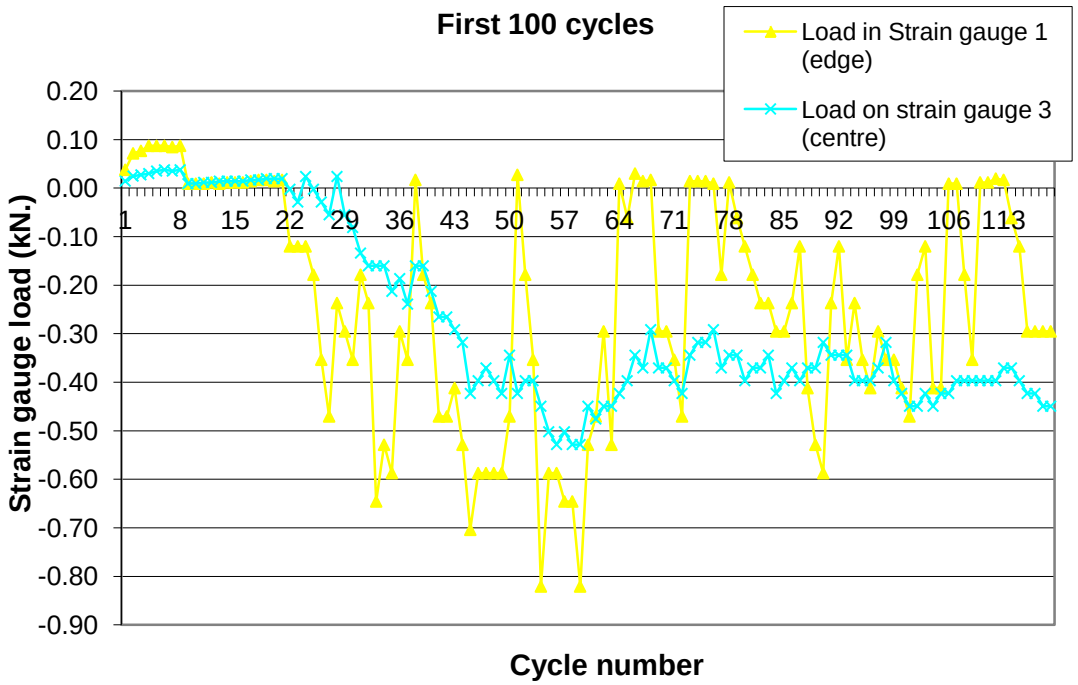

Figure 5.14 Load in strain gauge 1 and 3 for first 100 load cycles. Twenty simple cycles followed by uplift cycles were run.

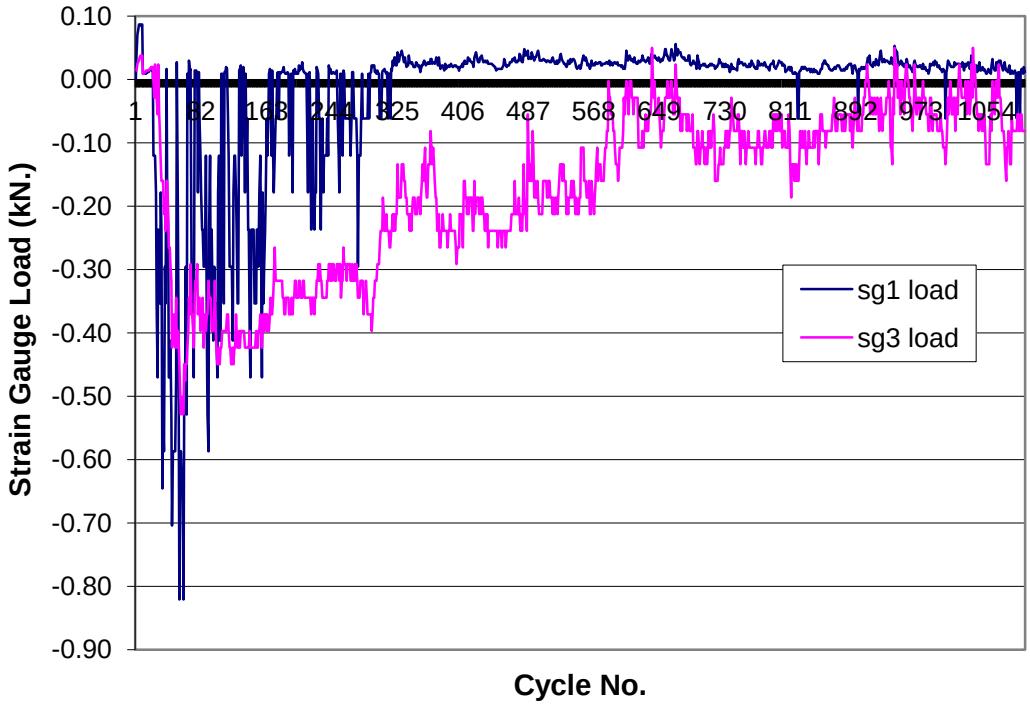

Figure 5.15 Complete strain gauge load data for all load cycles Strain gauge 1 and 3

Observations

In figure 5.14 for the first twenty simple load cycles the strain gauges are in tension and the load in both the edge strain gauge (strain gauge 1) and the central strain gauge (strain gauge 3) is equal at approximately 0.02kN, which is the load in the strain gauges with sleepers on bottom ballast as described in Chapter 4.

In the first ten load cycles the stress in the edge gauge is more than the middle gauge but after 10 simple cycles the load on both the strain gauges is the same. The reason for this could be that at the start of the test although the ballast was levelled out it had not been compacted. The instrumented sleeper was fixed in middle of the model assembly and due to difference in ballast level if all the sleepers were not bearing equally on to the bottom ballast the instrumented sleeper would be taking a large portion of the load but as can be seen from figure 5.14 after a few load cycles all the sleepers start bearing equally

onto the ballast and thus the load on the instrumented sleeper was reduced. For subsequent load cycles the load on the instrumented sleeper increases very gradually to 0.02kN for both the strain gauges.

With the start of the uplift load cycles the load on both strain gauge 1 and strain gauge 3 reduces and the load on both the gauges becomes negative, signifying that the strain gauges were in compression. This seems to imply that the sleeper is supported on its ends longitudinally causing compression in the strain gauges as the metal bars are bending in sagging. The compression load is greater in the middle gauge as compared to the edge gauge signifying that come crib ballast has moved in under the edge gauge but below the central portion of the sleeper there is still a void.

In approximately 80 uplift cycles the load on the edge gauge varies from 0.02 (tension) to negative load (compressive load), this signifies the dynamic state below the sleeper edge where the crib ballast is constantly moving into the void below the sleeper and is being compacted leading to more crib ballast moving into the void. This also implies that the crib ballast is migrating into the void below the sleeper at a faster rate from the sleeper ends as compared to the centre of the sleeper where the strain gauges were fixed. In the meanwhile the compressive load on the central gauge keeps on increasing to approximately –0.05kN.

Looking at figure 5.14 it can be seen that after the initial dynamic state below the edge gauge the load change has stabilised to a certain degree after approximately 300 load cycles, to increase to a maximum of approximately 0.05kN. Although compared to the middle gauge the stress changes in the edge gauge are more frequent as the crib ballast when filling the void below the sleeper moves to directly under the edge gauge first. The load on the central gauge slowly changes back from compressive load to tension load in approximately 1000 cycles. This implies that the crib ballast has moved into the centre of the sleeper cross-section in approximately 1000 load cycles.

6.0 Full scale test results

Full scale tests consisted of tests carried out on full scale ballast in a ballast box and on a full scale monoblock sleeper and rail assembly. The test results are described in detail in this chapter.

6.1 Box test

As described in chapter 4, box tests were carried out on a concrete sleeper pad placed in a ballast cross section enclosed within a wooden box. Boundary conditions of a small section of railway track were created within the box. As the tests were carried out in a ballast box the sleeper spacing (width of the box) was constant for all tests at 550mm. Tests were carried out on full scale railway ballast under full scale cyclic loading.

The basic aim of box tests was to validate the results of the model tests. Again as the test set up has been described in detail in chapter 4 this chapter will only concentrate on presenting the results.

6.1.1 Tests with 50mm bottom ballast and 50mm crib ballast

This test was similar to the initial model tests carried out for a sleeper spacing of 55mm. The bottom ballast below the sleeper for these tests was 50mm standard railway ballast and 50mm ballast was used as crib ballast. As mentioned in Chapter 4, the 50mm ballast was procured from a quarry, which supplies ballast to the railways. In a manner similar to the model test the sleeper pad was lowered on top of the bottom ballast with a minimum seating load of 5 kN. The LVDT was adjusted to read zero and this provided a datum for the test. The uplift height was input into the control panel of labview and the

number of simple and uplift cycles were specified. The smaller ballast was placed around the sleeper and the test started. The maximum load on the sleeper was 40kN. In the uplift cycles the sleeper was lifted up by 25mm after each load cycle thus simulating a void of size 25mm below the sleeper. 20 simple cycle followed by 20 uplift cycles were run. Results are shown as graph of maximum sleeper displacement for each load cycle in figure 6.1

6.1.1.1 Observations

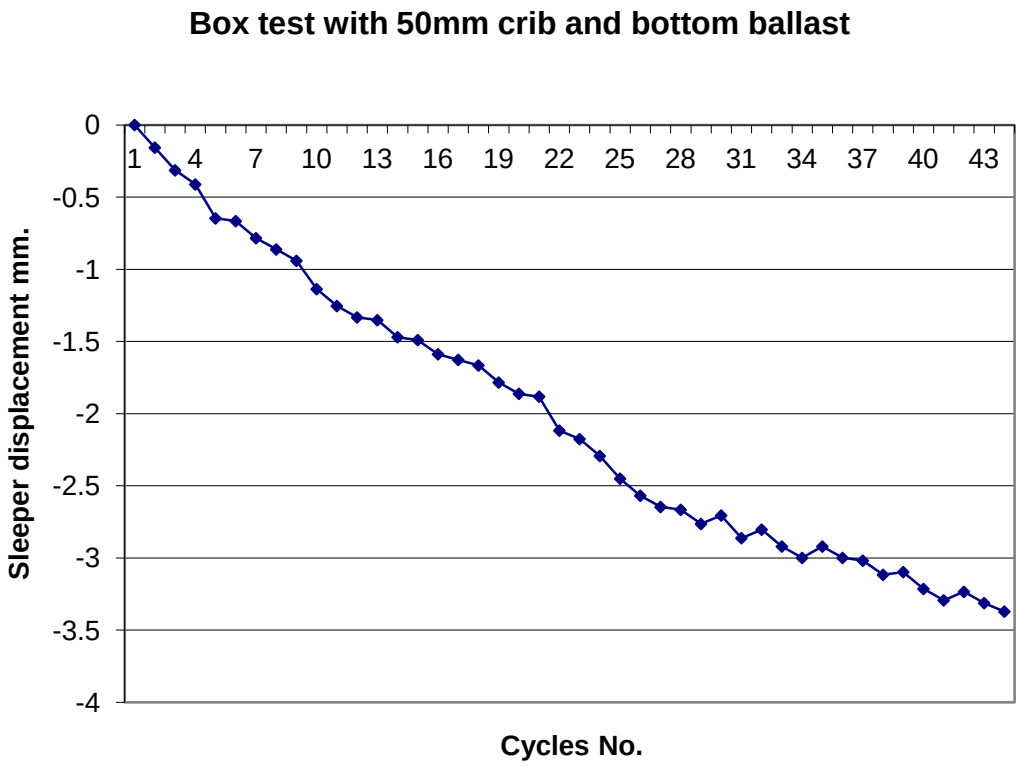

Figure 6.1 Box test with 50mm bottom and crib ballast.

There is no height correction for the sleeper in the uplift cycles i.e. the void below the sleeper is not filled up by the crib ballast. The results are similar to the results from the model test. A comparison has been done with the results from the model tests in figure 6.2

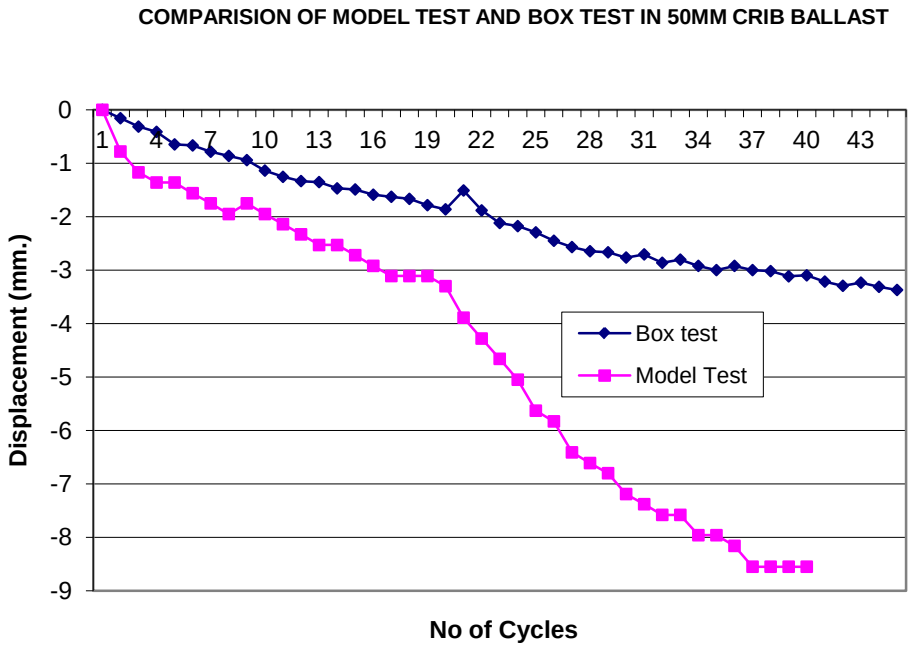

Figure 6.2 Model test and box test results

The model tests results are for 28mm sleeper at 55mm spacing. 5mm stone was used as bottom ballast and crib ballast in the model test. The model test results being tenth scale test results they were multiplied by ten to compare them with the full scale box test results.

It can be seen that the ballast compression for the model tests is more as compared to the box test. At the end of 40 load cycles the ballast compression for the box test is around 3.5mm while ballast compression for the model test is 8.5mm. Also ballast compression in the model test for the uplift cycles is double that for the simple load cycles i.e. after 20 simple cycles the ballast compression is 3mm. while after subsequent 20 uplift load cycles the ballast compression is 8.5mm. In the box test the ballast compression in the simple and uplift cycles is the same. A reason for this could be that the bottom ballast before the start of the model test was not well compressed while the bottom ballast before the start of the box test was compressed by running a few load cycles on it.

At the start of the model test the bottom ballast was placed on the sandpaper base and compressed by placing a sheet of plywood on top of it and running a few load cycles on the sheet of plywood. This levelled the bottom ballast and compressed it to some extent. In the box test when the sleeper was placed on the bottom ballast a few simple and uplift cycles were run without the crib ballast. This was done to check if the right maximum load was achieved in the load cycles and also to check if the sleeper was lifting up by the right amount in the uplift cycles. As mentioned earlier before loading the sleeper in the tests it was kept clear of the bottom ballast by at least 25mm, called as the position of 'rest' for the sleeper before the start of the test. It was then loaded by hydraulic oil pressure and under this pressure the sleeper travelled through the 25mm (or more) gap and was placed on the bottom ballast. This was done so that in the uplift cycles when the load was reduced to zero the oil pressure was dumped by the solenoid valve and this caused the sleeper to rise up to its position of 'rest' before the start of the test. The right level for the position of 'rest' for the sleeper at the start of the test was achieved by trial and error. The problem was that if the at 'rest' position was too high above the ballast the sleeper could not be loaded by hydraulic oil pressure and if the at 'rest' position was too low the correct uplift height was not achieved in the uplift cycles. Thus a few trial runs had to be carried out before the start of the test to position the sleeper to achieve the uplift height in the uplift cycles. Due to these trial runs the ballast below the sleeper was already compacted to some extent before the start of the test by 5-10 load cycles thus the final ballast compression in the box test is less as compared to the model test.

6.1.2 Tests with 50mm bottom ballast and smaller crib ballast

In these tests 50mm standard railway ballast was used as bottom ballast and tests were carried out with 20mm stoneblowing stone and 5mm aggregate as crib ballast. The uplift height was 25mm in the uplift cycles for both tests. 20 simple cycles followed by uplift cycles were run.

6.1.2.1 Test with 20mm crib ballast

The results for test run with 20mm crib ballast are shown in figure 6.3

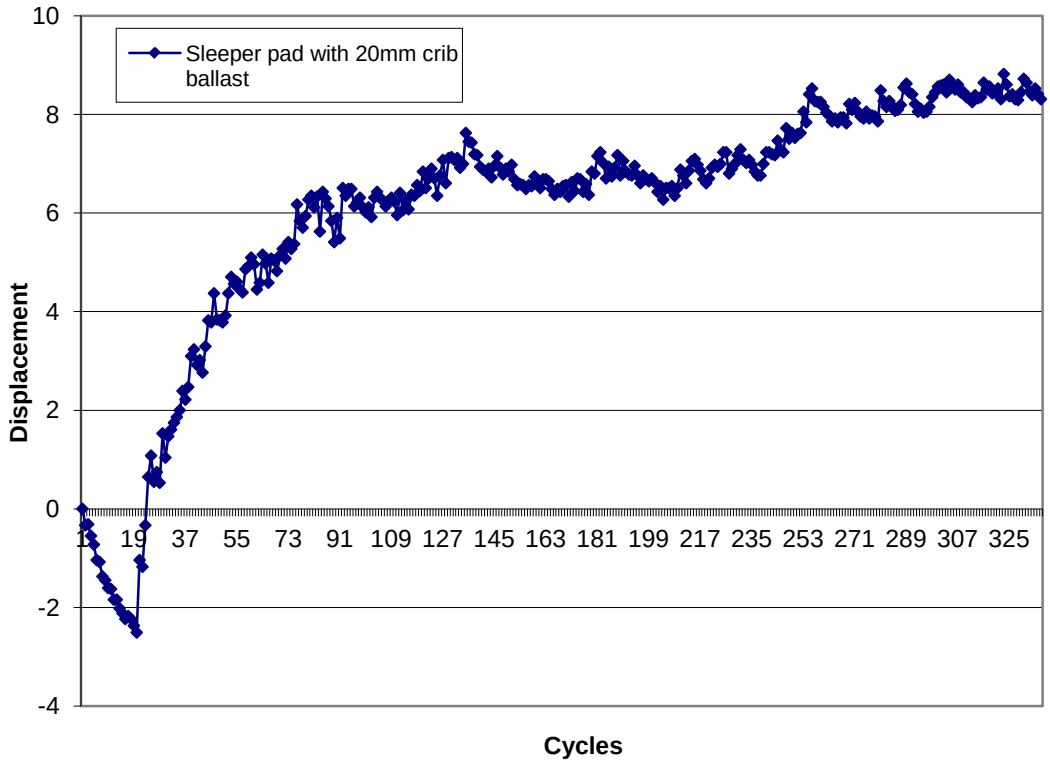

Figure 6.3 Box test with 20mm crib ballast, uplift height in uplift cycles 25mm

6.1.2.1.1 Observations

For the first 20 simple load cycles the sleeper displacement into ballast is similar to the results for the simple cycles shown in figure 6.3. In the uplift cycles the void below the sleeper fills up with the crib ballast migrating into the void and the sleeper can be seen gaining in height.

The movement of the crib ballast could be observed from the inspection window in the side of the box. In the first uplift cycle as the sleeper was lifted up crib ballast would flow into the void below the sleeper and some ballast was wedged in between the sleeper bottom and the bottom ballast. Thus it was not possible to push the sleeper back to its original position, this was as observed in the two dimensional glass model. The friction between the crib ballast particles and the sleeper sides was negligible compared to the load applied to the sleeper, although for the first few uplift cycles when maximum crib ballast movement was taking place it was possible to hear the sound of crib ballast in the void being compressed by the sleeper into the bottom ballast and also the grinding noise due to the resistance provided by crib ballast to the sleeper movement. Photographs taken while the box test was in progress are shown in figure6.5 a and 6.5b. It is possible to see through the inspection window that the crib ballast has migrated into the void below the sleeper and is mixing with the bottom ballast in approximately 50mm top layer of bottom ballast. It was observed during the box tests that with the vertical movement of the sleeper in the uplift cycles the mass of the crib ballast also moved some amount due to the friction with the sleeper walls. When the sleeper after rising up to its maximum uplift height was pushed down onto the ballast the crib ballast was also pressed down again due to the friction between the sleeper walls and the crib ballast. The crib ballast by the end of the test was sloping down from the edge of the box towards the sleeper as seen in the photograph. This was a common observation made on all full scale tests.

With the start of the uplift cycles the sleeper starts correcting in height, the height correction being very rapid in the first few cycles. The final sleeper height gain is 8mm in approximately 360 load cycles. Thus the sleeper has moved up by 8mm with respect to the datum zero level, leaving a final void size below the sleeper of 17mm. As described earlier the stoneblowing stone consists of stone sizes from 20mm down to 14mm with an average particle size of 17mm. Considering the relationship developed using the model test results of:

Final sleeper height correction = Void size - average particle size of crib ballast.

The sleeper height gain would be 8mm. Thus the test results validate the above equation developed from the model test results.

A comparison between the model test and box test results is given in figure 6.4. The model test results are for 28mm sleepers at 55mm spacing with 5mm bottom ballast and 2mm crib ballast. The model test results have been multiplied by ten to compare them with full scale test results. It can be seen that the rate of sleeper height correction in the box test is faster than that for the model test.

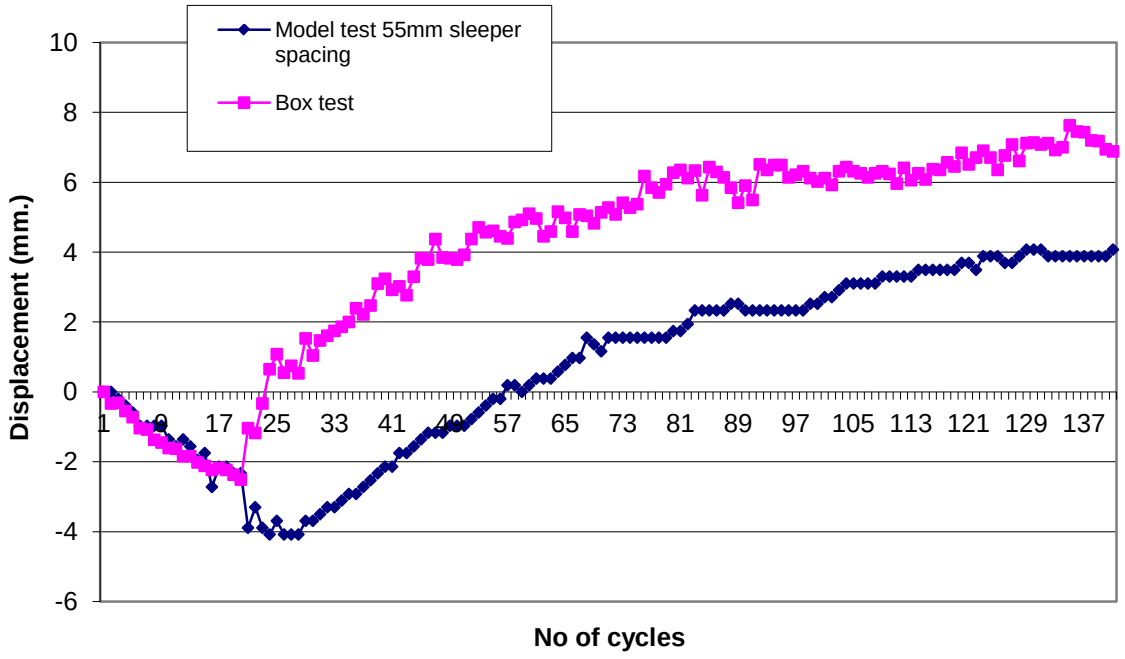

Figure 6.4 Comparison of box test and model test results

In approximately 120 uplift cycles the box test sleeper height gain is 7mm while the model test sleeper height gain is 4mm. Thus sleeper height gain in the uplift cycles is faster for box test. The possible reasons for this have been discussed in the section describing full scale tests with monoblock sleeper.

In the model tests after the end of the simple cycles in the first few uplift cycles there is no sleeper height gain, which is because of rearrangement of ballast particles under the sleeper for the first few uplift cycles but in the box test with the first uplift cycle the crib ballast flows into the void below the sleeper and the sleeper height gain in the first uplift cycle is maximum, thus more crib ballast is flowing into the void for the box test than can be compressed into the voids of the bottom ballast.

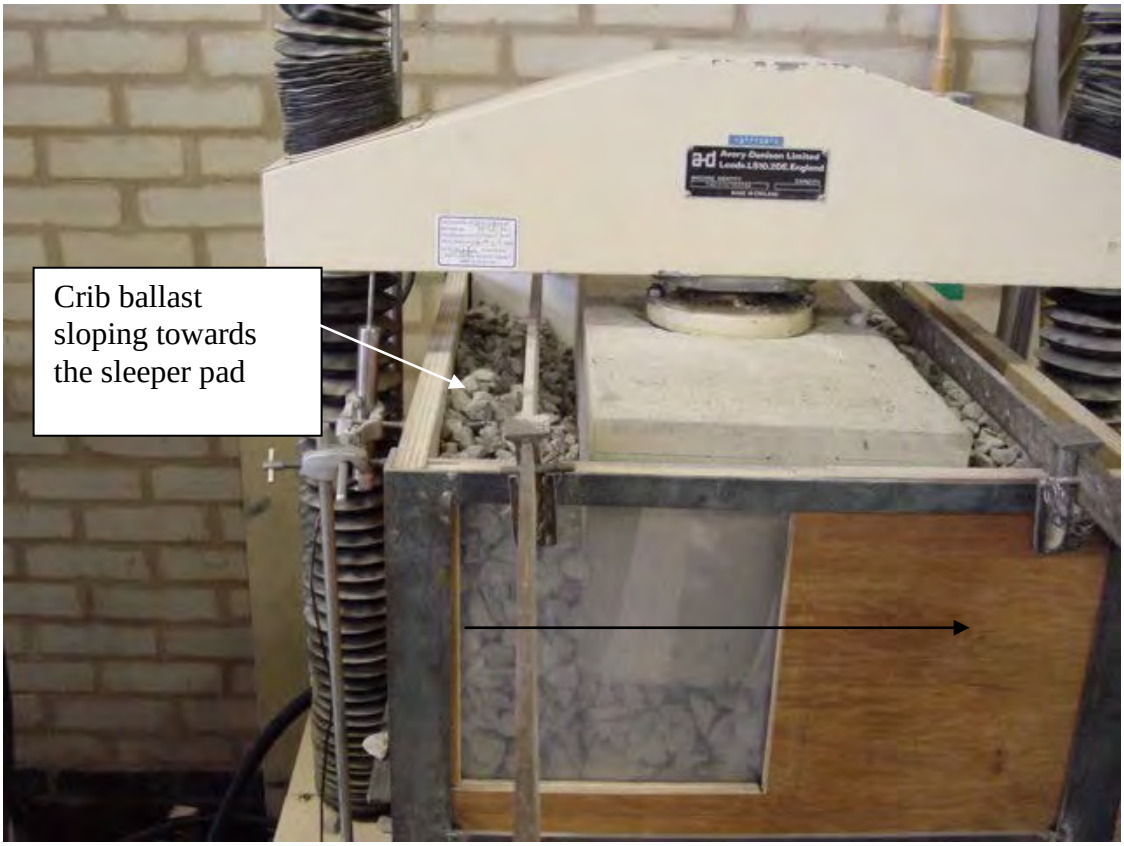

Figure 6.5a Box test with 20mm crib ballast

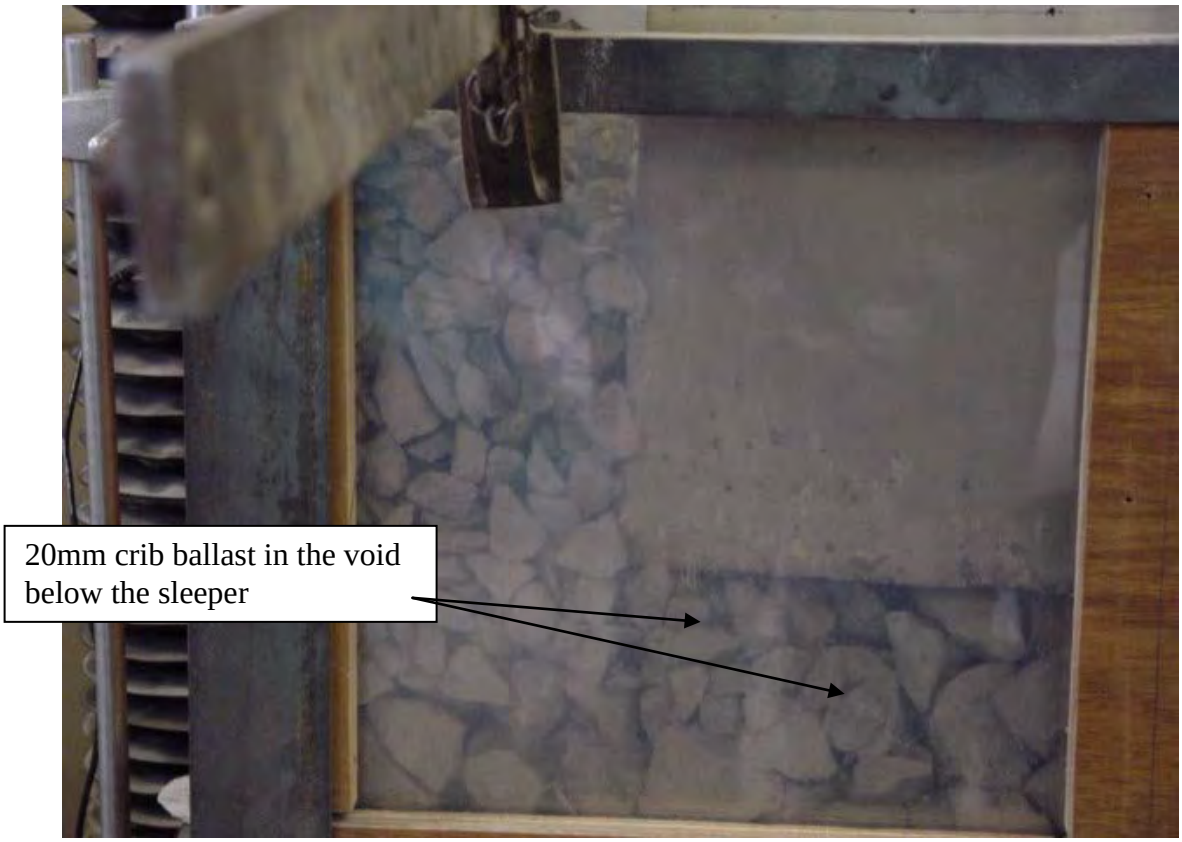

Figure 6.5b View through inspection window

6.1.2.2 Box test with 5mm crib ballast

Results for test with 5mm crib ballast are shown in figure 6.6. The results have been compared with box test carried out using 20mm crib ballast.

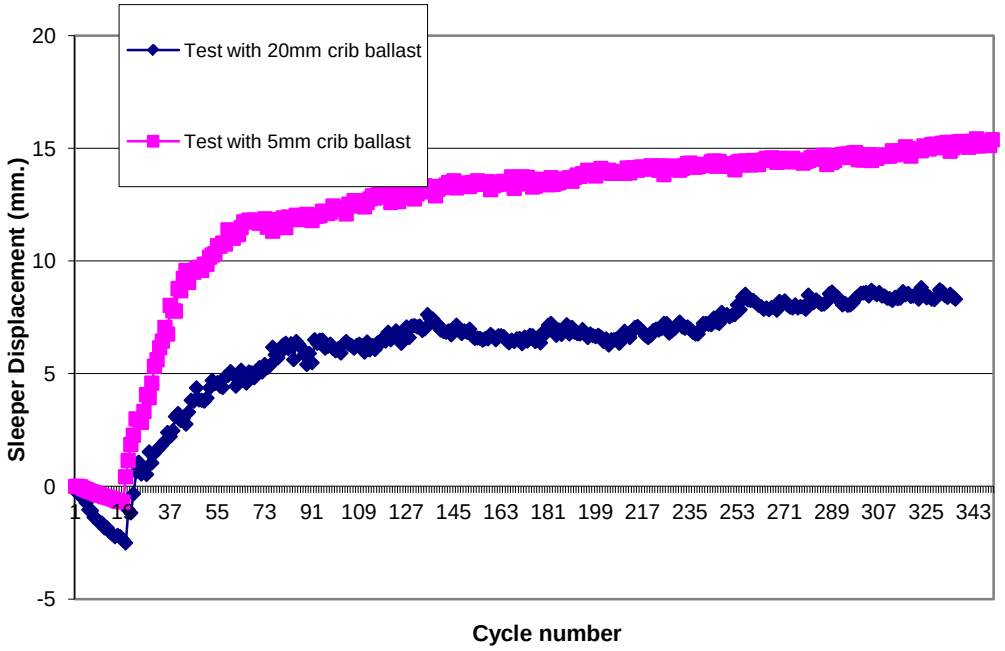

Figure 6.6 Box test results with 5mm and 20mm crib ballast.

For the test with 5mm crib ballast it was observed that the sleeper height correction was more as seen in the graph in figure 6.6. Through the inspection window it was observed that the 5mm crib ballast flowed more freely into the void below the sleeper as compared to the 20mm crib ballast, again the observation is similar to observations made in the two dimensional ballast cross-section. The friction between the sleeper sides and the crib ballast was less as less grinding and crunching noises were observed for the first few uplift cycles. This again is similar to the observations from the two dimensional ballast cross-section.

A photograph taken after the completion of the test is shown in figure 6.7. It was observed that as the 5mm ballast filled up the void below the sleeper the crib ballast sloped down towards the sleeper, with each uplift cycle a few particles would roll down the slope towards the sleeper. This was observed in all tests both model scale and full scale although this phenomenon was more prominent with smaller crib ballast. A photograph through the inspection window is also shown in figure 6.7 taken after completion of the test. It shows that the crib ballast has migrated to the centre of the sleeper cross-section.

Figure 6.7a Test with 5mm crib ballast - photograph taken after the test was complete.

Figure 6.7b Photograph showing movement of 5mm crib ballast to the centre of the sleeper cross-section.

The final sleeper height gain after 330 uplift cycles is just above 15mm. Thus there is a residual void size of 10mm under the sleeper after the test, which based on earlier observations should be 5mm for crib ballast size of 5mm. Thus the equation of, final sleeper height gain equals void size minus average particle size of crib ballast, is not satisfied. It can be seen from the graph that when the test was ended the sleeper was still correcting in height and the end point has not been reached for the curve.

A sieve analysis was then carried out on a random sample of the 5mm ballast. As mentioned earlier the 5mm ballast was used from the aggregate pile in the laboratory which was marked as 5mm aggregate. It had been supplied from the local builders merchant as granite stone of grading 5mm – 3mm. The sieve analysis on the 5mm aggregate revealed a different grading as given in table 6.1.

Table 6.1 5mm ballast gradation

Seive size mm.	Wt retained on sieve
10	0
5	44%
4	28%
2.8	16%
<2.8	12%

It can be seen that almost 50% of the 5mm aggregate sample consisted of stones more than 5mm in size while 28% of the sample consisted of stones of 5mm size. Thus the ballast particle size was 7mm instead of 5mm as assumed earlier. Thus the presence of particles in the crib ballast larger than 5mm in size has affected the results. This was also observed in model test results where presence in the crib ballast matrix of particles larger than the average size of the crib ballast or smaller than the average size of the crib ballast affected the final sleeper height gain in the uplift cycles. Also as discussed earlier the end point on the graph has not been reached in 330 uplift cycles thus the predicted final sleeper height gain has not been achieved.

The sleeper height gain for tests run with 5mm crib ballast and 20mm crib ballast after every 50 load cycles is shown in table 6.2.

Table 6.2 Sleeper uplift height gain

Crib ballast size (mm.)	Sleeper level relative to datum zero level (mm.)							
	Uplift cycle number							
	1	50	100	150	200	250	300	Final height

								gain
20	-1.03	5.2	6.5	6.3	6.9	8.2	8.5	8.5
5	0.428	11.73	12.87	13.619	14.22	14.4	14.93	15.0

It can be seen from table 6.2 that for both crib ballast sizes half of the final height gain is achieved in around 150 uplift cycles. For 20mm crib ballast the ballast bottom level below the sleeper has risen to 6.3mm above the datum zero level in 150 load cycles, the remaining 2mm height gain is achieved in subsequent 150 load cycles. Similarly for 5mm crib ballast in first 150 uplift cycles sleeper rises to 13.6mm above the datum level and in subsequent 150 uplift cycles the height gain is 1.5mm. It was observed that after the initial rapid height gain in the first few uplift cycles the sleeper height gain was more gradual. This it is assumed was because the ballast directly below the sleeper was being continuously rearranged after each load cycle. Crib ballast particles which migrated into the void below the sleeper in the initial few uplift cycles were compressed into the bottom ballast. With the void size reduced subsequent flow of crib ballast into the void was gradual and it was continuously being compacted into the bottom ballast as it gradually moved towards the centre of the sleeper.

6.1.3 Tests with 20mm bottom and crib ballast

These again were a repeat at full scale of model tests carried out using 2mm crib and bottom ballast. In these tests the 20mm stoneblowing stone was used as bottom ballast and crib ballast. The tests were run with only simple load cycles to compare the results with similar box test carried out with 50mm bottom ballast.

6.1.3.1 Observations

The results are given in figure 6.8 as graph of sleeper displacement for each cycle. Close to 300 load cycles were run and results were compared with similar test run with 50mm bottom ballast.

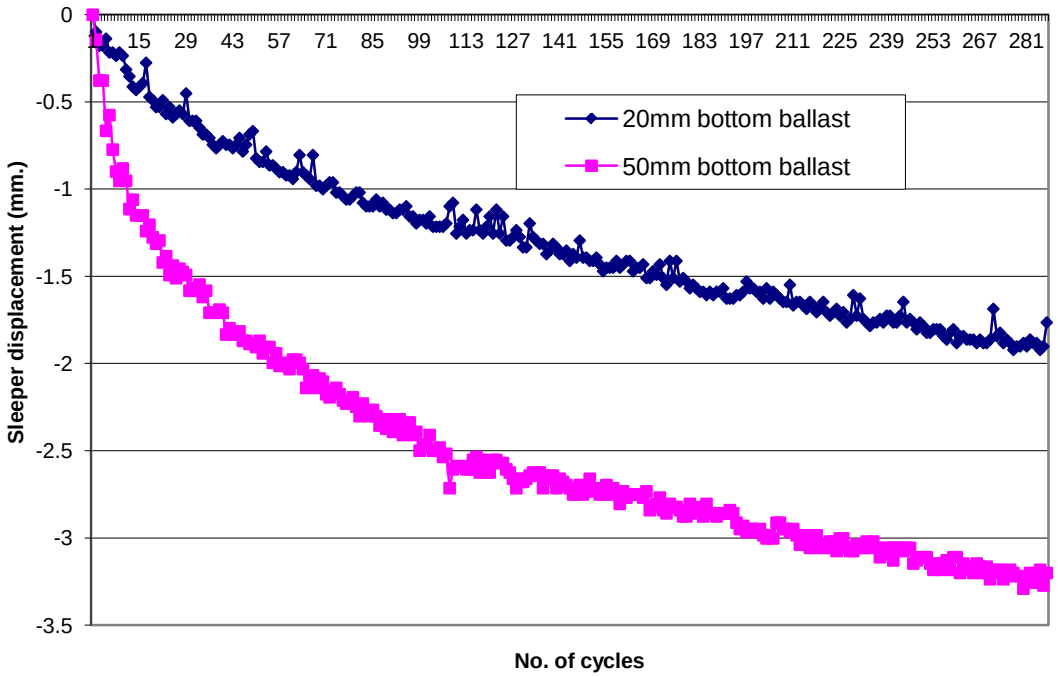

Figure 6.8 Simple cycles – test run with 50mm and 20mm bottom ballast

It can be seen that ballast compression for 20mm bottom ballast is less than that for 50mm crib ballast as sleeper displacement in the ballast is less for 20mm bottom ballast. In approximately 300 simple load cycles without uplift the sleeper displacement for 20mm bottom ballast is close to 2mm. while the sleeper displacement for 50mm bottom ballast is close to 3.5mm. This again reinforces the view that for smaller ballast below the sleeper the ballast inelastic compression is less. Similar observation has been made from the results of the model test carried out using 2mm crib ballast. For 20mm stone the number of particles contacting the sleeper underside is more than that for 50mm stone this leads to better load distribution below the sleeper, thus inelastic compression of ballast is reduced for a smaller ballast size.

6.1.4 Test with graded ballast

The results of both model and full scale tests with smaller crib ballast have indicated that any void below the sleeper will be filled up to the void size minus the average particle size of the crib ballast e.g. for 20mm stoneblowing stone the average particle size is 17mm and in the box test a void of size of 25mm is filled up by 8mm leaving a residual void of 17mm under the sleeper. This can be used as a simple rule to predict broadly the final sleeper height gain for a given void size and crib ballast particle size, thus help predict the residual void size below the sleeper for a given particle size of the crib ballast. In the literature review it has been discussed that the ballast on British Rail prior to introduction of tamping machines was small size ballast with majority of particles in the range of 12mm to 30mmn with a small proportion of ballast of size greater than 30mm. The ballast specification for Underground Railways (Anon 1973) has specified ballast as stone of size 1.5 inches (37.5mm) to 0.5 inches (12.5mm) with coarser ballast to be used at the bottom and smaller ballast to be used at the top. The test results have shown that with smaller crib ballast the void below the sleepers was filled up to the average particle size of the crib ballast. Thus in this test graded ballast was used in the crib with ballast particle size ranging from 40mm to 12mm with larger proportion of stones in the size range of 12-20mm. This specification of ballast simulated ballast specification prior to introduction of tampers on British Rail. This would perhaps present a means of altering the present ballast specifications and provide a compromise between large and small size ballast.

Thus tests have been carried out by mixing stones of 20mm and 10mm size with the standard railway ballast in different proportions to use as crib ballast. Tests run with three different ballast gradings have been compared :

1. Stoneblowing stone as crib ballast
2. 50-20 ballast. To develop this ballast grading the standard railway ballast was mixed with stoneblowing stone in the proportion of 1:2 by weight, respectively.

The grading of Standard railway ballast (50mm), stoneblowing stone (20mm) and the new mix gradations developed are given in table 6.3. In the test 20 simple load cycles followed by uplift cycles were run with uplift height in uplift cycles of 25mm.

Table 6.3 Mixed ballast grading

Sieve size (mm.)	% passing		
	Ballast size designation		
	50mm standard railway ballast	20mm stoneblowing stone	50-20 mix – 1:2 in proportion by weight
50	100		
37.5	30		77
28	0		67
20		100	
14		17	12
10		0	1
5			
4			
2.8			

Results are shown in graph again as maximum sleeper displacement for each loading cycle.

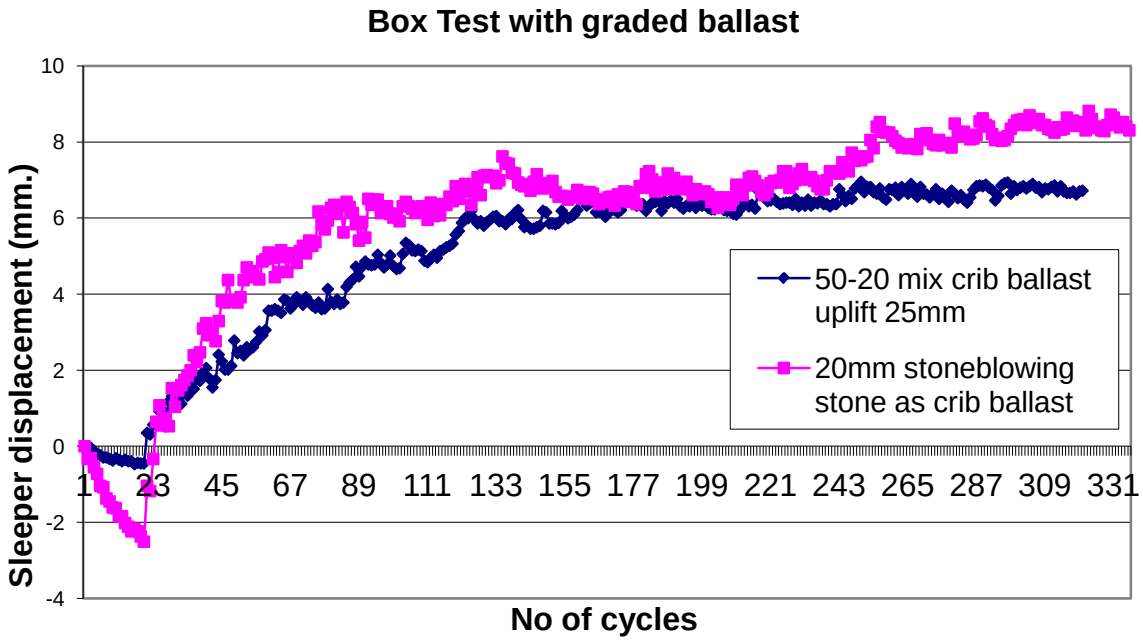

Figure 6.9 Tests with graded ballast

6.1.4.1 Observations

From table 6.3 it can be seen that in the mixed ballast matrix 67% of the particles are of the size 20-14 i.e. particle size 17mm. This size fraction is absent from the 50mm ballast specification, thus with the new grading a large proportion of smaller stones has been introduced in the standard railway ballast. Comparing the graph of sleeper displacement for 50-20 crib ballast with the graph for 20mm stoneblowing stone as crib ballast in figure 6.9 it is observed that the results are similar for both grading of crib ballast. Neglecting the sleeper displacement in simple load cycles the sleeper height gain in the uplift cycles for both crib ballast gradations is similar except that sleeper height correction for mix crib ballast initially is slow. In approximately 300 uplift cycles the sleeper height gain for 50-20 ballast is 7mm, same

as that for 20mm stoneblowing stone as crib ballast. The final sleeper height correction for 20mm crib ballast is 8.6mm while for 50-20 crib ballast is 6.8mm.

The initial slow rate of height gain for the sleeper could be due to the presence of large ballast particles 40mm size at the bottom of the crib close to the edge of the sleeper. It was observed while the test was running that with the vertical movement of the sleeper in the uplift cycles the smaller 20mm ballast filtered down to the bottom of the crib.

It has been observed earlier that the crib ballast would move vertically with the sleeper in the uplift cycles. As the ballast was a mix of 40mm and 20mm ballast a few 40mm ballast particles were visible in the top layer of crib ballast. The author placed a 20mm stoneblowing stone on top of a 40mm stone visible in the top layer of the crib ballast and observed the stones for a few uplift cycles. The 40mm stone was in the top layer of the crib ballast and was also adjacent to the sleeper thus in contact with the sleeper surface. With each upward movement of the sleeper the large ballast particle would move (rotate) upwards and then would move downward when the sleeper was loaded. In a few cycles the 20mm stone placed on top of the 40mm stone dropped into the ballast matrix below the 40mm stone. Thus it was assumed that with the vertical movement of the sleeper the smaller particles would filter down to the bottom of the crib.

The 20mm ballast flowed around the 40mm ballast to the crib bottom which is why the test results are similar to those with 20mm stoneblowing stone in the crib. This test indicated a very important property of the two layered ballast system that if a good proportion of smaller stones is present in the crib ballast the void size will be filled up to the size of the smaller stone in the crib ballast.

6.2 Full scale test on single sleeper and rail assembly

These tests were the last set of tests carried out on the two layered ballast system. As these tests were carried out on full scale sleeper and rail assembly they quite closely represented the live track conditions and were carried out to validate the results from the box test and the model test. These tests were carried out at three different sleeper spacing and crib ballast size was varied in different tests. Again the test set up has been described in detail in Chapter 4 so this chapter will concentrate on the results.

6.2.1 Initial tests with sleeper spacing 550mm

These tests were carried out with 50mm bottom ballast and 20mm crib ballast. The rigid panels forming the boundary for the ballast were placed 550mm apart thus simulating sleeper spacing of 550mm. 550mm is the absolute minimum sleeper spacing specified on British Rail. The sleeper was placed in the centre on 50mm standard railway bottom ballast. 20mm stoneblowing stone was used as crib ballast.

The first test of this type was carried out without any displacement transducers to measure sleeper displacement, sleeper displacement was measured manually by a tape measure relative to the steel beam on top of the sleeper. The steel beam was fixed on top of the sleeper to support the loading rams used for applying cyclic load to the sleeper. The sleeper, as explained earlier, was supported on springs to keep it off the ballast top by a distance equal to the amount of uplift required in uplift cycles. The sleeper level at zero load was measured relative to the steel beam and the sleeper was lowered on the 50mm bottom ballast with a minimum seating load of 10kN. The sleeper level at this load was then measured again relative to the steel beam. The difference between sleeper level at zero load and sleeper level at minimum seating load at the start of the test formed the uplift height in the uplift cycles. As explained earlier the sleeper was supported off the top of the ballast by springs at zero load so when in the uplift cycles the load was reduced to zero the sleepers would spring back to their original position supported by the springs, this formed the mechanism of the uplift cycles. The sleeper uplift measured was 30mm for the test.

With the sleeper seated on the ballast with a minimum seating load, crib ballast was filled around the sleeper and the test was started. First twenty cycles were simple loading cycles with the load cycled from 10kN to 60kN. Sleeper displacement was measured at maximum load for a few times in the simple cycles again relative to the steel beam above the sleeper. It was observed that the sleeper was progressively sinking into the bottom ballast by very small displacements. After the first twenty simple cycles the load was reduced to zero between subsequent cycles, which caused the sleeper to lift up supported by the springs, the uplift height being 30mm. After running 10 uplift cycles in the manner described above the sleeper level was measured at the maximum load and it was observed that the sleeper displacement at maximum load was less than that for the simple cycles.

Thus the void below the sleeper was being filled up by the smaller crib ballast and the sleeper started rising up out of the ballast.

It was tedious and inaccurate to measure sleeper displacement manually by using a tape measure so for all further tests displacement transducers were used to measure sleeper displacement. Displacement transducers were fixed to each rail to measure sleeper displacement and were connected to a data logger to log displacement readings. The setup has already been described in Chapter 4.

With the displacement transducers fixed to each rail the test was repeated. The void size below the sleeper measured at the start of the test was 30mm. The sleeper was lowered on the ballast with a minimum seating load and as with the model tests and box tests the sleeper level at this load was fixed as a datum zero level for the test. Twenty simple cycles followed by uplift cycles were run. The results are shown in figure 6.10 as graph of sleeper displacement for each load cycle. In the results for model test and box test the first displacement reading was subtracted from all the readings to eliminate the elastic compression of the test assembly from the readings. In the full scale tests a monoblock sleeper connected to the rail using standard pandrol fastenings was used thus it was assumed that any elastic compression of the test assembly would be small and thus this was ignored. The data recorded by the LVDT has been presented in the graph without any manipulation.

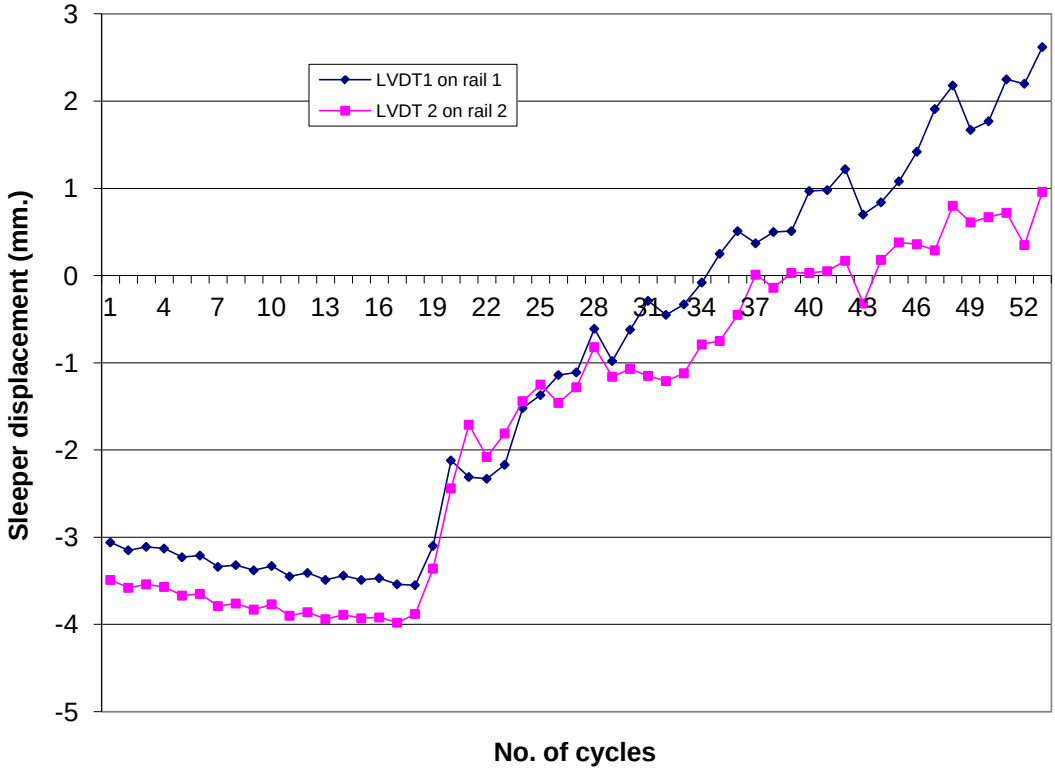

Figure 6.10 Full scale test for 550mm sleeper spacing, 20mm crib ballast.

6.2.1.1 Observations

The results are similar to those for box test and model test for similar sleeper spacing and crib ballast particle size. The two lines in the graph are readings from two LVDT each fixed on one rail. The sleeper for the first twenty displacement cycles moves down into the ballast as the ballast is slowly compressed by the cyclic load. The total sleeper displacement at the end of twenty uplift cycles is 4.0mm. For the uplift cycles as the

crib ballast migrates into the void below the sleeper the sleeper starts gaining in height. The total sleeper height gain in approximately 60 cycles is 2.6mm relative to the datum zero level.

At the end of the test the crib ballast was carefully removed and the sleeper lifted up to observe the extent by which the crib ballast had migrated to the centre of the sleeper cross-section. The photographs are shown in figure 6.11 a and 6.11b. It was observed that the crib ballast had moved in towards the centre of the sleeper cross-section on average by 80mm in approximately 50 uplift load cycles. In some locations the crib ballast had moved even further towards the centre of the sleeper cross section as seen in the close –up photograph. Thus the sleeper is not supported on its edge as the crib ballast fills up the void below the sleeper but the crib ballast is progressively moving towards the centre of the sleeper cross-section.

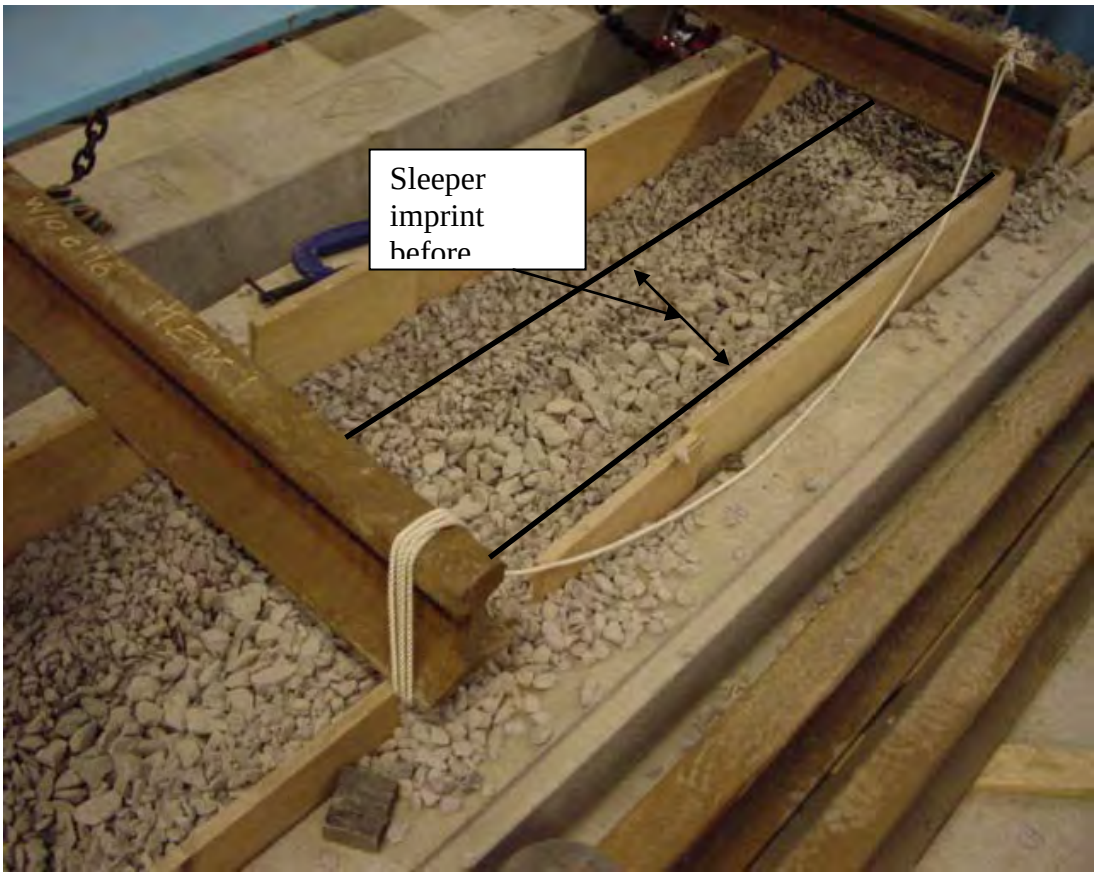

Figure 6.11a Movement of crib ballast below the sleeper

Figure 6.11b Movement of crib ballast below the sleeper

6.2.2 Tests with sleeper spacing 600mm.

600mm is the normal sleeper spacing on British rail and is the sleeper spacing adopted on the Channel Tunnel Rail. First a few tests with 50mm bottom ballast and 20mm crib ballast were repeated for this sleeper spacing and then a few tests were carried out with different sizes of crib ballast on 50mm bottom ballast. The aim was to observe the final sleeper height gain for different size of crib ballast.

6.2.2.1 Test with 50mm bottom and 20mm crib ballast.

The result is shown in figure 6.12 as a graph of sleeper displacement for each load cycle. Although displacement measurements were done on two rails data from one

displacement transducer has been shown in the graph for simplicity, the data from both the transducers were same for all the tests. The total void below the sleeper (uplift height) measured at the start of the test was 30mm.

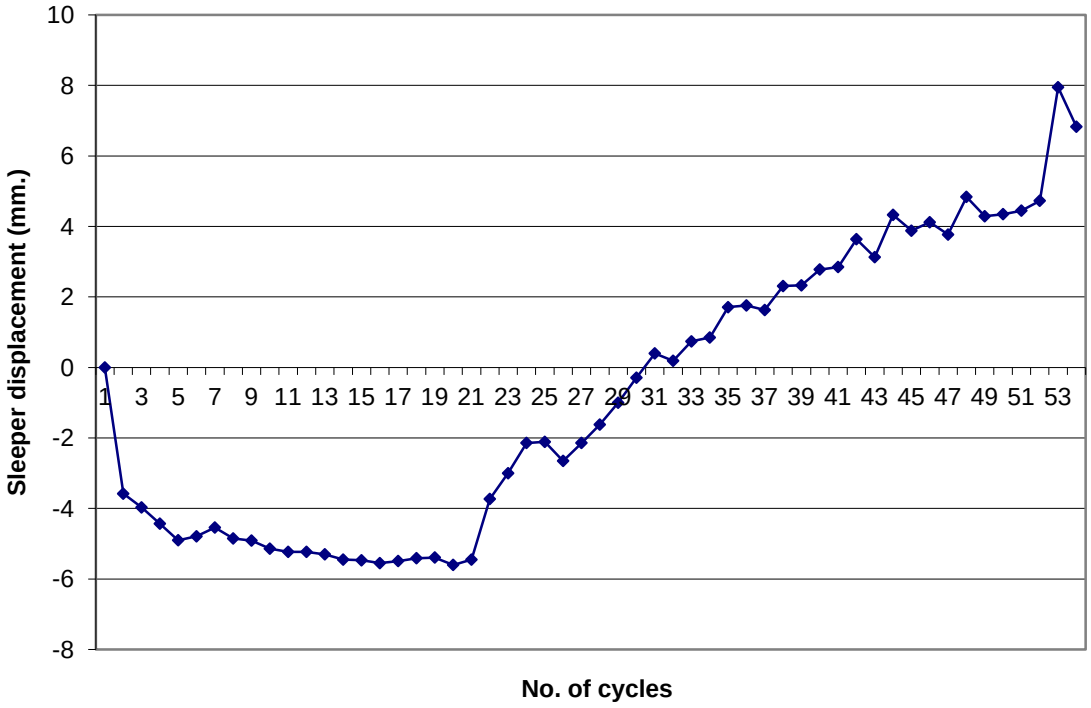

Figure6.12 Sleeper displacement for sleeper spacing 600mm with 20mm crib ballast. The total void size at the start of the test was 30mm.

6.2.2.1.1 Observations

Again the results confirm the fact that with smaller crib ballast any void below the sleeper will be filled up by the crib ballast with passage of traffic over the voided sleeper. At the end of the first twenty simple load cycles the sleeper displacement relative to the zero datum level into the ballast was 5.5mm while at the end of the uplift cycles the sleeper had lifted up to 8mm above the datum zero level in about 35 uplift cycles. Thus as the test progressed the sleeper vertical (uplift) movement of 30mm from the zero datum level

upwards was reduced to 22mm as the void filled up by 8mm relative to the datum zero level.

Comparing the results with box test and model test results, shown in figure 6.13. it is seen that the results from the box test and the full scale tests are similar. The sleeper displacement in the simple cycles for the box test is less as compared to the full scale test but that could be due to already well compacted ballast below the sleeper before starting the box test.

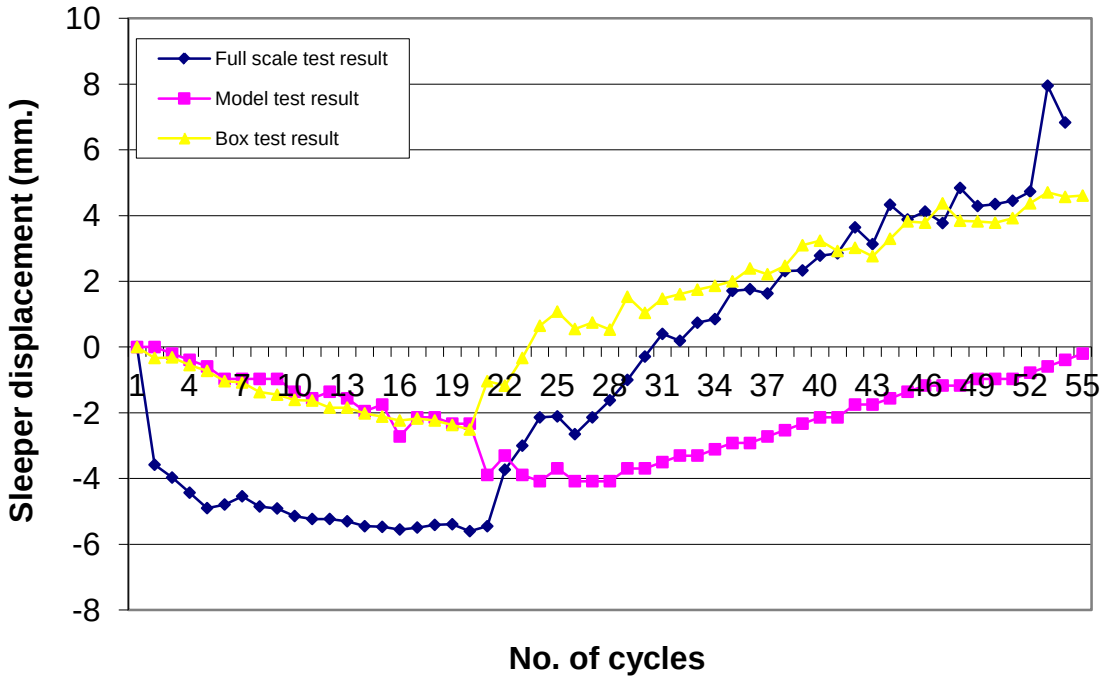

Figure 6.13 Comparison of results from full scale test, box test and model test.

In the uplift cycles it can be seen that sleeper height gain in the full scale test is quite rapid as compared to both the box test and the model test result. One reason for the rapid correction in sleeper height for the full scale test is that the void size below the

sleeper (or the uplift height in the uplift cycles) in the full scale test was 30mm instead of 25 for the box test and model test.

Comparing uplift cycles for all three tests the full scale test and box test results for the two layered ballast system are better than the model test. The reason for this the author assumes is the effect of gravity loading on model scale and full scale ballast. While scaling down all test parameters for the model test to 10^{th} scale of the full scale tests it was not possible to adjust the gravity loading on the model in proportion to the scale of the model. In all geotechnical model testing this is done by running tests in a centrifuge allowing to adjust gravity loading effect on the model i.e. using the centrifuge it is possible to increase or decrease gravity load as required on the model by creating artificial gravity force within the centrifuge. With the gravity force not adjusted for the model tests the gravity loading on ballast particle of size 20mm would be more than that on particle size scaled down to 2mm. Thus the flow of crib ballast into the void below the sleeper for the full scale tests is faster than that for the model tests and subsequently the final sleeper height gain is achieved quicker for the full scale tests than for the model tests. For the model tests a large number of load cycles are required to be run before the final sleeper height gain is achieved.

The predicted final sleeper height gain for the full scale test would be uplift height in the uplift cycles (30mm) minus the average particle size of crib ballast (17mm), which is 13mm. The maximum sleeper height gain for the full scale test is 8mm in approximately 30 uplift cycles which is less than the predicted height gain but it is clear from the graph that the end point had not been reached.

As mentioned earlier the loading for the full scale test was applied by manually controlling a valve on the hydraulic pump. The loading was applied very slowly and displacement reading taken at the same maximum load for each load cycle. It was observed in all earlier tests that after initial rapid sleeper height correction in the full scale tests the sleeper height gain for subsequent load cycles became progressively slow. As seen in the tests results described in figure 6.13 for the full scale test the first 6mm of sleeper height gain was achieved in 10 uplift cycles but subsequent 6mm sleeper height gain required 20 load cycles to be run. One limitation of applying the load manually was that it was not

possible to run a large number of load cycles in one test. Thus it was decided to try loading the sleeper with faster loading cycles to see if it made any difference to the results.

The test was thus stopped after approximately 30 uplift cycles and as the void below the sleeper was filled up by 8mm the sleeper remained suspended above the bottom ballast with a void below the sleeper 22mm in size. The test was then started as a new test with 22mm void below the sleeper. The void size was measured and confirmed to be 22 mm before the test was started. The sleeper was loaded to minimum seating load and the datum zero level for the test was fixed at the minimum seating load as described earlier. With the crib ballast already in place no simple load cycles were run. The uplift height as measured earlier was 22mm for the uplift load cycles. The load was cycled from zero to 60kN for the uplift cycles and the rate of load application was quicker compared to earlier tests. It has been mentioned earlier that with quicker rate of load application it was difficult to record the sleeper maximum displacement accurately. Thus to get around this problem it was decided not to take displacement readings for all uplift load cycles. For the fast loading cycles the aim was to simulate the pumping action of a voided sleeper at a quicker rate than the earlier tests thus no displacement readings were taken for the fast load cycles. Thus after running a few fast loading cycles a few loading cycles were run slowly to the correct maximum load and displacement readings were taken. In the fast loading cycles the rate of loading achieved was faster compared to earlier full scale tests but did not simulate live track loading. The results from the test are shown in figure 6.14

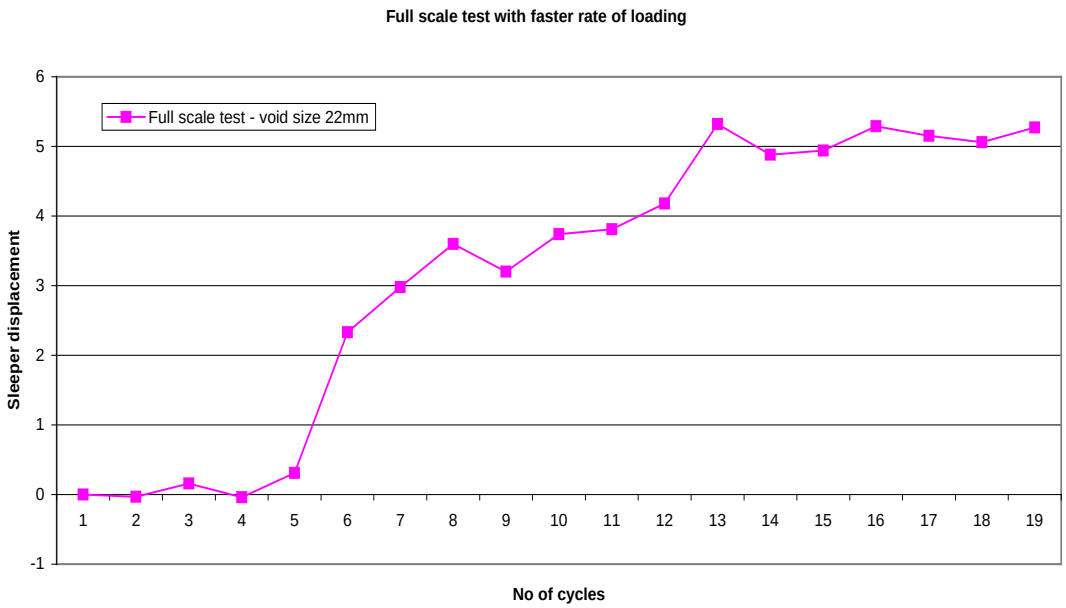

Figure 6.14 Full scale test with faster rate of loading – uplift cycles only.

For a void size below the sleeper of 22mm the predicted final sleeper height gain for an average particle size of 17mm would be 5mm. It can be seen from the graph in figure 6.14 the final sleeper height gain for the sleeper is 5mm. Thus a void size of 22mm was reduced to 17mm. This was achieved in 19 displacement readings thus approximately 30-40 uplift load cycles were run.

It was mentioned earlier in chapter 4 that the rate of loading for all testing on the two layered ballast system did not simulate actual live track loading but the total wheel load including the dynamic component of loading was simulated in all tests. It was assumed that if the two layered ballast system worked with a low rate of loading the system performance would be enhanced by faster rate of loading as in live track. The above results confirmed that assumption to be correct.

At the end of the test to confirm the size of the residual void below the sleeper, the two LVDT were scanned to read zero displacement for the sleeper at rest on the springs.

The sleeper was then lowered on the ballast and loaded to maximum load. LVDT reading was taken at maximum load, which was the size of void below the sleeper. Thus the final sleeper height gain could be cross checked in this manner.

6.2.2.2 Tests with 50mm bottom ballast with different sizes of crib ballast.

These tests were run with different sizes of crib ballast (smaller than 20mm stoneblowing stone) for each test to validate the observations of the model test and box test with crib ballast smaller than 20mm. Bottom ballast was 50mm size and 5mm, 10mm stones and sand were used as crib ballast. The 5mm and 10mm stone were used from the aggregate pile in the concrete laboratory and their grading is given in table 6.4.

Table 6.4 Grading of 5mm and 10mm aggregate used as crib ballast.

Seive size mm.	% passing (10mm aggregate)	% passing (5mm aggregate)
14	0	0
10	78	0
5	10	56
4	4	28
2.8	1.5	12
<2.8	0	0

It is seen from the sieve analysis that the aggregate was contaminated by stones of size larger than the specified maximum size. Sand used as crib ballast was assumed as having a particle size of 3mm.

Results are plotted in a single graph as maximum sleeper displacement for the uplift load cycles. The simple cycles have been neglected for simplicity. The graphs for tests with sand and 20mm stone as crib ballast have been plotted together while graphs for tests with 5mm and 10mm crib ballast have been plotted together.

6.2.2.2.1 Test with 20mm stone and sand as crib ballast

In both the tests the void below the sleeper was 38mm so the results are described together for comparison (Figure 6.15).

In the test with sand as crib ballast at the start of the test as the sand was being filled in the crib a lot of sand was lost in the voids of 50mm bottom ballast. This was similar to the observation made when using sand as crib ballast in the two dimensional cross-section of ballast described in chapter 5. Also during the test the level of sand in the crib went down as a lot of sand migrated into the void below the sleeper and also into voids in the bottom ballast, this did not occur with 5, 10 and 20mm stones as crib ballast. After approximately 100 load cycles the level of the crib ballast depleted as the void below the sleeper was filled up by the crib ballast. At this point the sleeper height gain with the uplift cycles became very slow. So the test was stopped and sleeper was maintained on top of the crib ballast with a minimum load of 10kN while sand was filled in again to the top of the sleeper. When the uplift cycles were recommenced the sleeper gained in height by another 4-5mm.

It is observed that the final sleeper height gain for test with sand as crib ballast is more than that for test with 20mm stone as crib ballast. Considering the sand particle size as 3mm the predicted final sleeper height gain would be (38-3) 35mm, the final sleeper height gain in the test is 33mm. Even in the last few load cycles when the test was stopped the sleeper was still correcting in height although very gradually. This observation is similar to that made when using sand as crib ballast in the two dimensional cross-section of ballast during the initial testing on the system. It was observed with sand ballast that even

for very small lifts small particles would still flow into the void below the sleeper, the same was observed in the full scale tests when with a void below the sleeper reduced to 5mm with every uplift cycle a slight gain in sleeper height was achieved. Thus using sand as crib ballast it is possible to completely fill up any void occurring below the sleeper but the fact that with sand in the crib the sleeper gains in height for very small lifts of a few mm could present a problem on live railway track. The 'precession wave effect' has been discussed in the literature review, which causes the sleepers in front of and behind the wheel to lift up by a few millimeters. Thus with sand as crib ballast when the sleeper would lift out of the ballast by a few millimetres under the precession wave effect, the sand from the crib would flow into this void and the sleeper would not return to its original position. Thus in this manner with each subsequent load cycle and the precession wave effect the sleeper would effectively be lifted out of the ballast and out of alignment.

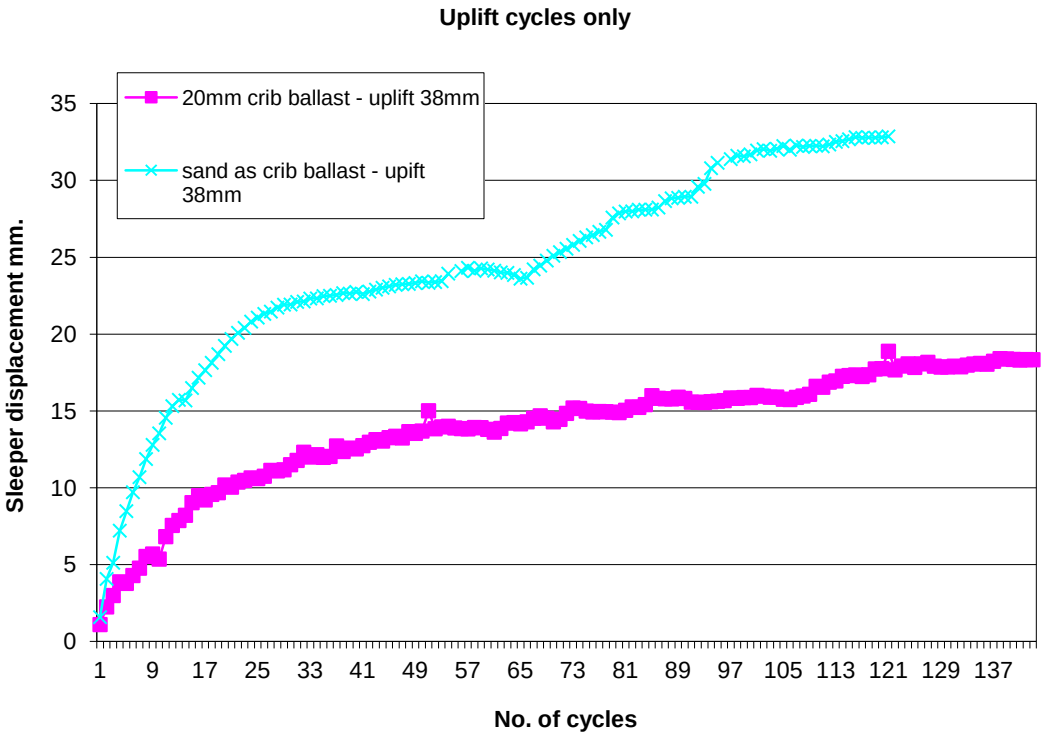

Figure 6.15 Tests with 20mm crib ballast and sand ballast compared

After the test with sand ballast was complete the sand from around the sleeper was removed carefully. The sleeper was then lifted to observe the distance the crib ballast had

moved towards the centre of the sleeper cross section, a photograph taken at that time is shown in figure 6.16. It was observed that the sand had completely covered the 50mm bottom ballast and below the sleeper imprint a neatly compacted layer of sand could be seen. From the photograph it can be seen that small pebbles of 2-5mm size were lying on the edge of the sleeper imprint at the end of the test. Thus as the void size below the sleeper reduced the larger particles in the crib ballast were filtered out while the smaller particles flowed around the larger particles and into the void below the sleeper. This has been observed earlier, when using the mixed gradation ballast consisting of stones from size 50mm down to 10mm in the box test.

With 20mm crib ballast the final sleeper height gain should be (38-17) 21mm while the final sleeper height gain when the test was stopped is 18mm. It was observed that very small corrections in height were still taking place when the test was stopped thus the end point for the graph had not been reached.

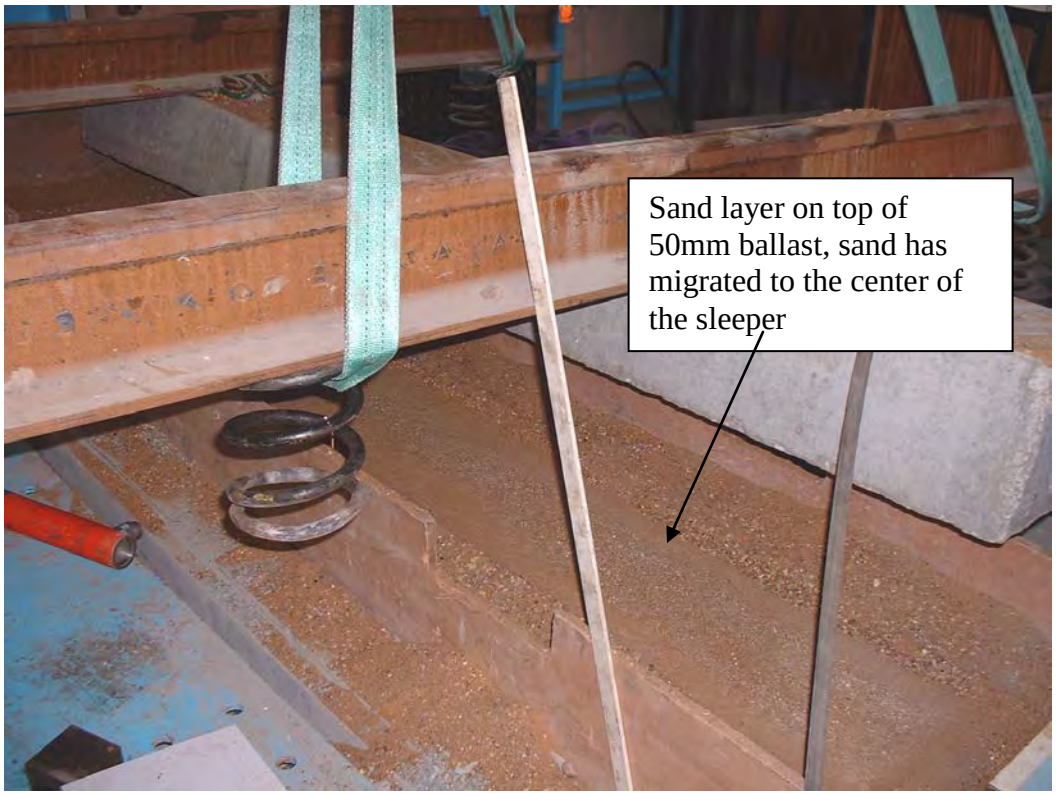

Figure 6.16 Test with sand as crib ballast

6.2.2.2.2 Test with 10mm and 5mm

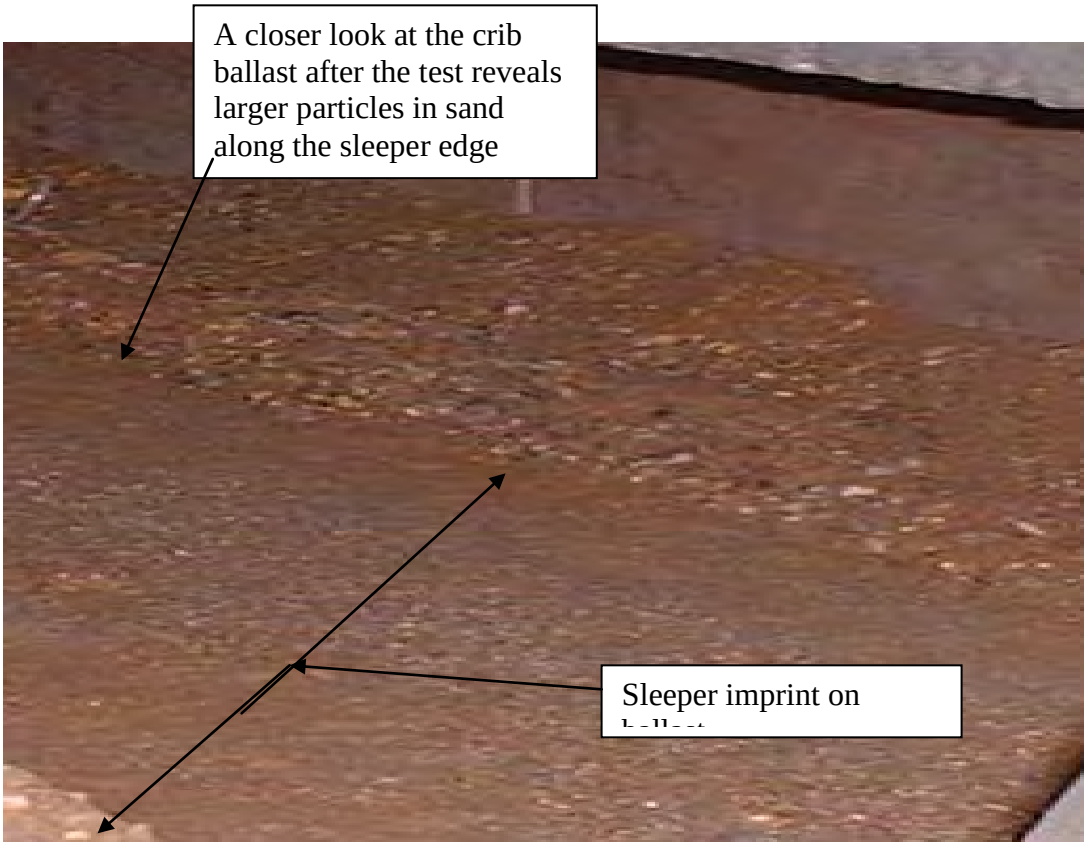

crib ballast

The uplift height for these tests was 30mm so the graphs have been plotted together for comparison. The graphs are shown in figure 6.17

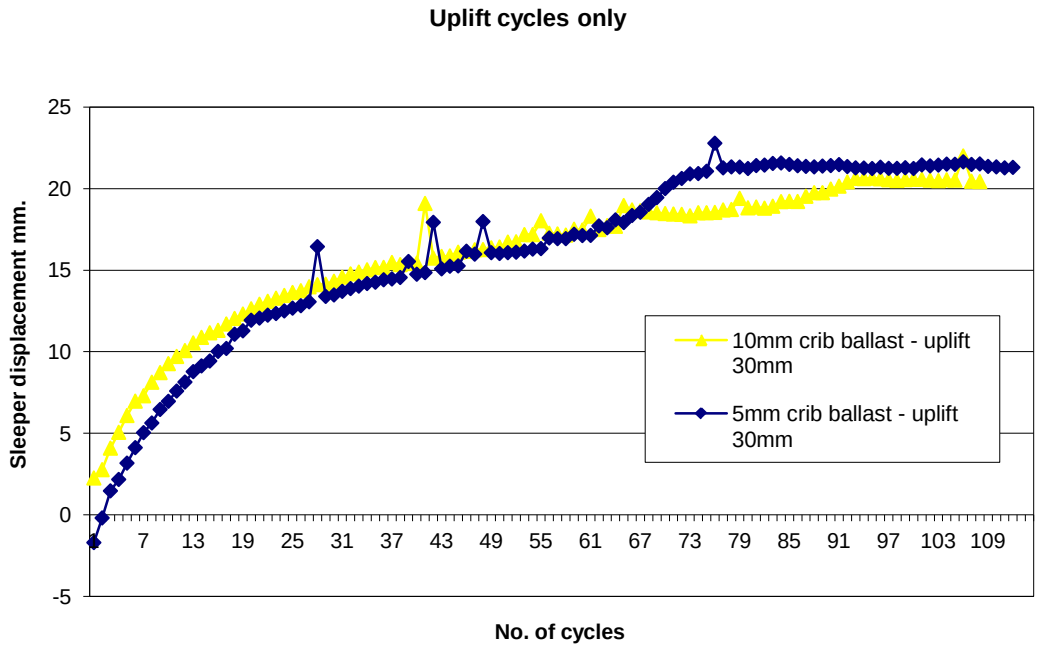

Figure 6.17 Tests with 10mm and 5mm crib ballast uplift cycles only.

The final uplift height gain for both the tests was not achieved as both the ballast samples were contaminated with larger size particles. From the ballast grading shown in table 6.4 it can be seen that the 10mm ballast sample consisted of 22% of stones of size 12mm while the 5mm ballast sample consisted of 44% of stones of size 7mm. The test was stopped when there was no appreciable sleeper height gain in the uplift cycles and the sleeper height gain at the end of the test was 21mm for the 10mm ballast and 22mm for 5mm crib ballast.

As described earlier displacement readings were taken by two LVDT fixed on the two rails. In the test with the 5 and 10mm crib ballast it was observed at the start of the test that the ballast below the sleeper was not level i.e. when the sleeper was loaded down onto the ballast surface the void readings from the two LVDT were not the same. For the test with 10mm crib ballast the void below one LVDT was 30mm while the void below the other LVDT was 26mm at the start of the test. Thus the bottom ballast was sloping in one direction, which is generally the case on live track when a track is given cant or superelevation on curves. Although the author was aware of the different void size at the two ends of the sleeper the test was run to check if the sleeper would loose its 'cant' level when the crib ballast would fill the void below the sleeper. The results from this test with 10mm crib ballast is shown in figure 6.18.

It is observed that the sleeper crosslevel at the end of the test is the same as the sleeper cross level at the start of the test. The void below the sleeper has been reduced but the void has reduced by the same amount each end of the sleeper. Thus the crib ballast has filled up the void but has maintained the same cross level of the sleeper.

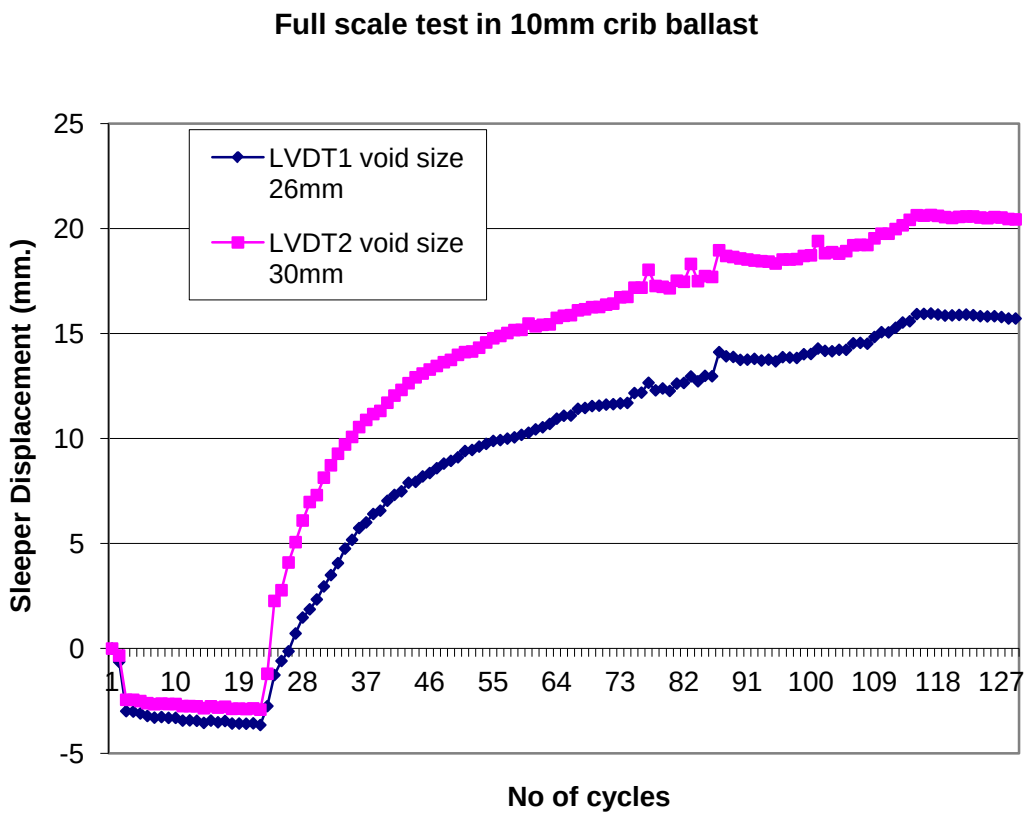

Figure 6.18 Full scale test in 10mm crib ballast with sloping bottom ballast.

6.2.2.3 Test with 20mm top and bottom ballast

This test was carried out with 20mm bottom and crib ballast, again it was a repeat of similar test carried out at model scale and in the box test. Sleeper spacing was 600mm and the uplift height in the uplift cycles was maintained at 38mm between each load cycle. The uplift height in the test carried out with 50mm bottom and 20mm crib ballast was 38mm thus the same uplift height was used for this test to allow comparison of results between the two tests. The crib ballast was filled in around the sleeper initially to approximately 30-50mm height in the crib. Using white paint the crib ballast stones close to the sleeper were marked out so that they could be identified from the rest of the crib ballast. The aim was to observe after the test the extent to which the crib ballast had migrated in the sleeper cross-section. Twenty simple load cycles were run followed by uplift cycles. The results are

shown in figure 6.19 as graph of maximum sleeper displacement for each load cycle. A comparison has been made with the test carried out with 50mm bottom and 20mm crib ballast.

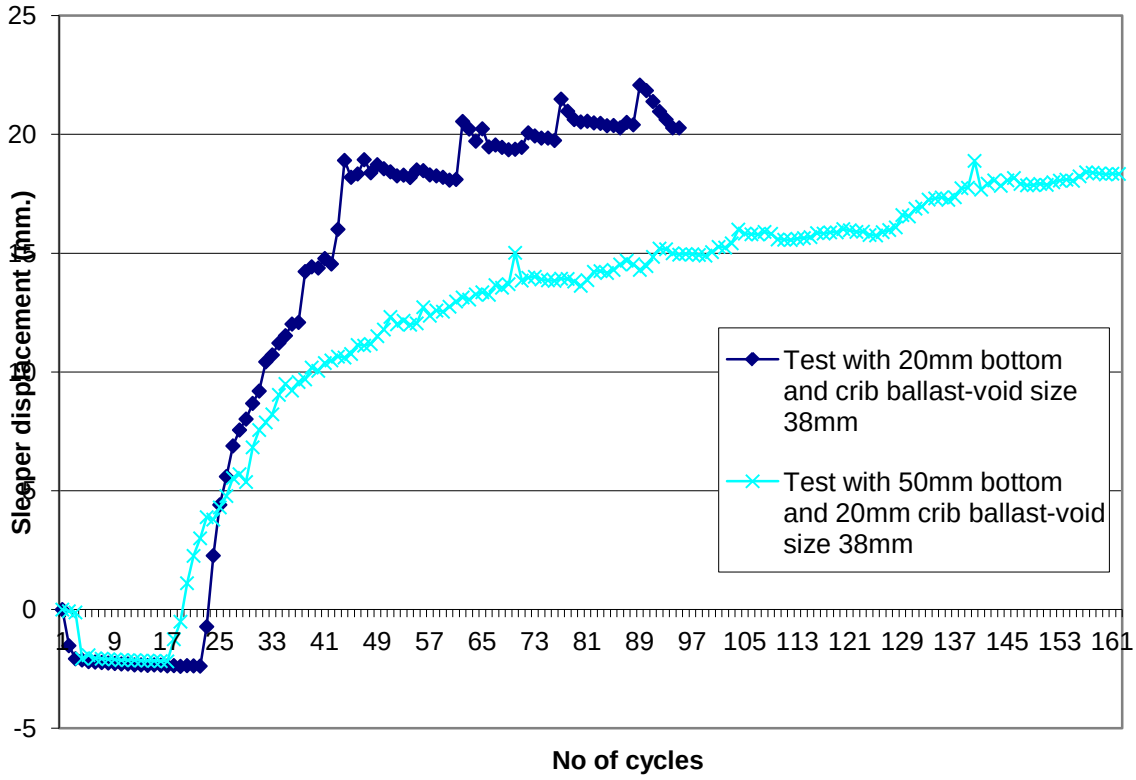

Figure 6.19 Comparison of test with 20mm and 50mm bottom ballast

6.2.2.3.1 Observations

The sleeper height gain is quicker for test with 20mm bottom ballast, this again validates the observation made in the model tests and box test. For test with 50mm bottom ballast the final sleeper height gain of 18mm occurs in approximately 140 uplift cycles and the end point of the graph has not been reached. For the test with 20mm bottom ballast the final sleeper height gain is 20mm in 75 uplift cycles and the end point for the graph has been reached. The predicted height gain for the uplift height 38mm with 17mm average size of crib ballast would be 21mm which defines the end point for the graphs.

Sleeper height gain in the first five uplift cycles for both tests are given in table 6.5

Table 6.5 Sleeper height gain.

Bottom ballast size	Sleeper level relative to datum zero level (mm.)						Total height gain (mm.)
	Last simple loading cycle reading (mm.)	Uplift cycle readings (mm.)					
20mm	-2.38	-0.72	2.27	4.4	5.6	6.8	7.5
50mm	-2.18	-1.25	-0.51	1.11	2.26	3.8	5.0

It is clear from the data in the table that the sleeper height gain in the first few uplift cycles for the test with 20mm bottom ballast is more as compared to test with 50mm crib ballast. In the first uplift cycle the sleeper height gain for test with 20mm bottom ballast is twice that for the test with 50mm bottom ballast. This is again similar to observations made for earlier tests with 20mm bottom and crib ballast. With a large size bottom ballast for the first few uplift cycles the smaller crib ballast is compacted into the voids in the bottom ballast and thus some of the sleeper height gain is lost.

At the end of the test the with the sleeper supported on the springs, the crib ballast was carefully removed from around the sleeper. The sleeper was then lifted and the bottom ballast below the sleeper was inspected to see by how much the crib ballast marked white before the test had migrated towards the centre of the sleeper. A photograph taken at that time is shown in figure 6.20. It was observed that the crib ballast painted white had migrated to the centre of the sleeper cross-section.

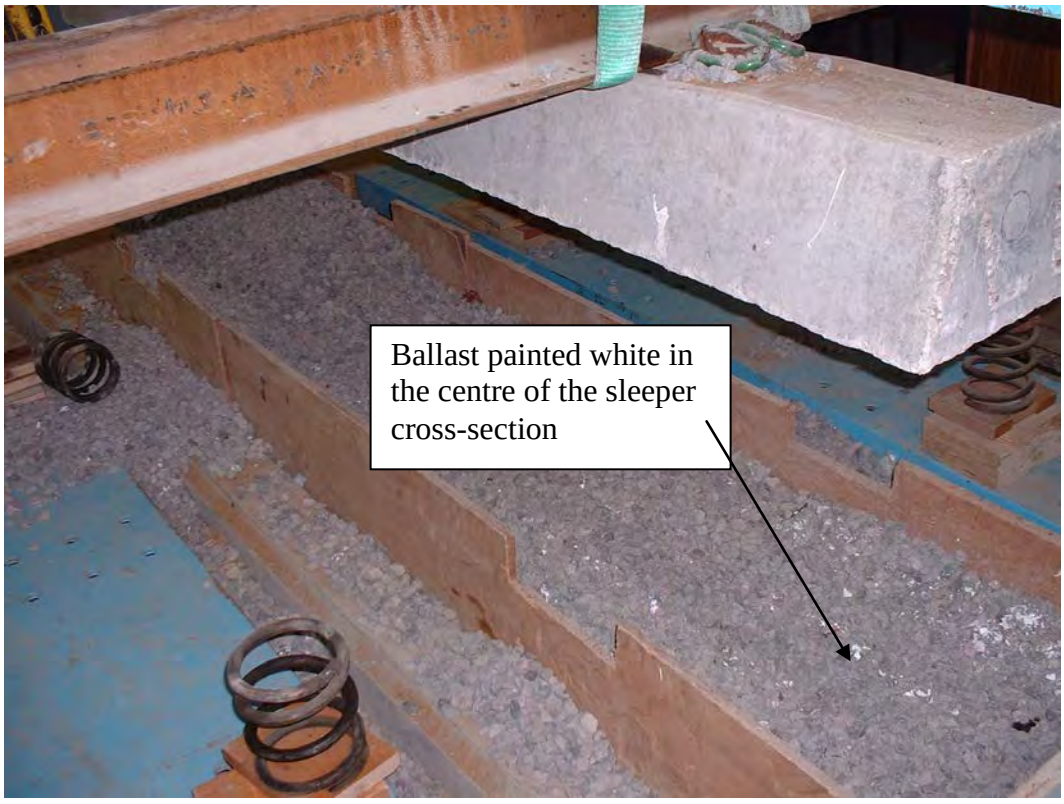

Figure 6.20 a Photograph of test with 20mm bottom and crib ballast

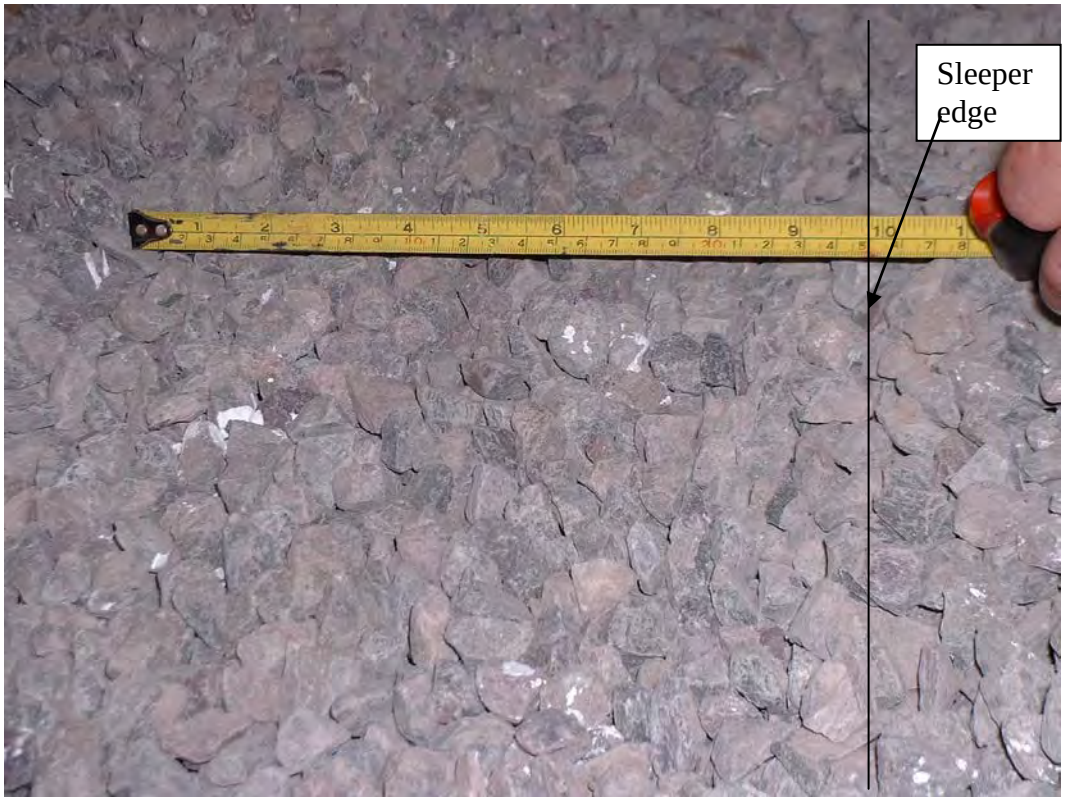

Figure 6.20 b Photograph of test with 20mm

bottom and crib ballast

6.2.2.4 Test to simulate the stoneblowing machine design uplift

It was observed in the type B model tests that if the sleeper assembly was lifted up by 4.5mm at intervals of 10 simple load cycles, enough smaller crib ballast will flow into the void below the sleeper in the one uplift cycle, to raise the sleeper level up by a height equal to the sleeper displacement in the subsequent 10 load cycles thus effectively maintaining the sleeper at the same level throughout the test. The graph is shown in Chapter 5. This implies that for even a single large lift of the sleeper assembly between load cycles the crib ballast migrates into the void created by lifting the sleeper up and the sleeper level is raised up. This can be related to the mechanical methods employed in maintaining the track top to the required level.

It has also been established from model tests and full scale tests that any void below the sleeper larger than the size of the crib ballast will be filled up by the crib ballast to an extent determined by the size of the crib ballast and the size of the void below the sleeper. The general relationship developed is that the void below the sleeper will be filled up to the void size minus the average particle size of the crib ballast. The average particle size for the standard railway ballast is 37mm neglecting particles smaller than 28mm. Thus using the above relationship if the void below the sleeper is more than 37mm some crib ballast would flow into the void below the sleeper i.e. if the void below the sleeper is 50 mm the void would be filled up by (50mm-37mm) 13mm or, if the sleeper is lifted up once, for maintenance purposes, by 50mm some crib ballast would flow into the void causing the sleeper to rise up.

It has been discussed in the literature review that to maintain a good ‘top’ on a line it must be lifted wherever it is low and the ballast must be packed firmly under the sleepers at the points wherever it has been lifted. From the early days of beater packing to modern mechanized maintenance of track this remains the fundamental principle of track maintenance. With manual methods of beater packing and measured shovel packing the crib ballast is cleared to the sleeper bottom before the sleeper is lifted up to the required

level thus there would be no crib ballast present which could potentially flow into the void below the sleeper also the lift given to the track is very small.

For mechanized maintenance of track using tampers or stoneblowers the track is lifted up without removing the crib ballast. As discussed earlier to achieve greater durability of track maintenance by tamping, wherever possible high lift tamping is used. In high lift tamping the lift given is greater than 25mm and Selig and Waters (Selig and Waters 1994) have defined high lift as being in excess of the sieve size, which will retain 50% of the sample of ballast being tamped. 50mm ballast on British Rail typically consists of 30% - 70% of stones of size retained on 37.5mm sieve. Thus a lift greater than 37mm would be considered a high lift on British Rail.

For the stoneblowing process the track needs to be lifted up by the amount required to correct track geometry and an extra 45mm to allow blowing of stones of 20mm size under the sleeper i.e. if the track geometry is to be corrected by 5mm the total uplift given to the track by the stoneblower is 50mm. This extra 45mm of lift above that required for correcting track geometry is called the ‘design overlift’ of the stoneblower. The stones are blown below the sleeper into the void and the track is lowered back on the new stones. It has been observed that the track just after stoneblowing looks worse than it was pre maintenance and in some cases the track geometry just after stoneblowing has been found to be worse than the track geometry prior to stoneblowing. The reason for this has been attributed to the ‘design overlift’ of the track by 45mm. It is assumed that the track when lowered down on the ballast bed after stoneblowing does not return back through the full 45mm overlift given to the track and that subsequent traffic is required to compact the track back to its correct level as designed by the stoneblower. From the results of the model and full scale tests and the type B model runs it was realized that giving a high uplift to the track of more than 37mm would cause the crib ballast to migrate into the void below the sleeper thus this could in some way affect the post maintenance track geometry of the track (Ball 2003).

To understand if the observations made on model and full scale test with smaller crib ballast would apply to standard railway ballast in case of high lifts given to the track, a full scale test with a high uplift was carried out in the laboratory.

The sleeper spacing was simulated at 600mm and both top and bottom ballast were standard 50mm railway ballast. The test was run with 20 simple cycles followed by uplift cycles. The uplift height in the uplift cycles was kept 45mm, this simulated the high uplift given to the track while correcting track geometry using tampers or stoneblowers. The results are plotted as graph of maximum sleeper displacement for each load cycle in figure 6.21

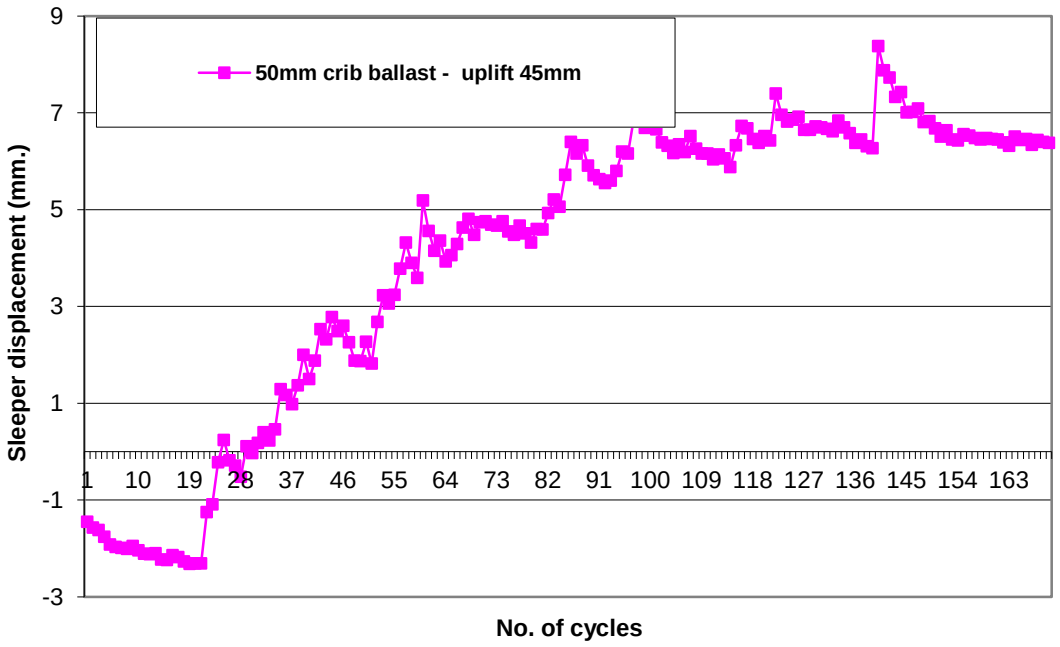

Figure 6.21 Simulation of high uplift used by tampers or stoneblowers in full scale test.

6.2.2.4.1 Observations

It can be seen from the graph that the sleeper starts correcting in height from the first uplift cycle. The height gain in the first uplift cycle is approximately 1.2mm and in three uplift cycles the sleeper has moved back to its zero level rising up by 2.3mm. Thus even a single lift given to the sleeper larger than 37mm will cause the crib ballast to migrate into the void below the sleeper causing the sleeper to rise up. The predicted maximum height gain for crib ballast average particle size 37mm and uplift height 45mm is 8mm. The sleeper has corrected to 7mm above the datum zero level. This again demonstrates that the void size will be filled up to the average size of the crib ballast.

It was observed during the test that during the uplift cycles when the sleeper was lifted up some crib ballast would flow into the void below the sleeper and the sleeper was pressed down again with some difficulty. The sleeper could not be pressed back to its original position even after the first uplift cycle. When the load was applied again after the sleeper had been lifted, due to the resistance provided by the crib ballast and the ballast which had migrated into the void the sleeper became unbalanced, although eventually the ballast was compressed to some extent by the heavy load applied to the sleeper. This was observed throughout the test starting from the first uplift cycle. Kinks in the graph can be observed where a large stone from the crib has migrated into the void below the sleeper and then is compacted to some extent by subsequent load cycles into the bottom ballast. Even after approximately 100 uplift load cycles the sleeper vertical movement was not smooth.

The above test results confirm that for large uplift given to the track by stoneblower or tamper the sleeper would undergo some permanent height gain. The higher the uplift given to the track the larger the height gain by the sleeper.

When the tamper or the stoneblower arrives on site it undertakes a measurement run in which all track parameters are measured. The on-board computer then designs a geometric profile for the track and the tamper or the stoneblower implements this design to the track. In the stoneblower depending on the amount of lift to be given to the track the amount of stones to be blown under the track is calculated. As the tamper and the stoneblower do not account for the lift given to the track by the crib ballast flowing into the

void below the sleeper, as seen above in the test result, the track vertical alignment would be overcorrected. The problem with the tampers would not be severe as the tampers vibrate and compact the ballast but as the stoneblowers depend on new stone being blown below the sleeper for correcting geometry faults the stones from the crib ballast would leave the track overcorrected by a significant amount. Also the stoneblower blows 20mm stone below the sleeper so stones of size 28-37mm added with the stoneblowing stone would prevent stoneblower design track geometry to be implemented.

6.2.3 Tests with sleeper spacing at 800mm.

This was the last test carried out on the full scale test assembly. The rigid panels forming the boundary for the ballast were moved to a distance 800mm apart thus the sleeper centre distance was simulated at a spacing of 800mm which is more than the maximum recommended sleeper spacing on British Rail. The maximum sleeper spacing tested in the model test was 80mm (10^{th} scale of 800mm), thus this test was a repeat of the model test at full scale. 50mm bottom and 20mm crib ballast were used in the test and twenty simple load cycles followed by uplift cycles were run. The uplift height in the uplift cycles was 32mm The results are shown in figure 6.21 as graph of maximum sleeper displacement for each load cycle.

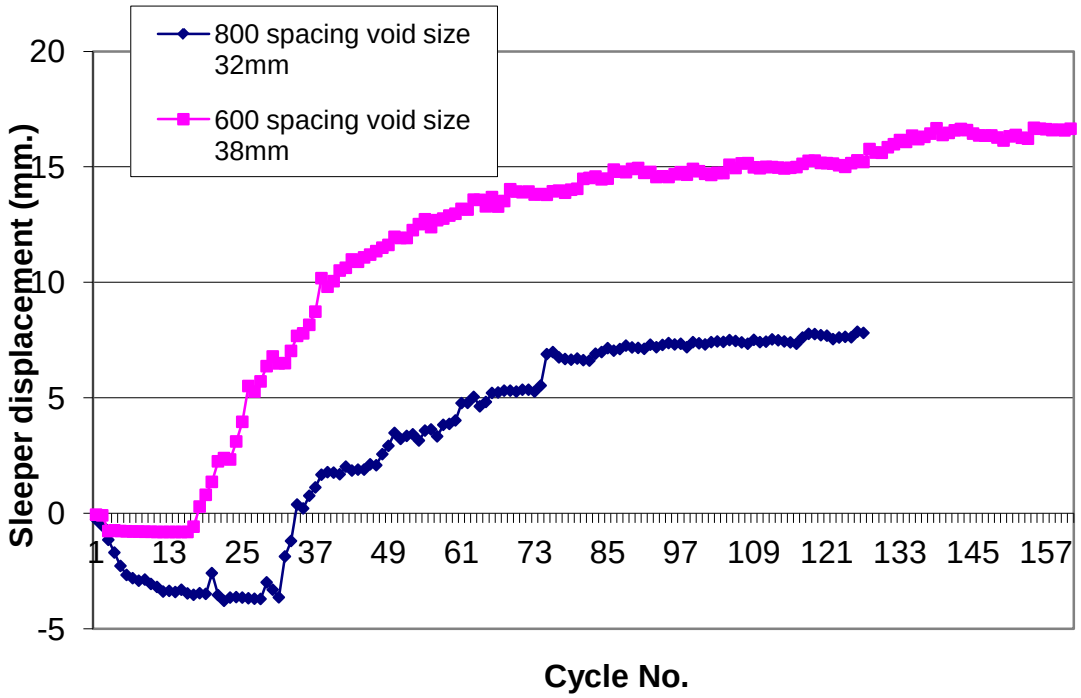

Figure 6.22 Tests with sleeper spacing 600mm and 800mm compared. Crib ballast size for both tests was 20mm stoneblowing stone.

6.2.3.1 Observations

Similar to observation made in the model test the sleeper height gain in the uplift cycles is slow for sleeper spacing of 800mm as compared to sleeper spacing of 600mm. For the test with 600mm sleeper spacing the final height gain is equal to void size minus average particle size of the crib ballast i.e. approximately 17mm, while this is not observed for the test result for sleeper spacing 800mm. For sleeper spacing 800mm the predicted height gain was 14mm while the total height gain in approximately 130 load cycles is approximately 8mm. Thus optimum sleeper spacing for performance of the two layered ballast system is 600mm.

7. Discussion on results

7.1 Introduction

In this chapter all observations made on model and full scale test results have been summarized. An attempt has been made to compare test results with previous research on ballast, although from the literature review carried out by the author it is evident that the concept of using smaller stone as crib ballast has not been researched before. Smaller ballast or graded ballast with a proportion of smaller stone was the British Rail standard untill early 1980's but the aspect of voids below the sleepers being filled up by smaller ballast from the crib has never been reported before. This phenomenon has either been overlooked or more likely taken for granted by early railway men and the author has not come across any published literature on this subject. All research on ballast has concentrated on ballast settlement or inelastic compression under sustained cyclic loading and ballast deterioration over time under sustained cyclic loading. The aim was to develop specifications for ballast to improve ballast performance and to develop maintenance models for maintenance of ballasted railway track. Recently research has been carried out on two layered ballast system (Anderson and Key 2000), this relates to the use of stoneblower for track maintenance. As discussed in the literature review the stoneblower aligns the sleeper in the vertical plane by placing 20mm stone below the sleeper on an already compacted ballast bed. Tests have been carried out to study the long term effect of having two layers of different stone sizes below the sleeper. Some tests have been carried out with graded or smaller ballast but the area of attention has been the ballast directly below the sleeper to observe the inelastic compression of the ballast and again ballast degradation under loads.

Mathematical models for track settlement have been developed but are generally empirical in nature. There is no generally accepted equation for track settlement and different railways around the world refer to their own settlement models (Dahlberg 2001).

All track settlement models are developed with track settlement as a function of number of loading cycles or the loading on the track.

In this chapter an attempt has been made to develop empirical equations for sleeper height gain in the uplift cycles for model tests, box tests and full scale tests. Also to relate box test results to earlier research carried out by Selig and Waters (1994), a few box tests were carried out with standard railway ballast below the sleepers and in the crib, subject to sustained cyclic loading without uplift (simple load cycles). Results were compared with results from similar box tests carried out by Selig and Waters (1994).

7.2 Ballast compression under sustained cyclic loading.

Settlement equation proposed by Selig and Waters (1994, p8.34) was selected to analyse test data from box tests.

Based on laboratory tests as reported in the literature review, Selig and Waters (1994, p8.34) have proposed the following power relationship for settlement of ballast,

$$S_N = S_1 N^b \qquad (7.1)$$

Where S_N is the settlement after N load cycles

S_1 is the settlement from the first load cycle

b is track constant

The best fit equation found by Selig and Waters (1994, p8.35) for their data was for b value of 0.17.

Data from box test results was used to calculate the values of the constants in equation proposed by Selig and Waters (1994). To facilitate this a few box tests were run with 50mm bottom ballast and 20mm bottom ballast with simple load cycles to simulate sustained cyclic loading of a sleeper under traffic, no uplift cycles were run. The results are

shown in figure 7.1 as graph of sleeper displacement for each load cycle. In all previous graphs sleeper displacement into ballast or ballast compression in the simple load cycles has been represented as negative values but to be able to compare the results with those of Selig and Waters (1994) the data values are represented as positive values. The best fit power equation (equation (1)) has also been drawn in figure 7.1 for the box test data values.

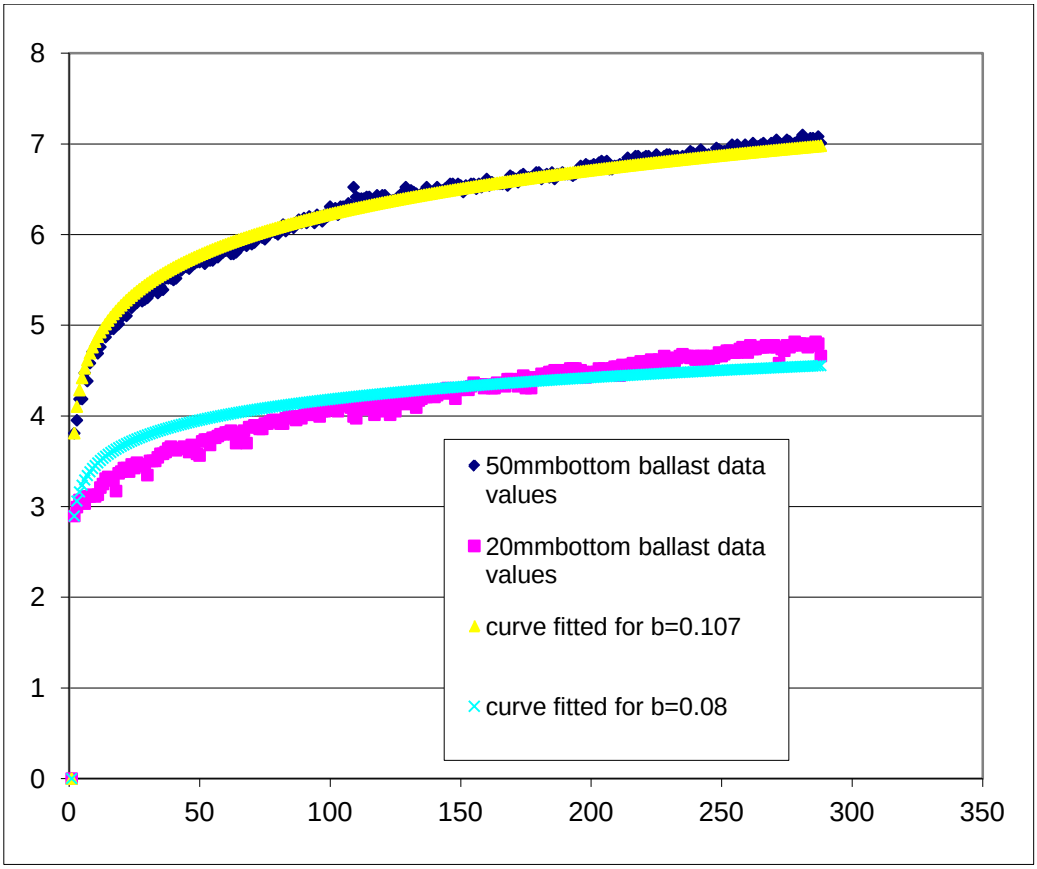

Figure 7.1 Comparison of box test results with Selig and Waters (1994), curve fitting using equation 7.1.

7.2.1 Observations

Selig and Waters (1994) have investigated trends for ballast settlement for 2 million or more cycles while the box tests have been run for approximately 300 load cycles. The

purpose of the above tests with simple load cycles was to compare the trends of the results with those of Selig and Waters (1994) to validate the box test set up.

It can be seen that the graph for b = 0.11 is a good fit for the settlement data of the box test with 50mm bottom ballast while the graph for b = 0.08 is the best fit for settlement data of the box tests with 20mm bottom ballast. The power equation is not a very good fit to the data for the box test with 20mm bottom ballast, this could be because the settlement behaviour of 20mm ballast is different from 50mm ballast and the proposed power equation by Selig and Waters (1994) has been developed based on observations on 50mm standard railway ballast. Also the best fit for Selig and Waters (1994, p8.35) data is for value of exponent b as 0.17 while the for box test carried out by the author with 50mm bottom ballast the best fit is for b as 0.11. A cause for this could be that the tests by Selig and Waters (1994) were carried out for an axle load of 390 kN (39 tons) which is the standard axle load on American Railway while the tests by the author were carried out at 200kN axle load which is the standard axle load on British Rail (Profillidis 1995, p36). For a higher axle load the settlement would be more and also more rapid which is why the value of exponent b for tests data of Selig and Waters (1994) is greater than that for the author's tests.

7.3 Sleeper height gain in uplift cycles for Type A runs

It has been demonstrated by model tests and full scale laboratory tests, for type A runs, that any void below the sleeper larger than the average particle size of the crib ballast will be filled up to the average particle size of the crib ballast when the sleeper moves vertically in the void under traffic. Thus the final sleeper height gain can be given by the equation,

Final sleeper height gain = Void size – average particle size of the crib ballast (7.2)

A few graphs of sleeper uplift height gain against cycle number are shown in figure 7.2. The graphs include data from model tests, box test and full scale single sleeper test for

type A runs. The type A runs involve running 20 simple load cycles on the sleeper (s) without uplift, followed by uplift cycles in which the sleeper is lifted up by a predetermined amount after each load cycle. In the graph in figure 7.2 only the uplift cycle readings have been plotted against cycle number. It can be seen that the form of the curve for the uplift cycles is similar for all tests and can be represented by the first term of Sato's equation described in the literature review as

$$y = A\ (1 - e^{-cx}) \qquad (7.3)$$

Where

A = Final sleeper height gain = Total void size – average particle size of crib ballast

y = Sleeper height gain for load cycle x

c = constant

The term A is the maximum sleeper height gain. Thus for x = 0, y is zero and the value of c controls the number of loading cycles required to attain the maximum height gain.

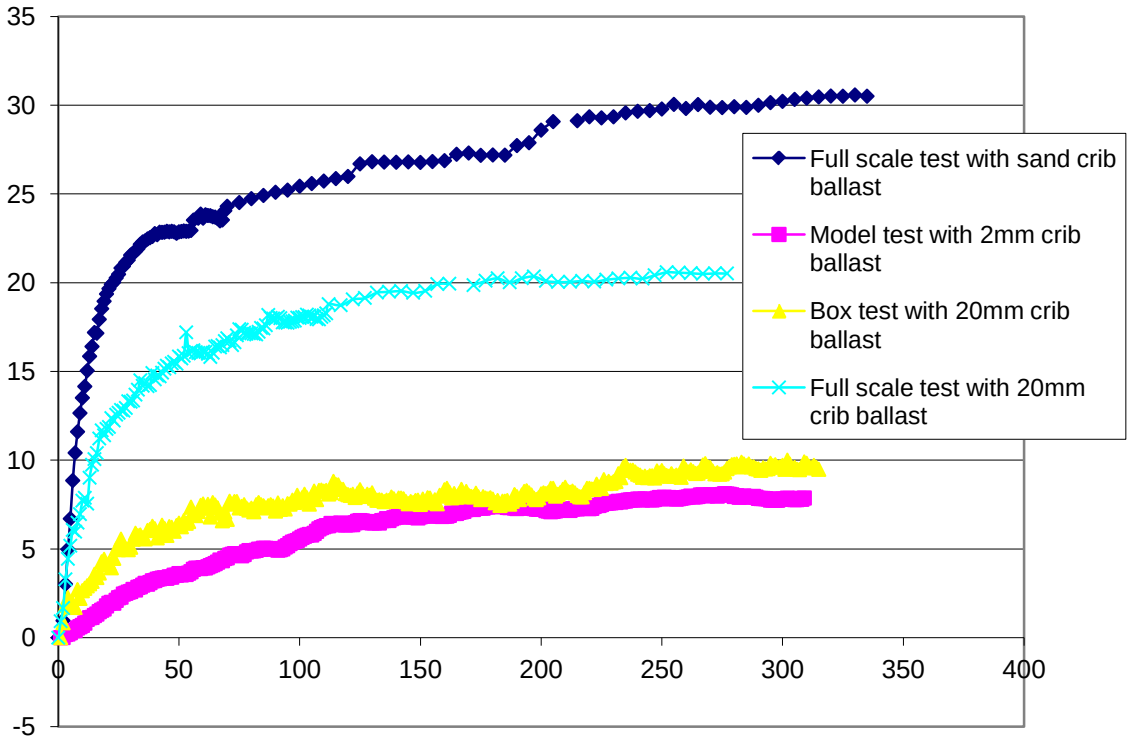

Figure 7.2 Sleeper uplift height gain for different tests.

As described in the literature review Sato's equation for predicting track settlement has two terms as shown in equation (7.4).

$$y = A\ (1 - e^{-cx}) + ßx \qquad (7.4)$$

The first term in the equation $A\ (1 - e^{-cx})$ is for the short term settlement of the track immediately after tamping. A is the total track settlement immediately after tamping while c controls how quickly the settlement occurs. The term ßx is for long term settlement of track. The value of ß is chosen such that the term ßx becomes relevant only after the initial settlement has taken place. For the mathematical modelling of the data from the tests on the two layered ballast system only the first term of Sato's equation was used because with the second term the sleeper height gain for infinite number of load cycles would be infinite i.e. the equation does not have an asymptote. As seen from the model and full scale tests, the maximum sleeper height gain is limited by the void size below the sleeper and the size of stone used as crib ballast. Thus the first term of Sato's equation was used for empirical modeling to describe the sleeper height gain in the uplift cycles.

To carry out empirical modelling of the test data, taking logarithm of both sides of equation (7.3) the graph of ln(Ap - y) (Ap is the predicted height gain using equation 7.2) was plotted against cycle number (x), the value of Ap was calculated using equation (7.2) and y was the sleeper height gain obtained from the test data. The slope of the graph gave the value of c. Substituting the values of Ap and c in equation (7.3) a graph of sleeper height gain (y) against cycle number (x) was plotted against cycle number and compared with the graph of data values from the test. To check if the best fit to the test data had been achieved the Root Mean Square (RMS) error for the two data values (y measured in the test and y predicted by equation) was calculated.

The above procedure for carrying out the modelling has been described for a typical model test data set. A typical graph of a model test on wooden monoblock sleepers at 60mm spacing with 5mm bottom and 2mm crib ballast is shown in figure 7.3. Only positive displacement readings from the uplift cycle have been shown. The model test readings have been multiplied by 10 to allow comparison with full scale test results. The final sleeper height gain in approximately 1000 uplift cycles is 8mm which is equal to the uplift height minus average particle size of the crib ballast.

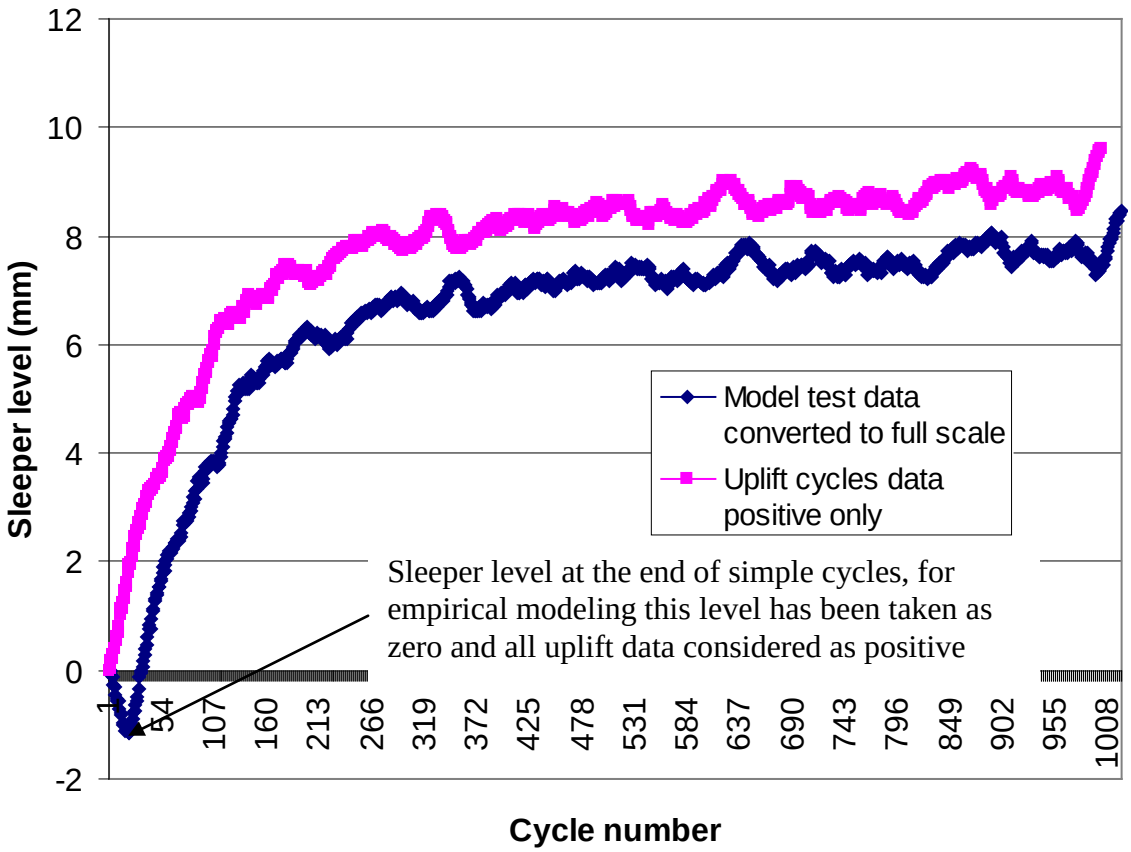

Figure 7.3 Model test for sleepers at 60mm spacing with 2mm crib ballast, sleeper level relative to the datum zero level for simple and uplift cycles.

In figure 7.3 the uplift height gain values were all considered as positive. As described earlier in chapter 4, for each Type A run 20 simple cycles were run followed by uplift cycles, the downward displacement of the sleeper into the ballast was taken as negative. After 20 simple load cycles without uplift, at the start of the uplift cycles the sleeper level was a few mm below the datum zero level for all the tests and thus as the sleeper started lifting up gradually (in the uplift cycles) the first few displacement readings were negative before the sleeper reached the original datum zero level, this is clear from the graph of sleeper level Vs cycle number in figure 7.3. In the graph in figure 7.3 the sleeper displacement into ballast is 1.1mm at the end of 20 simple cycles, this was taken as zero for the uplift cycle readings and all the readings were adjusted accordingly (as positive) as shown in figure 7.3. The final sleeper height gain for the adjusted sleeper displacement readings was approximately 9mm.

Assuming a value of Ap equal to total void size minus the average particle size the graph for natural log of (A-y) Vs cycle number (x) was plotted as shown in figure7.4. A linear trendline was fitted through the graph of log (Ap-y) Vs (x) and the slope of the trendline gave the value of c. Using the estimated value of Ap and the value of c obtained from the trendline, ‘y’ values were calculated for each cycle number and plotted against the cycle number as shown in figure 7.4. The root mean square error between the calculated ‘y’ values and ‘y’ values from experimental data was determined. It was observed that the RMS error was not minimum for the estimated Ap and c values obtained as described above. Thus the RMS value was observed while changing both Ap and c and the best fit curve obtained for minimum RMS value. For the test data in figure 7.4 the RMS error is minimum for Ae = 8.6 (Ae is the A obtained from empirical modelling and is different from Ap) and c = 0.01. Thus ‘Ap’ estimated based on void size and average particle size of crib ballast was 8mm while ‘Ae’ obtained by empirical modelling is 8.6mm. The value of c obtained from graph of ln(Ap-y) Vs (x) for all empirical modelling was used as a starting point for curve fitting but the best fit values for Ae and c were obtained for the minimum RMS error by trial and error procedure as described above.

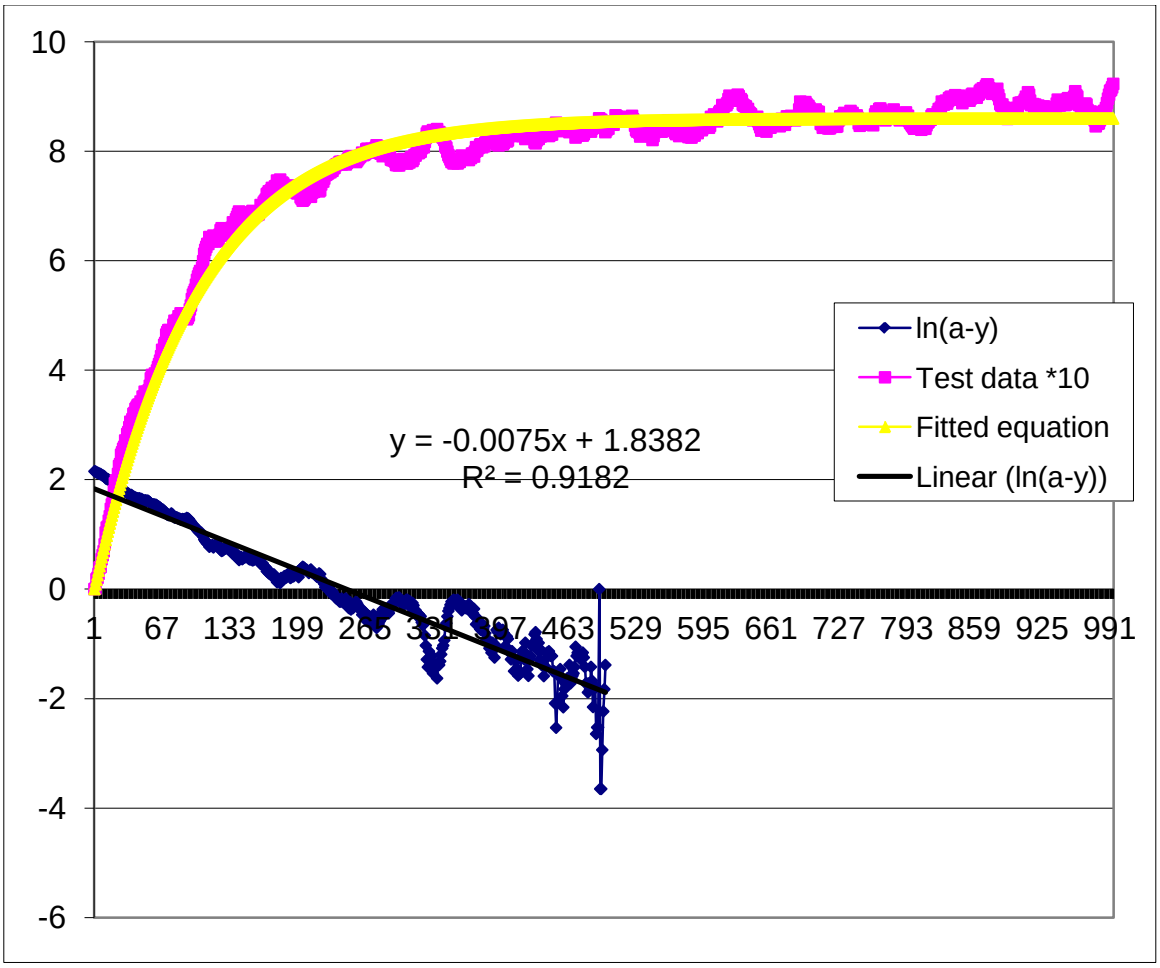

Figure 7.4 Empirical modelling of model test data for sleeper spacing 600mm and 20mm crib ballast uplift height 25mm, data has been converted to equivalent full scale.

While repeating the above mentioned process of optimising A and c by trial and error, for box tests and full scale tests it was realised that a good fit was not obtained for the test data even for the minimum RMS error, an example is shown in figure 7.5.

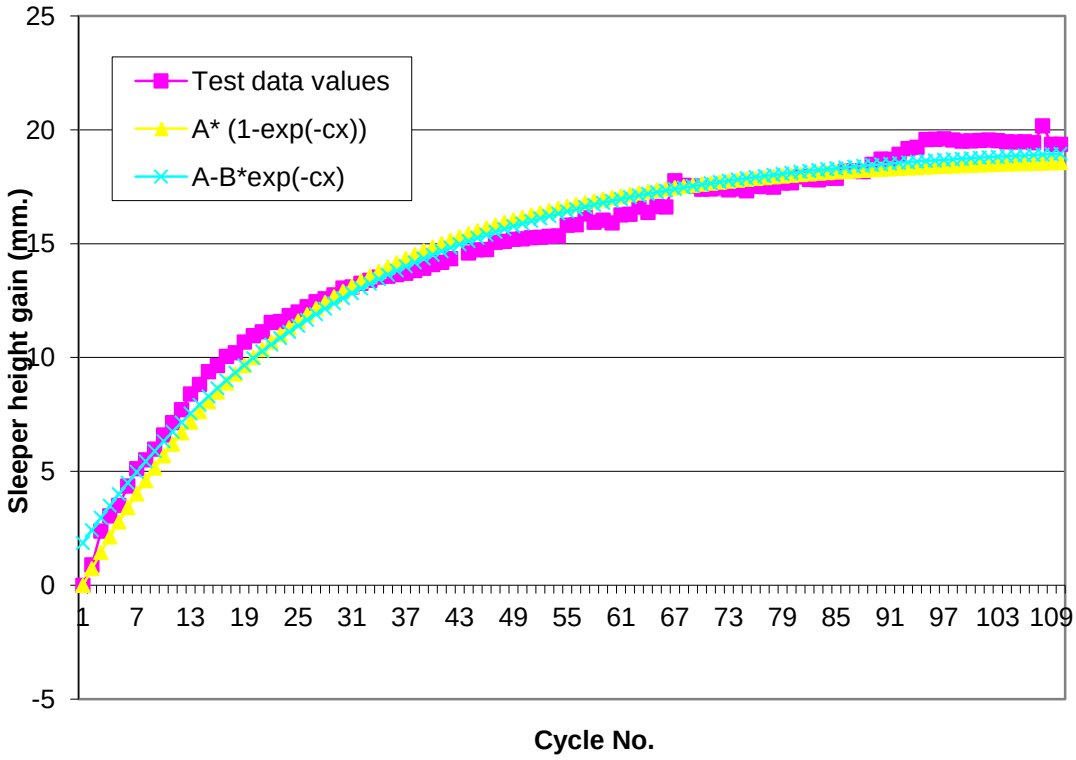

Figure 7.5 Box test with 10mm crib ballast, 50mm bottom ballast, uplift height 25mm.

As shown in figure7.5 for the curve to start from zero it was not possible to define a best fit curve for the data, thus a new term B was introduced in equation (7.3) as shown in equation (7.4).

$$Y = A - B\,(e^{-cx}) \qquad (7.4)$$

Thus for x = 0, y is not zero thus the curve does not start at the origin. It was decided to try and fit this curve to the data values. The RMS error was calculated and the best fit curve to the data was the one with the minimum RMS error. As it was not possible to determine the best fit curve to the data for three constants A, B, c manually by trial and error, a program

was written in Visual Basic within Excel to find a best fit curve for the data values and define the values of parameters A, B and c. The algorithm would optimise the value of A, B and c for the minimum RMS error between the calculated 'y' values and 'y' values from experimental data. The program is shown in the appendix.

For the test data shown in figure 7.5 the RMS error for 'y' values calculated using equation (3) is 8.25 while the RMS error for 'y' values calculated using equation (7.4) is 6.28. Thus the algorithm has been able to optimise further on the RMS value by introduction of the term B as shown in equation (7.4).

The best fit equation for all data sets was calculated using equation (7.4) and the optimisation program. The results for all type A runs are shown in table 7.1. Figures 7.6, 7.7 and 7.8 show some examples of curve fitting using equation (7.4)

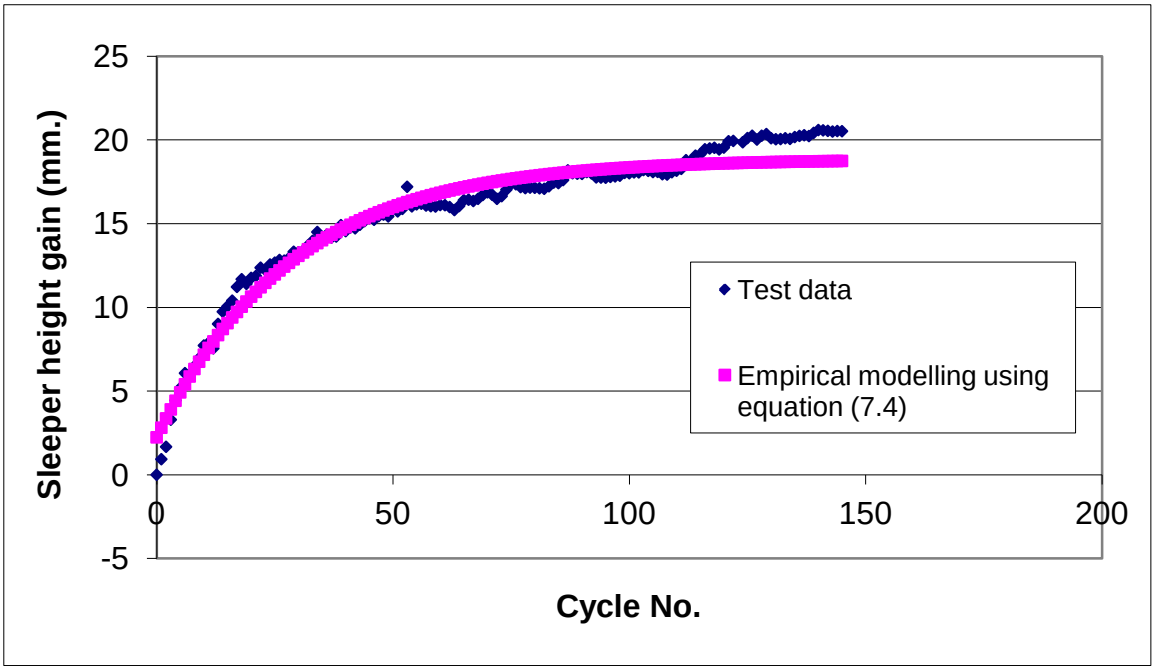

Figure 7.6 Full scale test with 20mm crib ballast, curve fitting using equation (7.4)

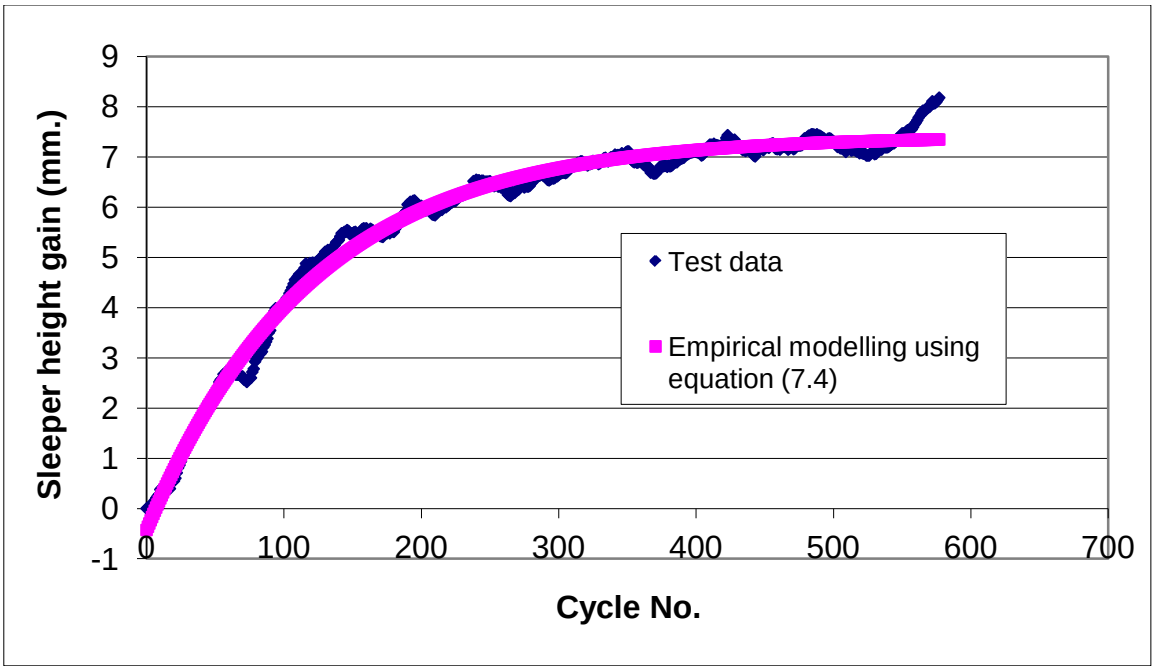

Figure 7.7 Model test with 45mm sleeper spacing 2mm crib ballast

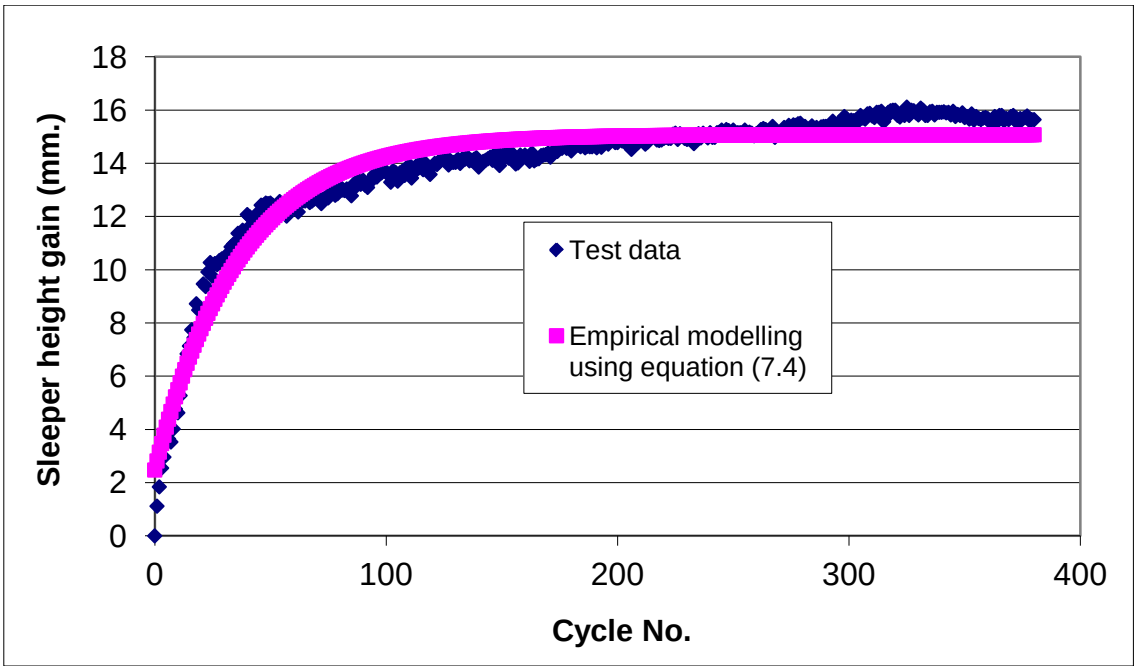

Figure 7.8 Box test with 7mm crib ballast

Table 7.1 Results of empirical modelling

Test type	Total void size	Average particle size (mm.)	A predicted (Ap) (mm.)=	A empirical (Ae) from empirical	A maximum (Am) observed	Constant B	Constant c

		(mm.)		Void size – average crib ballast particle size	modelling	from test data (mm.)		
Model test	Twin block sleeper at 45mm spacing	30	17	13	3.7	3.2	3.21	0.002
	Twin block sleeper at 60mm spacing	28.9	17	11.9	5.27	5.4	5.29	0.0061
	Twin block sleeper at 70mm spacing	32	17	15	3.68	3.7	3.43	0.0061
	Twin block sleeper at 80mm spacing	30.5	17	13.5	4.72	4.8	4.46	0.007
	Monoblock sleeper at 45mm spacing	27	17	10	7.41	7.4	7.817	0.0084
	Monoblock sleeper at 60mm spacing	26	17	9	8.62	8.72	8.2	0.0097
	Monoblock sleeper at 70mm spacing	25.6	17	8.6	6.196	5.82	7.58	0.0193
	Monoblock sleeper at 80mm spacing	30.1	17	13.1	4.91	4.7	5.13	0.011

Table 7.1 cont'd

Test type		Total void size (mm.)	Average particle size (mm.)	A predicted (Ap) (mm.)= Void size – average crib ballast particle size	A empirical (Ae) from empirical modelling	A maximum (Am) from test data (mm.)	Constant B	Constant c
Full scale box test	With 20mm crib ballast	26.17	17	9.17	8.89	9.6	7.04	0.0193
	With 5mm crib ballast	25.6	7	18.6	15.09	15.7	12.61	0.0273
	40-20 mix crib ballast				10.15		7.79	0.0218
Full scale test with 50mm bottom ballast	20mm crib ballast	41	17	24	18.87	20.41	16.56	0.0352
	20mm crib ballast quick loading cycles	21	17	4	5.68	5.04	6.16	0.214
	10mm crib ballast	29.1	10	19.1	19.48	19.5	17.54	0.0325
	7mm crib ballast	34.4	7	27.4	26.51	24	22.35	0.0207

	Sand as crib ballast	41.6	4	37.6	27.36	30.3	24.2	0.0427
	50mm crib ballast	47	37	10	9.37	8.7	8.75	0.0264
Full scale test 800mm sleeper spacing 50mm bottom ballast	20mm crib ballast	35.7	17	18.7	11.86	11.33	9.71	0.0340
Full scale test with 20mm crib&	20mm crib ballast	36.5	17	19.5	17.75	17.7	17.32	0.0608

Table 7.1 cont'd

Test Type		Total void size (mm.)	Average particle size (mm.)	A predicted (Ap) (mm.)= Void size – average crib ballast particle size	A empirical (Ae) from empirical modelling	A maximum (Am) from test data (mm.)	Constant B	Constant c
Model tests on sand paper uplift height 25mm	Particle size range							
	23-20	25	21.5	3.5	3.59	3.3	3.64	0.0280
	20-17	25	18.5	6.5	5.45	5.3	4.2098	0.0097
	17-14	25	15.5	9.5	5.17	5.39	3.52	0.0177
	14-12	25	13	12	9.04	9.17	5.5	0.0192
Model test on sand paper crib ballast average particle size 1.7mm	Uplift height (mm)							
	Uplift 45	45	17	28	25.5	25.26	11.5	0.038
	Uplift 35	35	17	18	10.46	16.9	8.17	0.027

	Uplift 25	25	17	8	9.45	10	8.09	0.1389
Model test with 20mm bottom ballast		26	17	9	7.16	7.19	6.81	0.041

In table 7.1 all test described are type A runs i.e. tests run with 20 simple loading cycles followed by uplift cycles. The tests have been classified as model tests, box tests and full scale tests. The tests have been further classified based on the sleeper type used (for model tests), sleeper spacing, size of crib ballast used, size of bottom ballast used and also in one instance for a full scale test, based on the speed of loading cycles. The total void size at the start of the uplift cycles for the tests is given and also the average particle size. The Ap (the predicted final sleeper height gain) is calculated based on equation 7.2 and Ae is the final sleeper height gain as derived from the empirical analysis of the data. These are compared with the Am, the actual final sleeper height gain from the test data. The final sleeper height gain (Am) for the test data was taken as the average of last ten sleeper height gain readings for the test. In the last two columns the values of constants B and c as defined in equation 7.4. The results presented in table 7.1 are discussed in the succeeding article.

7.4 Observations on empirical analysis and discussion on results

7.4.1 Amaximum (Am) Vs Aempirical (Ae)

Amaximum (Am) was the final sleeper height gain observed in the tests while Aempirical (Ae) was the final sleeper height gain as predicted by the empirical modelling of the test data using equation 7.4. Graph of Am against Ae is shown in figure 7.9, this includes data for all model and full scale tests. A line of equality is also plotted to study the accuracy of the empirical modelling.

It is seen from figure 7.9 that all data sets are clustered on or very close to the line of equality which shows that the empirical modelling of the data can be used to predict the

final sleeper height gain for the two layered ballast system. For two tests the Ae value is greater than the Am value, which implies that the test was stopped before the final sleeper height gain was achieved and the empirical modelling suggests that if run for further cycles the sleeper height gain would be more than that achieved in the test.

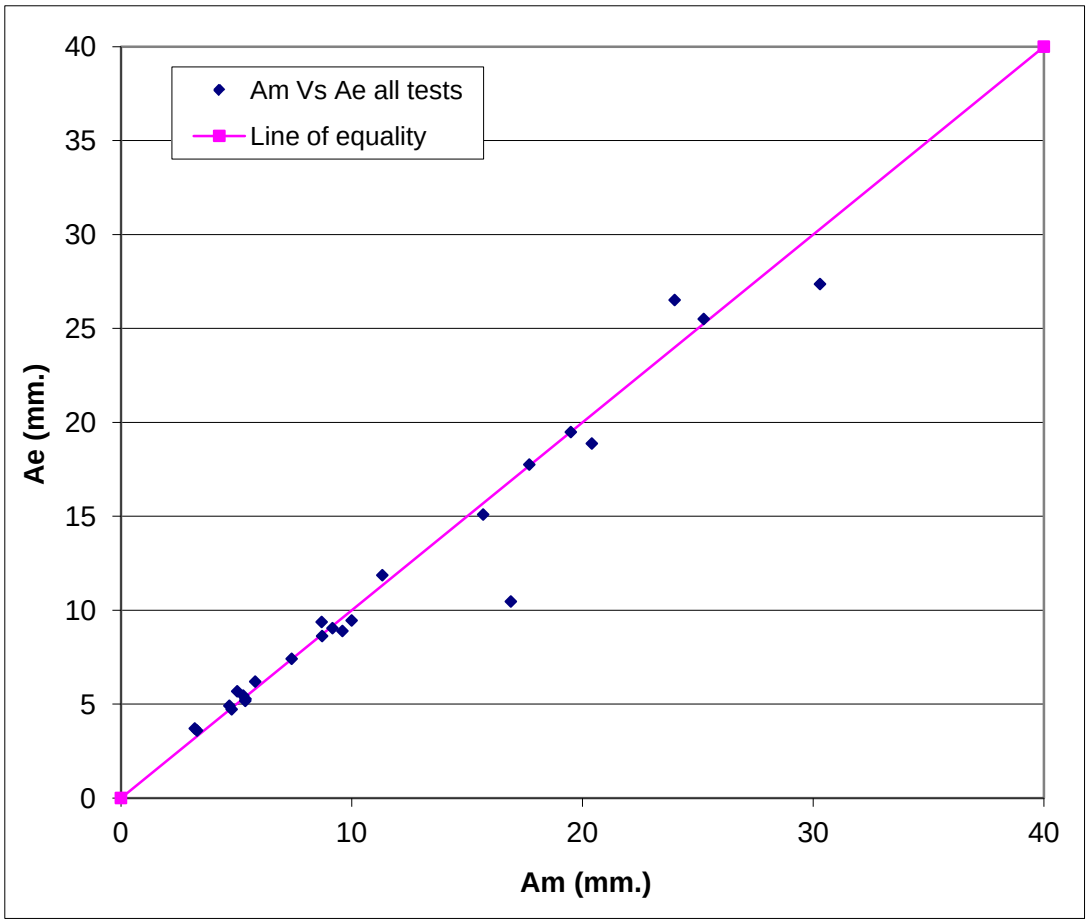

Figure 7.9 Am (maximum height gain observed from test data) Vs Ae (maximum height gain from empirical modelling) for all test data.

7.4.2 Parameter – sleeper spacing

One parameter affecting the performance of the two layered ballast system is the sleeper spacing. Model tests on both monoblock sleepers and twin block sleepers were run at different sleeper spacing to understand the effect of sleeper spacing on the performance of the two layered ballast system. Full scale box tests were limited to sleeper spacing 550mm for all box tests but full scale tests on monoblock sleeper were run with two different

sleeper spacing of 600mm and 800mm. The graph of sleeper spacing Vs Ae/Ap is given in figure 7.10

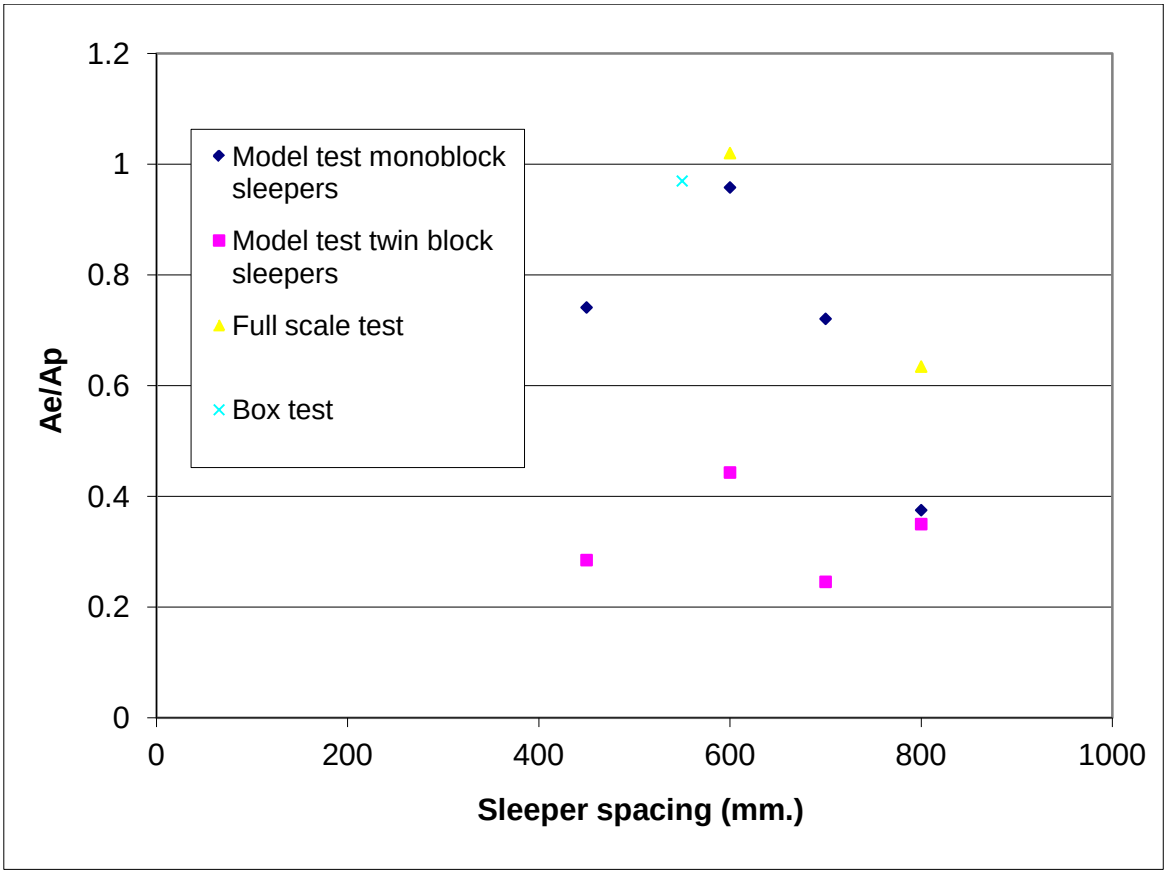

Figure 7.10 Sleeper spacing Vs Ae (from empirical modelling) / Ap (void size minus average particle size).

It can be seen from figure 7.10 that the maximum sleeper height gain is achieved for sleeper spacing 550-600mm for both model and full scale tests. For model tests on monoblock sleepers, box test and full scale test Ae/Ap is approximately equal to one for sleeper spacing 550-600mm while for sleeper spacing less than or greater than 600mm the ratio Ae/Ap is less than 1. For twin block sleepers Ae/Ap ratio is maximum for sleeper spacing 600mm at approximately 0.45 as shown in figure 7.10, while for sleeper spacing greater than or less than 600mm Ae/Ap is less than 0.45. Thus again sleeper spacing for optimum performance of the two layered ballast system is 550-600mm, which is the standard sleeper spacing on the railway.

The reason for reduced sleeper height gain for sleeper spacing greater than 600mm is that the ballast pressure under the sleeper is increased as the sleepers are spaced further apart. It has been discussed earlier that for current industry standard of sleeper spacing 40% of the wheel load is borne by the sleeper directly under the wheel while the rest of the load is distributed to adjoining sleepers. With sleepers spaced further apart the percentage of the wheel load taken by the sleeper directly under the wheel would be greater leading to higher ballast pressure under the sleeper. This would cause increased track settlement as is seen in the results of the model tests with 50mm bottom and crib ballast, discussed in Chapter 5 where ballast inelastic compression under load for sleepers spaced 800mm centers was twice that of sleepers spaced at 450mm centers. For tests run with 20mm crib ballast, the crib ballast migrating into the void below the sleeper would be compressed into the voids in the bottom ballast. For tests run with 20mm crib ballast, sleeper spacing 800mm, for the first few uplift cycles the sleeper height gain due to migration of the crib ballast would be greater than the ballast inelastic compression but after a few cycles the rate of sleeper height gain would reduce and eventually a state of equilibrium would be reached where the ballast inelastic compression would be equal to the sleeper height gain due to the migration of crib ballast. This equilibrium would last while there was sufficient smaller ballast in the crib, if all the crib ballast is used up the track will start deteriorating again.

Another observation made by the author while running the tests was that the movement of the crib ballast in the uplift cycles was affected by the frictional forces developing between the crib ballast particles and the crib boundary, which in case of the model test was the adjoining sleepers and in case of full scale tests was the face of the sleeper and the boundary condition imposed at the center distance of two sleepers. The forces acting on the crib ballast can be described as :

a. Frictional forces between the crib ballast particles and sleeper face.

b. Particle interlocking and frictional forces within the crib ballast particles (these were very high for large stone ballast).

c. Gravity force (Self Weight of crib ballast particles)

In the uplift cycles the crib ballast would move into the void below the sleeper under the effect of gravity, which would have to be greater than the combined effect of the frictional forces and interparticle locking forces, acting on the crib ballast. It was observed in the uplift cycles that due to the frictional forces between the sleeper face and the interlocking forces between crib ballast particles with each uplift cycle the crib ballast was also lifted up by a small amount. Thus the ballast was slowly vibrated with every uplift cycle but the effect of this vibration on sleeper height gain would depend on the sleeper spacing as described further.

For very closely spaced sleepers the effect of inter - particle locking forces would cause close packing of the crib ballast particles and the effect of frictional forces between the crib ballast particles and the sleeper face would extend through the full width of the crib. For the first few uplift cycles the ballast self weight would counter the frictional forces and the ballast would flow into the void below the sleeper but with subsequent cycles with vertical movement of the sleeper and reducing volume of the crib ballast, the ballast confined between two sleepers would be packed into a self supporting stable state and no more sleeper height gain would occur.

For optimum sleeper spacing of 550-600mm the effect of frictional forces would not extend through the full width of the crib. The crib ballast directly in contact with the face of the sleeper would be moved upwards when the sleeper lifted up but adjacent stones in the crib would move towards the sleeper to fill in the void. Thus the slow ‘vibration’ of the crib ballast in the uplift cycles helped the ballast to move into the void below the sleeper. Also the sleeper height gain for the uplift cycles was more than the inelastic compression of ballast under the loads thus sleeper height gain was maximum for sleeper spacing of 550-

600mm. As the rate of loading on all the tests was slow and did not simulate live track loading the author is of the opinion that in live track conditions the ‘vibration’ of the crib ballast due to vertical movement of the sleeper as described above will cause the void below the sleeper to be filled up at a faster rate as compared to laboratory tests. This was demonstrated by the full scale test run with faster loading cycles where the rate of sleeper height gain was quicker as compared to similar test with slow loading cycles.

It is seen from the results in figure 7.10 that for twin block sleepers the maximum sleeper height gain is less as compared to the monoblock sleepers. It has been discussed in the literature review that the ballast pressure under the twin block sleepers is very high as compared to monoblock sleepers. The ballast below twin block sleepers has to be compacted and maintained to a very high standard else track geometry for twin block sleepers deteriorates rapidly for poorly compacted and poorly maintained track. This applies to the test results for twin block sleepers with the two layered ballast system. The ballast for the model tests in the laboratory was laid on steel substrate to the required depth but was not compacted to a very high degree. A plywood board was placed on the ballast and a few loading cycles run on the plywood board, the aim was to level the ballast rather than compact it and the test was started. It was not possible to achieve the live track standard for ballast compaction in the laboratory. This is one reason for the poor results from the tests with the twin block sleepers. The other reason is the high ballast pressure under the twin block sleepers, similar to widely spaced monoblock sleepers. After a few uplift cycles, the inelastic compression of the ballast would balance the sleeper height gain in the uplift cycles, thus the final sleeper height gain for the tests with the twin block sleepers was less than that for monoblock sleepers.

7.4.3 Parameter – Uplift height and crib ballast particle size

7.4.3.1 Model tests carried out without bottom ballast on sandpaper

These tests have been reported in detail in earlier Chapters. For these tests the effect of the bottom ballast as a variable was omitted and the tests were carried out by placing the model sleeper assembly directly on the sandpaper base. For all the tests sleeper spacing was maintained as constant at 550mm. Different size of crib ballast were used for one set of tests with the uplift height kept constant while different uplift heights were used for the other set of tests with crib ballast size kept constant. The graph of average particle size / Void size Vs Ae / Void size for all the tests is shown in figure 7.11.

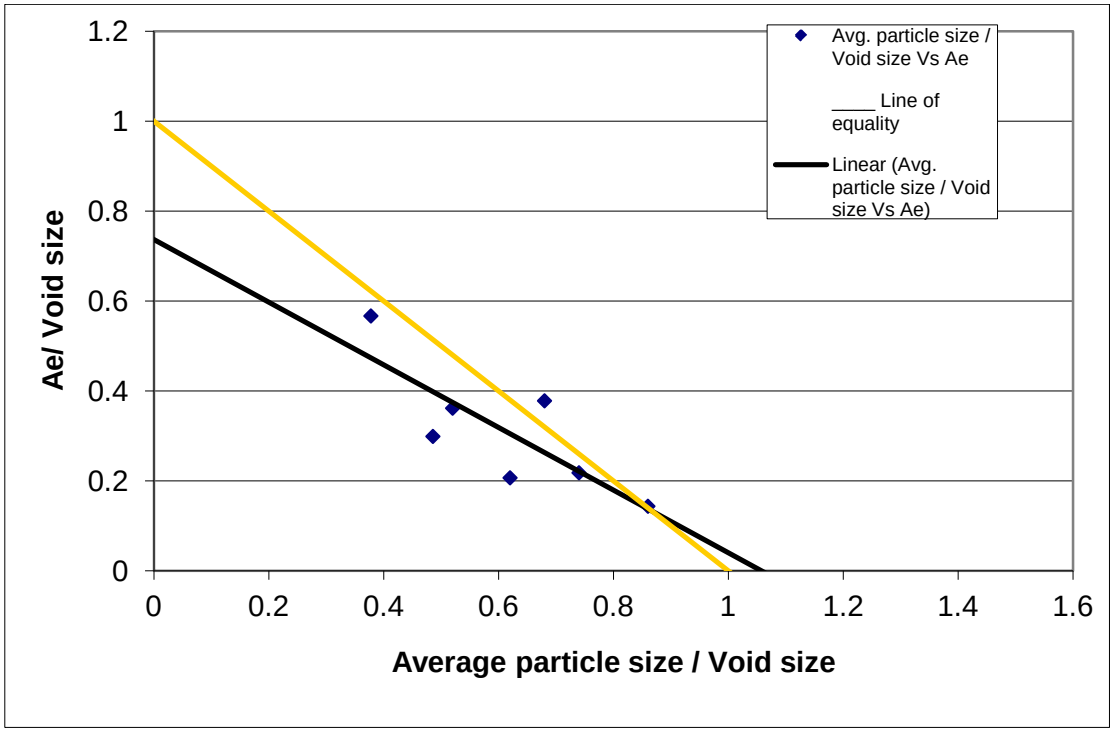

Figure 7.11 Model tests without bottom ballast (tests run by placing sleeper assembly directly on sandpaper base).

For the graph in figure 7.11 a linear trendline was drawn through the data points and extended till it crossed the axes. As discussed earlier Ap is the predicted eight gain using

equation (7.2) where the final sleeper height gain is equal to void size below the sleeper minus the average particle size of the crib ballast and Ae is the value obtained from the empirical modeling (equation 7.4). A line of equality was drawn using Ap as shown in figure 7.11i.e. the line of equality is graph of Ap/void size Vs Average particle size / void size. For the line of equality using Ap, when the ratio of Average particle size / Void size is unity there is no sleeper height gain as Ap is zero i.e. when the average particle size of the crib ballast is equal to the void size below the sleeper there is no sleeper height gain for the uplift cycles. When the ratio of average particle size/void size is zero the sleeper height gain is maximum i.e. equal to the void size below the sleeper. This allowed comparision to be made with graph plotted using Ae.

Comparing with graph using Ae in figure 7.11 it can be seen that Ae/Void size is zero for ratio of average particle size / void size greater than 1. This implies that for no sleeper height gain to take place in the uplift cycles, the average particle size of the crib ballast should be slightly larger than the void size below the sleeper.

Again for ratio of average particle size / void size equal to zero Ae/void size is approximately equal to 0.8. This implies that the final sleeper height gain for all void sizes and crib ballast particle sizes will not be greater than the void size below the sleeper i.e. the void below the sleeper will fill up depending on the void size below the sleeper and the crib ballast average particle size but the sleeper will not rise above its original level in the ballast.

7.4.3.2 Full scale tests (including box tests):

Both the box test and full scale test results are discussed in this section, the results include tests carried out with 50mm and 20mm bottom ballast and different crib ballast sizes. The sleeper spacing for the box tests was 550mm while for full scale tests was 600mm which is the optimum spacing range for performance of the two layered ballast system.

Graph of Average crib ballast particle size / Void size Vs Ae/Void size is shown in figure 7.12.

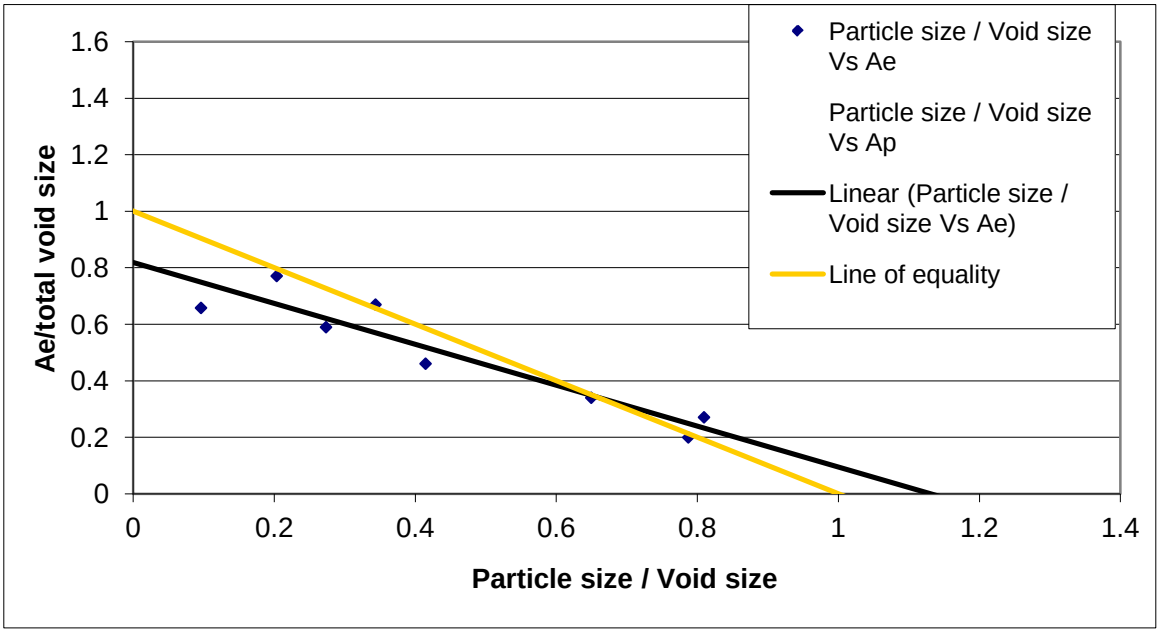

Figure 7.12 Full scale tests

Again similar to model tests the line of equality represents graph of Average particle size / Void size Vs Ap/void size. It is observed that sleeper height gain is zero for average crib ballast particle size larger than the void size below the sleeper, from figure 7.12 for Ae/total void size equal to zero the average particle size / void size is approximately 1.1 which is similar to the results for the model tests. For ratio average particle size /void size equal to zero the Ae/total void size is approximately 0.8, again similar to the observations made from model tests. Thus the sleeper height gain is not greater than the total void size below the sleeper even for small crib ballast size, thus the

sleeper will not gradually climb out of the ballast even for infinitesimally small crib ballast particle size.

It has been discussed earlier that on live track, the sleepers are pushed down into the void into the ballast under the wheel load but just in front of the advancing wheel the sleepers are lifted up by 1-2mm, this effect was not simulated in the testing carried out in the laboratory, thus it is expected that for crib ballast of size smaller than 2mm (sand) the sleeper would continue to rise out of the ballast even after the void below the sleeper has been filled up, under the effect of the uplift in front of each advancing wheel.

7.4.4 Constant c and B

In equation 7.4 used for empirical modelling the constant c controls how fast the final sleeper height gain is achieved while B is a constant introduced to get a best fit of the equation to the data. The effect of c and B on the two layered ballast system have been discussed in this section.

7.4.4.1 Effect of sleeper spacing on constant c in model tests

To understand the effect of the sleeper spacing, in model tests, on c a graph of sleeper spacing Vs c (Constant) is shown in figure 7.13.

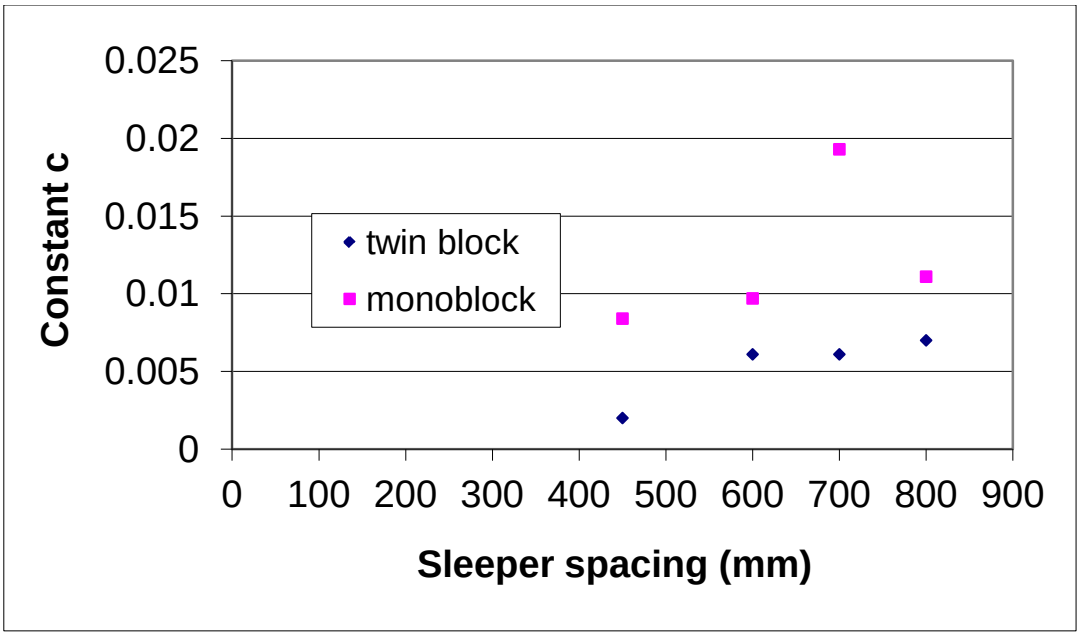

Figure 7.13 Value of constant c for different sleeper spacing

It can be seen from figure 7.13 that the c values for tests carried out with monoblock sleepers are higher than those for twinblock sleepers, thus the final sleeper height gain is attenuated quicker for monoblock sleepers. The trend of the graph suggests that the c value is higher for increased sleeper spacing. This implies that although the final sleeper height gain for widely spaced sleepers is less the height gain is attenuated quickly.

7.4.4.2 Model tests on sandpaper base compared with model tests on 50mm bottom ballast

Graph of average crib ballast particle size/ void size Vs c is shown in figure 7.14. A comparison is made with c values for model tests carried out with 50mm bottom ballast with different sleeper spacing.

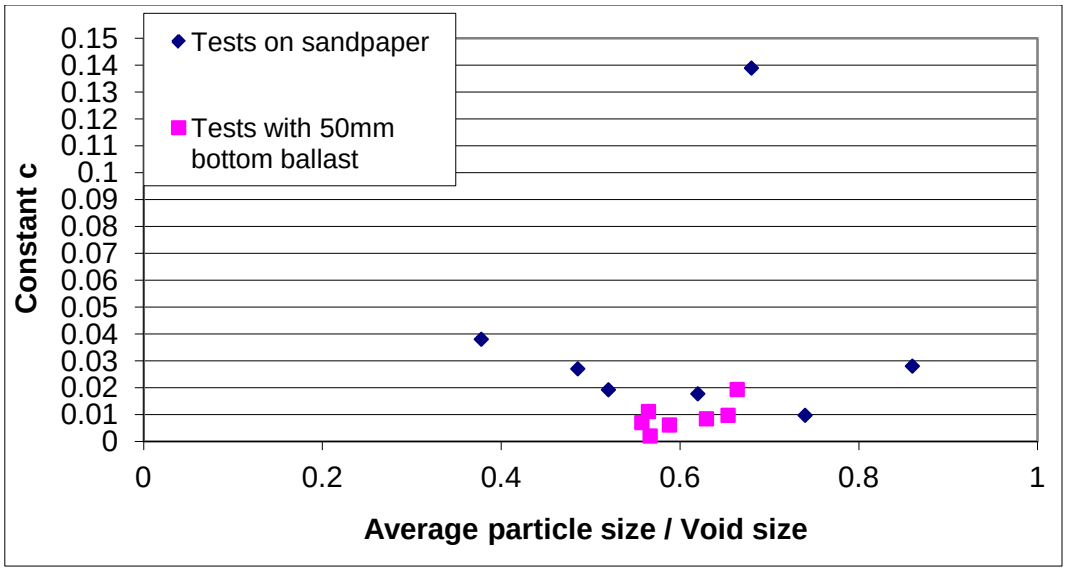

Figure 7.14 Average particle size / void size Vs c

It is observed that for tests carried out on sandpaper without bottom ballast the c values are higher than those for tests carried out on 50mm bottom ballast. This implies that with 50mm bottom ballast the sleeper height gain in the test is slower compared to tests without bottom ballast. This reinforces the point that for the initial uplift cycles a percentage of the crib ballast migrating into the void below the sleeper is lost in the voids of the bottom ballast and for all subsequent load cycles a part of the sleeper height gain is offset by the elastic compression of the bottom ballast, thus sleeper height gain is slow compared to tests carried out on sandpaper with no bottom ballast.

No definite trend for value of c relating to crib ballast particle size and void size below the sleeper can be seen but in the graph in figure 7.14 it can be seen that the value of c is higher for lower value of (average particle size/void size) implying that for larger void size or smaller particle size the uplift height gain is quicker.

7.4.4.3 Model tests on 50mm bottom ballast compared to full scale test with 50mm bottom ballast

It has been discussed in Chapter 5 that the sleeper height gain in the model tests was slower as compared to the full scale tests. The reason for this is that the effect of gravity could not be modelled at 10^{th} scale without carrying out the model tests in a centrifuge to create artificial scaled down gravity effect. With empirical modelling the value of constant c would determine the how fast the final sleeper height gain was achieved, thus graph of Ae/Ap Vs value of constant c has been plotted in figure 7.15 for all model tests and full scale tests on 50mm bottom ballast, including box test.

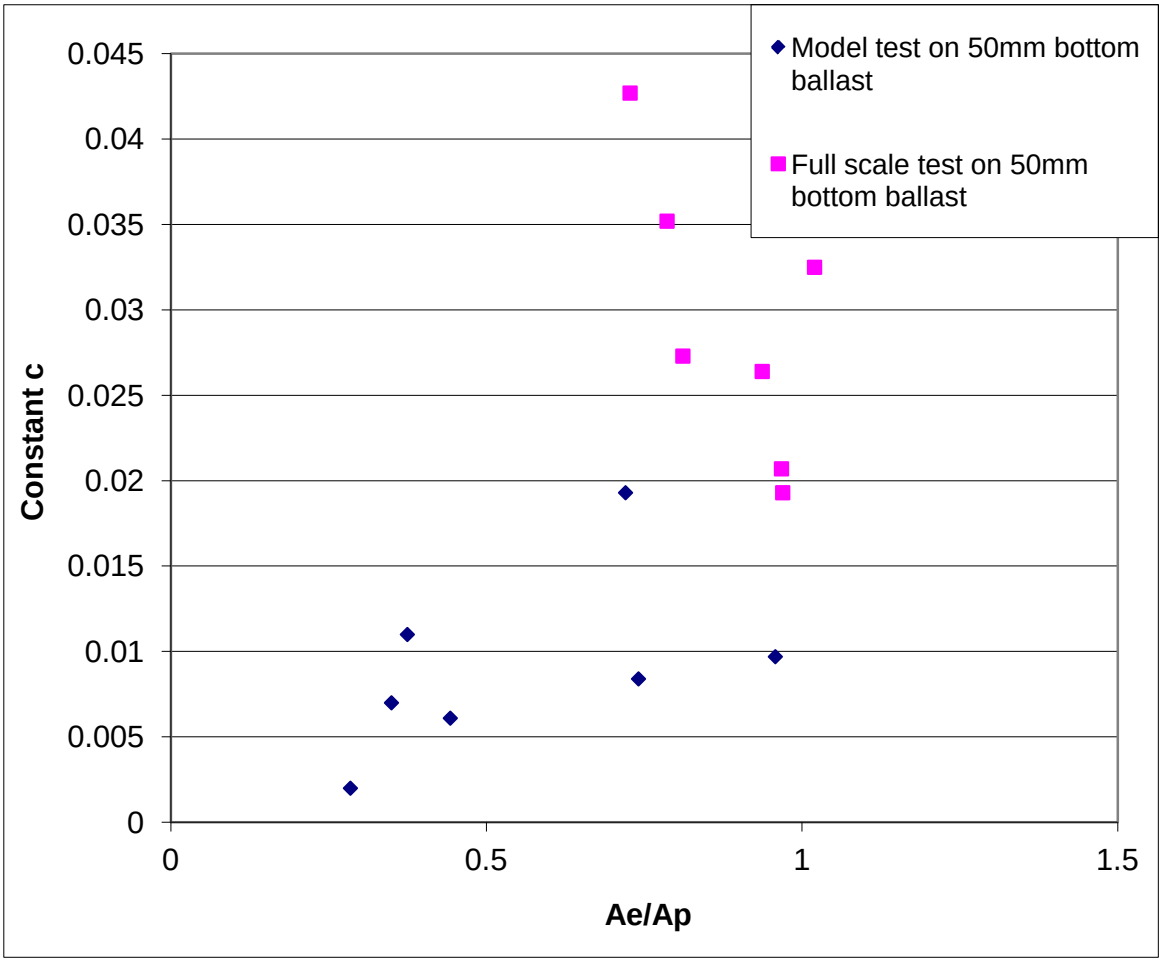

Figure 7.15 Model tests and Full scale tests (including box test) on 50mm bottom ballast, Ae is the A value from empirical modeling and Ap is the predicted value of A using equation 7.2.

It can be seen from figure 7.15 that the for the model test results the value of c is lower as compared to full scale test results e.g. for model with monoblock sleepers with 600mm spacing and 20 mm crib ballast the value of c is 0.0097 while for similar box test the value of c is 0.0193 and for similar full scale test the value of c is 0.0352. The final sleeper height gain for the above mentioned model test was achieved in approximately 800 load cycles while the final sleeper height gain for the box test was achieved in approximately 300 load cycles and for the full scale test was achieved in approximately 250 load cycles.

7.4.4.4 Void size and crib ballast particle size Vs c for full scale test.

In the graph in figure 7.16 Average crib ballast particle size / Void size is plotted against value of constant 'c' from empirical modelling.

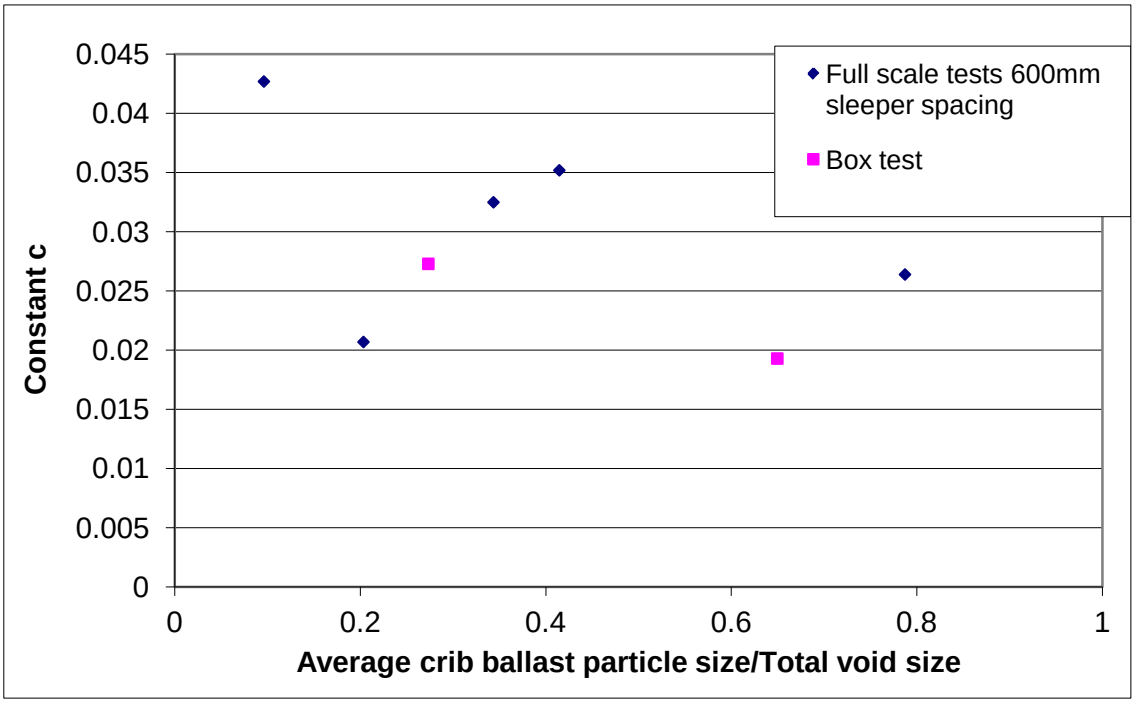

Figure 7.16 Box tests and full scale tests 50mm bottom ballast – value of constant c

The trend of the graphs shows conclusively that for lower value of ratio of average crib ballast particle size and Total void size below the sleeper the value of constant c is higher i.e. for smaller crib ballast particle size or large void size below the sleeper the sleeper height gain will be faster, e.g. the value of constant c for sand as crib ballast is the highest at 0.04 as compared to the test with 50mm crib ballast for which the value of c is 0.026. The same can be seen for the two box tests results wherein for box test with 20mm crib ballast the value of c is 0.0193 and the value of c for box test with 7mm crib ballast is 0.0273.

In the graph in figure 7.16 the value of c for the full scale test run with faster loading cycles is not shown for clarity of the graph. As discussed earlier one full scale test was run with faster loading cycles and it was observed that the sleeper height gain was faster than that observed for all ballast particle sizes and uplift heights in the full scale tests. The value of c for the test run with fast loading cycles was 0.214, which is the maximum value of c for all laboratory tests carried out on the two layered ballast system. The ratio of average crib ballast particle size to the total void size below the sleeper for the test was 0.8 which is higher as compared to all full scale test but the value of constant c was still higher as compared to all full scale and model test carried out on the two layered ballast system. Thus it seems that the rate of loading is perhaps the most important factor in deciding how fast the final sleeper height gain will be achieved.

7.4.4.5 Tests run on 20mm crib and bottom ballast.

Model test with monoblock sleepers and full scale test (Type A runs) were run on 20mm bottom ballast with 20mm crib ballast to understand the effect of smaller ballast under the sleeper on the two layered ballast system.

For both model and full scale tests with 20mm bottom ballast it was observed that the ballast inelastic compression in the simple load cycles was less than that observed for tests run with 50mm bottom ballast. The sleeper height gain in the uplift cycles was also

quicker for the test run with 20mm bottom ballast. In the empirical modelling for the tests run with 20mm bottom ballast the value of c for the full scale test was 0.0608 while the value of c for similar full scale test with 50mm bottom ballast was 0.03. For model test on 20mm bottom ballast value of c was 0.041 while for test run with 50mm bottom ballast the value of c was 0.0097. Thus the value of c is higher for tests run on 20mm bottom ballast as compared to tests run on 50mm bottom ballast.

As discussed earlier two important factors affecting the sleeper height gain in the uplift cycles are :

1. Ballast inelastic compression under the load (as observed from tests with wider sleeper spacing and twin block sleepers)
2. Void size in the bottom ballast (observed when comparing model test run on sandpaper and 50mm bottom ballast)

Considering the factors mentioned above for tests run with 20mm bottom ballast, the ballast inelastic compression for 20mm bottom ballast is less than that for 50mm bottom ballast. As explained earlier this is due to large number of contact points below the sleeper for 20mm ballast and better load distribution under the sleeper for 20mm bottom ballast. Thus in the uplift cycles very small portion of the sleeper height gain would be offset by the inelastic compression of the bottom ballast as compared to test run with 50mm bottom ballast.

For the test with 20mm bottom and crib ballast, in the uplift cycles when the crib ballast would flow into the void below the sleeper, as both the bottom ballast and the crib ballast are of the same size the crib ballast would not be lost in the voids of the bottom ballast, as it occurs for test with 50mm bottom ballast thus the sleeper height gain is quicker as compared to test with 50mm crib ballast.

7.4.4.6 Constant B

As mentioned earlier the constant B was introduced to allow better curve fitting to the test data. To analyse the effect of constant B a graph of Ae Vs B is plotted in figure 7.16. It can be seen that all data points on the graph in figure 7.17 are clustered around the line of equality. This implies that there is no significant difference in the value of Ae and B but introducing the constant B in the equation allows better fitting of the data to be carried out.

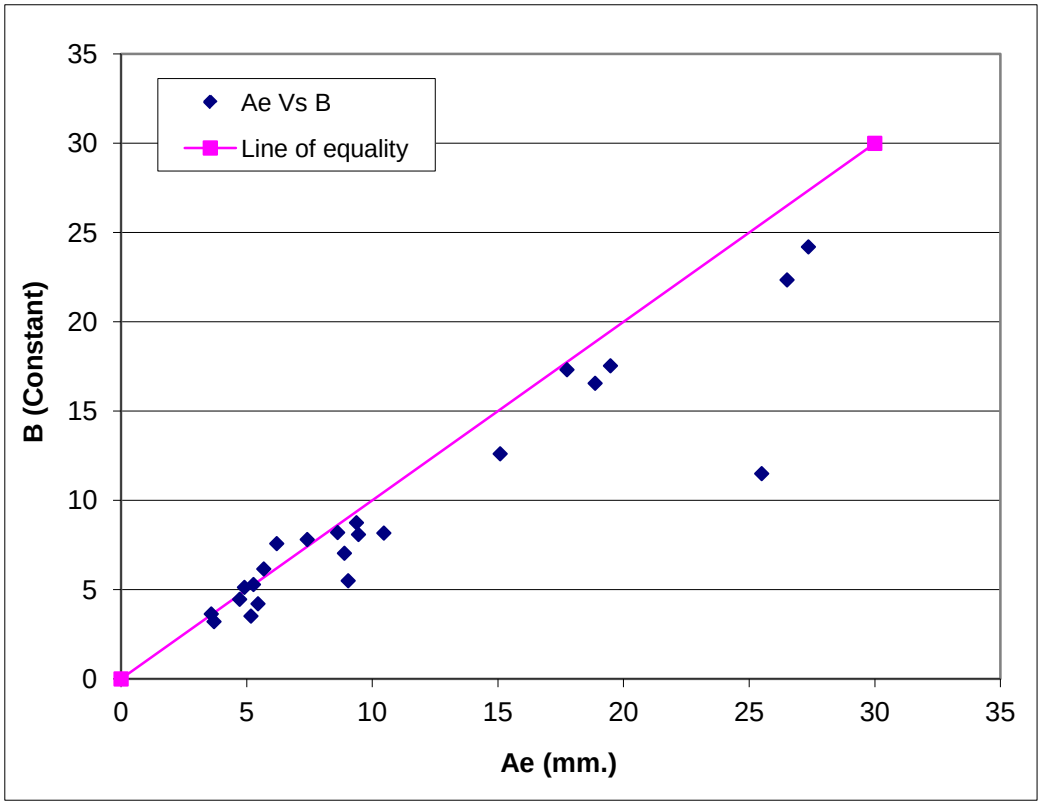

Figure 7.17 Ae Vs B for all test data

8. Live track trials

8.1 Introduction

The final stage of the project must involve trials of the proposed two layered ballast system on live track. The live track trials have not been carried out to date because Balfour Beatty Rail (Project Sponsors), due to change in policy by Network Rail, are not given any incentive to bring this research to its logical conclusion. Preparation had been done for the live track trials to be carried out by selecting a location for the trials at Gillingham in Dorset (a track length with voided sleepers – void size approximately 15mm to 25mm was selected), developing a method of displacement measurement on site by digital video photography, looking at access arrangements and logistics of material supply. The live track trials presented an opportunity to observe the performance of the two layered ballast system under live track conditions and also to validate the assumptions made regarding boundary conditions and loading conditions for tests carried out in the laboratory. A method statement was prepared to carry out the live track trials. The method statement and the technique of displacement measurement by digital video photography, developed for the live track trials are described in brief in this chapter.

8.2. Methodology for carrying out the live track trials

The first requirement for the live track trials was selection of a site with a length of track with voided sleepers. The aim was to measure the existing voids below the sleepers,

replace crib ballast by smaller size stone and monitor the voids below the sleepers over a duration of time. The site had to be easily accessible by road to allow smaller ballast to be taken to site by road and also to allow periodic visits to be undertaken to site to monitor the voids below the sleepers in the track.

It was decided that once a site had been identified the void size below the sleepers would be measured. If possible a track geometry recording equipment was to be used to measure track geometry prior to the trials or the latest HSTRC data for the section of track could be used to record geometry of track prior to the trials. The existing crib ballast removed to the bottom of the void around the sleepers and smaller crib ballast filled in around the sleepers. The displacement of the sleeper in the void would be measured subsequently over a period of time. Displacement measurement when the first train passed over the section of the track, after smaller size stones were put in the crib, was critical as maximum sleeper height gain would occur in first few loading cycles. Any HSTRC runs on the track subsequent to the testing would give data for comparison with data from HSTRC run before the test.

8.2.1 Displacement measurement using digital video photography

The most important aspect of the test was displacement measurement of the sleeper as it moved in the void under traffic. The requirement was for a measurement method, which would not require going close to the track or working on the track. The present method to measure voids below the sleepers is to use a void meter as described in Chapter 2. This would require going out on live track to install a void meter and then read it and reset it frequently as it would be disturbed by the vibrations of the passing trains, also void meter readings are not very accurate. Thus it was decided to use digital video photography to remotely measure and monitor the void below the sleepers. This method was ideal for the purpose as the video could be set up a good distance away from the track and thus periodic monitoring could be carried out without having to go out on live track.

High speed filming is used for measuring speed of objects and distance moved by objects, in the field of sports or bio-mechanics. High speed filming can be used to measure velocity of a ball, distance jumped by an athelete etc. In the video the image is reduced to a fraction of its original size and thus the video image has to be calibrated to give the real life measurements. To calibrate the video images any object of known dimensions has to be placed in the camera's field of view during the filming. Knowing the actual dimensions of the object and the dimensions as they appear in the video the images can be calibrated to give real life dimensions. A reference point is usually required in the moving object being filmed if displacement is to be measured e.g. if measuring movement of the sleeper or the rail a small indicator, which is clearly visible when filming can be fixed onto the rail or sleeper.

Once high speed video has been acquired the video has to be split up in individual frames. The frames when viewed on any photo-imaging software on the computer will be composed of pixels. With a known measurement in the field of view of the camera the pixels can be calibrated to real life dimensions. When measuring displacement of an object e.g. rail, the movement of the indicator fixed on the object can be monitored in successive frames and the number of pixels the indicator has moved can be measured giving the real life displacement as the pixels are already calibrated to real life dimensions.

In preparation for the full scale trials a trial for displacement measurement of a rail in live track was carried out as described. The location selected to position the camera was the car park of Coventry Railway station. The car park extends beyond the station platform and thus from the edge of the car park the Coventry Birmingham and Coventry Nuneaton railway lines can be photographed easily. A digital video camera of speed 25 frames per second was selected for recording the movement of the rail under traffic. First the railway line was observed by the naked eye under traffic and a rail moving under traffic and easily visible from the car park was selected. The camera was zoom was adjusted to get a close-up of the rail. The movement of the rail was recorded under traffic, using digital video. The video was taken back to the technicians in Coventry University Arts department who split the video in to frames.

As it was not possible to go on to the live track and fix a known measurement in the field of view of the camera the depth of the rail was selected as a known measurement. The problem with this approach was that it was difficult to get sharp edges on the rail to measure distance from, this problem was noted and it was decided to use a fixed known measurement when carrying out the live track trials. An approximate fixed edge was located on the rail and the pixels calibrated using the rail height. The same fixed edge was then observed in successive frames and the maximum movement of the rail was calculated as 7mm from the calibration of the pixels. The two frames used to measure displacement are shown in figure 8.1. Thus a method was devised to remotely monitor track movement.

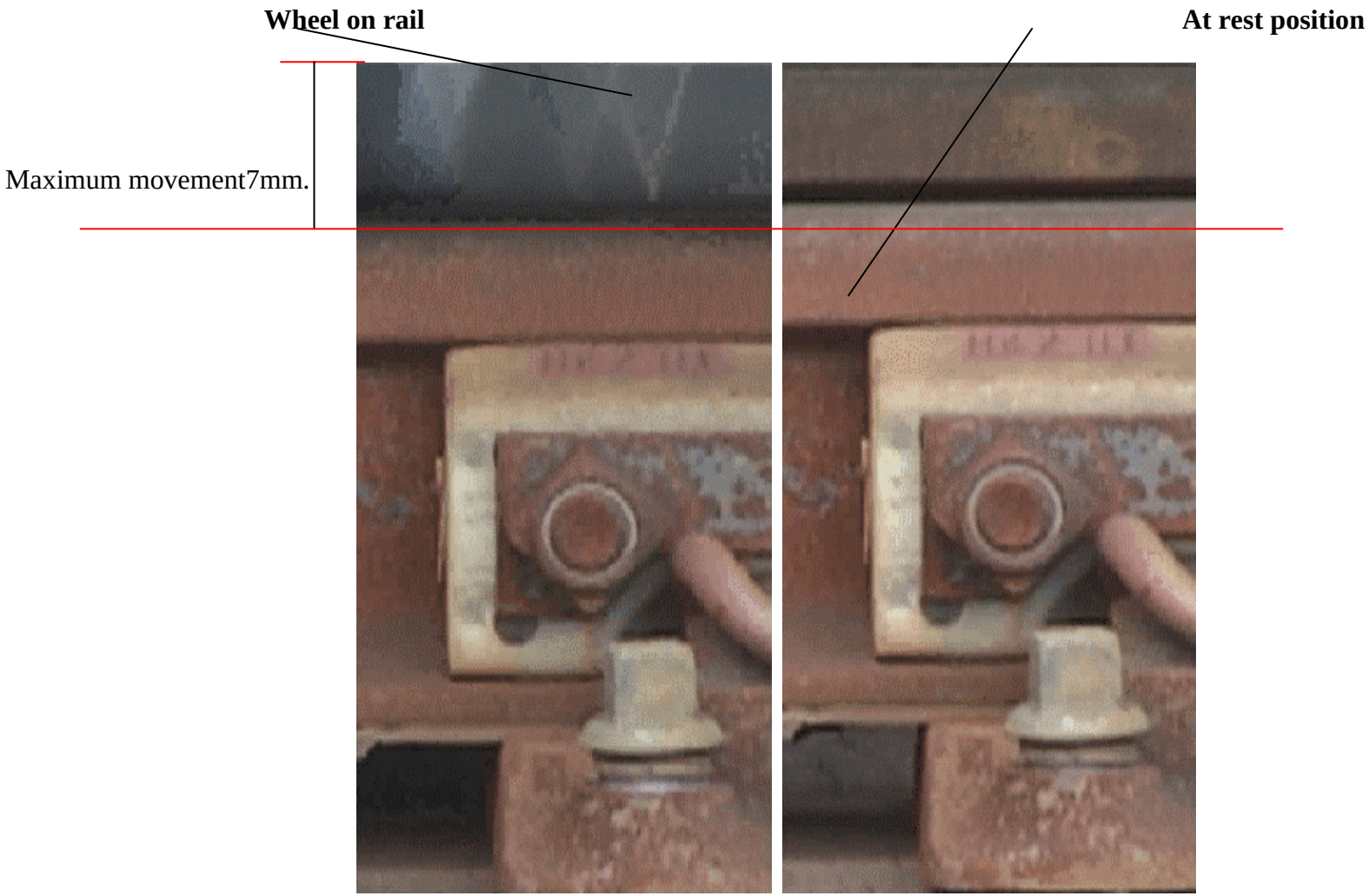
Wheel on rail
At rest position
Maximum movement7mm.

Maximum displacement position **At rest position**

Figure 8.1 Frames selected from digital video to measure maximum rail displacement

For the actual live track trials, in consultation with the sponsors Balfour Beatty it was decided to use small tell tales as a reference object fixed on the side of the rail. These could be monitored in successive frames to calculated displacement. The height and width of the tell tale could be used as a reference to calibrate the video images to real life measurements.

The method statement for the live track trials is given below:

Selection of location.

The trial should be carried out on a stretch of track with at least 5 sleepers with voids beneath them sufficient to cause more than 15mm of vertical movement when a train passes. Ideally the movement should be approximately 25mm or more.

Procedure

Voids below sleepers

1. Track survey look for low spots on track and sections with loose sleepers. Fix tell tales on the rail above loose sleepers.
2. Use digital video photography to record accurately existing displacement of sleepers.
3. Check recent maintenance record on track and any data on track geometry recorded earlier.
4. Carry out a run of standard track geometry recording equipment (if easily available) on section of track and record track geometry information and if possible void size.
5. Remove crib ballast from the section of track with the selected sleepers up to sleeper bottom and replace with 20mm stone leave one sleeper with standard 50mm crib ballast.

6. Set up video camera and measure displacement for passage of first train (critical) – record total number of axles passing and change in sleeper displacement for 20mm stone as crib ballast and 50mm stone as crib ballast.

Track settlement

1. Arrange for dynamic track stabiliser. Raise sleepers to required level (using a jack) and compact 20mm crib ballast and observe if it fills the void below the sleeper.
2. Arrange a run of track geometry recording instrument on the track and compare readings of standard deviation.

Long term monitoring

1. Monitor sleeper displacement for as long as possible and keep record of number of trains passing between each displacement measurement and approximate number of axles passing the track section.
2. Monitor track geometry with track geometry measuring equipment for a longer duration to measure track durability.
3. If possible remove sleeper and take photographs of movement of crib ballast below sleepers at different stages.

9. Conclusions and suggestions for further study

The following conclusions can be derived from the research on the two layered ballast system:

1. Following from discussion on railway track maintenance using Tampers and Stoneblowers in section 2.6.3.2 and 2.6.4.2 in the Literature Review it can be

concluded that, mechanised stoneblowing should replace tamping as the industry mainstay for railway track geometry maintenance.

2. From discussion in Literature Review on damage caused to ballast by the tamping process, it is evident that the use of tamping should be minimized to prolong life of ballast.

3. The problem with ‘track roughness’ after stoneblowing is due to excessive ‘design overlift’ required to allow 20mm stones to be blown into the void below the sleeper, this allows large crib ballast to migrate into the void. This has been demonstrated by ‘Type B’ model tests and full scale test with ‘uplift height 45mm’. Use of smaller stone of size 5-12mm should be considered for stoneblowing to overcome the problems with ‘design overlift’ of the stoneblowers as no ‘design overlift’ would be required for smaller size stones.

4. The proposed two layered ballast system is effective in reducing voids below the sleepers by filling it with smaller crib ballast for track with monoblock concrete or wooden sleepers, the system is not effective on track with twin block sleepers or steel sleepers. This has been demonstrated by model tests and full scale tests carried out in the laboratory on the proposed system.

5. It has been discussed in Literature Review that voids below sleepers are a major maintenance problem on the Railway. With smaller crib ballast the void below the sleeper would be limited to within certain tolerances, thus use of the proposed system could potentially lead to major reduction in track maintenance costs.

6. From results of tests using graded ballast, described in section 6.1.4, it is evident that use of graded ballast or smaller ballast to pre 1980’s specification should be reintroduced on the railways, to keep voids below sleepers to a minimum.

7. Empirical modeling of test data, from the tests carried out on the proposed system has demonstrated that for a lower value of ratio of average particle size of the crib ballast/void size below the sleeper, the sleeper height gain is maximum and the maximum height gain is attenuated at a faster rate i.e. the value of the variables Ae and c are maximum.

Suggestions for further study

1. The next logical step in this research is to carry out live track trials using the proposed two layered ballast system with smaller crib ballast. Long term monitoring of the live track trials should be carried out, this will also help study the effect, if any, on track drainage due to the use of the proposed system. All the laboratory tests have been continued until the maximum sleeper height gain was achieved (approximately 500-1000 cycles i.e. 500-1000 axles in live track). This is equivalent to a single days traffic on lightly trafficked lines in the UK. The long term effect of the two layered ballast system was not studied. Long term monitoring of the track with the proposed system should be carried out both in the laboratory and in live track conditions.

2. It has been observed in the full scale tests that the performance of the two layered ballast system improved for faster rate of loading. It has been mentioned earlier that the loading in all the tests did not simulate the rate of loading on live railway track i.e. the rate of loading was slow although the total load applied was equal to the standard axle load on British Rail. Thus the effect of faster rate of loading on the proposed system should be investigated both in laboratory tests and when carrying out live track trials.

3. Tests with twin block sleepers have shown that for increased ballast pressure below the sleeper and poorly compacted ballast the performance of the two layered ballast

system is not optimum, thus further tests should be carried out on both twin block and monoblock sleepers with higher axle loads and properly compacted ballast.

4. As with the stoneblowing process, the use of the proposed system will eventually produce a two layered ballast cross-section under the sleeper, with 20mm stone on 50mm stone. The effect of having a two layered ballast cross-section below the sleeper on track stiffness should be studied.

5. The effect of the proposed system on ballast fouling has not been studied. Some crib ballast particle breakage is likely to take place when the smaller crib ballast moves into the void below the sleeper. The track fouling caused by the use of the proposed system should be compared with track fouling due to the use of stoneblowers and tampers.

References:

Ahlf, R. E. (1995) Ballast Basics: Part I, *Railway Track and Structures*, April, pp 14-15

Anderson W.F., Wilde C., Thompson J. (2002) Experiences with the stoneblower on the UK East Coast Main Line, *Proceedings of the Railway Engineering Conference*, Edinburgh, ECS Publications

Anderson, W.F. Key, A.J. (2000) Model Testing Of A Two Layered Railway Track Ballast, *Proceedings of American Society of Civil Engineers, Journal of Geotechnical and Geo-environmental Engineering*, vol. 126, Part 4, pp 317-323

Anon (1973) *Track Laying For Underground Haulage*, British Coal Board, 1973

Anon (1989) In Crossties What is the State of the Art, *Railway Track and Structures*, November.

Arora, S.P. Saxena, S.C. (1988) *A Text Book of Railway Engineering*, New Delhi, Dhanpat Rai and Sons

Ball M., *Railway Ballast Maintenance*, Final year project, School of Science and the Environment, Coventry University, 2003.

Bonnet, C.F. (1996) *Practical Railway Engineering*, London, Imperial College Press

Claisse P.A. and Calla C. (2003) Tests on a two layered ballast system, *Proceedings of Railway Engineering Conference*, Edinburgh, ECS Publications

Coenraad, E. (2001) *Modern Railway Track*, MRT-Productions.

Computer Boards Inc. (1994) *CIO-DAS16/M1* Users Manual, Manchester

Computer boards Inc. (1994) *Universal library programmers manual*, Manchester

Conder, F.R. (1983) *The Men Who Built the Railways*, edited by Simmons J. London, Telford.

Coombs, D.H. (1971) British Railway Track – Design Construction and Maintenance, Nottingham, The Permanent Way Institution

Cope, D.L. Ellis J.B. (2001) *British Railway Track vol.4 : Plain Line Maintenance*, Permanent Way Institution.

Cope, G. H (1993) *British Railway Track, Design, Construction and Maintenance*, The Permanent Way Institution

Dahlberg T. (2001) Some railroad settlement models – a critical review, *Proceedings of the Institution of Mechanical Engineers*, Vol 215, Part F, pp 289-300

Eisenmann, J. (1995) Ballastless Track as an Alternative to Ballasted Track, *Rail International*, November.

Frazer, I.R. (1938) Measured Shovel Packing, *Journal of The Permanent Way Institution*, Volume LVI. Pp79-95

Hamnett R.A. (1956) British Railway Track – Design, Construction and Maintenance, Nottingham, The Permanent Way Institution

Hamnett, R.A. (1943) *British Railway Track – Design, Construction and Maintenance*, Nottingham, The Permanent Way Institution

Harsco track technology (1997) *Stoneblower brochure*

Heeler, C.L. (1979) *British Railway Track – Design, Construction and Maintenance*, Nottingham, The Permanent Way Institution.

Holbourn P.(2003) *Tests On A Two Layered Ballast System*, Final year project, School of Science and the Environment, Coventry University

Hope R. (2000) Steel sleepers invade concrete territory, *Railway Gazette Internationa*l, February, pp 96-98.

Indraratna, B. Ionescu, D. Christie, H.D. (1998) Shear behaviour of railway ballast based on large scale triaxial tests, *ASCE Journal of Geotechnical and Geoenvironmental Engineering*, vol. 124, No. 5, May , pp 439-449

Ishikawa, T. Sekine, E. (2002) Effect of Moving Wheel Load on Cyclic Deformation of Railroad Ballast, *Proceedings of International Railway Engineering Conference*, Edinburgh, ECS Publications

Keedwell, M.J. *Rail Support* (2003), Patent Number 759400, July, Australia.

Keedwell, M.J. *Rail Support*, (2003), Patent Number 6502760 B2, January, USA.

Lechner, B. Leykauf, G. (2002) Development of Ballastless Track Systems in Germany – Design Characteristics and Experiences In Situ, *Proceedings of Railway Engineering Conference*, Edinburgh, ECS Publications

Leeves C.G., (1992) Standards for Track Components, Cost Effective Maintenance of Railway Track, London, Thomas Telford.

Li, D. Selig, E.T. (1998a) Method for Railroad Track Foundation Design I: Development, *ASCE Journal of Geotechnical and Geoenvironmental Engineering* vol 124 no 4, April, pp 316-322.

Li, D. Selig, E.T. (1998b) Method for Railroad Track Foundation Design II: Applications, *Journal of Geotechnical and Geoenvironmental Engineering* vol 124 no 4, April, pp 316-322.

Marshall J. (1989) *The Guinness Railway Book*, U.K.

Mc Dougall (1931) Modern Maintenance of Permanent Way, *The Journal of The Permanent Way Institution*, vol. XLIX, pp 290-306

Mc Michael, P. L. Strange P. R. (1992), BR Adopts New Maintenance Process, *International Railway Journal.*

National Instruments Corporation (2000) *Labview Measurements Manual*, Texas, July

Profillidis V.A. (1995) *Railway Engineering*, Avebury Technical, England
Railtrack Standard, *RT/CE/P/027* 1996

Randell, W. (1913) Track beds and ballast, *Proceedings of Journal of Permanent Way Institution*, vol. xxxI, pp 82-87

RMC brochure 2000

Rolt L.T.C. (1968) *Railway Engineering*, Macmillan, London

Selig E. T. (1998) Ballast's Part : Its Key Roles and Qualities, *Railway Track and Structures*, March, pp 21-35

Selig E.T. (1998) Ballast Performance: Considering more Key Factors, *Railway Track and Structures*, July, pp 17 – 20

Selig E.T.(1984) *Ballast for Heavy Duty Track*: Track Technology, Thomas Telford Ltd., London

Selig, E.T. and Stewart, H.E. (1982) Predicted and Measured Resilient Response of Track, *ASCE Journal of Geotechnical Engineering Division,* vol. 108, November, pp 1423-1442.

Selig, E.T. Waters, J.M. (1994) *Track Geotechnology and Substructure Management*, London, Telford.

Shahu, J.T. Kameswara Rao, N.S. Yudhbir (1999) Parametric Study of Resilient Response of Tracks with a Sub Ballast layer, *Canadian Geotechnical Journal* vol 36 part 6, pp 1137-1150.

Sharpe, P. Lewis, W.H. Musgrave, P.A. Total Trackbed Solution West Coast Route Modernisation (WCRM), *Proceedings of Railway Engineering Conference*, Edinburgh, ECS Publications.

Shenton M.J (1984), *Ballast Deformation and Track Deterioration*, Track Technology, London, Thomas Telford Ltd.

Strange P. (2003), Engineer Network Rail, *Private Communication on Stoneblower Development*.

Taylor H.P.J (1993), The Railway Sleeper: 50 years of Pretensioned, Prestressed Concrete, *The Structural Engineer, v*ol 71, No 16, August, pp 281-288

Tazwell B. (1928), Lifting and packing, *Journal and Proceedings of The Permanent Way Institution*, pp 179-184

Tratman, R.E.E. (1909), 3rd ed. *Railway Track and Track Work*, New York, Mc Graw-Hill Book Company.

Wakui, H. Matsumoto, N. Inoue, H. *Technological Innovation in Railway Structure System with Ladder Track System, Web page:* *www.rtri.or.jp/infoce/wcrr97/b131/b131.html*

Wanek, M. (2001) Tie Market: A Real Sleeper, *Railway Track and Structures* (Internet Edition), October.

Watanabe et al (1984), Civil Engineering Maintenance of High Speed Railways, *Track Technology*, London, Thomas Telford Ltd.

Wood T. (2002), *Private Communication with Tim Wood - Scott Wilson Railway on Ballast Specification*